



UNIVERSITY OF  
LIVERPOOL

# **Towards Improved Models for the Study of the Multi-mechanistic Toxicity of Drug-induced Liver Injury**

Thesis submitted in accordance with the requirements of the University of Liverpool  
for the degree of Doctor of Philosophy

By

**Sophie Louise Penman**

October 2020

## **Declaration**

This thesis is the result of my own work. The material contained within this thesis has not been presented, nor is currently being presented, either wholly or in part for any other degree or qualification.

Sophie Louise Penman

This research was carried out in the Department of Molecular and Clinical Pharmacology, University of Liverpool, UK, in collaboration with Servier.

## CONTENTS

Abstract	iv
Acknowledgements	vi
Publications	vii
Abbreviations	ix
Chapter 1: General Introduction	1
Chapter 2: Investigation of HepaRG Cells for Studying Transporter Regulation in Bile Acid and Mitochondrial Toxicity	40
Chapter 3: Investigation of Bile Acid-induced Mitochondrial Dysfunction in Isolated Mitochondria and HepaRG Cells	69
Chapter 4: Assessment of the Mitotoxic and Cholestatic Potential of Flucloxacillin in HepaRG Cells	111
Chapter 5: Assessment of the Impact of Mitochondrial Genetic Variation and Susceptibility to Toxicity Using HepG2 Transmitochondrial Cybrids	126
Chapter 6: Final Discussion	172
Bibliography	180

## ABSTRACT

The detection of adverse drug reactions (ADRs) post-market poses a significant concern for patient health and the pharmaceutical industry given the high cost of drug development and the potential for fatalities. The liver is one of the most reported cases of toxicity and therefore, the detection of drug-induced liver injury (DILI) preclinically is imperative. Whilst rare, cases of DILI that are idiosyncratic are the most problematic as they are characterised by a complex dose-related relationship, lack of predictability from the pharmacology of the drug and interindividual variation. Notably, it is acknowledged that the toxicity of idiosyncratic DILI is multi-mechanistic.

Advancements in the field have identified many *in vitro* assays to evaluate the potential for a compound to cause DILI however, if these are not conducted in an appropriate model, the results can lack *in vivo* applicability. HepG2 cells are the most common cell line used during preclinical DILI screening however, their utility is limited for certain mechanisms associated with DILI. If limitations of the models are not accounted for, toxicity can be missed, over-estimated or bear little relevance to the toxicity seen in humans.

Therefore, the aim of this research was to assess the utility of different hepatic models for their appropriateness in studying mechanisms of toxicity associated with DILI. Biliary transporter alterations and mitochondrial dysfunction are frequently reported to be implicated in DILI and so the utility of HepG2 and HepaRG cells for studying these mechanisms was evaluated. Whilst it is acknowledged that DILI arises due to a combination of drug-related mechanisms, individual susceptibility factors are also involved, but fail to be incorporated into preclinical models. The final aim of this thesis was to use HepG2 trans-mitochondrial cybrids to assess the effect of mitochondrial DNA (mtDNA) variation upon susceptibility to mitochondrial dysfunction with a compound associated with idiosyncratic DILI.

Initial investigations revealed that HepaRG cells possess a more suitable phenotype for assessments of transporter regulation and mitochondrial dysfunction than HepG2 cells. Following this confirmation, the ability of bile acid (BA) mixtures to cause transporter toxicity and mitochondrial dysfunction were evaluated. It was identified that pathological concentrations of BA mixtures caused a temporal reduction in the activity and expression of key biliary transporters. Subsequent experiments investigated the mitotoxic potential of BAs in isolated mitochondria and HepaRG whole cells. Taken collectively, alterations in mitochondrial membrane potential (MMP), ATP content in galactose media and

extracellular flux analysis did not reveal mitochondrial dysfunction as a mechanism of BA-induced toxicity. Finally, an mtDNA haplogroup-toxicity association study using haplogroups B, H and J was conducted to assess differential toxicity to tolcapone. A significant difference in susceptibility to tolcapone-induced mitochondrial toxicity was detected between haplogroups following 2 hours dosing. However, extended dosing regimens of 24 hours resulted in a reversal in susceptibility to toxicity. Studies of mitochondrial dynamics and biogenesis revealed that there are complex molecular pathways governing mitochondrial protection and susceptibility to toxicity dependent on mtDNA haplogroup. Specifically, differences in mtDNA copy number, which was used as a surrogate marker for biogenesis, was identified to be temporally different amongst the haplogroups.

To conclude, it is likely that idiosyncratic DILI occurs due to a combination of mechanisms in conjunction with personal susceptibility factors. However, failure to employ the correct model can lead to the generation of data that lacks *in vivo* applicability. Following the use of appropriate, physiologically relevant preclinical models, this research identified biliary transporter dysfunction as a mechanism of BA-induced toxicity but not mitochondrial dysfunction. Additionally, HepG2 transmitochondrial cybrids were identified as a novel model for assessing the role of mtDNA variation and its contributions towards idiosyncratic DILI. Ultimately, the use of the most appropriate and physiologically relevant models is likely to improve the predictivity of DILI screening, leading to improvements in drug safety.

## ACKNOWLEDGEMENTS

I would firstly like to thank my supervisors, Dr Amy Chadwick, Dr Parveen Sharma, Professor Kevin Park and Professor Richard Weaver, as well as the Medical Research Council (MRC) and Servier for providing me with the opportunity and funding to undertake this PhD. In particular, I would like to say a special thank you to Amy for your guidance and support. No question was ever too silly and you were always there encouraging me, thank you.

A thank you must also go to Dr Neil Kitteringham and Dr Dammy Olayanju. You're both probably unaware of the impact you had on me, but thank you for encouraging shy, self-doubting, 20 year old me of my abilities. If it hadn't been for your kind words and inspiration, I never would have had the courage to pursue this PhD.

A special thank you must be extended to both past and present members of Team Bioenergetics: Carol, Laleh, Amy, Sammie, Rebecca and Robyn. Each one of you has supported me over the years and helped me grow as a scientist. Carol, thank you for sharing your extensive cell culture wisdom and lab knowledge with me. Your help was immeasurable during the early years of my PhD and I don't know what I would have done without you. Rob and Chris, whilst you weren't in Team Bioenergetics, sharing an office with you for the last year has been so much fun and you made coming into work an enjoyable experience.

Thank you to all of my wonderful friends in both Liverpool and Hatfield for your support during my PhD. Shai, Grace and Christina, thank you for all of the fun times over the last 4 years. I appreciate all of the times you listened to me rant over one too many G&Ts. Pip, thank you for agreeing to all of my holiday demands. Our trips and talks of fabulousness always gave me something to look forward to when times in the lab were tough. Ameze, Mary, Jazz and Tanesha, each of you has helped me in a different way throughout this PhD. You truly are the best friends a girl could ask for! Thank you for being by my side throughout.

It would be impossible to thank my family enough. Mum, Sammy, Granny (BFF) and Grandad, you have all worked so hard to make every want or dream of mine a reality – this work is yours as much as it is mine. Thank you for the monthly care packages of chocolate or the money for cookie dough whenever I was feeling stressed – it really helped. To Chris, the best supporter. Thank you for your constant patience, love and support. Who else would care to learn the difference between a HepG2 and HepaRG cell if they didn't have to?! You. Thank you for taking a genuine interest in my research and always encouraging me.

Most importantly, I'd like to dedicate this thesis to my late Father, Andrew Penman. Whilst I doubt you'd have understood anything in this thesis, I would have loved to read it to you over a drink. I hope I am making you proud. This is all for you.

## PUBLICATIONS

**S.L. Penman**, P. Sharma, H. Aerts, B.K. Park, R.J. Weaver, A.E Chadwick, Differential toxic effects of bile acid mixtures in isolated mitochondria and physiologically relevant HepaRG cells, *Toxicology in Vitro* (2019). <https://doi.org/10.1016/j.tiv.2019.104595>.

**S.L. Penman**, A.S. Carter, A.E. Chadwick, Investigating the importance of individual mitochondrial genotype in susceptibility to drug-induced toxicity, *Biochemical Society of Transactions* (2020). <https://doi.org/10.1042/BST20190233>

**S.L. Penman**, R.L. Jensen, R.T. Kiy, A.E. Chadwick, The mitochondrial paradox, *eLife* (2020). <https://elifesciences.org/articles/59140>

**S.L. Penman**, R.T. Kiy, R.L. Jensen, C. Beoku-Betts, A. Alfirevic, D. Back, S.H. Khoo, A. Owen, M. Pirmohamed, B.K. Park, X. Meng, C.E Goldring, A.E. Chadwick, Safety perspectives on presently considered drugs for the treatment of COVID-19, *British Journal of Pharmacology* (2020). <https://doi.org/10.1111/bph.15204>

C.E. Jolly, O. Douglas, L. Kamalian, R.E. Jenkins, A.J. Beckett, **S.L. Penman**, D.P. Williams, M. Monshouwer, D. Simic, J. Snoeys, B.K. Park, A.E. Chadwick, The utility of a differentiated preclinical liver model, HepaRG cells, in investigating delayed toxicity via inhibition of mitochondria-replication induced by fialuridine, *Toxicology and Applied Pharmacology* (2020). <https://doi.org/10.1016/j.taap.2020.115163>

J.C Waddington, S. Ali, **S.L. Penman**, P. Whitaker, J. Hamlett, A.E. Chadwick, D.J. Naisbitt, B.K. Park, X. Meng, Cell membrane transporters facilitate the accumulation of hepatocellular flucloxacillin protein adducts: Implication in flucloxacillin-induced liver injury, *Chemical Research in Toxicology* (2020). <https://doi.org/10.1021/acs.chemrestox.0c00400>

S.W. Jones, **S.L. Penman**, N.S. French, B.K. Park, A.E. Chadwick,  
Investigating Dihydroorotate Dehydrogenase Inhibitor Mediated  
Mitochondrial Dysfunction in Hepatic in vitro Models, *Toxicology in  
Vitro* (2020). *Manuscript under review*

## ABBREVIATIONS

ANT	Adenine nucleotide translocase
ADP	Adenosine diphosphate
ATP	Adenosine triphosphate
ADR	Adverse drug reactions
$\alpha$	Alpha-
ASBT	Apical sodium-dependent bile acid transporter
AIF	Apoptosome-inducing factor
ALR	ATP-linked respiration
BR	Basal respiration
Bax	B-cell lymphoma 2-associated X protein
$\beta$	Beta-
BCA	Bicinchoninic acid
BA	Bile acid
BSEP	Bile salt export pump
BSA	Bovine serum albumin
FCCP	carbonyl cyanide-4- trifluoromethoxyphenylhydrazone
COMT	Catechol-O-methyl transferase
CMFDA	Cell Tracker 5- chloromethylfluorescein diacetate
CDCA	Chenodeoxycholic acid
CA	Cholic acid
CAR	Constitutive androstane receptor
CBB	Coomassie Brilliant Blue
CK	Creatine kinase
CypD	Cyclophilin D
Cyt b	Cytochrome b
COX	Cytochrome c oxidase
CYP	Cytochrome P450
$\Delta/\delta$	Delta-
AKR1D1	$\Delta^4$ -3-oxosteroid 5 $\beta$ -reductase
DCA	Deoxycholic acid
DNA	Deoxyribonucleic acid
FADH <sub>2</sub>	Dihydroflavin adenine dinucleotide

DMSO	Dimethyl sulfoxide
DIC	Drug-induced cholestasis
DILI	Drug-induced liver injury
DIMT	Drug-induced mitochondrial toxicity
DMEM	Dulbecco's Modified Eagle Medium
ETC	Electron transport chain
ER	Endoplasmic reticulum
ECL	Enhanced chemiluminescence
$\epsilon$	Epsilon
EGTA	Ethylene-bis(oxyethylenitrilo)tetraacetic acid
EDTA	Ethylenediaminetetraacetic acid
ECACC	European Collection of Cell Cultures
ECAR	Extracellular acidification rate
XFe96	Extracellular flux analyser
ECM	Extracellular matrix
FXR	Farnesoid x receptor
FBS	Fetal bovine serum
FAD	Flavin adenine dinucleotide
FMN	Flavin mononucleotide
FDA	Food and Drug Administration
$\gamma$	Gamma
GSMF	Glutathione-methylfluorescein
GST	Glutathione S-transferase
GCA	Glycocholic acid
HBSS	Hank's Balanced Salt Solution
Hsp27	Heat shock protein 27
Hsp60	Heat shock protein 60
Hsp70	Heat shock protein 70
HK	Hexokinase
HRP	Horseradish peroxidase
HLA	Human leukocyte antigen
IMVs	Inner membrane vesicles
Fe-S	Iron-sulphur
LDH	Lactate dehydrogenase

LHON	Leber's hereditary optic neuropathy
LCA	Lithocholic acid
Lamp2	Lysosome-associated membrane protein 2
MR	Maximum respiration
mRNA	Messenger Ribonucleic acid
μ-	Micro-
m-	Milli-
mtDAMPs	Mitochondria specific damage associated molecular patterns
mtDNA	Mitochondrial DNA
MMP	Mitochondrial membrane potential
MOMP	Mitochondrial outer membrane permeabilisation
MPT	Mitochondrial permeability transition
POLRMT	Mitochondrial RNA polymerase
TFAM	Mitochondrial transcription factor A
M	Molar
MRCA	Most recent common ancestor
MRP	Multidrug resistance-associated proteins
MDR	Multidrug resistance protein
ND	NADH dehydrogenase
NHS	National Health Services
NGS	Next generation sequencing
NADH	Nicotinamide adenine dinucleotide
TMPD	N,N,N',N'-tetramethyl-p-phenylenediamine
NASH	Non-alcoholic steatohepatitis
NMR	Non-mitochondrial respiration
NRF	Nuclear receptor factors
NRTI	Nucleoside reverse transcriptase inhibitor
OATP	Organic anion-transporting polypeptide
OST	Organic solute and steroid transporter
O <sub>H</sub>	Origins of replication of the heavy strand
O <sub>L</sub>	Origins of replication of the light strand
OXPPOS	Oxidative phosphorylation
OCR	Oxygen consumption rate
PFA	Paraformaldehyde

PBR	Peripheral benzodiazepine receptor
Pgp	Permeability glycoprotein
PMP70	peroxisomal membrane protein 70
PPAR	Peroxisome proliferator-activated receptor
PGC1- $\alpha$	Peroxisome proliferator-activated receptor gamma coactivator 1-alpha
PBS	Phosphate buffered saline
PI3K	Phosphoinositide 3-kinase
PEG	Polyethylene glycol
PCR	Polymerase chain reaction
PVA	Polyvinyl alcohol
PXR	Pregnane X receptor
PHH	Primary human hepatocytes
PFIC	Progressive familial intrahepatic cholestasis
AKT	Protein kinase B
PL	Proton leak
PCC	Pump controlled cell rupture
RIPA	Radio-Immunoprecipitation Assay
ROS	Reactive oxygen species
RT-PCR	Real-time polymerase chain reaction
rPFO	Recombinant perfringolysin O
REDOX	Reduction–oxidation reaction
Rh123	Rhodamine 123
$\rho 0$	Rho zero cells
SimPops™	Simulated human population
SNPs	Single nucleotide polymorphisms
NTCP	Sodium-dependent taurocholate co-transporting polypeptide
SDS	Sodium dodecyl sulphate
SRC	Spare respiratory capacity
TCDCA	Taurochenodeoxycholic acid
TCA	Taurocholic acid
TMRM	Tetramethylrhodamine methyl ester
tRNA	Transfer RNA
TBS-T	Tris Buffered Saline-Tween
ULA	Ultra-low attachment

UGT	Uridine diphosphate glucuronosyltransferase
UDCA	Ursodeoxycholic acid
VDAC	Voltage-dependent anion channel
2D	2-dimension
TES	2-[(2-Hydroxy-1,1-bis(hydroxymethyl)ethyl)amino]ethanesulfonic acid
3D	3-dimension
HSD3B7	3 $\beta$ -hydroxysteroid dehydrogenase type 7
MOPS	3-(N-morpholino)propanesulfonic acid
HEPES	4-(2-hydroxyethyl)-1-piperazineethanesulfonic acid
JC-1	5,5',6,6'-tetrachloro-1,1',3,3'-tetraethyl benzimidazol carbocyanine iodide

# **Chapter 1**

## **General Introduction**

**CONTENTS**

1.1	DRUG-INDUCED LIVER INJURY	3
1.1.1	Human Liver Physiology	4
1.1.2	Drug Metabolism and Biliary Transporters	5
1.1.3	Preclinical Hepatic Models for the Assessment of Drug-Induced Liver Injury	9
1.1.4	Common Assays used to Assess Drug-Induced Liver Injury	13
1.2	BILE	16
1.2.1	Bile Acid Synthesis	17
1.2.2	Bile Acid Modification	20
1.2.3	Bile Acid Regulation	21
1.2.3	Bile Acid-Induced Toxicity	21
1.3	MITOCHONDRIAL STRUCTURE AND FUNCTION	22
1.3.1	Mitochondrial Structure	22
1.3.2	Oxidative Phosphorylation	24
1.3.3	Additional Features of the Mitochondria	28
1.3.4	Mitochondrial Stress Management	29
1.4	THE MITOCHONDRIAL GENOME	30
1.4.1	Mitochondrial DNA Structure	30
1.4.2	Mitochondrial Heteroplasmy	32
1.4.3	Mitochondrial Haplogroups	33
1.5	DRUG-INDUCED MITOCHONDRIAL TOXICITY	34
1.5.1	Models for the Assessment of Drug-Induced Mitochondrial Toxicity	35
1.6	THESIS AIMS AND OBJECTIVES	39

## 1.1 DRUG-INDUCED LIVER INJURY

Adverse drug reactions (ADRs) are a major burden to the National Health Services (NHS), accounting for 6.5 % of hospital admissions in 2004 (Pirmohamed et al., 2004). It is estimated that ADRs cost the NHS £466 million annually due to them being the 7<sup>th</sup> leading cause of death (Pirmohamed et al., 2004; Wester et al., 2008). However, ADRs are not just a hospital problem; they represent a major pharmaceutical concern. In 2015, it was estimated that the cost of getting a drug from bench to market cost \$2.6 billion (DiMasi et al., 2015). During 1975 – 1999, of the 548 new drugs that were approved, 10.2 % acquired black box warnings or were withdrawn from the market due to ADRs (Lasser et al., 2002). For this reason, there is a great pharmaceutical concern as millions of pounds and time could be wasted.

Drug-induced liver injury (DILI), alongside drug-induced cardiac toxicity, are recognised as the current leading causes of drug attrition and withdrawal from the market (Stevens and Baker, 2009). Whilst clinical reports of DILI are rare at 1 in 10,000 to 1 in 100,000 patients, the consequences of its acquisition can be severe (Larrey, 2002). In the USA, more than 50 % of acute liver failures are attributed to DILI and shockingly, 75 % of these cases result in liver transplantation or death (Lee, 2003; Ostapowicz et al., 2002). The majority of cases of adverse liver reactions are idiosyncratic, meaning they are not predictable from the known pharmacology of the drug, have delayed onset, have no clear dose-dependent relationship and are often life threatening (Utrecht and Naisbitt, 2013).

DILI can present itself in many pathological forms. Various clinicopathological presentations of DILI include: acute hepatic necrosis, acute liver failure, bland cholestasis, cirrhosis and nodular regeneration (Tujios and Fontana, 2011). One of the most common forms of DILI is cholestasis, occurring in 20 – 40 % of reported cases (Sharanek et al., 2016).

A variety of *in vitro* assays have been developed to assess the ability of a compound to cause DILI however, it is recognised that the toxicity of DILI is multi-mechanistic, which has contributed to the difficulty in detecting DILI preclinically (Tujios and Fontana, 2011). Additionally, failure to employ appropriate models for specific mechanisms of toxicity can result in toxicity being undetected, missed or exaggerated during preclinical screening. Therefore, it is essential that the appropriateness of models are evaluated prior to drug screening in order to deliver results with *in vivo* relevance and predictive value.

### 1.1.1 Human Liver Physiology

The liver is a complex organ and so any models used to examine the effects of drugs on hepatic function must consider these intricacies. In order to do this, models need to be based upon a more reproducible physiology of the liver.

The human liver is the largest organ within the body accounting for 2 – 3 % of a person's average body weight. It is situated in the upper right quadrant of the abdomen and is protected by the rib cages. The liver receives a large blood supply with 25 % coming from the hepatic artery, which transports blood from the aorta, and 75 % coming from the portal vein, which supplies blood from the gastrointestinal tract, gallbladder and pancreas (Abdel-Misih and Bloomston, 2010). The liver is divided into hexagonal functional units called liver lobules, which are composed of hepatocytes and sinusoids (figure 1.1) (Jacobs et al., 2010).

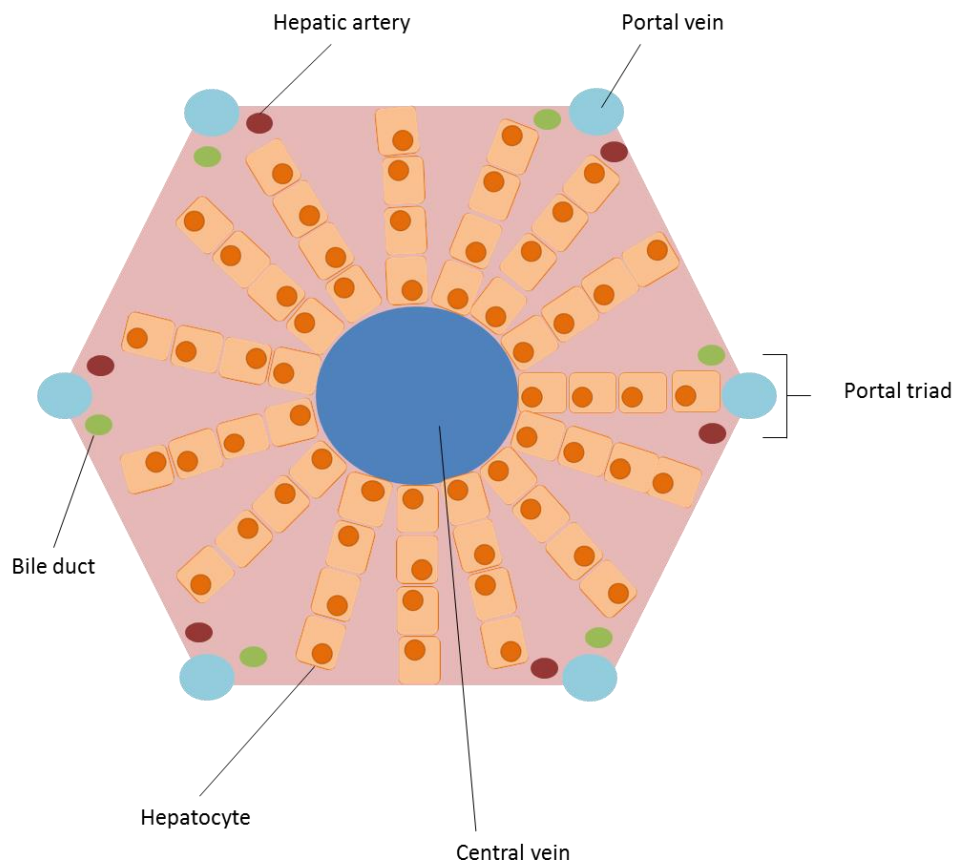


**Figure 1.1: Example of a liver lobule.** The liver lobule is composed of hepatocytes surrounding a central vein and the portal triad which is situated at the periphery of the lobule.

The portal triad is a component of the liver lobule and includes the hepatic vein, hepatic artery, bile duct, lymphatic vessels and the vagus nerve. The main cells within the liver lobules are hepatocytes, which closely neighbour each other and can be seen as long cords surrounding a central vein. The cords of hepatocytes spread across the lobule and face sinusoids on either side (figure 1.2) (Kietzmann, 2017). Neighbouring hepatocytes form bile canaliculi at their cell-cell contact domains (Gissen and Arias, 2015). Hepatocytes make bile and it is secreted into the bile canaliculi where it passes through the biliary tract to either the gallbladder or the duodenum (Boyer, 2013). Sinusoidal cells make up the remainder of the liver lobule and include Kupffer cells, stellate cells and endothelial cells which line the sinusoids (Jacobs et al., 2010; Kietzmann, 2017). There is a small space between the apical membrane of the hepatocytes and the endothelial cells lining the sinusoids called the Space of Disse. The Space of Disse is important in the absorption of molecules into hepatocytes and is where stellate cells reside for storage of fat and vitamin A (Kietzmann, 2017).

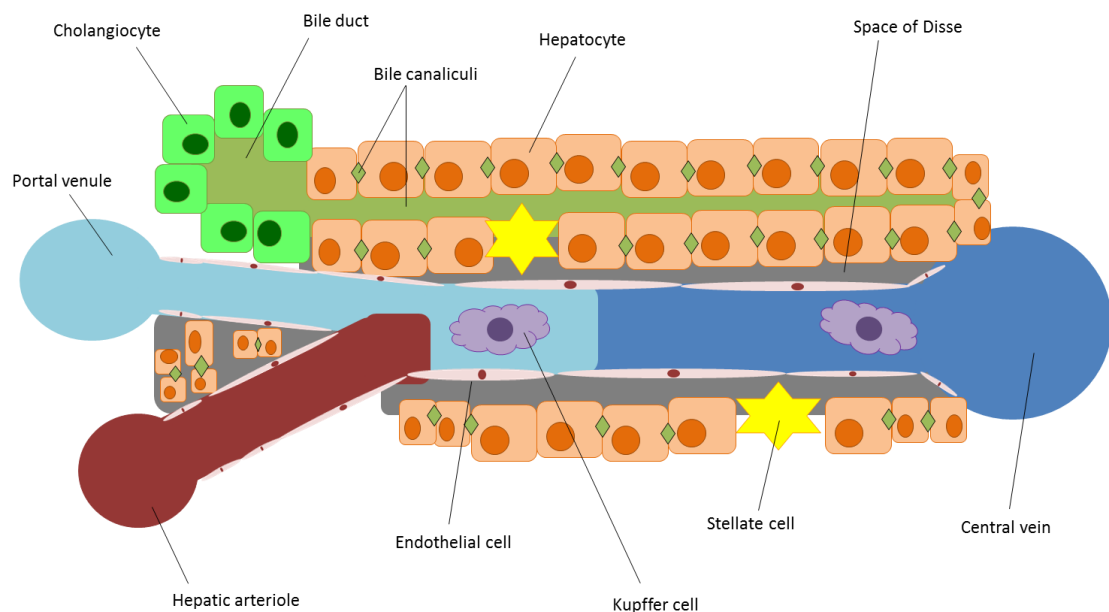


**Figure 1.2: Illustration of the cells and sinusoids within the liver.** The liver is composed of multiple cell types but the most prominent are the hepatocytes, which are the parenchymal cells of the liver.

### 1.1.2 Drug Metabolism and Biliary Transporters

The most abundant cells within the human liver are hepatocytes, which are responsible for the function of the liver and form 85 % of the liver's mass (Perkins et al., 2006). Hepatocytes

like to grow close together, which aids in the ability of hepatocytes to polarise (Gissen and Arias, 2015). Polarised hepatocytes express a basolateral (sinusoidal) membrane and an apical (canalicular) membrane (Müsch, 2014). The ability of adjacent cells to polarise results in a large branched bile canaliculus network that spreads across the liver (Müsch, 2014).

One of the main roles of the liver is the biotransformation of lipophilic compounds into hydrophilic derivatives for drug metabolism (Park et al., 2005). Due to this, hepatocytes express enzymes involved in phase 1 and phase 2 metabolism (Kietzmann, 2017). Drug metabolism can occur in three phases which include: phase 1 (bioactivation/functionalisation) via the cytochrome P450 (CYP) family of enzymes; phase 2 (conjugation/detoxification) and phase 3 (transport/excretion) (Pachkoria et al., 2007). In order for drugs and xenobiotics to reach their target they usually have to cross many membranes. For this reason, drugs and xenobiotics tend to be non-polar and lipophilic. In order for drugs to be excreted into the bile or urine they must be converted to more hydrophilic compounds. It is the job of the CYP family of enzymes to incorporate or unmask functional groups on xenobiotics to make them more polar species (Porter and Coon, 1991). Occasionally, compounds can undergo biotransformation during phase 1 metabolism, which leads to the formation of toxic metabolites (Park et al., 2005). The products of phase 1 metabolism are further manipulated to increase their hydrophilicity and excretion by phase 2 metabolism (Jancova et al., 2010). Various phase 2 reactions include sulfation, glucuronidation, glutathione conjugation, methylation, acetylation and amino acid conjugation (Jancova et al., 2010; Zamek-Gliszczyński et al., 2006). The conjugated compounds formed from phase 2 metabolism are often too hydrophilic to passively diffuse across the cell membrane and will therefore be removed from hepatocytes via transporters (Zamek-Gliszczyński et al., 2006).

Polarised hepatocytes express influx and efflux transporters on their basolateral and canalicular membranes, which facilitates in a two-way flow system (figure 1.3). Transporters situated at the sinusoidal membrane aid in the uptake and secretion of sinusoidal blood molecules, drugs, bile acids (BAs) and xenobiotics, whereas canalicular transporters enable the efflux of BAs from hepatocytes into the bile canaliculi (Treyer and Müsch, 2013). The ability of hepatocytes to polarise is important for the overall function of the liver and defects in polarisation can result in disease (Gissen and Arias, 2015). The majority of BA and bile salt uptake is facilitated by the transporter sodium-dependent taurocholate co-transporting polypeptide (NTCP) (Meier and Stieger, 2002). During bile salt influx, two Na<sup>+</sup> molecules are

exchanged with one taurocholate molecule (Trauner and Boyer, 2003). The  $\text{Na}^+$  gradient is maintained by the  $\text{Na}^+ \text{K}^+$ -ATPase as well as the negative intracellular potential (Hagenbuch and Dawson, 2004). NTCP is able to transport all bile salts across the basolateral membrane but has highest affinity for the taurine-conjugated bile salts taurocholic acid (TCA) and taurochenodeoxycholic acid (TCDCA) (Hagenbuch and Dawson, 2004). Sodium-independent hepatocyte uptake of BAs at the basolateral membrane is mediated by different members of the superfamily of organic anion-transporting polypeptides (OATPs) (Meier and Stieger, 2002). OATPs can carry a range of substrates including conjugated and unconjugated BAs, bilirubin, drugs and a variety of steroids however, BA uptake is less significant than that by the NTCP (Trauner and Boyer, 2003). The uptake of these substrates is mediated by three members of the OATP family, which includes OATP1, 2 and 4 (Trauner and Boyer, 2003). OATP3 is expressed in the small intestine but not the liver and so does not have any function in BA uptake within hepatocytes (Walters et al., 2000). The adenosine triphosphate (ATP) - dependent transporter family, multidrug resistance-associated proteins (MRPs), are multi-specific efflux transporters for organic anions located at both the basolateral and canalicular membranes of hepatocytes (Homolya et al., 2003). In hepatocytes MRP1, 3, 4, 5 and 6 are expressed on the basolateral membrane and are able to transport bile salts, nucleosides and drugs into the blood (Borst et al., 2000). Additionally, the organic solute and steroid transporters -alpha and -beta ( $\text{OST}\alpha/\beta$ ) are capable of transporting BAs and conjugated steroids across the basolateral membrane into the blood (Ballatori et al.). Under physiological conditions, BA efflux via the basolateral membrane is negligible, however during cholestasis the expression of  $\text{OST}\alpha$ ,  $\text{OST}\beta$ , MRP3 and MRP4 are upregulated to act as a compensatory mechanism (Boyer et al., 2006; Trauner and Boyer, 2003). This adaptive response helps prevent the toxic accumulation of bile salts within the hepatocytes. However, drugs or genetic polymorphisms resulting in defects in MRP3 or 4 can worsen the problem and lead to a greater build-up of BAs within hepatocytes (Yang et al., 2013).

The transport of bile salts across the canalicular membrane is the rate limiting step in the formation of bile (Trauner and Boyer, 2003). The main transporter responsible for the efflux of bile salts across the canalicular membrane is the ATP-dependent transporter, bile salt export pump (BSEP) (Kullak-Ublick et al., 2000). BSEP has high affinity for TCA, glycocholic acid (GCA), chenodeoxycholic acid (CDCA) and deoxycholic acid (DCA) (Byrne et al., 2002). The genetic condition, progressive familial intrahepatic cholestasis (PFIC), refers to a group of autosomal recessive conditions where there are defects in the biliary transporters, which leads to disruptions in bile formation (Jacquemin, 2012). In patients suffering from PFIC-2,

there is a mutation in the gene for BSEP, which results in its absence from the canalicular membrane and causes extremely low levels of bile salts, thus highlighting its importance in bile salt transport (Strautnieks et al., 1998). A variety of drugs with cholestatic liabilities are known to directly inhibit BSEP (Stieger et al., 2000). This inhibition is usually cis-inhibition however certain inhibitors such as; progesterone and estradiol 17 $\beta$ -glucuronide, are secreted into the bile canaliculi by MRP2 and then trans-inhibit BSEP (Stieger et al., 2000). The anti-diabetic drug, troglitazone, causes cholestasis by inhibiting BSEP, however its major metabolite, troglitazone sulphate, is known to inhibit MRP4 (Yang et al., 2013). Experimental work has shown that drugs which inhibit both BSEP and MRP4 have an enhanced risk of causing cholestasis (Köck et al., 2014). MRP2 is another ATP-dependent transporter located on the canalicular membrane of hepatocytes and is responsible for transporting glucuronidated and sulphated BAs into the bile canaliculi (Akita et al., 2001). MRP2 is the only member of the multidrug resistance-associated protein family localised on the canalicular membrane and serves an important role in regulating bile salt-independent flow via the excretion of glutathione (Pauli-Magnus and Meier, 2006). In addition to transporting bile salts, MRP2 transports a wide variety of substrates including many cancer chemotherapeutics, antibiotics, leukotrienes, conjugated bilirubin and heavy metals (Gerk and Vore, 2002). During cholestasis, the levels of MRP2 are drastically decreased (Kullak-Ublick et al., 2000). Multidrug resistance protein-3 (MDR3) is an ATP-dependent floppase present at the canalicular membrane that translocates phosphatidylcholine from the hepatocytes into the bile canaliculi (van Helvoort et al., 1996). Phosphatidylcholine is essential for the physiological transport of BAs into the bile canaliculi as it forms mixed micelles with cholesterol and BAs, thus preventing damage to cholangiocytes via the detergent actions of BAs (Stapelbroek et al., 2010). A genetic mutation in MDR3 results in the genetic condition PFIC3 that is characterised by fibrosis, bile duct proliferation and recurrent gallstones due to cholesterol saturation (de Vree et al., 1998; Stapelbroek et al., 2010). Permeability glycoprotein (Pgp) is another canalicular transporter that aids in the excretion of bile salts, organic cations and a wide variety of drugs (Pauli-Magnus and Meier, 2006). The excretion of bile salts via Pgp is less efficient than that of BSEP with studies showing that Pgp has a five times lower affinity for bile salts than BSEP (Lam et al., 2005). However, when the liver is in a state of cholestatic injury, the levels of Pgp are upregulated in order to aid in the expulsion of accumulating bile salts in the hepatocytes (Schrenk et al., 1993).

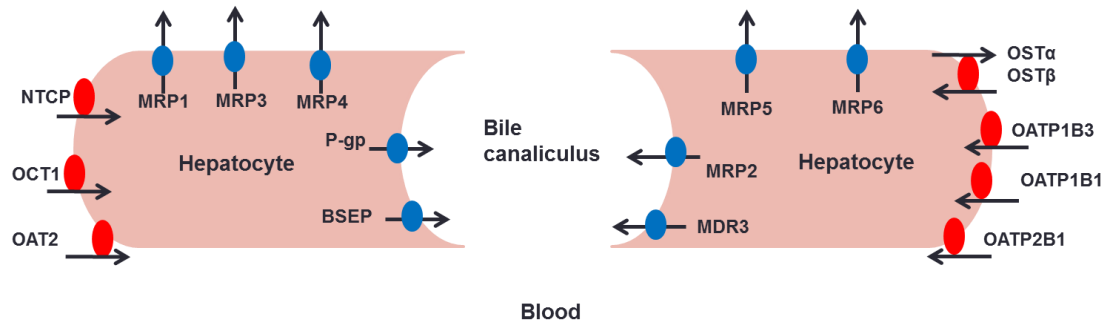


**Figure 1.3 Example of the biliary transporters within hepatocytes.** Uptake transporters (red) are located at the basolateral membrane and are responsible for the influx of drugs, xenobiotics and BAs from the blood into the hepatocytes. Efflux transporters (blue) are located at both the basolateral and canalicular membrane. Figure adapted from (Pauli-Magnus and Meier, 2006).

### 1.1.3 Preclinical Hepatic Models for the Assessment of Drug-Induced Liver Injury

#### 1.1.3.1 Introduction

There are a multitude of models that can be used for the preclinical screening of DILI. As such, a certain model may be better suited for detecting specific mechanisms of toxicity associated with DIL over others (Atienzar et al., 2016). Prior to conducting *in vitro* assays, limitations of the model should be evaluated to ensure that the preclinical question can be answered based upon the physiology of the model. For example, drug-induced cholestasis (DIC) occurs when there is impairment in the flow of bile from the liver to the duodenum, which occurs due to constraints on canalicular transporters, thus preventing BA efflux from hepatocytes (Woolbright and Jaeschke, 2015). It is therefore essential that models used to study DIC have functional biliary transporters in order to recapitulate the correct pathophysiology of the insult. Similarly, if the toxicity of a drug is elicited by its metabolite, the appropriate model would be one with CYP enzymes and metabolic capabilities. Failure to employ appropriate models can lead to the generation of results that lack *in vivo* relevance and predictive value.

Primary human hepatocytes (PHH) isolated from human tissue biopsies can be cultured in 2-dimension (2D) or 3-dimension (3D) and are recognised as the 'gold standard' cells to use in DILI studies as they closely resemble normal hepatocytes found within the human body (Atienzar et al., 2016). Functioning PHH show phase 1 and 2 metabolic enzyme activity, glucose metabolism, urea formation and albumin production as well as other hepatocyte indicators when cultured appropriately (Knobeloch et al., 2012). However, there are some

issues associated with PHH in toxicology studies. The availability of PHH from liver resections is not substantial for high-throughput studies and the quality of the hepatocytes is dependent on the lifestyle of the donor and any pathologies they may have had (Godoy et al., 2013). Additionally, there is a high degree of donor variation in regards to gene expression and function, which impacts the reproducibility and predictability of PHH in detecting hepatotoxins (Atienzar et al., 2016). PHH are limited to acute drug exposure studies as after 72 hours they undergo dedifferentiation, which sees their hepatocyte features such as function, morphology and structure lost, thus reducing their physiological relevance (Godoy et al., 2013; Heslop et al., 2017).

An alternative to PHH is the use of immortalised hepatic carcinoma cell lines. Typical cell lines used in DILI toxicology studies are HepG2 and HepaRG cells, which alleviate some of the limitations associated with PHH but also have their own restrictions (Atienzar et al., 2016)

#### *1.1.3.2 HepG2 Cells*

HepG2 cells are the most widely used hepatic cell line for toxicology studies due to their stable phenotype and high availability (Donato et al., 2015). The tumour-derived HepG2 cells were first established in 1975 from a tumour liver biopsy of a 15 year old Caucasian male from Argentina with differentiated hepatocellular carcinoma (Aden et al., 1979). HepG2 cells are non-tumorigenic cells with a high proliferation rate and have an epithelial morphology (Donato et al., 2015; Mersch-Sundermann et al., 2004). Analysis of the supernatant fluid of HepG2 cells revealed that 17 out of 20 characteristic proteins of PHH were conserved in HepG2 cells (Knowles et al., 1980). Abundant levels of some of these liver proteins were albumin, hepatocyte nuclear factors and conjugating enzymes (Choi et al., 2015). Functional characterisation of HepG2 cells revealed that certain metabolic enzymes were lacking or undetectable with differences between HepG2 cells and PHH occurring due to transporter and enzyme differences (Donato et al., 2015). When grown in monolayer, HepG2 cells do not polarise and thus express non-functioning transporters however, manipulation of cell culture conditions and growth of HepG2 cells as 3D spheroids leads to the formation of functional bile canaliculi (Miyamoto et al., 2015). Proteomic analysis revealed that there is a low expression of some CYP450 enzymes and phase 2 metabolism enzymes such as glutathione S-transferase (GST) and uridine diphosphate glucuronosyltransferase (UGT) proteins (Sison-Young et al., 2015). Messenger ribonucleic acid (mRNA) analysis via polymerase chain reaction (PCR) revealed that HepG2 cells have a low expression of the efflux transporters P-

gp and BSEP and low expression of the influx transporters OATP1B1 and OCT1 (Donato et al., 2015; Louisa et al., 2016).

Despite these differences, HepG2 cells are widely used as preclinical models for pharmacology and toxicology studies over the 'gold standard' PHH. HepG2 cells are useful for studying toxicity of parent drugs on the liver but due to them having low levels of CYP enzymes they are unable to test the toxicity of drug metabolites (Gerets et al., 2012b). Due to HepG2 cells being cancer-derived, their availability is unlimited, which poses benefits over PHH whose supply is scarce. HepG2 cells have an altered bioenergetic phenotype compared to PHH (Kamalian et al., 2015). Due to their tumorigenic origin, they have the ability to use glycolysis alongside oxidative phosphorylation (OXPHOS) in order to increase their ATP supply and grow in anaerobic conditions, thus allowing investigations of mitochondrial dysfunction to be conducted (Marroquin et al., 2007).

#### *1.1.3.3 HepaRG Cells*

The hepatoma-derived HepaRG cells were first obtained from a differentiated liver tumour of a female hepatocarcinoma patient who was also suffering from chronic hepatitis C (Gripon et al., 2002). HepaRG cells are unique in that they are an immortalised, bipotent, progenitor cell line capable of differentiating into hepatocytes or primitive biliary-like cells (Cerec et al., 2007; Guillouzo et al., 2007). On plating, undifferentiated HepaRG cells spend 7 days in growth media during which they proliferate and grow until they reach confluency (Marion et al., 2010). HepaRG cells spend days 7-14 in growth media, however enter a stationary phase where they do not proliferate but start to undergo differentiation into either hepatocytes or primitive biliary-like cells (Marion et al., 2010). At day 14, HepaRG cells are cultured in differentiation media which contains 1.7 % dimethyl sulfoxide (DMSO) and resultantly forces the cells to commit to either the hepatocyte or biliary-like cell lineage (Cerec et al., 2007; Guillouzo et al., 2007). Interestingly, HepaRG cells possess the unique ability that they are able to undergo transdifferentiation (Cerec et al., 2007). If HepaRG cells are trypsinised and re-seeded at a low density prior to culture in differentiation media, they have the ability to de-differentiate and regain progenitor properties (figure 1.4) (Cerec et al., 2007).

Differentiated HepaRG cells have functioning bile canaliculi and similar levels of CYP enzymes and other proteins involved in drug metabolism and excretion as PHH (Aninat et al., 2006; Cerec et al., 2007). A comparison of the mRNA levels of CYP enzymes in HepG2 and HepaRG

cells revealed that the only phase 1 enzyme with greater quantities in HepG2 cells was glutathione transferase M3 (Gerets et al., 2012b). The enzyme CYP3A4 is responsible for the metabolism of a wide variety of drugs and was found to be 19.1 x greater in HepaRG cells than HepG2 cells (Gripon et al., 2002). Additionally, proteomic analysis revealed that the levels of CYP3A4 were greater in HepaRG cells when compared to cryopreserved PHH (Sison-Young et al., 2015). The enzyme CYP4B1 was found to be significantly higher in HepaRG cells than PHH but all other phase 1 enzymes were marginally decreased (Gerets et al., 2012b). A variety of phase 2 enzymes such as GST and some UGTs were expressed at equivalent levels in HepaRG cells as PHH (Sison-Young et al., 2015). Hepatocytes express a variety of influx and efflux transporters on their basolateral and canalicular membrane, which are responsible for controlling the transport of BAs, drugs and xenobiotics (Faber et al., 2003). HepaRG cells have a higher expression of liver transporters compared with HepG2 cells however, the levels are slightly lower when compared with PHH (Sison-Young et al., 2015). Conversely, proteomic analysis revealed that the levels of the transporters MRP – 1, 3 and Pgp, were greater in HepaRG cells than PHH (Sison-Young et al., 2015). HepaRG cells express the key nuclear receptors, pregnane X receptor (PXR), peroxisome proliferator-activated receptor (PPAR), farnesoid x receptor (FXR) and constitutive androstane receptor (CAR) (Aninat et al., 2006; Brobst and L. Staudinger, 2017). Consequently, due to the similar features mentioned above between HepaRG cells and PHH, HepaRG cells have been acknowledged as a suitable alternative to the “gold standard” PHH in toxicology studies.

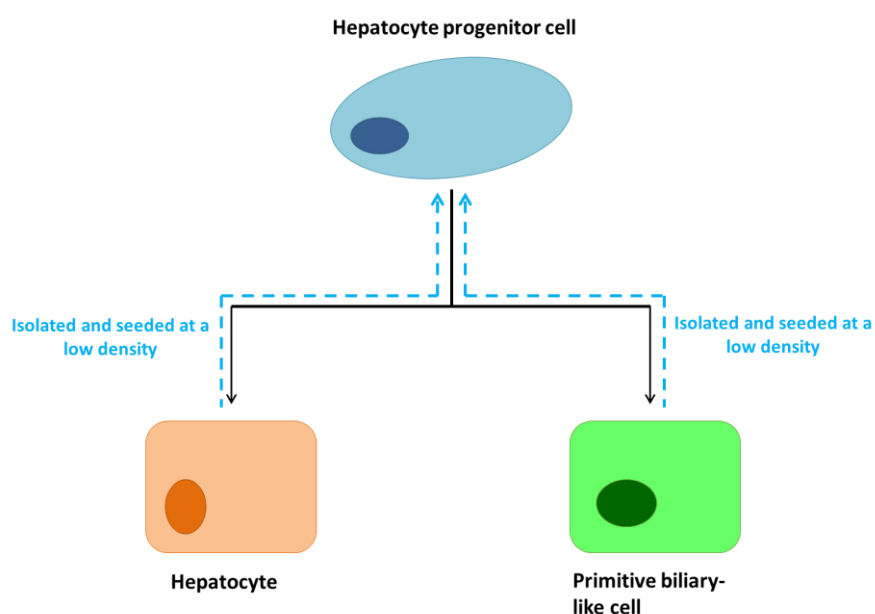


**Figure 1.4: Differentiation and transdifferentiation of HepaRG cells.** The HepaRG progenitor cell is grown to confluency in growth media for two weeks. After this, the presence of 1.7 % DMSO in the differentiation media forces the hepatocyte progenitor cell to commit to differentiate into either

hepatocytes or primitive biliary-like cells. If the hepatocytes and primitive biliary-like cells are isolated, purified and seeded at a low-density, they can undergo transdifferentiation and repeat the differentiation process.

#### 1.1.4 Common Assays used to Assess Drug-Induced Liver Injury

Whilst mitochondrial toxicity and biliary transporter alterations are recognised as major mechanisms of hepatotoxicity and will be assessed in this thesis, advancements in the field have identified multiple *in vitro* assays for the screening of DILI (table 1.1) (Aleo et al., 2014; Kenna and Uetrecht, 2018). Due to the multi-mechanistic toxicity of DILI, no single *in vitro* assay appears to have greater predictive value to a clinical manifestation of toxicity than the other (Atienzar et al., 2016; Kenna and Uetrecht, 2018). Nonetheless, predictivity can be increased by conducting the assays in the most appropriate preclinical models.

**Table 1.1: Common parameters assessed by *in vitro* assays during DILI studies.**

Source	Common <i>in vitro</i> assays for DILI studies
(Haugland, 1996; O'Brien et al., 2006).	<b>New deoxyribonucleic acid (DNA) synthesis:</b> In order to establish the effect of a test compound on cell division, DNA synthesis can be measured by the incorporation of the radioactive nucleoside <sup>3</sup> H-thymidine into new strands of DNA during mitosis. A liquid scintillator is used to detect new DNA synthesis from cells due to the integration of the radioactive nucleoside in DNA.
(Lin and Goodell, 2011; Persson et al., 2013).	<b>Nuclear area:</b> Hoechst 33342 is a cell permeable fluorescent dye that binds to adenine-thymine region in nuclear DNA. Hoechst 33342 is excited by ultraviolet light at around 350 nm and emits blue fluorescent light around an emission spectrum of 460 nm. In microscopic studies, Hoechst 33342 staining can be used to determine nuclear number and measure nuclear area.
(Colombo et al., 1965; O'Brien et al., 2006).	<b>Protein synthesis:</b> Methionine is an essential amino acid during protein translation. New protein synthesis can be measured over time by the pulse-incorporation of the radioactive nucleoside <sup>4</sup> C-methionine into new strands of protein during amino acid assembly. Liquid scintillation is used to detect protein synthesis due to the incorporation of the radioactive amino acid in protein.
(Nair et al., 2011; O'Brien et al., 2006).	<b>Intracellular calcium levels:</b> Fluo-4AM is a cell permeable, green, fluorescent dye that binds to intracellular calcium. Fluo-4AM is excited by ultraviolet light at around 488 nm and emits light on binding to calcium. Fluo-4AM can be used in microscopy, flow cytometry and

---

plate-based assays to determine intracellular calcium levels as the fluorescent signal is proportional calcium binding.

(Rice et al., 1986).	<b>Glutathione depletion:</b> Monochlorobimane is a fluorescent probe used for quantification of glutathione levels. Monochlorobimane is non-fluorescent until bound to glutathione. Kinetic analysis of fluorescent detection permits determination of glutathione levels as the two are proportional.
(Lorico et al., 1986; McCord and Fridovich, 1969).	<b>Superoxide secretion:</b> Cytochrome c can act as a scavenger molecule and react with superoxides to produce ferrocytochrome c which can be spectrophotometrically detected at 550 nm.
(Gurtu et al., 1997).	<b>Caspase-3 activity:</b> The peptide sequence Aspartic acid-Glutamic acid-Valine-Aspartic acid-Glycine DEVD is tagged with the chromophore p-nitroaniline. Caspase-3 protease activity is assessed by the spectrophotometric detection of the free p-nitroaniline. Comparison of the difference in absorbance between test compounds and a control determines a fold change in caspase-3 activity.
(Byrne et al.; Gerloff et al., 1998).	<b>BSEP activity in membrane vesicle:</b> Baculoviruses containing BSEP cDNA are generated. Vesicles are incubated with [ <sup>3</sup> H]-taurocholate in the presence and absence of ATP and the test compound for 30 seconds. BSEP inhibition by test compounds is measured by scintillation counting
(Persson et al., 2013; Zuliani et al., 2003)	<b>Membrane integrity:</b> TOTO-3 is a cell impermeable dimeric cyanine acid dye which has a high affinity for nucleic acids. Unbound TOTO-3 exhibits weak fluorescence however on binding to DNA and RNA this fluorescence increases. TOTO-3 is excited at 633 nm and emits light around 660 nm. Cells with compromised membrane integrity such as necrotic or late apoptotic cells will exhibit high TOTO-3 binding.
(Crouch et al., 1993; Kamalian et al., 2015; Nachlas et al., 1960).	<b>Cell viability:</b> Non-viable cells are unable to synthesise ATP and during injury release lactate dehydrogenase (LDH) as a biomarker of damage. Therefore, combined results from ATP and LDH assays provide information of cell viability. ATP measurements are based on a luminescent assay in which luciferin is catalysed by luciferase to oxyluciferin and luminescent light. The luminescent signal is proportional to the amount of ATP present. The LDH assay is a colorimetric assay which relies on a 2 part reaction. LDH reduces NAD <sup>+</sup> to nicotinamide adenine dinucleotide (NADH) and H <sup>+</sup> by the oxidation of lactate to pyruvate. In the second part of the reaction, 2 H <sup>+</sup> are transferred from NADH to the tetrazolium salt; which is supplied in the assay kit, which is reduced to a red formazan. The colour intensity of the formazan is proportional to the amount of lysed cells.

---

(Chazotte, 2011a; Persson et al., 2013). **Lysosomal activity:** LysoTracker Green is a fluorescent dye used for staining lysosomes and tracking lysosomal activity in live and fixed cells. LysoTracker Green is excited at 504 nm and emits light around 511 nm.

(Chazotte, 2011b; Scaduto and Grotyohann, 1999). **Mitochondrial damage – Mitochondrial membrane potential (MMP) loss:** A variety of lipophilic cationic fluorescent dyes can be used to measure MMP in microscopic studies. Tetramethylrhodamine, methyl ester (TMRM) and rhodamine123 accumulate in the matrix of healthy mitochondria and an orange-red/red fluorescent signal is detected. On loss of MMP the dyes are released from the mitochondria and the relative fluorescence signal increases. MitoTracker orange is another fluorescent dye used to assess MMP. MitoTracker orange is cell permeable and accumulates in the mitochondria but forms covalent bonds with proteins preventing loss of dye after cell fixation. Loss of MMP is detected as a decrease in the incorporation of MitoTracker orange in cells.

(Hynes et al., 2006; Hynes et al., 2013; Nadanaciva et al., 2012) **Mitochondrial damage – oxygen consumption rate:** Oxygen consumption rate (OCR) is an informative measure of mitochondrial function. Mitochondrial impairment can be detected by changes in OCR and an increase in extracellular acidification rate (ECAR), which is an indirect measurement of glycolysis. OCR can be monitored in isolated mitochondria and whole cells via multiple methods. A phosphorescent oxygen-sensitive probe which is quenched by oxygen can be used. During OXPHOS, oxygen is depleted as it is used by the electron transport chain (ETC). This results in a reduction in the quenching effect and leads to an increase in phosphorescent emission which is proportional to OCR. The development of the metabolic flux analyser has allowed the comprehensive investigation of mitochondria via high-throughput screening. Fluorescent probes are coupled with fibre-optics which deliver light and excite oxygen and pH sensors in every well at 530 and 470 nm separately. This causes the oxygen and pH sensors to emit a fluorescent signals at 650 and 530 nm respectively, which is detected by photodetectors within the plate.

(Barker, 1944; Khetani et al., 2013) **Albumin and urea secretion:** Urea is a waste product of protein catabolism and an indicator of liver function. Urea concentrations can be determined by a colorimetric reaction in which diacetyl monoxmine and urea are heated under acidic conditions to yield a yellow coloured compound which is relative to the amount of urea secreted. Albumin is an important protein found within the blood. It is essential for regulating the oncotic pressure and serving as a carrier for molecules with low water solubility. Low levels of albumin are an indicator of liver injury. Albumin content can be assessed using an enzyme-linked immunosorbent assay in which the compound 3,3',5,5'-tetramethylbenzidine is catalysed by horseradish peroxidase to a blue compound. On the addition of acid, the blue compound is converted to a yellow compound. The intensity of the yellow compound is proportional to the amount of albumin in the well of the plate.

## 1.2 BILE

Bile is an essential fluid in the human body, responsible for aiding in the digestion of lipids in the small intestine (Thomas et al., 2008). Without bile, dietary fats would be insoluble and lead to patients being deficient in essential fatty acids and fat-soluble vitamins (Werner et al., 2004). The major constituents of bile are water, BAs, cholesterol, phospholipids and bilirubin (Thomas et al., 2008). BAs are amphipathic molecules as they have a hydrophilic face composed of hydroxyl groups and carboxyl groups, and a hydrophobic face composed of methyl groups (figure 1.5) (Chiang, 2013). The amphipathic nature of BAs is essential for the digestion and absorption of fats and fat-soluble vitamins (Lefebvre et al., 2009). BAs act as detergent molecules which mean that they emulsify hydrophobic compounds such as dietary lipids into micelles for easy digestion and excretion into the small intestine (Hofmann, 1999a; Lefebvre et al., 2009). BAs also aid in the motility of the digestive tract due to the release of motilin as well as reducing bacteria flora of the small intestine due to the release of mucin (Hofmann, 1999b). In addition to these roles, it has recently been noted that BAs can act as signalling molecules (Thomas et al., 2008). BAs are endogenous ligands for the nuclear receptors FXR and PXR, and binding to these receptors initiates gene transcription of a variety of enzymes involved in metabolic homeostasis (Chiang, 2002; Xie et al., 2001). BAs can activate G protein-coupled receptors such as G protein-coupled BA receptor, and play a role in energy metabolism and liver and gallbladder physiology (Thomas et al., 2008).

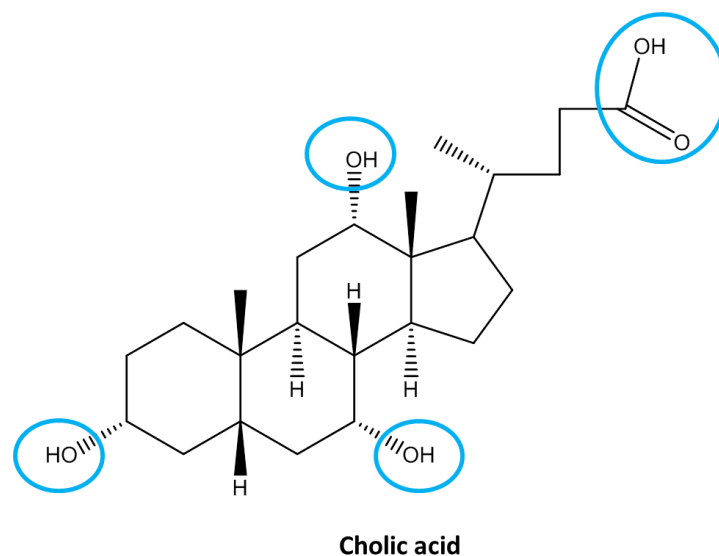


**Figure 1.5: Chemical structure of the primary BA, cholic acid (CA).** BAs are amphipathic molecules as they contain both hydrophobic and hydrophilic faces. Circled in blue are the polar regions of CA which

include hydroxyl and carboxyl groups. The remainder of the molecule (cyclohexane and methyl groups) form the hydrophobic regions.

### 1.2.1 Bile Acid Synthesis

The liver is the only organ within the human body that is capable of the *de novo* synthesis of BAs (Russell, 2003). BA synthesis is a complex procedure, which involves many enzymes. The liver is the only organ to contain all 14 enzymes required to synthesise the two primary BAs, CA and CDCA (Chiang, 2009). There are two pathways for the synthesis of BAs. The classical pathway is the most common of the two pathways and takes place via the endoplasmic reticulum (ER) and peroxisomes in hepatocytes (figure 1.6) (Ferdinandusse and Houten, 2006). The second route of BA synthesis is called the alternative pathway and occurs when the classical pathway is downregulated (Axelson et al., 1989; Pandak et al., 2002). The alternative pathway is also known as the acidic pathway due to the production of acidic intermediates and takes place via the mitochondria (Li and Apte, 2015).

The first step in the classical pathway of BA synthesis is the oxidation of a side chain and the addition of a hydroxyl group onto cholesterol which is initiated by the enzyme CYP7A1 and yields the product 7 $\alpha$ -hydroxycholesterol (figure 1.6) (Lefebvre et al., 2009). Ring structure modification of the 7 $\alpha$ -hydroxycholesterol is catalysed by the enzyme 3  $\beta$ -hydroxysteroid dehydrogenase type 7 (HSD3B7) and yields the cholesterol intermediate 4-Cholesten-7 $\alpha$ -ol-3-one (Ferdinandusse and Houten, 2006). This intermediate can be catalysed by two potential enzymes. If catalysis takes place due to CYP8B1 then the final product will be CA (Russell, 2003). If catalysis take place by  $\Delta^4$ -3-oxosteroid 5 $\beta$ -reductase (AKR1D1) then CDCA will be produced (Ferdinandusse and Houten, 2006). The classical pathway is responsible for around 90 % of BA production in the liver and both CA and CDCA are produced in equal amounts (Li and Apte, 2015).

In contrast, the alternative pathway is deemed a minor route of synthesis as it produces around 10 % of the total BA pool under physiological conditions and only creates CDCA. The enzyme CYP27A1 is located in the mitochondrial inner membrane and catalyses the first hydroxylation reaction which sees cholesterol converted to 27-hydroxycholesterol. The second hydroxylation reaction takes place by CYP7B1 and yields an oxysterol intermediate which is then converted to CDCA (Li and Apte, 2015).

Before BAs are released into the bile canaliculi they will be conjugated with one of the amino acids glycine or taurine (Lefebvre et al., 2009). This increases the water solubility of the compounds and they are now referred to as bile salts (Lefebvre et al., 2009; Maillette de Buy Wenniger and Beuers, 2010a). The pKa of BAs is around 5-6 which means that if present within the intestine, whose pH is around 3-5, the BAs would exist in their protonated form and thus be insoluble in water (Fini and Roda, 1987; Hofmann, 1999b; Maillette de Buy Wenniger and Beuers, 2010a). Conjugating BAs with taurine or glycine lowers the pKa to 1-4 which means that in the intestine the bile salts are in their deprotonated form and thus more soluble in water and able to emulsify fats (Hofmann, 1963; Lefebvre et al., 2009; Maillette de Buy Wenniger and Beuers, 2010a). In humans, DCA and lithocholic acid (LCA) are the main secondary BAs and are formed due to reduction of the hydroxyl groups of BAs by intestinal bacteria (Lefebvre et al., 2009).

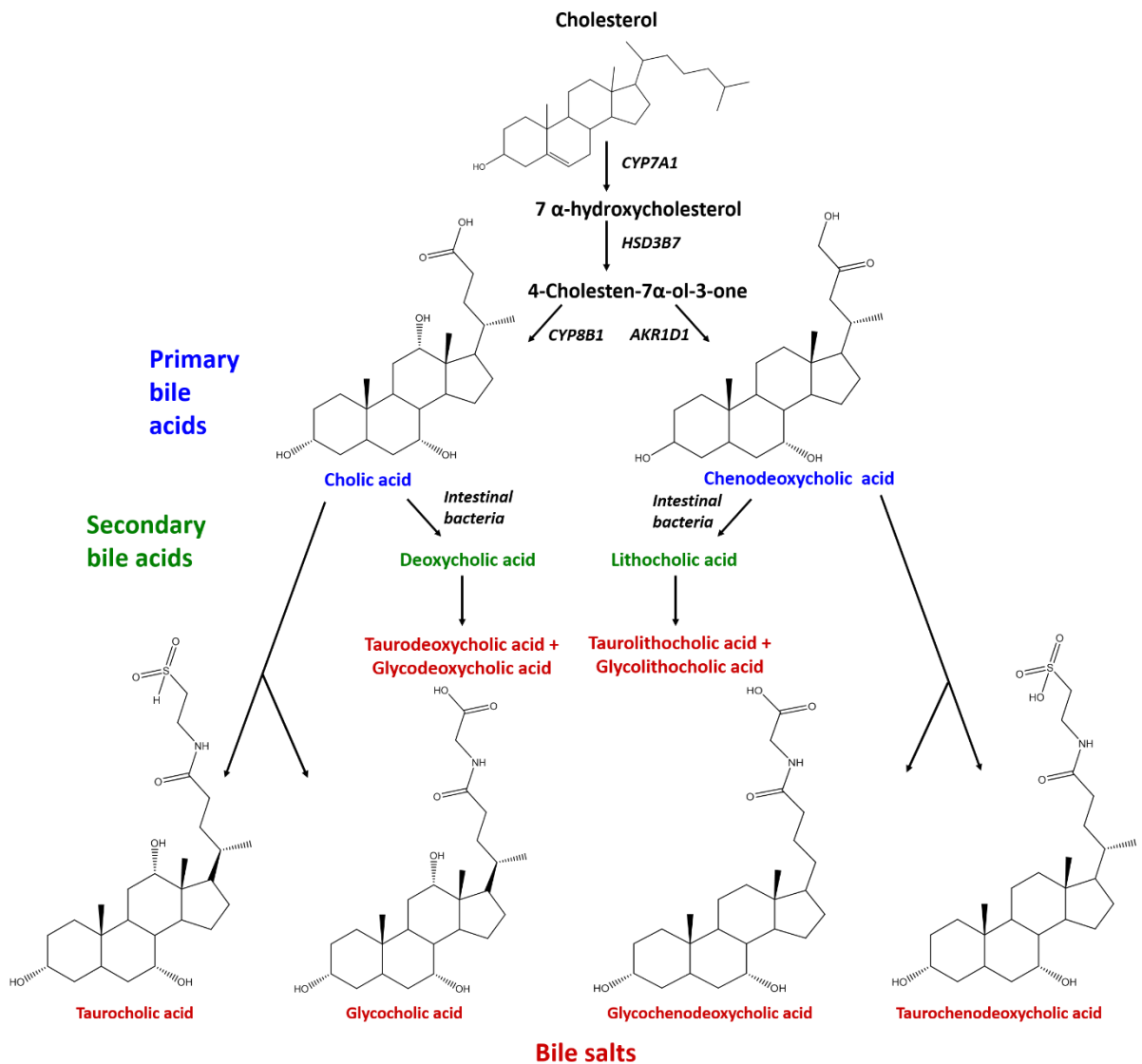


**Figure 1.6: The classical pathway of BA synthesis.** The classical pathway represents around 90 % of total BA production. Cholesterol is converted into either of the primary BAs, CA or CDCA. Actions of intestinal bacteria lead to the conversion of the primary BAs into the secondary BAs, DCA or LCA. Bile salts are formed due to the conjugation of the primary and secondary BAs with the amino acids taurine or glycine.

### 1.2.2 Bile Acid Modification

BA release and modification relies on the actions of hepatocytes and cholangiocytes. Cholangiocytes are the epithelial cells that line the bile duct and their main role is the modification of hepatic bile as it is transported through the biliary tree (Tabibian et al., 2013). During the interdigestive period, bile will be stored in the gallbladder until it is needed (Lefebvre et al., 2009). Upon digestion, the acidic pH of the duodenum stimulates endocrine cells to release secretin (Tabibian et al., 2013). Secretin promotes cholangiocytes to release  $\text{HCO}_3^-$  and  $\text{H}_2\text{O}$  which modifies bile by determining the alkalinity and pH of bile (Tabibian et al., 2013). Additionally, a  $\text{HCO}_3^-$  umbrella is formed on the apical membrane of cholangiocytes which prevents the protonation of glycine-conjugated BAs, thus offering protection from hydrophobic bile constituents (Hohenester et al., 2012; Tabibian et al., 2013). Cholangiocytes are also able to absorb a small amount of BAs (Tabibian et al., 2013). Unconjugated BAs are protonated and then are able to passively diffuse into cholangiocytes whereas conjugated BAs are transported across the apical and basolateral membrane by transporters such as the apical sodium-dependent bile acid transporter (ASBT) and  $\text{OST}\alpha/\beta$  (Benedetti et al., 1997; Hofmann, 2009). In this method, bile is returned to the hepatocytes via cholangiocytes and the peribiliary vascular plexus rather than being transported into the small intestine (Hofmann, 2009). This method is called cholehepatic shunt (figure 1.7) (Hofmann, 2009).

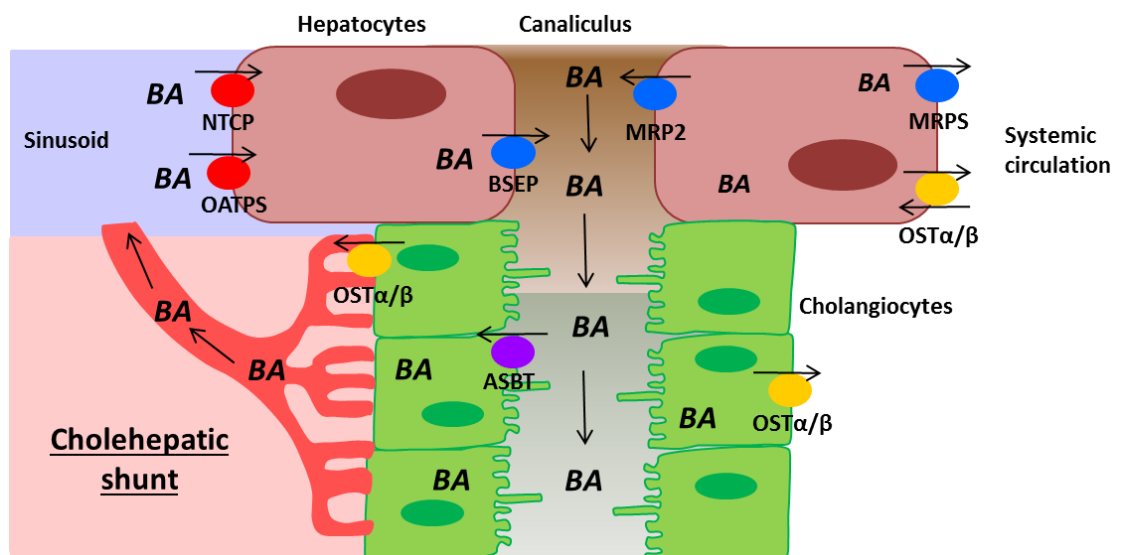


**Figure 1.7: Illustration of cholehepatic shunting of BAs.** BAs are synthesised by hepatocytes and then transported into the bile canaliculus where they travel through the biliary tree. Unconjugated BAs are protonated and can undergo passive diffusion into cholangiocytes. Conjugated BAs are transported into the cholangiocytes by ASBT and then returned to the hepatocytes by cholehepatic shunting. Adapted from (Tabibian et al., 2013).

### 1.2.3 Bile Acid Regulation

The synthesis of bile is tightly regulated as BAs can be derived from two sources (Maillette de Buy Wenniger and Beuers, 2010b). They are either directly synthesised via hepatocytes or resurfaced due to enterohepatic circulation. During enterohepatic circulation, BAs, bilirubin, cholesterol and drugs pass through the liver and undergo intestinal absorption before being reabsorbed back into the liver (Hofmann, 1999a; Roberts et al., 2002). Enterohepatic circulation of BAs is tightly regulated. If the levels of bile salts returning to hepatocytes are low then the biosynthesis of BAs will be increased. Since BAs are synthesised from cholesterol, an upregulation in the biosynthesis of BAs leads to an equal amount of cholesterol biosynthesis (Hofmann, 1999a). Bile salts secreted into the bile canaliculi will be stored in the gallbladder and released after a meal in order to aid in the digestion of lipids (Lefebvre et al., 2009). If the levels of BAs within hepatocytes are too high they will be spilled over into the systemic circulation where they will be reabsorbed by the kidneys and finally circulated back to the liver via the blood (Chiang, 2009). Bile salts secreted by the gallbladder pass through the intestinal tract and will either be reabsorbed in the upper intestine by passive diffusion or will be reabsorbed in the ileum and then transported back to the hepatocytes (Chiang, 2009). Roughly 5 % of BAs secreted by the gallbladder will be lost into the faeces (Lefebvre et al., 2009). Enterohepatic circulation of BAs prevents the cells from wasting energy metabolising more BAs because approximately 95 % of bile salts secreted into the duodenum will be returned to the hepatocytes (Hofmann, 1999a).

### 1.2.4 Bile Acid-Induced Toxicity

DIC represents the most frequent clinical manifestation of DILI, occurring in 20 – 40 % of reported cases (Sharanek et al., 2016). Drugs can elicit constraints on biliary transporters and prevent the efflux of BAs from hepatocytes (Woolbright and Jaeschke, 2015). Despite being involved in many physiological processes, the retention of BAs during DIC can cause toxicity (Attili et al., 1986). Research to ascertain the mechanisms of BA-induced toxicity have been conducted in a variety of models and have revealed that toxicity is multi-mechanistic and depending on the cell model used, can cause apoptosis or necrosis of hepatocytes (Perez and Briz, 2009). BA hydrophobicity is a determining factor for whether toxicity or protection will occur, with the more hydrophobic BAs causing greater levels of hepatocyte injury (Perez and Briz, 2009). BA hydrophobicity is dependent on the number, position and orientation of the hydroxyl groups, along with amidation taking place at the carbon 24 position (Perez and Briz, 2009). The secondary BA LCA is recognised as one of the

most hydrophobic and cytotoxic BAs whilst the secondary BA ursodeoxycholic acid (UDCA) is a hydrophilic BA and used in the treatment of cholestatic liver injury (figure 1.17) (Padda et al., 2011; Perez and Briz, 2009). Due to BAs detergent actions on lipid components, the accumulation of BAs in hepatocytes during cholestasis can lead to the destruction of cellular membranes (Billington et al., 1980). Other mechanisms associated with BA toxicity include the generation of ROS, which leads to oxidative stress, alterations to bile canaliculi dynamics, mitochondrial dysfunction, ER stress and activation of hepatocyte death receptors, which leads to apoptosis and necrosis (Adachi et al., 2014; Fahey et al., 1995; Perez and Briz, 2009; Sharanek et al., 2016). A vast amount of research has been conducted in isolated mitochondria, rodent hepatocytes and HepG2 cells in which mitochondria dysfunction has been revealed as a major route of BA-induced toxicity (Palmeira and Rolo, 2004; Rolo et al., 2004; Schulz et al., 2013).

### **1.3 MITOCHONDRIAL STRUCTURE AND FUNCTION**

Mitochondria are important organelles ubiquitously expressed within cells. The main function of the mitochondria are the production of energy in the form of ATP via the oxidation of reduced electron carriers and the phosphorylation of adenosine diphosphate (ADP). Mitochondria are also involved in other processes such as reactive oxygen species (ROS) production, steroid and heme synthesis, calcium signalling and the regulation of apoptosis (Duchen and Szabadkai, 2010; van der Giezen and Tovar, 2005). Additionally, mitochondria contain their own genome, thus contributing to interindividual variation. Mitochondria have a wealth of structural and functional features, which can be targeted by a compound and lead to toxicity. Consequently, mitochondria have developed a variety of compensatory mechanisms of protection in order to minimise the potential for damage (Valera-Alberni and Canto, 2018).

#### **1.3.1 Mitochondrial Structure**

The mitochondria are a double-membraned organelle; the outer membrane and the inner membrane are separated by the intermembrane space (figure 1.8). The outer membrane encloses the entire organelle and is in interaction with the rest of the cell. The outer membrane has a homogenous structure containing many essential membrane proteins such as porins, and contains a low amount of the lipid cardiolipin (de Kroon et al., 1997; Walther and Rapaport, 2009). Porins are highly abundant within the outer membrane structure and

are important in the diffusion of small molecules into the intermembrane space. One of the most ample porins within the outer membrane of the mitochondria is the voltage-dependent anion channel (VDAC) (Mannella, 1998). Considerable evidence suggests that VDAC forms the outer pore constituent of the mitochondrial permeability transition (MPT) pore, whose opening leads to apoptosis (Vianello et al., 2012). The permeability of the outer membrane of the mitochondria can be accounted for due to VDAC and its ability to allow small molecules up to 5 kDa to diffuse across the membrane (Lemasters and Holmuhamedov, 2006). Larger molecules can only cross the outer membrane via translocases, which actively transport from the cytosol into the intermembrane space (Perry et al., 2008). Due to the exclusive permeability of the outer membrane, the composition of the intermembrane space is similar to that of the cytosol of the cell (Herrmann and Riemer, 2010). Additionally, the intermembrane space contains many pro-apoptotic proteins such as cytochrome c, apoptosome-inducing factor (AIF) and endonuclease G (Munoz-Pinedo et al., 2006). The inner membrane folds on itself to form invaginations called cristae. These invaginations increase the surface area of the inner membrane for enhanced energy production. The inner membrane is less permeable to ions and small molecules than the outer membrane, but does allow the passage of small gases. Given that the inner membrane is the site of OXPHOS, it contains specific ion transporters which aid in the development of an electrochemical membrane potential (Kühlbrandt, 2015). The inner membrane is composed of the phospholipid cardiolipin which is found in the membranes of most bacteria (Schlame and Ren, 2009). Cardiolipin is a highly acidic molecule composed of two phosphatidic moieties connected to a glycerol backbone (Paradies et al., 2014). One of the most abundant proteins in the mitochondria is the adenine nucleotide translocase (ANT), which is located at the inner membrane of the mitochondria (Brand et al., 2005; Liu and Chen, 2013). ANT is responsible for the transport of ADP or ATP across the inner membrane of the mitochondria (Liu and Chen, 2013). In addition to VDAC, ANT has been hypothesised to be a part of the MPT pore along with many other proteins such as cyclophilin D (CypD), the peripheral benzodiazepine receptor (PBR), hexokinase (HK) and creatine kinase (CK) (Bernardi, 1999). Within the inner membrane, enzymes and proteins utilised in energy production are situated. Folding of the inner membrane creates a space in the middle of the organelle called the matrix. The matrix contains the mitochondria's DNA (mtDNA) and a large amount of proteins and enzymes required for ATP synthesis (Mazunin et al., 2015).

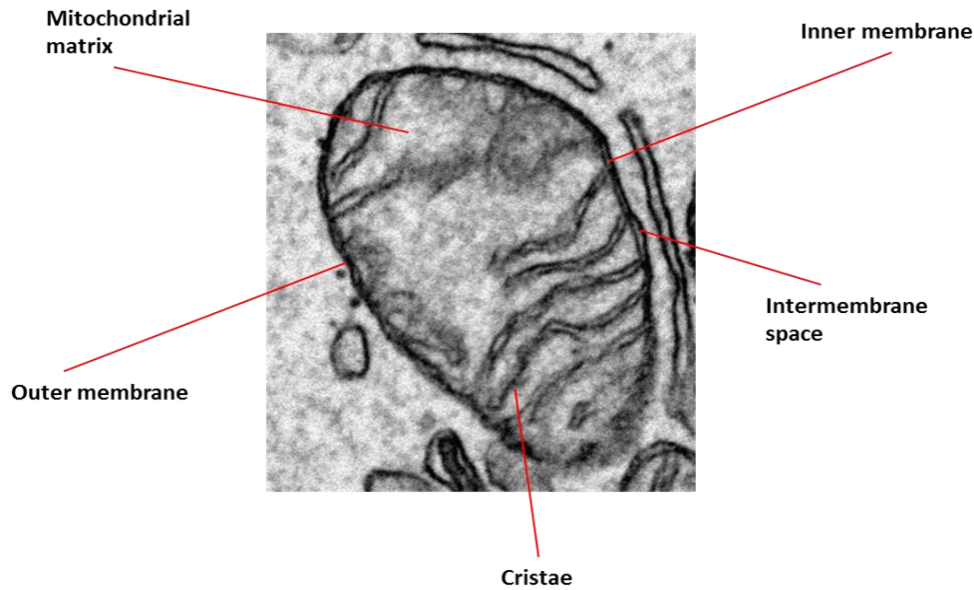


**Figure 1.8: Electron microscopic image illustrating structural features of the mitochondria.** The mitochondria are a double-membraned organelle separated by the intermembrane space. Folding of the mitochondrial inner membrane increases the surface area for enhanced APT production and the folds are known as cristae. The space surrounded by the inner membrane is known as the mitochondrial matrix.

### 1.3.2 Oxidative Phosphorylation

Different organs will have different amounts of mitochondria dependent on their requirement for ATP. For example, the liver has a high metabolic demand and therefore is mitochondria rich (Degli Esposti et al., 2012). Cellular respiration is a multi-step process (figure 1.9) with the initial stage, glycolysis, taking place in the cytosol of the cell. During glycolysis, food is broken down via metabolic reactions so that glucose is converted to pyruvate with the production of two molecules of ATP and two molecules of the reducing agent nicotinamide adenine dinucleotide (NADH) (Hüttemann et al., 2007). Pyruvate is transported into the mitochondria where the pyruvate dehydrogenase complex converts the molecule into acetylCoA, which is used in the Krebs cycle (Patel and Korotchkina, 2006). The Krebs cycle takes place in the mitochondrial matrix and is an eight step process where one molecule of acetylCoA is oxidised to yield the electron carriers, NADH and dihydroflavin adenine dinucleotide ( $\text{FADH}_2$ ), as well as carbon dioxide as a waste product (Krebs, 1937). The final step of aerobic respiration is OXPHOS, which takes place at the mitochondrial inner membrane (Hüttemann et al., 2007). The respiratory chain is comprised of over 85 proteins which assemble themselves into four complexes and together with cytochrome c and ubiquinone catalyse the electron transfer from NADH and  $\text{FADH}_2$  to molecular oxygen (figure

1.10) (Wojtczak and Zablocki, 2008). ATP generation during OXPHOS occurs via the coupling of two processes, the oxidation of reduced electron carriers and the phosphorylation of ADP. The coupling of these two processes is dependent on the impermeability of the inner mitochondrial membrane and the generation of a proton motive force, which then drives the translocation of protons from the intermembrane space into the matrix via ATP synthase leading to the generation of ATP (Wojtczak and Zablocki, 2008).

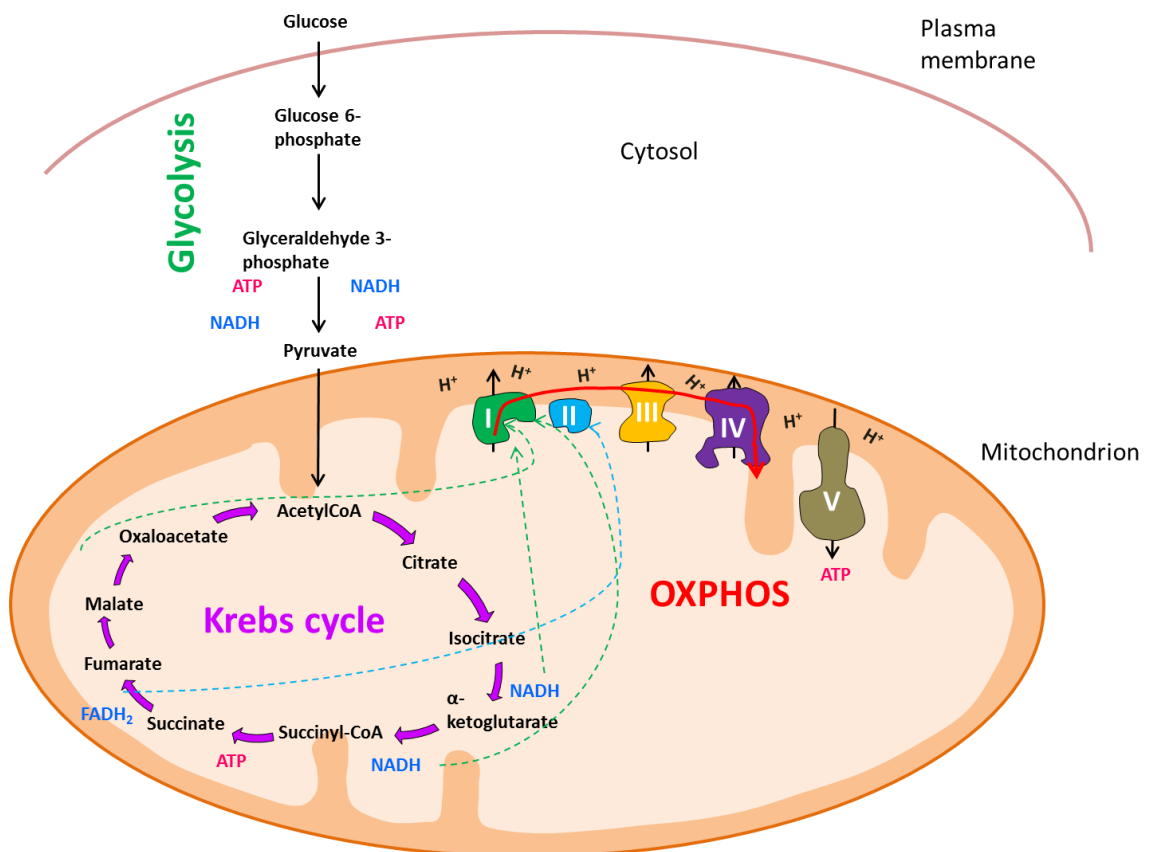


**Figure 1.9: Schematic representation of the stages involved in aerobic respiration.** Glycolysis takes place within the cell cytoplasm and sees glucose converted into pyruvate. Pyruvate is transported into the mitochondria where it is converted to acetylCoA which is fed into the Krebs cycle. The Krebs cycle is an 8 step conversion in which the electron carriers **NADH** and **FADH<sub>2</sub>** are created. The electrons from **NADH** and **FADH<sub>2</sub>** are transferred to the ETC in order to generate ATP. Figure adapted from (Kruiswijk et al., 2015).

### 1.3.2.1 The Electrochemical Gradient

#### 1.3.2.1.1 Complex I

Complex I is a large 'L' shaped protein that protrudes into the mitochondrial matrix (Friedrich and Bottcher, 2004). Complex I binds NADH and 2-electron oxidation takes place, transferring the electrons to flavin mononucleotide (FMN) (Mimaki et al., 2012). The electrons undergo passage through a series of iron-sulphur (Fe-S) clusters, finally reducing ubiquinone to ubiquinol (Mimaki et al., 2012). The transport of 4 H<sup>+</sup> across the inner membrane into the intermembrane space aids in sustaining the proton motive force required for ATP production (Hirst, 2009).

#### 1.3.2.1.2 Complex II

Complex II is an alternative entry point for electrons to enter the electron transport chain (ETC). It links the citric acid cycle with OXPHOS as succinate is oxidised to fumarate and ubiquinone is reduced to ubiquinol. Two electrons from FADH<sub>2</sub> are passed alongside Fe-S clusters to enable the reduction of ubiquinone (Dudkina et al., 2008). The release of energy is low throughput and so there is no proton translocation from complex II (Dudkina et al., 2008).

#### 1.3.2.1.3 Complex III

Electrons from complex I and complex II are fed into complex III where they are passed from ubiquinol to cytochrome c. Complex III is a dimer unit containing cytochrome c (including one heme group) and the cytochrome b<sub>1</sub> complex (including two heme groups) as well as two Fe-S centres (Solmaz and Hunte, 2008). Ubiquinol binds to complex III and undergoes 2-electron oxidation known as the Q cycle. One electron is passed onto the Fe-S centre, which then donates this electron to cytochrome c. The other electron is passed onto cytochrome b, which then reduces a ubiquinone molecule and forms the free radical, semiubiquinone. In order to prevent superoxide formation, a second ubiquinol molecule must bind to complex III for another round of the Q cycle. One of the electrons passed on from ubiquinol is used to reduce the semiubiquinone to ubiquinol. The process is cyclic as the ubiquinol can be reused in the Q cycle (Brandt and Trumpower, 1994). During electron transfer, four protons are translocated across the inner membrane into the intermembrane space (Schultz and Chan, 2001).

### 1.3.2.1.4 Complex IV

The electrons from the reduced cytochrome c generated by complex III are transferred to complex IV which is the terminal oxidase of the ETC (Dudkina et al., 2008; Solmaz and Hunte, 2008). Complex IV is the final complex in the ETC. Complex IV mediates the transfer of electrons from cytochrome c to oxygen, which reduces the latter to water (Dudkina et al., 2008). The actions of complex IV contributes to the proton gradient as four protons are pumped into the intermembrane space (Dudkina et al., 2008).

### 1.3.2.1.5 ATP Synthase and ATP Generation

The final component of the ETC is ATP synthase. ATP synthase is a large protein complex that consists of two regions, the  $F_0$  region situated within the inner mitochondrial membrane and the  $F_1$  region residing in the mitochondrial matrix (Jonckheere et al., 2012). Protons that were pumped into the intermembrane space during OXPHOS diffuse back into the mitochondrial matrix via the the  $F_0$  region of ATP synthase. The movement of the positively charged protons back into the negatively charged matrix creates an electrochemical gradient. Energy from the electrochemical gradient initiates conformational changes of the catalytic site within the  $F_1$  region of ATP synthases leading to the release of ATP into the mitochondrial matrix (Boyer, 1993; Capaldi and Aggeler, 2002).

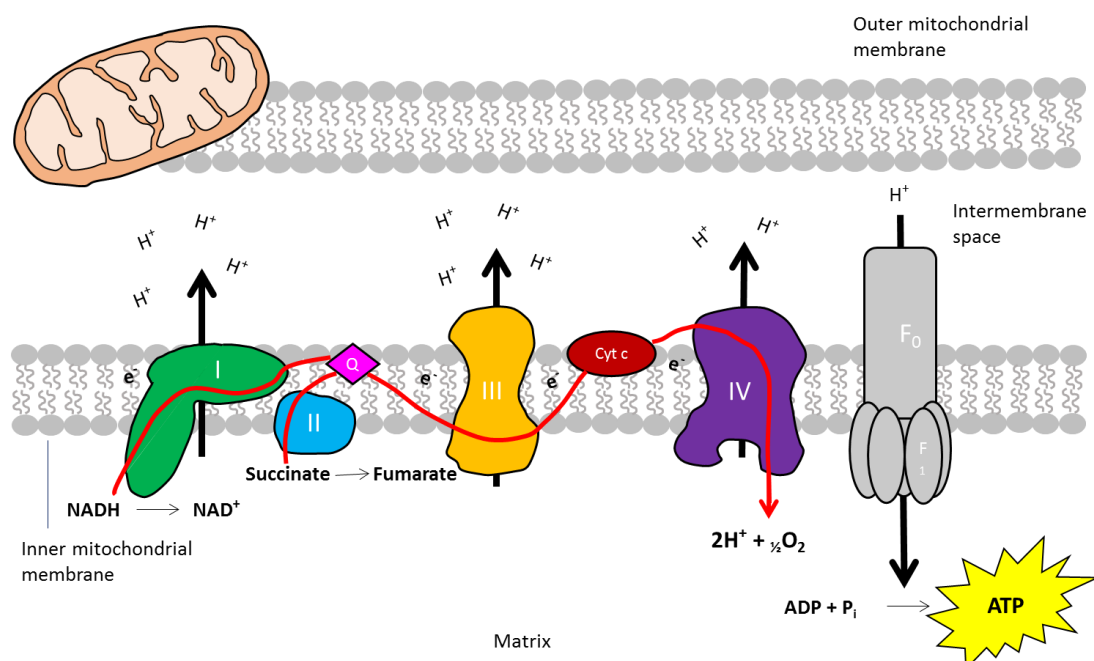


**Figure 1.10: Illustration of the ETC.** The ETC is situated at the inner membrane of the mitochondria and is composed of five complexes important in the production of ATP. Electrons are transferred from electron donors to electron acceptors within the complexes via reduction and oxidation reactions. This is coupled with the transfer of H<sup>+</sup> across the membrane which creates an electrochemical proton gradient that drives the production of ATP through ATP synthase.

### 1.3.3 Additional Features of the Mitochondria

#### 1.3.3.1 Reactive Oxygen Species Production

Other than ATP production, mitochondria are an important organelle because they are involved in the regulation of cell death and apoptosis, and the production of ROS and  $\text{Ca}^{2+}$  signalling (Duchen and Szabadkai, 2010). The mitochondria are one of the sources of ROS as they are produced by complexes 1 and 3 during OXPHOS (Turrens, 2003). During OXPHOS, superoxide is produced by the one electron reduction of oxygen (Murphy, 2009). The mitochondria contain their own superoxide dismutase, which converts superoxide to hydrogen peroxide (Weisiger and Fridovich, 1973). Excessive ROS production could be detrimental to mitochondria by allowing damage to mtDNA, proteins and lipids (Hollensworth et al., 2000; Kirkinezos et al., 2005).

#### 1.3.3.2 Calcium Signalling and Apoptosis

Calcium is vital for cell function and is involved in many cell signalling processes. Although the ER is recognised as the main calcium store, the mitochondria have the capacity to accumulate calcium (Contreras et al., 2010). However, pathological levels of calcium can be detrimental to the mitochondria via the opening of the MPT pore and the subsequent induction of apoptosis or necrosis. The exact molecular composition of the MPT pore remains widely debated however, the illustration in figure 1.11 is the most widely accepted configuration of the pore. The MPT is described as a sudden increase in the permeability of the mitochondrial inner membrane initiated by calcium and other small molecules such as inorganic phosphate and ROS (Hunter et al., 1976; Kim et al., 2003). Opening of the MPT pore leads to the diffusion of solutes with a molecular mass up to 1.5kD entering the mitochondrial matrix, thus increasing the volume of the mitochondrial matrix and causing the organelle to swell (Kim et al., 2003). A process known as mitochondrial outer membrane permeabilisation (MOMP) follows, which is when the outer membrane ruptures due to mitochondria swelling (Zamzami et al., 2005). Initiation of MOMP is the determining factor for the mitochondria to undergo apoptosis.

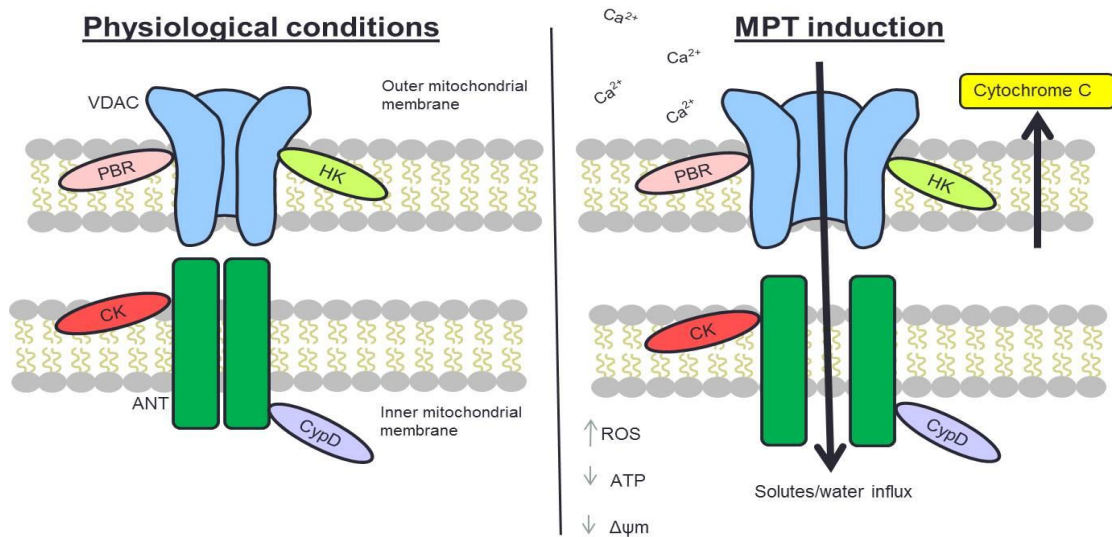


**Figure 1.11: Example of the current proposed structure of the MPT pore.** Components of MPT pore situated within the mitochondrial outer membrane include VDAC, PBR and HK. Constituents within the inner mitochondrial membrane include ANT, CypD and CK. Adapted from (Paul et al., 2008).

### 1.3.4 Mitochondrial Stress Management

The mitochondria have a wealth of structural and functional features that increase their likelihood of injury. In order to prevent this insult from causing damage, the mitochondria have evolved to be able to detect and adapt to insult in order to protect mitochondrial function. The activation of compensatory mechanisms of protection typically involve a complex cascade of events and examples include mitochondrial dynamics, mitophagy, biogenesis and the mitochondrial unfolded protein response (Valera-Alberni and Canto, 2018).

#### 1.3.4.1 Mitochondrial Dynamics

Mitochondria are dynamic organelles, continuously changing their shape via fission and fusion in both physiological and pathological conditions (Rosdahl et al., 2016). Cycling through both processes is necessary for the maintenance of mitochondria health. The main function of fusion is the appropriate distribution of mtDNA, lipids and proteins across all mitochondria (Rosdahl et al., 2016). Additionally, fusion can help mitigate mitochondrial stress imposed by environmental damage and genetic mutations by allowing fused mitochondria to share the burden (Yoneda et al., 1994). Fission is essential for the creation

of new mitochondria but also serves as a quality control point, enabling the removal of damaged mitochondria by mitophagy (Youle and van der Bliek, 2012).

#### *1.3.4.2 Mitochondrial Biogenesis*

Mitochondrial biogenesis is the process by which cells increase their mitochondrial mass, typically in response to an increase in ATP demand or compromised ATP synthesis (Valera-Alberni and Canto, 2018). Mitochondrial biogenesis is a complex signalling cascade requiring coordination between mtDNA and nuclear DNA as both encode mitochondrial proteins (Valera-Alberni and Canto, 2018). The transcriptional co-activator, peroxisome proliferator-activated receptor gamma coactivator 1-alpha (PGC1- $\alpha$ ), is regarded as the master regulator of mitochondrial biogenesis and on detection of an energy deficit stimulus, initiates the signalling cascade for biogenesis (Medeiros, 2008; Valera-Alberni and Canto, 2018). PGC1- $\alpha$  initiates the biogenesis cascade by activating the nuclear receptor factors 1 and 2 (NRF1 and NRF2) (Scarpulla, 2008). NRF1 and NRF2 are responsible for regulating the expression of subunits of the ETC that are encoded by nuclear DNA as well as the mitochondrial transcription factor A (TFAM) (Evans and Scarpulla, 1990; Virbasius and Scarpulla, 1994). TFAM is responsible for controlling mtDNA replication and ensures correct unwinding of mtDNA in order for the mitochondrial RNA polymerase (POLRMT) to bind to mtDNA promoters for transcription (Gureev et al., 2019).

## **1.4 THE MITOCHONDRIAL GENOME**

Cases of toxicity that are idiosyncratic present the most uncertainty to drug development as they typically only occur when the novel agent is tested on a large population post market (Mosedale and Watkins, 2017). Whilst it is acknowledged that DILI can arise due to a plethora of mechanisms, it is also governed by complex genetic and non-genetic factors giving rise to interindividual variation (Chalasani and Björnsson, 2010; Roth and Lee, 2017; Ulrich, 2007). The mitochondria contain their own genome and thus offer another source of interindividual variation, which could account for some of the idiosyncrasies associated with DILI (Boelsterli and Lim, 2007).

### **1.4.1 Mitochondrial DNA Structure**

MtDNA is a double-stranded, circular molecule composed of 16,569 base pairs (Calvo and Mootha, 2010). The two strands are different due to their nucleotide content. The heavy

strand is rich in guanine and the light strand is rich in cytosine (Calvo and Mootha, 2010). MtDNA encodes 37 genes of which 22 encode for transfer RNA (tRNA) and two for ribosomal RNA (rRNA) (Anderson et al., 1981). The remaining thirteen genes encode for structural subunits of the ETC with the remaining respiratory chain subunits being encoded for by the nuclear genome (figure 1.12) (Calvo and Mootha, 2010). MtDNA are packaged into DNA-protein complexes termed mitochondrial nucleoids, which are important in protection and enabling efficient replication (Kukat et al., 2011). The mitochondrial nucleoid is coupled with TFAM, which is important in regulating mtDNA copy number. On average, a mitochondrial nucleoid contains 1.4 mtDNA molecules (Kukat et al., 2011). A mitochondrion contains around ten copies of mtDNA but the exact numbers vary in accordance with the bioenergetic needs of the tissues (Schon et al., 2012).

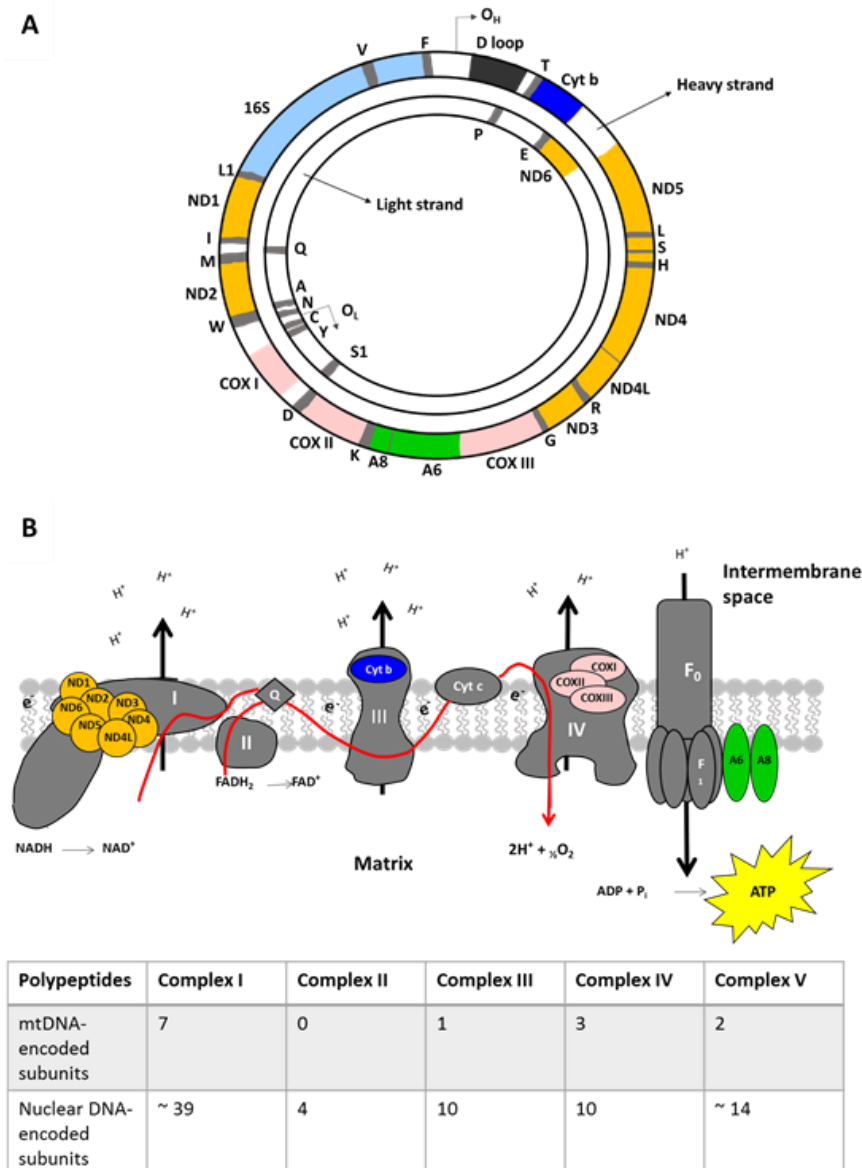


**Figure 1.12: Mitochondrial DNA structure and schematic representation of the ETC and the proteins encoded by the mtDNA.** A: Human mtDNA is double-strand, circular molecule responsible for encoding 37 genes. B: The mtDNA encodes 13 proteins which are shown in colour. The colours correspond to the colours of the polypeptide-coding gene in figure X1. Abbreviations: ND, NADH dehydrogenase; Q, ubiquinone; cyt b, cytochrome *b*; COX, cytochrome *c* oxidase; A, ATPase;  $O_H$ , origins of replication of the heavy strand;  $O_L$ , origins of replication of the light strand. Copied from (Penman et al., 2020b).

### 1.4.2 Mitochondrial Heteroplasmy

Unlike nuclear DNA, which is replicated during interphase for cell division, mtDNA is constantly replicated independent of the cell cycle in a process called relaxed replication (Stewart and Chinnery, 2015). The mitochondrial genome is lacking in histones and other

repair systems utilised by the nuclear genome for repair (Denver et al., 2000). Additionally, the proximity of mtDNA to ROS, coupled with the aforementioned high replication rate, offer explanations to the high mutation rate associated with mtDNA (Burr et al., 2018; Lagouge and Larsson, 2013).

By definition, the “normal state” of a cell would be homoplasmy which is where all copies of the mtDNA would share the same sequence (Burr et al., 2018). Due to the high mutation rate associated with mtDNA, it is very common for cells to have both wild-type mtDNA and mutant mtDNA in a process called heteroplasmy (Stewart and Chinnery, 2015). Heteroplasmy is constantly changing within a cell due to the random separation of mtDNA during cell division. During cell division, daughter cells can receive different proportions of mtDNA in a process called vegetative segregation (Stewart and Chinnery, 2015). Mutations in mtDNA accumulate over the lifetime of an individual but are unlikely to instigate a cellular phenotype until a critical threshold is reached (Schon et al., 2012). The threshold effect infers that cells can survive damage over time but as the burden of mutant mtDNA increases compared to wild-type mtDNA, a critical point is reached on which there is rapid cell death and some form of pathogenic phenotype (Burr et al., 2018). It is estimated that this critical point is when the percentage of mtDNA mutations reaches 60 – 80 % (Stewart and Chinnery, 2015).

### **1.4.3 Mitochondrial Haplogroups**

Progressive accumulation of mtDNA mutations through the maternal lineage led to the creation of haplogroups. A haplogroup is characterised by groups of individuals sharing groups of genes with similar single nucleotide polymorphisms (SNPs) in their mtDNA that was inherited from our ancestral ‘mitochondrial Eve’ (Ienco et al., 2011; Mitchell et al., 2014; Stewart and Chinnery, 2015). Mitochondrial haplogroups are confined to different ethnic groups due to the maternal inheritance of mtDNA and the lack of recombination (Stewart and Chinnery, 2015). It is estimated that mitochondrial Eve, the matrilineal most recent common ancestor (MRCA), lived approximately 200,000 years ago in Africa. Due to population migration, new SNPs in the mtDNA that were advantageous for the different environmental conditions were selected for and have remained within specific ethnic groups and thus their haplogroup (Ruiz-Pesini et al., 2004; Stewart and Chinnery, 2015). Haplogroup H is the most common in Europe accounting for 40 % of the European population and is estimated to contain around 90 sub-haplogroups (Stewart and Chinnery, 2015; van Oven and Kayser, 2009).

## 1.5 DRUG-INDUCED MITOCHONDRIAL TOXICITY

Drug-induced mitochondrial toxicity (DIMIT) has been reported as a determinant of DILI with 50 % of drugs with black box warnings for DILI also having mitochondrial burdens (Boelsterli and Lim, 2007). Whilst the incidence of DIMIT is low, it is grossly undervalued as the consequences can be critical. The link between DILI and DIMIT is underlined by the heteroplasmy and mitochondrial hypothesis. Low levels of heteroplasmy are not dangerous as the cell can withstand the functional effects of mutant mitochondria via compensatory mechanisms (DiMauro and Schon, 2003). Furthermore, cells with a high turnover rate; such as hepatic parenchymal cells, can endure high levels of heteroplasmy due to the aforementioned threshold effect (Stewart and Chinnery, 2015). This postponed but then sudden death mirrors what is seen in the clinic, as most idiosyncratic DILI cases are delayed but then have a sudden onset of action, which provides evidence as to why the mitochondria are hypothesised to be a contributing factor of DILI. In addition, certain structural features of the mitochondria make them more susceptible to being targeted by a drug (Boelsterli and Lim, 2007). Table 1.2 presents a selection of drugs with dual liver and mitochondrial liabilities.

**Table 1.2: Selected compounds possessing both DILI and mitochondrial liabilities along with their mechanisms of mitochondrial toxicity.**

Source	Drug	Clinical use	Mitochondrial involvement
(Fromenty et al., 1990a; Fromenty et al., 1990b)	Amiodarone	Anti-arrhythmic	Inhibition of complex I and II. Decrease in state 3 respiration. Loss of MMP. Biphasic effect on state 4 respiration (increase followed by decrease). Inhibition of $\beta$ -oxidation of fatty acids.
(Kennedy et al., 1996)	Perhexilline	Antianginal	Reduction in fatty acid metabolism by the inhibition of carnitine palmitoyltransferase-1.
(Fromenty and Pessayre, 1995)	Valproate	Antiepileptic	Inhibition of fatty acid oxidation via the sequestering of coenzyme A and carnitine.
(Le Dinh et al., 1988)	Amineptine	Antidepressant	Inhibition of fatty acid oxidation
(Coe et al., 2007)	Flutamide	Nonsteroidal antiandrogen	Decrease in respiration due to the inhibition of complex I.
(Moreno-Sanchez et al., 1999)	Diclofenac	Nonsteroidal anti-inflammatory agent	Inhibition of ATP synthesis via prevention of activity of ATPase and adenine nucleotide translocase. Mitochondrial membrane depolarisation.

(Kon et al., 2004)	Paracetamol	Pain killer	Induction of MPT.
(Masubuchi et al., 2006; Nadanaciva et al., 2007b)	Troglitazone	Anti-diabetic	Inhibition of complex IV and V leading to an inhibition of ADP-driven respiration. Initiation of MPT pore opening.
(Brinkman and Kakuda, 2000)	Nucleoside reverse transcriptase inhibitor (NRTIs) (Zidovudine and stavudine)	Antiviral (anti-HIV)	Inhibition of mitochondrial DNA polymerase- $\gamma$ causing a reduction in mitochondrial DNA.
(Cui et al., 1995; Lewis et al., 1996)	Fialuridine	Antiviral (anti-HBV)	Incorporation of fialuridine into the mitochondrial DNA and inhibition of mitochondrial DNA polymerase- $\gamma$ leading to mitochondrial dysfunction.
(Dykens et al., 2008; Nadanaciva et al., 2007a)	Nefazodone	Antidepressant	Decrease in respiration due to the inhibition of complexes I and IV.
(Nissinen et al., 1997)	Tolcapone	Antiparkinsonian	Acts as an uncoupler of the ETC.

## 1.5.1 Models for the Assessment of Drug-Induced Mitochondrial Toxicity

### 1.5.1.1 Introduction

*In vitro* models for the assessment of mitochondrial dysfunction have traditionally used isolated mitochondrial or whole cells. Whilst both models have their advantages, it is imperative to consider their disadvantages when determining what is the most appropriate model for the assessment of DIMT. In most cases, if the compound of interest is effecting the production of ATP then the use of isolated mitochondria is appropriate. However, if the compound disturbs any of the other functions the mitochondria are involved in, then the use of whole or permeabilised cells may be better suited. It is essential that the appropriate *in*

*vitro* model is employed in drug toxicology studies in order to gain full mechanistic insight and not allow mitochondrial toxicity to go undetected (Brand M and Nicholls D 2011).

#### *1.5.1.2 Isolated Mitochondria*

Isolated mitochondria have been extensively used in DIMT studies in order to determine direct interactions between a compound and the mitochondria as there are no interferences from cytosolic fractions (Brand M and Nicholls D 2011). Mitochondrial isolations have been validated for a variety of cell types and tissues and are easy to perform (Schmitt et al., 2015). Despite its ease, practical limitations include the large sample size needed per isolation, the risk of mitochondrial damage during the procedure and the loss of mitochondrial activity over time meaning that experiments have to be performed immediately (Brand M and Nicholls D 2011; Perry et al., 2013). Additionally, the removal of the mitochondria from their cellular setting prevents physiological interactions between other mitochondria and organelles (Brand M and Nicholls D 2011). The lack of cellular context means that cellular protective mechanisms such as fission, fusion and mitophagy cannot take place, thus enabling artificial toxicity to be concluded. Conversely, mitochondrial toxicity can go undetected if the compound causes toxicity via multiple mechanisms or needs to be metabolised.

#### *1.5.1.3 Whole Cells*

Many techniques for bioenergetic research have been developed for use in whole cells, thus alleviating the problems associated with isolated mitochondria. Predominantly, whole cells offer the advantage of greater physiological relevance as interactions between mitochondria and other organelles are maintained. Additionally, the sample size required for many plate-based assays are small in comparison with the amount of cells needed for isolated mitochondria experiments. Usage of whole cells add extra mechanistic insight into bioenergetics as glycolysis can be measured by measurements of extracellular acidification (ECAR) or lactate production (Brand M and Nicholls D 2011). A limitation of whole cells is that many substrates and inhibitors needed for the assessment of mitochondria function are cell-impermeable, thus requiring experimental aims and conditions to be optimised to allow usage of extracellular substrates (Brand M and Nicholls D 2011).

#### 1.5.1.4 Permeabilised Cells

Plasma membrane permeabilisation can alleviate some of the problems associated with intact cells and isolated mitochondria. The compounds traditionally used for permeabilisation (digitonin, saponin and recombinant perfringolysin O (rPFO)) interact with cholesterol in the cellular plasma membrane (Kuznetsov et al., 2008; Salabei et al., 2014). The low cholesterol content of the mitochondria and ER means that these organelles do not undergo permeabilisation and remain intact (Kuznetsov et al., 2008). Permeabilisation of the plasma membrane allows compounds that are cell-impermeable to access the mitochondria thereby allowing analysis of individual complexes within the ETC (Brand M and Nicholls D 2011). Similar to whole cells, assays using permeabilised cells require fewer cells and are faster than mitochondrial isolations, thus limiting damage to mitochondria as associated with isolated mitochondria (Brand M and Nicholls D 2011; Kuznetsov et al., 2008).

#### 1.5.1.5 Transmitochondrial Cybrids

As both mtDNA and nuclear DNA regulate mitochondrial function, it can be difficult to determine which genome is responsible for any mitochondrial alterations. The generation of transmitochondrial cybrids has advanced understandings of the role of mtDNA in mitochondrial dysfunction by allowing the effects of mtDNA upon cellular behaviour to be investigated against a stable nuclear background. Facilitation of cybrids generation begins with the production of a Rho zero cell ( $\rho 0$ ) (Wilkins et al., 2014). A  $\rho 0$  cell is a cell devoid of its mtDNA. The most common method for the production of  $\rho 0$  cells is the depletion of mtDNA with ethidium bromide (Wiseman and Attardi, 1978). Ethidium bromide is a positively-charged DNA intercalator that is attracted to the negatively-charged mtDNA found with the negatively-charged mitochondrial matrix. Intercalation of ethidium bromide into the mtDNA leads to a failure of DNA replication and ultimate elimination of mtDNA (Wilkins et al., 2014). Cybrids are created by the fusion of  $\rho 0$  cells with either anucleated cells (platelets) or enucleated cells (cytoplast) from individuals (figure 1.13). Fusion of the two cell types requires polyethylene glycol (PEG) and supplemented media containing bromodeoxyuridine and lacking in pyruvate or uridine (Schon et al., 2012). Due to a functioning ETC, cybrids are able to generate their own pyruvate and uridine whereas  $\rho 0$  cells are auxotrophic for uridine and pyruvate. Consequently, uridine and pyruvate are omitted from the cybrid selection media in order to eliminate any  $\rho 0$  cells that have not undergone the fusion (Schon et al., 2012). Due to the nuclear DNA being constant from the  $\rho 0$  cell, any differences observed in cellular function can be attributed to the donor mtDNA

(Wilkins et al., 2014). The term cybrids was adopted in 1974 to distinguish between a hybrid, which is the fusion of two nucleated cells (Bunn et al., 1974).

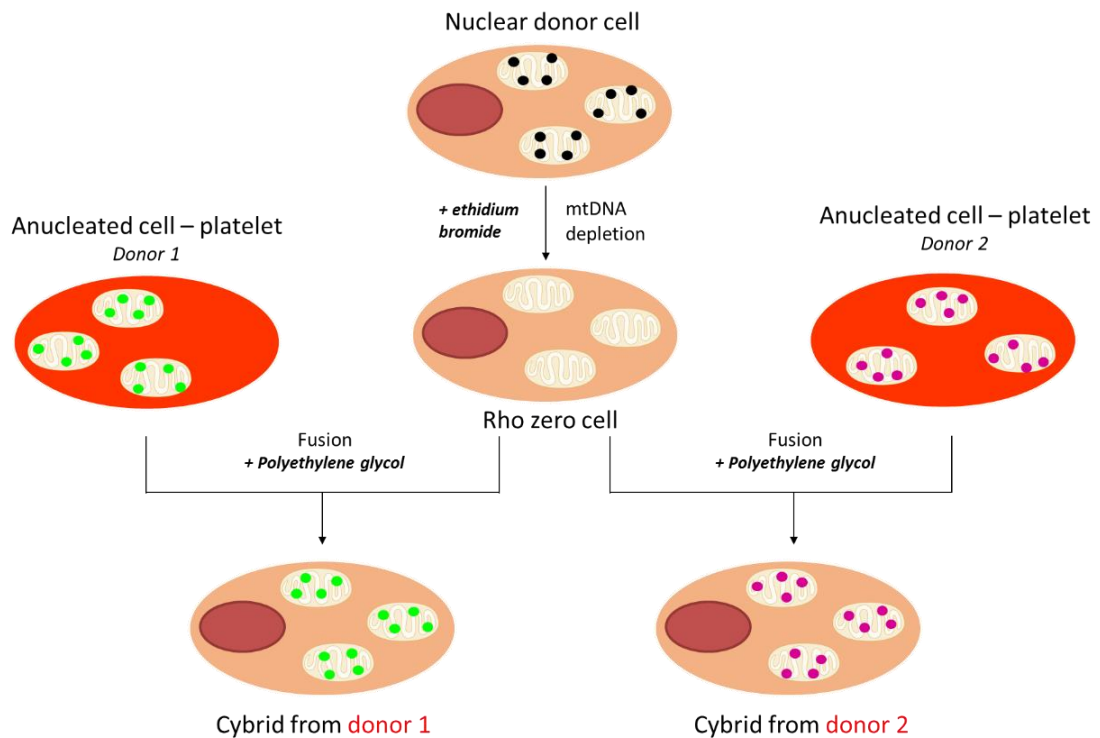


**Figure 1.13: The generation of transmitochondrial cybrids from p0 cells and platelets.** A nuclear donor cell is devoid of its mtDNA using the DNA-intercalator ethidium bromide to produce a p0 cell. Platelets are anucleated cells and can be isolated from patient blood donations. Platelets are fused with p0 cells using polyethylene glycol to produce transmitochondrial cells. Both cybrids will have the same nuclear DNA background but will have different mtDNA from the different platelet donors. Adapted from (Schon et al., 2012).

## 1.6 THESIS AIMS AND OBJECTIVES

Mitochondrial dysfunction and biliary transporter alterations are recognised as major mechanisms of hepatotoxicity and so it is essential that investigations of toxicity by these means are performed using the most appropriate and physiologically relevant models in order to improve predictivity of DILI screening.

Therefore, the overall aim of the research presented in this thesis was to assess the pharmacological and toxicological utility of advanced hepatic models, including HepaRG cells and HepG2 transmitochondrial cybrids, for the study of biliary transporter alterations and mitochondrial dysfunction. Furthermore, it is acknowledged that alongside drug-related mechanisms, individual susceptibility factors are important in defining susceptibility to toxicity. However, such factors are rarely incorporated into preclinical models. The final aim of this thesis was to use HepG2 transmitochondrial cybrids to assess the effect of mtDNA variation upon susceptibility to mitochondrial dysfunction with tolcapone, a compound associated with idiosyncratic DILI. In order to achieve these aims, the following objectives were created:

**Objective 1:** To define the utility of HepaRG cells over HepG2 cells for studies of cholestatic dysfunction.

**Objective 2:** To determine if biliary transporter alterations and mitochondrial dysfunction are mechanisms of toxicity of BAs and flucloxacillin in HepaRG cells and isolated mitochondria.

**Objective 3:** To assess the translatability of mitochondrial dysfunction detected in isolated mitochondria and whole cells.

**Objective 4:** To assess the effects of mtDNA variation upon susceptibility to tolcapone-induced mitochondrial dysfunction using HepG2 transmitochondrial cybrids.

**Chapter 2**  
**Characterisation of HepaRG cells for**  
**the Study of Bile Acid-induced Biliary**  
**Transporter Dysfunction**

**CONTENTS**

2.1	INTRODUCTION	42
2.2	MATERIALS AND METHODS	44
2.2.1	Materials	44
2.2.2	HepG2 Cell Culture	44
2.2.3	HepaRG Cell Culture	44
2.2.4	Bile Acid Treatment	47
2.2.5	Proteomic Analysis of Biliary Transporters in HepaRG Cells and HepG2 Cells	47
2.2.6	Fluorescence Imaging of Biliary Transporters	49
2.2.7	Statistical Analysis	51
2.3	RESULTS	52
2.3.1	Comparison of Transporter Expression Between HepaRG Cells and HepG2 Cells	52
2.3.2	Examining Biliary Transporter Localisation and Function in HepG2 Cells	53
2.3.3	Examining Biliary Transporter Localisation and Function in HepaRG Cells	54
2.3.4	Determining Biliary Transporter Inhibition in HepaRG Cells	56
2.3.5	Assessment of the Effects of BA Mixtures on Biliary Transporter Function and Expression in HepaRG Cells	57
2.3.6	Assessment of the Effects of Rotenone on Biliary Transporter Function and Expression in HepaRG Cells	60
2.4	DISCUSSION	62
2.5	CONCLUSION	68

## 2.1 INTRODUCTION

Drug-induced cholestasis (DIC) represents the most frequent clinical manifestation of DILI, occurring in 20 – 40 % of reported cases (Sgro et al., 2002). BAs are recognised as the causative agents of toxicity in intrahepatic cholestasis (Perez and Briz, 2009; Woolbright and Jaeschke, 2015). Mechanistic studies in rodent hepatocytes, HepG2 cells and isolated mitochondria have elucidated various pathways of BA-induced damage, revealing DIC to be a complex, multifactorial disease (Perez and Briz, 2009; Sharanek et al., 2016). However, a vast amount of research has shown BA-induced mitochondrial toxicity as a key event in the toxicity of DIC (Palmeira and Rolo, 2004; Rolo et al., 2004; Schulz et al., 2013). Whilst valuable, there are some limitations associated with this past research. Importantly, much of this research has been conducted using single BAs and as a result, may have overlooked the effects a BA milieu would have on hepatocytes (Woolbright and Jaeschke, 2015). During cholestasis, hepatocytes are exposed to multiple BAs and so the exposure of hepatocytes to single BAs experimentally bears little resemblance to the *in vivo* pathophysiology (Woolbright and Jaeschke, 2015).

It is acknowledged that the toxicity of DILI is multi-mechanistic however, it is currently unknown whether there is a mechanistic link between the various processes. Therefore, there is a need for further research to delineate a pathway of toxicity for DIC (Aleo et al., 2014). For example, research by Aleo *et al* found that there was a mechanistic link between the inhibition of BSEP and mitochondrial function with severity to human DILI. During a drug screen of compounds associated with high, low and no DILI concern, it was discovered that compounds with a dual potency to inhibit mitochondrial function and BSEP were associated with a more severe case of DILI (Aleo et al., 2014). This association was further strengthened by work from the Food and Drug Administration (FDA) in which 67 % of drugs withdrawn from the market or issued with a black box warning were found to be potent inhibitors of both mitochondrial function and BSEP, implying that there could be interplay between these mechanisms of toxicity (Aleo et al., 2014). Whilst strong associations between BAs and mitochondrial toxicity have been elucidated, the link with biliary transporter toxicity and accumulation of BAs has yet to be investigated. Therefore, it was hypothesised that toxicologically relevant concentrations of BA mixtures would impair mitochondrial bioenergetics, which would consequently lead to a reduction in the expression and activity of ATP-dependent biliary transporters.

The research presented in this chapter aimed to define the utility of HepaRG cells for such studies of cholestatic dysfunction. Following this, it was determined if the BA mixtures exerted alterations upon biliary transporters. The BAs selected for the mixture were the 6 most abundant BAs found within human plasma during physiological levels of healthy patients (Xiang et al., 2010). In order to determine how much deviation from “normal” was needed to elicit a response, the concentrations of the BAs were increased to a 10, 100 and 1000 x BA mix (table 2.2) (Penman et al., 2019).

The physiological phenotype of HepaRG and HepG2 cells were defined with respect to biliary transporter activity. Primarily, western blotting and fluorescence imaging was used to assess the localisation, expression and function of biliary transporters. Many drugs with cholestatic liabilities are known inhibitors of BSEP and MRP transporters, and so the ability of these transporters to be inhibited by compounds was assessed (Köck et al., 2014). Finally, time-dependent effects of the BA mixtures on transporter protein activities were assessed in HepaRG cells. In order to confirm a mechanistic link between mitochondrial and transporter inhibition, the mitotoxic potential of the BA mixtures will need to be assessed in the next experimental chapter of this thesis.

## 2.2 MATERIALS AND METHODS

### 2.2.1 Materials

HepG2 cells were purchased from European Collection of Cell Cultures (ECACC, Salisbury, UK). HepaRG cells, basal media, growth and differentiation additives were purchased from Biopredic International (Saint Grégoire, France). Dulbecco's Modified Eagle Medium (DMEM), fetal bovine serum (FBS), 4-(2-hydroxyethyl)-1-piperazineethanesulfonic acid (HEPES), 1 x phosphate buffered saline (PBS), Hank's balanced salt solution (HBSS), rat tail collagen I, NUPAGE 4-12 % gels, Cell Tracker 5- chloromethylfluorescein diacetate (CMFDA) and trypsin were purchased from Life Technologies (Paisley, UK). Glass cover slips were purchased from Appleton Woods (Birmingham, UK). Nunc flasks, 6-well plates, 12-well plates, microscope slides and dimethyl sulfoxide (DMSO) were purchased from Fisher Scientific (Loughborough, UK). L-glutamine, sucrose, 3-(N-morpholino)propanesulfonic acid (MOPS), phosphoric acid, bovine serum albumin (BSA), bicinchoninic acid (BCA) kit and all bile acids and salts were purchased from Sigma Aldrich (Missouri, USA). Nitrocellulose membrane and enhanced chemiluminescence (ECL) were purchased from GE Healthcare (Buckinghamshire, UK). All antibodies were purchased from Abcam (Cambridge, UK).

### 2.2.2 HepG2 Cell Culture

HepG2 cells were cultured (37 °C in 5 % CO<sub>2</sub>) in DMEM high-glucose medium (glucose; 25 mM) supplemented with 10 % v/v FBS, sodium pyruvate (1 mM), L-glutamine (4 mM) and HEPES (1 mM). HepG2 cells were used up to passage 20. HepG2 cells were routinely tested for mycoplasma.

### 2.2.3 HepaRG Cell Culture

Undifferentiated HepaRG cells were supplied by the manufacturers at passage 12. Cells were thawed and grown (37 °C in 5 % CO<sub>2</sub>) in a T25 flask for 2 weeks in HepaRG base medium supplemented with HepaRG growth additives (growth media) in order to amplify the population.

Every 2 weeks, undifferentiated HepaRG cells were dissociated from the T25 flask using 0.05 % trypsin, which was neutralised using growth media. Cells were counted using 0.05 % trypan blue. Cells were seeded into different experimental flasks and plates dependent on the

experiment. Seeding densities were supplied by the manufacturer and are based upon the number of cells/cm<sup>2</sup> and the number of cells/mL (table 2.1).

**Table 2.1: Undifferentiated HepaRG cell seeding densities as supplied by the manufacturers.**

Culture plate	Number cells /well x 10 <sup>6</sup>	Volume of media /well	Cells/cm <sup>2</sup>	Cells/mL
T75 flask	2	14 mL	0.026 x 10 <sup>6</sup>	0.14 x 10 <sup>6</sup>
T25	0.5	5 mL	0.02 x 10 <sup>6</sup>	0.1 x 10 <sup>6</sup>
6 well plate	0.2	2 mL	0.022 x 10 <sup>6</sup>	0.1 x 10 <sup>6</sup>
24 well plate	0.055	500 µL	0.028 x 10 <sup>6</sup>	0.11 x 10 <sup>6</sup>
12 well plate with coverslips	0.08	800 µL	0.02 x 10 <sup>6</sup>	0.1 x 10 <sup>6</sup>
96 well plate	0.009	100 µL	0.028 x 10 <sup>6</sup>	0.09 x 10 <sup>6</sup>
XF Cell Culture 96 well Microplate	0.005	100 µL	0.028 x 10 <sup>6</sup>	0.05 x 10 <sup>6</sup>

Cells were grown in growth media for 2 weeks. Thereafter, cells were grown in HepaRG base media supplemented with HepaRG differentiation additive (differentiation media) for an additional 2 weeks. At this point, cells were fully differentiated and could be maintained in differentiation media for an additional 4 weeks until ready for experimental use, with twice-weekly media changes required (figure 2.1). HepaRG cells were routinely tested for mycoplasma and were used to passage 20.

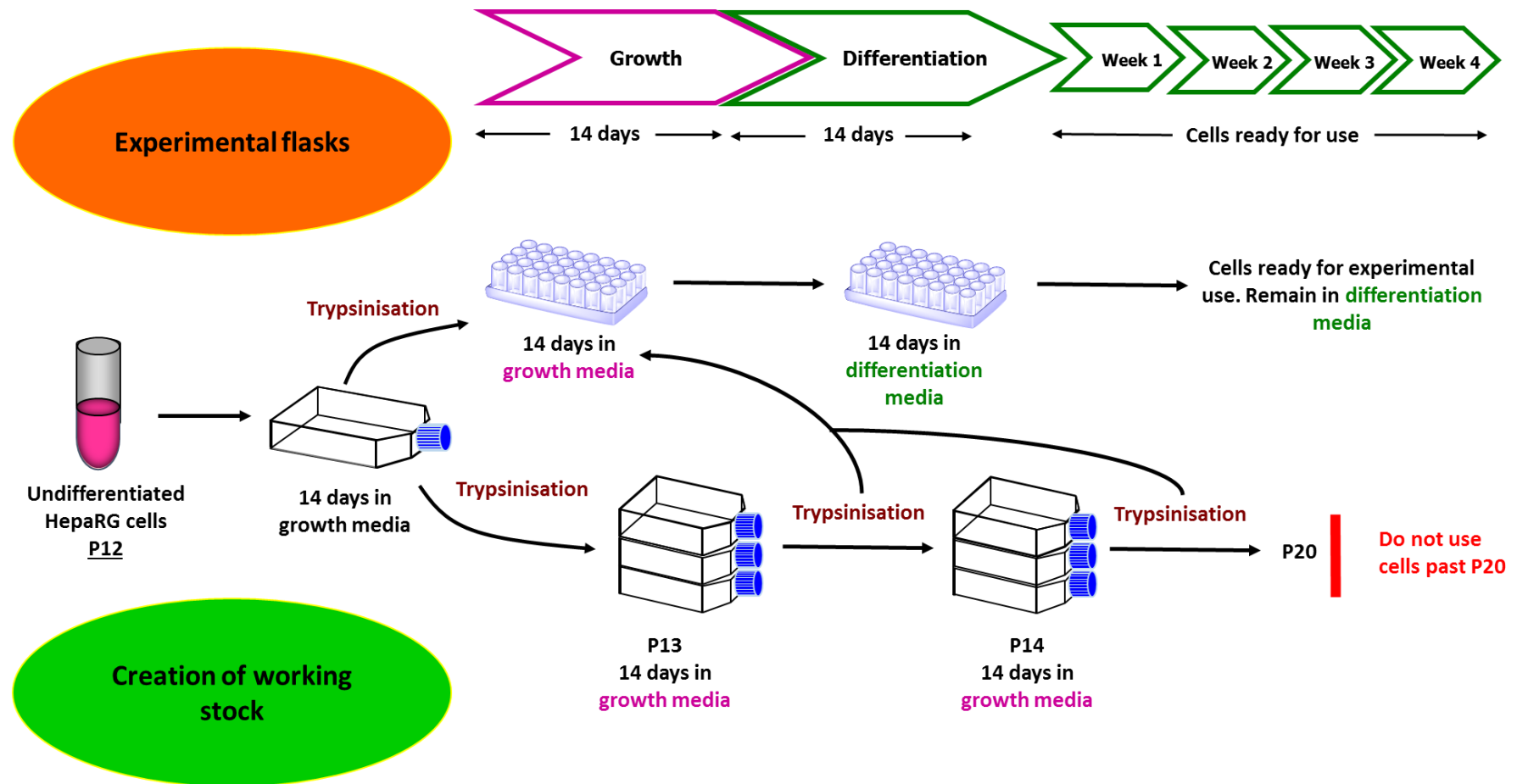


**Figure 2.1: HepaRG cell culture.** Undifferentiated HepaRG cells are supplied by the manufacturers at passage 12. They are grown in growth media for 2 weeks until they reach confluency. After this, the media is swapped to contain 1.7 % DMSO (differentiation media) for an additional 2 weeks. The cells are now differentiated and can be kept in differentiation media for 4 weeks until they are used for experimental purposes.

### 2.2.4 Bile Acid Treatment

HepaRG cells were treated once differentiated into mature hepatocytes. BA mixtures were prepared as 200 x stock solutions in DMSO and the final solvent concentration was diluted to 0.5 % with a vehicle control in each experiment. HepaRG cells were treated for 24 and 72 h or 1 and 2 weeks (compounds were replenished twice a week). A mixture containing the 6 most abundant BAs found within human plasma at physiological levels was prepared as the 1 x BA mixture (Xiang et al., 2010) (table 2.2). The concentrations of the individual BAs were increased in order to create a 10, 100 and 1000 x BA mixture.

**Table 2.2: Composition of the BA mixtures and the concentrations of the individual BAs within the mixtures.** The concentrations of the BAs were increased in order to generate a 1, 10, 100 and 1000 x BA mixture.

<b>Bile acid</b>	<b>Concentration in 1 x BA (<math>\mu\text{M}</math>)</b>	<b>Concentration in 10 x BA (<math>\mu\text{M}</math>)</b>	<b>Concentration in 100 x BA (<math>\mu\text{M}</math>)</b>	<b>Concentration in 1000 x BA (<math>\mu\text{M}</math>)</b>
Cholic acid	0.41	4.1	41	410
Chenodeoxycholic acid	0.64	6.4	64	640
Deoxycholic acid	0.48	4.8	48	480
Lithocholic acid	0.008	0.08	0.8	8
Ursodeoxycholic acid	0.14	1.4	14	140
Glycochenodeoxycholic acid	0.8	8	80	800
<b>Sum</b>	<b>2.478</b>	<b>24.78</b>	<b>247.8</b>	<b>2478</b>

### 2.2.5 Proteomic Analysis of Biliary Transporters in HepaRG Cells and HepG2 Cells

#### 2.2.5.1 Assay Preparation

Undifferentiated HepaRG cells were plated onto 6-well plates at  $2 \times 10^5$  cells/well and cultured to differentiation as described in Section 2.2.3. To assess the biliary transporter expression in untreated HepaRG cells, cells were lysed in Radio-Immunoprecipitation Assay (RIPA) buffer once differentiated. To assess the effects of BA mixtures on biliary transporter

expression, cells were treated for 24 and 72 h or 1 and 2 weeks as described in Section 2.2.4 and then lysed in RIPA buffer.

HepG2 cells were collected by trypsinisation with 0.25 % trypsin and seeded onto collagen coated (50 µg/mL in 0.02 M acetic acid) 6-well plates at  $1 \times 10^6$  cells/well. Cells were cultured as described in Section 2.2.2. Following 24 h in culture, HepG2 cells were lysed in RIPA buffer to assess biliary transporter expression in untreated cells.

### 2.2.5.2 Bicinchoninic Acid Assay (BCA) for Protein Quantification

Standards in the range of 0 – 1 mg/mL BSA were added in duplicate to a 96-well plate and samples diluted in the appropriate amount of diluent. The copper sulphate solution was diluted 1:50 in the BCA solution and 200 µL was added to each well. The plate was incubated for 30 mins at 37 °C and the absorbance read at 562 nm using a Varioskan™ Flash multimode plate reader with SkanIt™ software. This assay is centred around 2 reactions in which a colorimetric reaction occurs that is proportional to the amount of protein in the sample (figure 2.2) (Smith et al., 1985). Peptide bonds within proteins reduce  $\text{Cu}^{2+}$  to  $\text{Cu}^+$  and two molecules of BCA bind with each  $\text{Cu}^+$  forming a purple coloured complex that absorbs light at 562 nm (Smith et al., 1985).

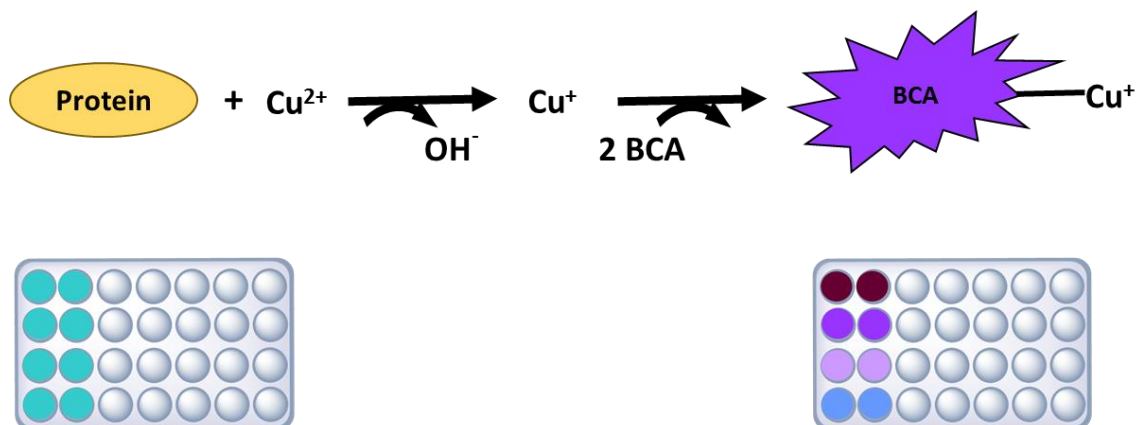


**Figure 2.2: Illustration of the BCA assay used for protein quantification.**  $\text{Cu}^{2+}$  is reduced by peptide bonds. The resulting  $\text{Cu}^+$  reacts with 2 molecules of BCA to form a purple complex that is proportional to the amount of protein within the sample.

### 2.2.5.3 Western Blot Analysis

20 µg of each sample was mixed with 5 µL of sample-loading dye. Samples were heat denatured at 37 °C for 30 mins before being loaded into NuPAGE® 4-12 % Bis-Tris pre-cast

gels together with 5  $\mu$ L of Precision Plus Protein™ molecular weight marker. The proteins were separated by molecular weight in a MOPS-sodium dodecyl sulphate (SDS) buffer (50 mM MOPS, 50 mM Tris-base, 0.1 % (w/v) SDS, 1 mM ethylenediaminetetraacetic acid (EDTA)) at 170 V for 1 h.

The gel was transferred onto a nitrocellulose membrane for 1 h at 220 V in transfer buffer (25 mM Tris-base, 192 mM glycine, 20 % (v/v) methanol) and blocked using 10 % (w/v) non-fat milk in Tris buffered saline-tween (TBS-T) (137 mM NaCl, 2.7 mM KCl, 19 mM Tris-base, 0.01 % (v/v) Tween-20, pH 7.4) at room temperature for 1 h. Incubation and dilution conditions for the primary and secondary antibodies were dependent on the protein of interest (table 2.3). Primary antibodies were diluted in 5 % (w/v) non-fat milk TBS-T and incubated overnight at 4 °C. The membranes were washed in TBS-T and incubated with the appropriate horseradish peroxidase (HRP)-conjugated secondary antibody (1:10,000), diluted in 5 % (w/v) non-fat milk TBS-T for 2 h at 4 °C. Protein bands were visualised using an ECL system. Briefly, the substrate luminol is oxidised by hydrogen peroxide in the presence of the catalyst HRP to yield a chemiluminescent product (Khan et al., 2014). As the product decays to a lower energy state, photons of light are released which can be captured by X-ray films (Khan et al., 2014). Densitometry analysis was performed with Image J 1.48 software.

**Table 2.3: Western blot incubation conditions for primary and secondary antibodies.** Summary of primary antibodies, dilution conditions and appropriate secondary HRP-conjugated secondary antibody.

Protein	Antibody product code	Molecular weight (kDa)	Primary antibody (in 5 % milk)	HRP-conjugated Secondary antibody (in 5 % milk)
MRP1	ab3369	190	1:200	Anti-mouse
MRP2	ab3373	174	1:40	Anti-mouse
BSEP	ab155421	146	1:750	Anti-rabbit
NTCP	ab131084	38	1:100	Anti-rabbit
GAPDH	ab8245	37	1:5000	Anti-mouse

## 2.2.6 Fluorescence Imaging of Biliary Transporters

### 2.2.6.1 Assay preparation

Undifferentiated HepaRG cells were plated onto collagen coated (50  $\mu$ g/mL in 0.02 M acetic acid) glass coverslides in 12-well plates at  $8 \times 10^4$  cells/well and cultured until differentiation as described in Section 2.2.3. To assess the effect of BA mixtures on biliary transporter activity, differentiated HepaRG cells were treated for 24 h as described in Section 2.2.4.

HepG2 cells were collected by trypsinisation with 0.25 % trypsin and seeded onto collagen coated (50 µg/mL in 0.02 M acetic acid) glass coverslides in 12-well plates at  $2 \times 10^6$  cells/well. Cells were cultured as described in Section 2.2.2.

### 2.2.6.2 Immunofluorescence Analysis of Biliary Transporters

Cells were washed twice with PBS and then fixed in 4 % (w/v) paraformaldehyde (PFA) for 30 mins at 4 °C. Cells were again washed twice in PBS and then permeabilised with two 15 min washes in permeabilisation buffer (0.2 % (v/v) Tween-20 and 0.5 % (v/v) Triton X-100 in PBS) at 4 °C. Non-specific binding was blocked using 5 % (w/v) BSA reconstituted in permeabilisation buffer for 1 h at room temperature. Incubation and dilution conditions for the primary and secondary antibodies were dependent on the protein of interest (table 2.4). Primary antibodies were diluted in 5 % (w/v) BSA permeabilisation buffer and incubated with the sample overnight at 4 °C. Cells were washed 3 times for 15 mins in permeabilisation buffer before being incubated in the dark with secondary Alexa Fluor® conjugated secondary antibodies (488 nm/568 nm) (1:1000) diluted in 5 % (w/v) BSA permeabilisation buffer for 1 h at room temperature. Cells were washed in PBS and then incubated in the dark with Hoechst (nucleus) (1:5000) and phalloidin (filamentous-actin) (1:250) dyes; diluted in PBS at room temperature for 20 mins. Samples were mounted onto glass microslides with Pro-Long Gold anti-fade reagent and left to dry overnight at 4 °C. Maximum intensity projection images and snap images were taken using a Zeiss Axio Observer.Z1 widefield florescent microscope with Apotome using 40 x oil objective.

**Table 2.4: Immunofluorescence incubation conditions for primary and secondary antibodies.**

Protein	Antibody product code	Primary antibody (in 5% BSA)	Secondary antibody (in 5% BSA)
MRP2	ab3373	1:200	Anti-mouse
BSEP	ab155421	1:750	Anti-rabbit
NTCP	ab131084	1:200	Anti-rabbit

### 2.2.6.3 Analysis of MRP2 and Pgp Function

HepG2 cells were incubated with CMFDA (5 µM) and Hoechst (1:5000) in HBSS for 30 mins at 37 °C. CMFDA passively diffuses from the incubation media across the cell membrane. Within the cell it is converted into the impermeable MRP2 and Pgp substrate, glutathione-methylfluorescein (GSMF) (Forster et al., 2008). Cells were washed with HBSS to eliminate excess CMFDA and then mounted with Pro-long gold onto glass microslides. Snap images

with Apotome were taken using a Zeiss Axio Observer.Z1 widefield florescent microscope with Apotome using 40 x oil objective.

HepaRG cells were incubated with CMFDA (5  $\mu$ M) and Hoechst (1:5000) with or without MK571 (30  $\mu$ M) and bosentan (50  $\mu$ M) in HBSS for 30 mins at 37 °C and treated as described above.

### **2.2.7 Statistical Analysis**

Data is expressed from a minimum of three independent experiments. Unless specified otherwise, all results are expressed as mean  $\pm$  standard error of the mean (SEM). Normality was assessed using a Shapiro-Wilk statistical test. An unpaired t test was used to compare transporter expression between HepG2 cells and HepaRG cells. Statistical significance compared to the control was determined by a one-way ANOVA with a Dunnett's test for parametric data or a Kruskal-Wallis test for non-parametric data using StatsDirect 3.0.171. Results were considered significant when  $P < 0.05$ .

## 2.3 RESULTS

### 2.3.1 Comparison of Transporter Expression between HepaRG Cells and HepG2 cells

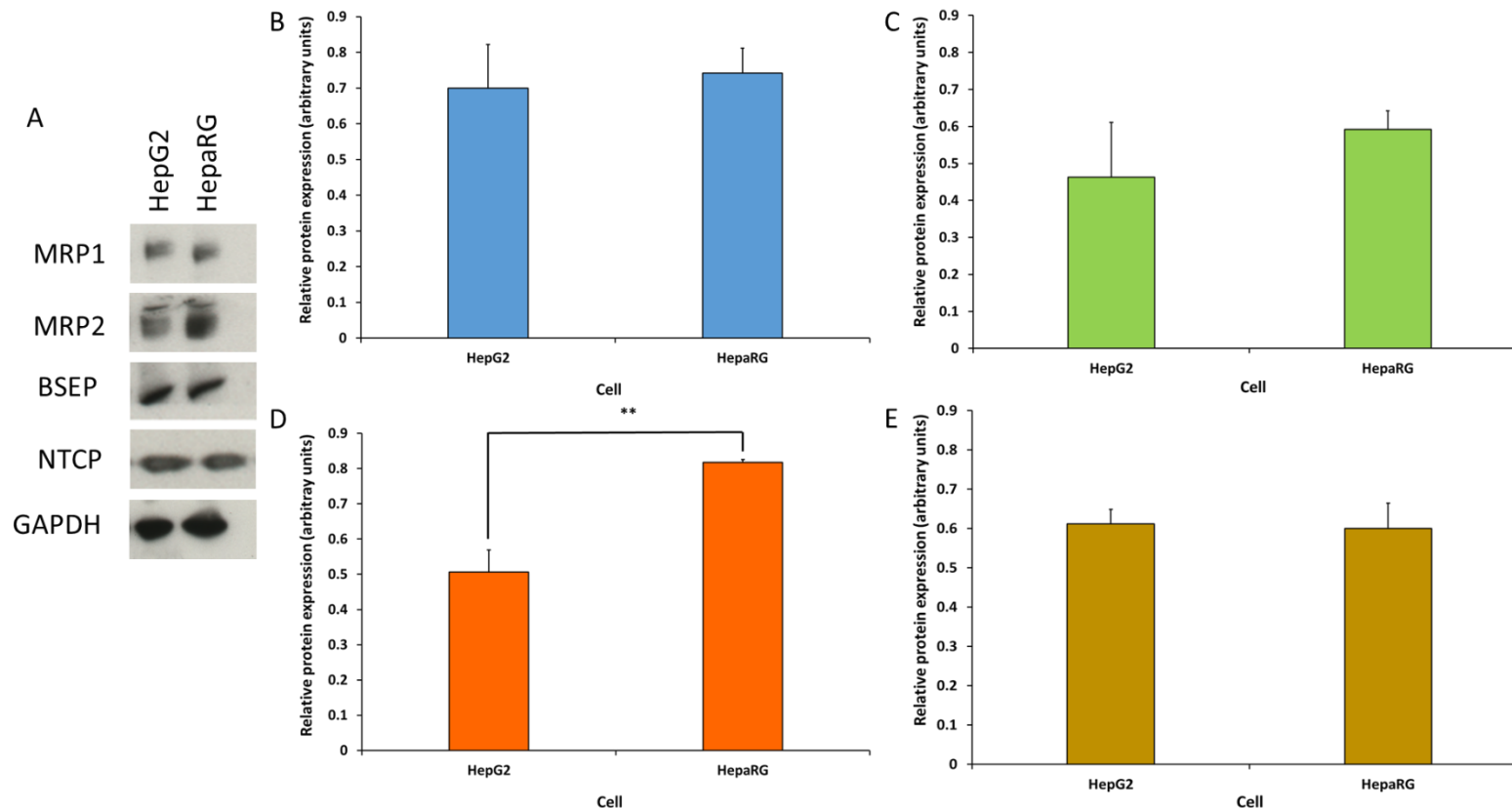


**Figure 2.3: Differences in biliary transporter expression between HepG2 and HepaRG cells.** (A) 20  $\mu$ g of lysate protein was separated by gel electrophoresis and probed for influx and efflux biliary transporters. GAPDH was used as a loading control. The bands were quantified using Image J and differences in (B) BSEP, (C) NTCP, (D) MRP2 (E) MRP1 between HepG2 and HepaRG cells were assessed. Statistical significance was determined by an un-paired t-test. \*  $p < 0.05$ , \*\* $p < 0.01$ , \*\*\* $p < 0.001$ , \*\*\*\* $p < 0.0001$ .

Differences in biliary transporter expression between HepG2 and HepaRG cells were assessed via western blot. There were no significant differences between the levels of BSEP, NTCP and MRP1 between the two cell lines. In contrast, the expression of MRP2 was significantly greater in HepaRG cells than HepG2 cells by 60 % (figure 2.3A).

### 2.3.2 Examining Biliary Transporter Localisation and Function in HepG2 Cells

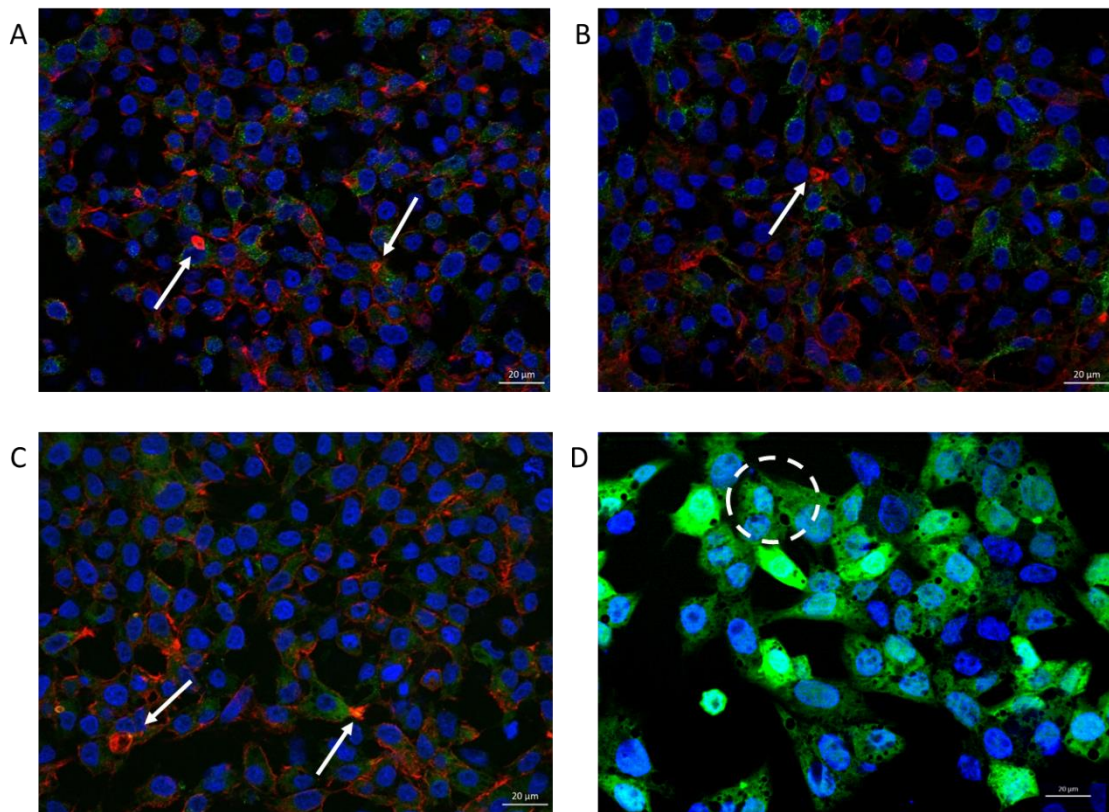


**Figure 2.4: Biliary transporter localisation and function in HepG2 cells.** Cells were fixed with 4 % PFA and stained with primary antibodies specific for influx and efflux transporters (green), Hoechst (blue) and phalloidin (red). (A) BSEP localisation, (B) NTCP localisation, (C) MRP2 localisation. (D) HepG2 cells were incubated with CMFDA (green) and Hoechst. Snap images with Apotome were taken using a Zeiss microscope using 40 x oil objective. Arrows represent suspected bile canaliculi. Dotted circle indicates an example of a cell where CMFDA is retained with the cytoplasm. Scale bar = 20 µm.

In order to function correctly, hepatocytes must polarise. This involves the establishment of bile canaliculi between neighbouring cells and the correct localisation of biliary transporters to the basolateral or canalicular membrane (Gissen and Arias, 2015). Following the confirmation of biliary transporter expression in HepG2 cells (figure 2.3), immunofluorescence was used to analyse transporter localisation. HepG2 cells were stained with Hoechst (blue) to stain the nucleus, phalloidin (red) to stain F-actin structures and the

appropriate biliary transporter antibody (green) (figure 2.4A - C). The actin structures formed dense circular regions (white arrows in figure 2.4A - C), which were suspected bile canaliculi. HepG2 cells failed to polarise as the canalicular transporters BSEP and MRP2 did not localise at the canalicular membrane but were retained within the cell cytoplasm (figure 2.4A and C). Additionally, the influx transporter NTCP was not expressed on the basolateral membrane (figure 2.4B). The functionality of MRP2 and Pgp was assessed using the green fluorescent dye CMFDA (Forster et al., 2008). In HepG2 cells, there was retention of CMFDA in the cell cytoplasm (figure 2.4D), indicating that MRP2 and Pgp were not functional.

### **2.3.3 Examining Biliary Transporter Localisation and Function in HepaRG Cells**

Once differentiated, HepaRG cells are a heterogeneous population of hepatocytes and primitive biliary-like cells (Marion et al., 2010). The hepatocyte colonies can be distinguished due to the formation of bile canaliculi (figure 2.5A and C, white arrows). HepaRG cells polarised as BSEP and MRP2 correctly localised at the canalicular membrane (figure 2.5A and C) and NTCP localised to the basolateral membrane (figure 2.5B). HepaRG cells expressed functioning biliary transporters as seen by the efflux of CMFDA into the bile canaliculi by MRP2 and Pgp transporters (figure 2.5D).

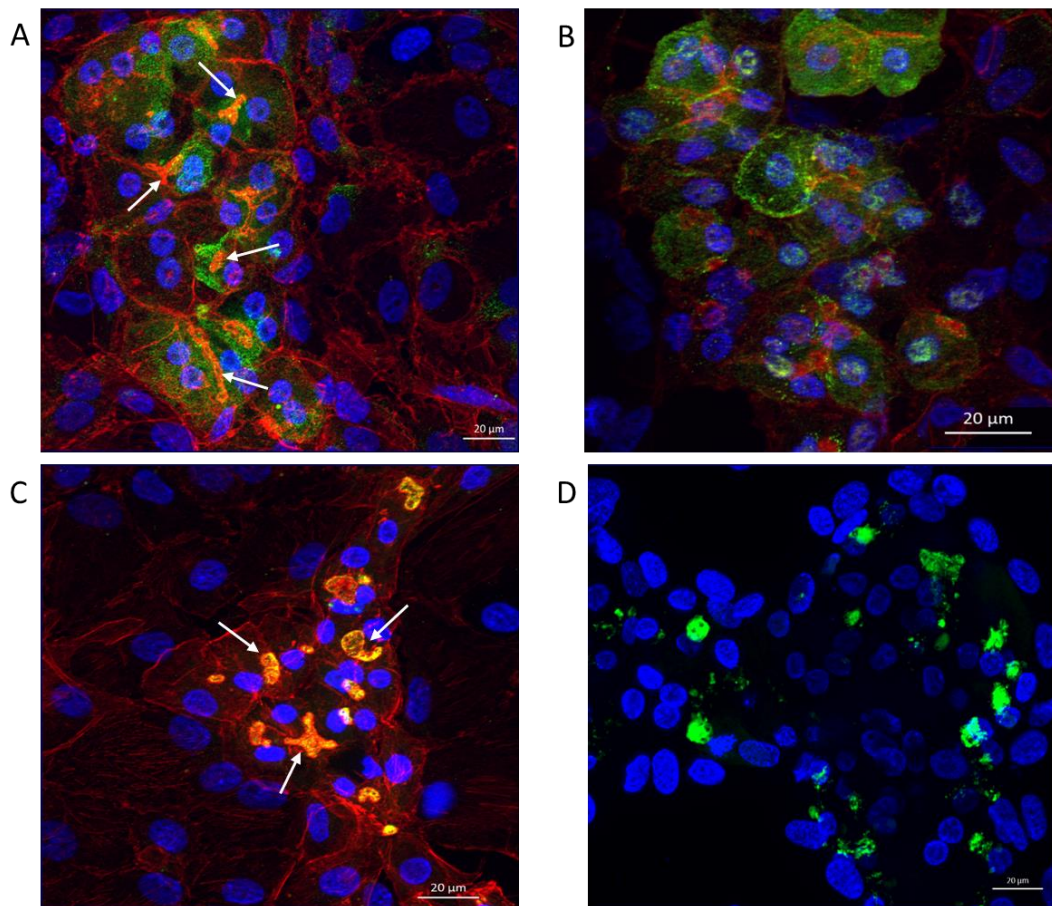


**Figure 2.5: Biliary transporter localisation and function in HepaRG cells.** Cells were fixed with 4 % PFA and stained with primary antibodies specific for influx and efflux transporters (green), Hoechst (blue) and phalloidin (red). (A) BSEP localisation, (B) NTCP localisation, (C) MRP2 localisation. (D) HepG2 cells were incubated with CMFDA (green) and Hoechst. Maximum intensity images with Apotome were taken using a Zeiss microscope using 40 x oil objective. Arrows represent bile canaliculi. Scale bar = 20 μm.

### 2.3.4 Determining Biliary Transporter Inhibition in HepaRG Cells

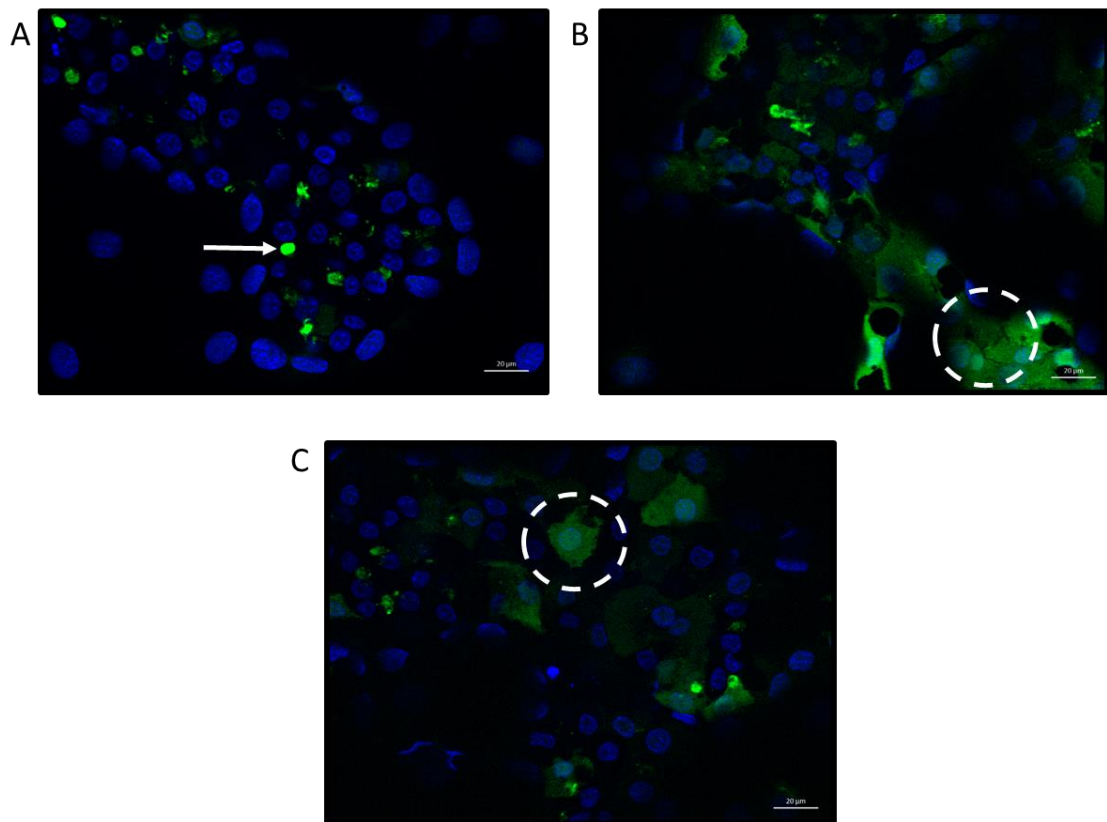


**Figure 2.6: Biliary transporter function and inhibition in HepaRG cells.** HepaRG cells were incubated with (A) CMFDA and Hoechst only for 30 mins, (B) CMFDA, Hoechst and the MRP inhibitor MK571 for 30 mins, (C) CMFDA, Hoechst and the BSEP inhibitor bosentan for 30 mins. Maximum intensity images with Apotome were taken using a Zeiss microscope using 40 x oil objective. Arrow indicates CMFDA within the bile canaliculi whereas the dotted circles indicate CMFDA retained within the cell cytoplasm. Scale bar = 20 µm.

During DIC, biliary transporters can be inhibited leading to the retainment of BAs within hepatocytes (Woolbright and Jaeschke, 2015). Therefore, it was essential that the biliary transporters in HepaRG cells could be inhibited in order to recapture the transporter inhibition seen in DIC. HepaRG cells were treated with known BSEP and MRP inhibitors, bosentan and MK571, and the transport of CMFDA into the bile canaliculi was evaluated. Sole inhibition of BSEP or MRP2 prevented the efflux of CMFDA into the bile canaliculi and it was retained within the cell cytoplasm (figure 2.6B and C).

### 2.3.5 Assessment of the Effects of BA Mixtures on Biliary Transporter Function and Expression in HepaRG Cells

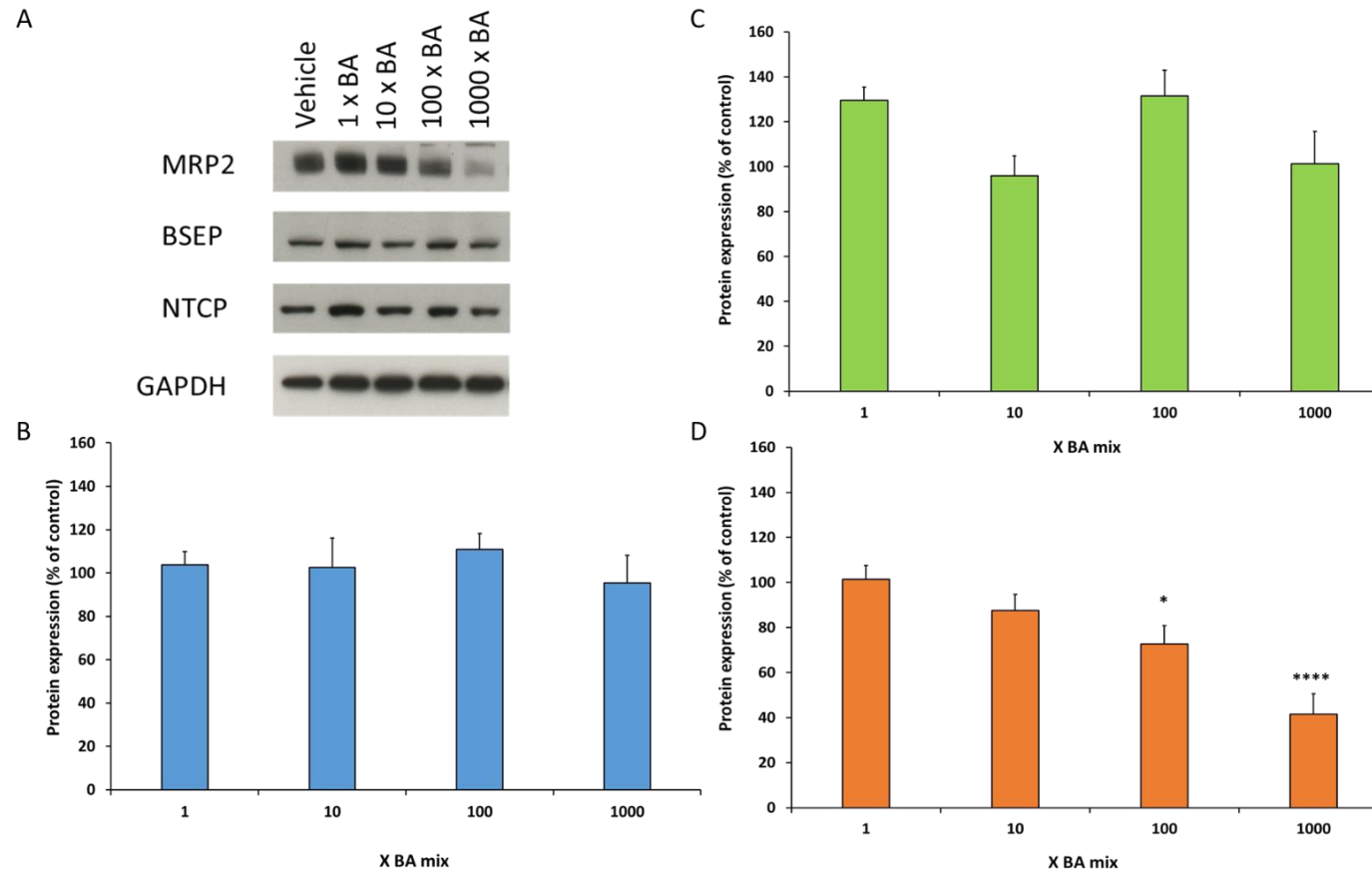


**Figure 2.7: The effects of 24 h BA mix treatment on biliary transporter expression.** (A) 20  $\mu$ g of lysate protein was separated by gel electrophoresis and probed for influx and efflux biliary transporters. GAPDH was used as a loading control. The bands were quantified using Image J and differences in (B) BSEP, (C) NTCP, (D) MRP2 expression compared to the control were assessed.

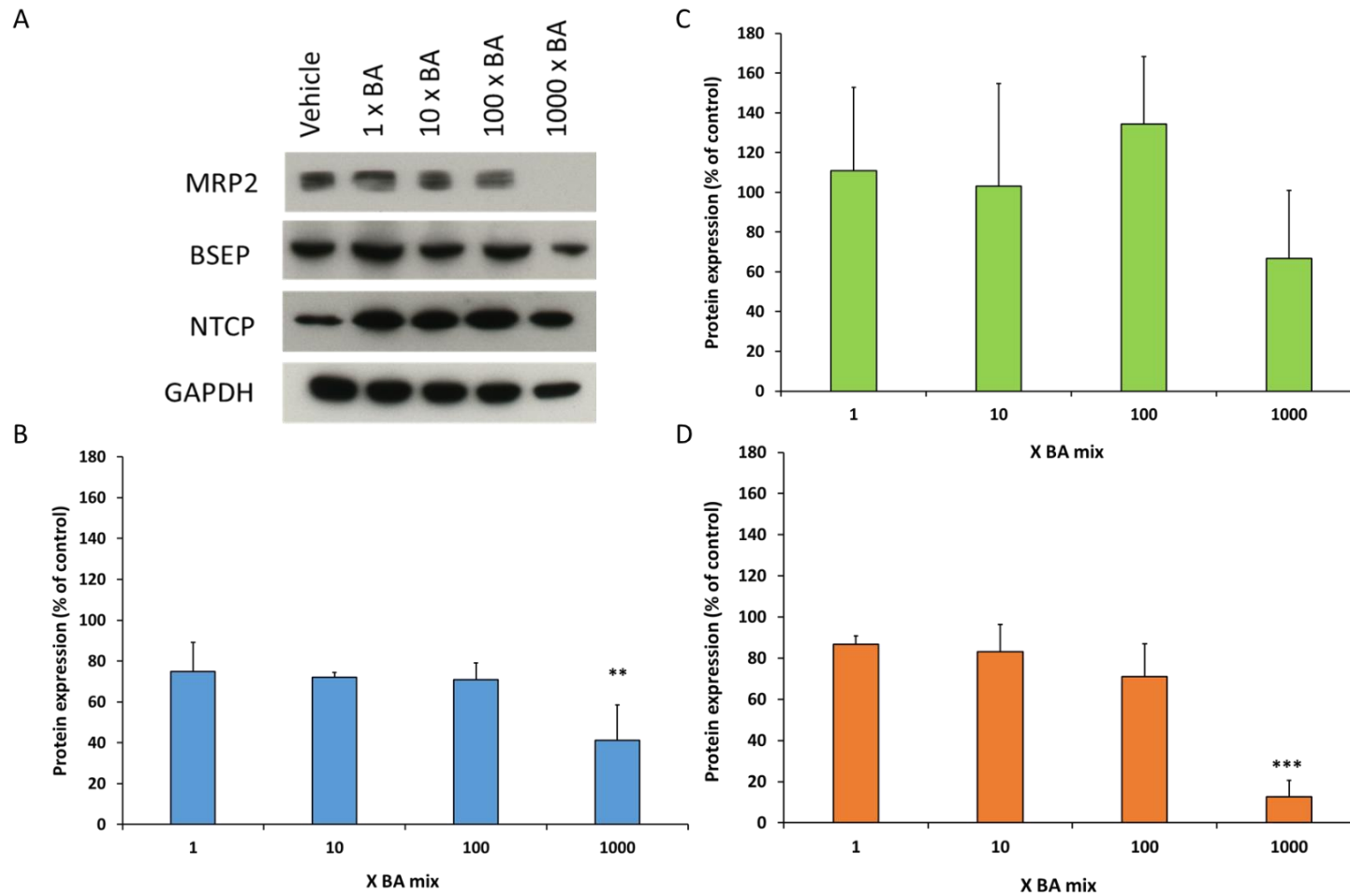


**Figure 2.8: The effects of 2 weeks BA mix treatment on biliary transporter expression.** (A) 20  $\mu$ g of lysate protein was separated by gel electrophoresis and probed for influx and efflux biliary transporters. GAPDH was used as a loading control. The bands were quantified using Image J and differences in (B) BSEP, (C) NTCP, (D) MRP2 expression compared to the control were assessed.

The expression of biliary transporters important in BA influx and efflux was assessed over time in HepaRG cells following BA mix treatment. There was a temporal reduction in the expression of BSEP and MRP2 (figure 2.7D, 2.8B and 2.8D). Following 24 h BA mix treatment, the expression of MRP2 had significantly reduced by  $27.2 \pm 8.0 \%$  with the 100 x BA mix and by  $58.4 \pm 8.9 \%$  with the 1000 x BA mix. Following 24 h BA mix treatment, the expression of other biliary transporters remained unchanged. However, following 2 weeks of treatment, there was a significant reduction in the expression of BSEP by  $58.7 \pm 17.3 \%$  following 1000 x BA mix treatment (figure 2.8B). Additionally, following 2 weeks of treatment, there was negligible expression of MRP2 after treatment with the 1000 x BA mix with a significant reduction in expression of  $87.5 \pm 8.1 \%$  (figure 2.8D). Furthermore, after 24 h BA mix treatment, the activity of MRP2 and Pgp had been reduced as indicated by the retainment of CMFDA within the cell cytoplasm (figure 2.9).

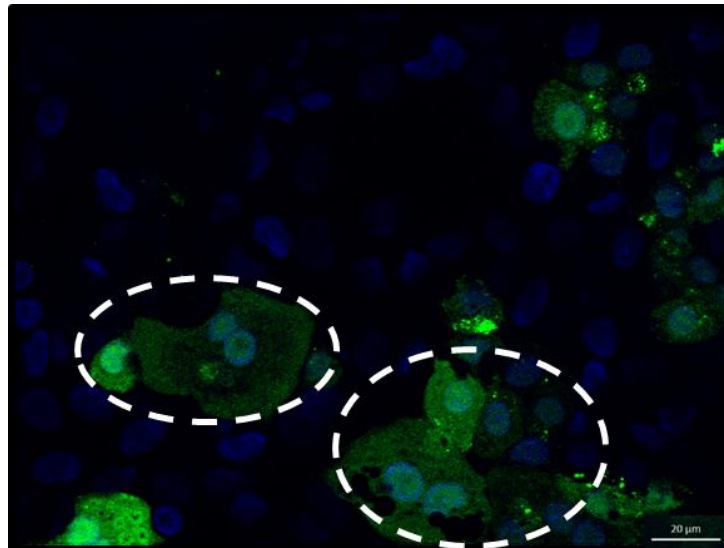


**Figure 2.9: Effects of 24 h BA mixtures on MRP2 and Pgp activity.** Transporter inhibition following 24 h 1000 x BA mix treatment. Dotted circle indicates CMFDA retainment in the cytoplasm due to failed activity of MRP2 and Pgp transporters. Scale bar = 20  $\mu\text{m}$ .

### 2.3.6 Assessment of the Effects of Rotenone on Biliary Transporter Function and Expression in HepaRG Cells

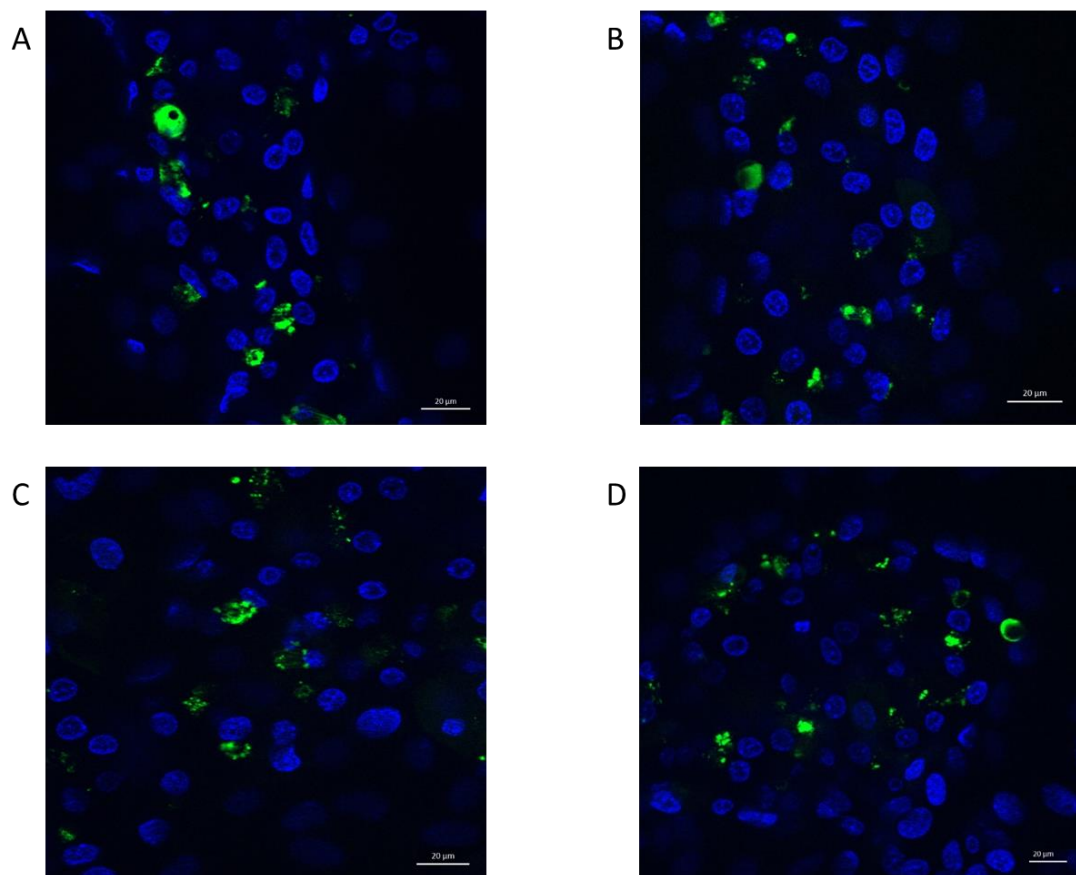


**Figure 2.10: The effects of rotenone on biliary transporter function in HepaRG cells.** HepaRG cells were treated (A) Vehicle, (B) 0.001  $\mu\text{M}$  rotenone, (C) 0.01  $\mu\text{M}$  rotenone, (D) 0.1  $\mu\text{M}$  rotenone for 24 h and incubated with CMFDA and Hoechst for 30 mins. Maximum intensity images with Apoptome were taken using a Zeiss microscope using 40 x oil objective. Scale bar = 20  $\mu\text{m}$ .

Rotenone is a known mitochondrial toxin and is a potent complex I inhibitor (Lindahl and Oberg, 1961). The effects of rotenone on biliary transporter function and expression were assessed in HepaRG cells following 24 h treatment. Rotenone did not exert any changes in the activity of MRP2 or Pgp as indicated by the efflux of CMFDA into the bile canaliculi (figure 2.10). Additionally, there were no differences in the expression of BSEP, NTCP and MRP2 compared to the control following 24 h rotenone treatment (figure 2.11).

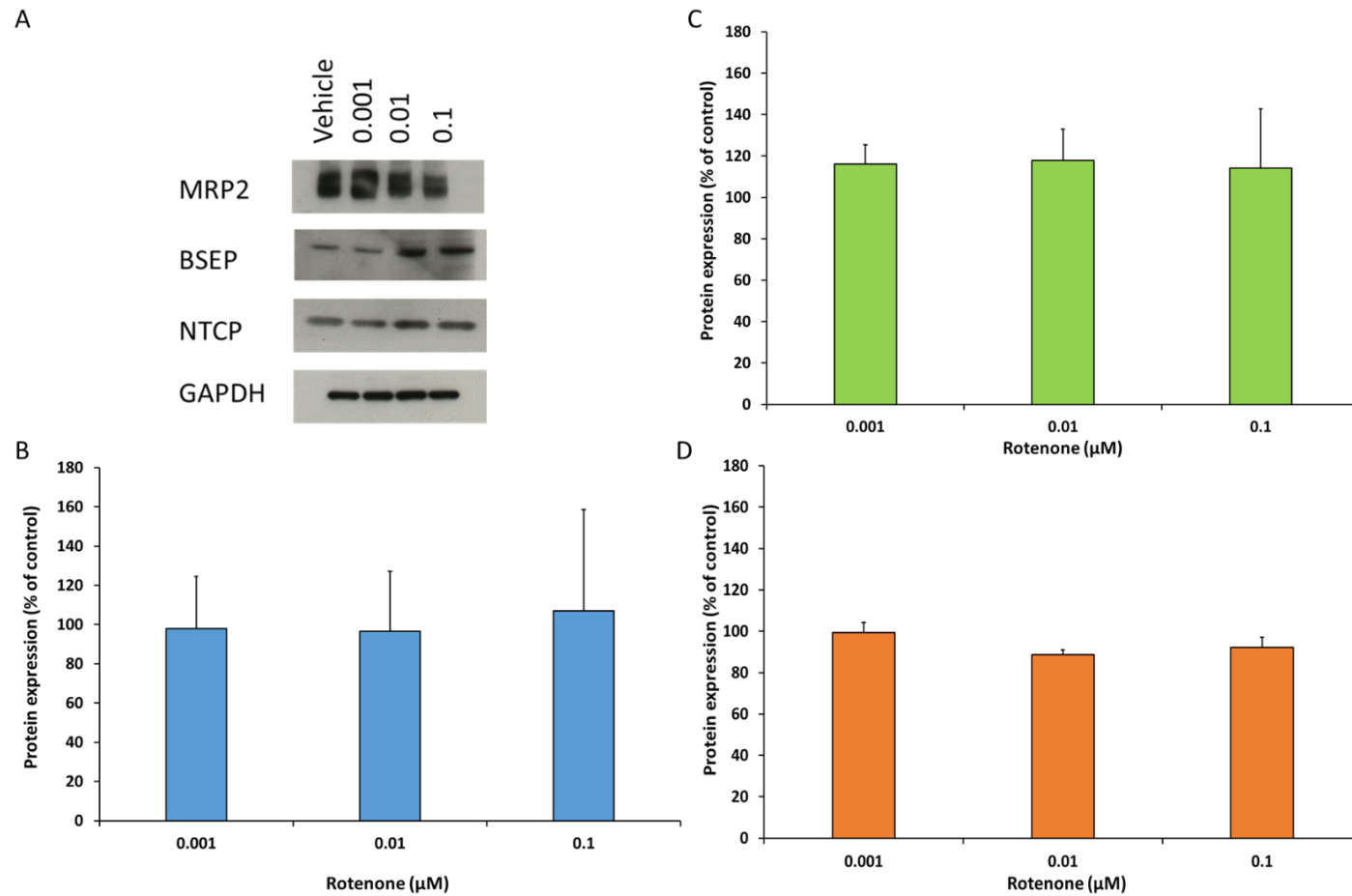


**Figure 2.11: The effects of 24 h rotenone on biliary transporter expression in HepaRG cells.** (A) 20  $\mu\text{g}$  of lysate protein was separated by gel electrophoresis and probed for influx and efflux biliary transporters. GAPDH was used as a loading control. The bands were quantified using Image J and differences in (B) BSEP, (C) NTCP, (D) MRP2 expression compared to the control were assessed.

## 2.4 DISCUSSION

HepG2 cells are the most common hepatic cell line used for the identification of compounds with DILI liabilities. However, the findings presented in this chapter have shown that they are not a physiologically relevant cell line for cholestatic studies as they fail to polarise and therefore do not express functioning biliary transporters required for BA transport (Gerets et al., 2012a).

The ability of hepatocytes to polarise is an important function that is necessary for the correct flow of bile. Failures in BA secretion from hepatocytes can lead to cholestatic disease (Gissen and Arias, 2015). Whilst it has been shown that some hydrophobic BAs can enter the cell via passive diffusion, active transporter-mediated uptake and efflux is the major route of BA transport, thus requiring a cell line that can encapsulate this movement (Hofmann et al., 1999). The observation of similar transporter expression in HepG2 cells and HepaRG cells, notably NTCP (figure 2.3A and 2.3C), differs to observations in the literature. Various research has shown that HepG2 cells have low levels or no NTCP mRNA (Kullak-Ublick et al., 1996; Libra et al., 2006; Marin et al., 2003; Su et al., 2004; Wang et al., 2020). Due to this observation, many researchers transfect HepG2 cells with NTCP in order to increase expression and enable substrate influx (Sun et al., 2017). The HepG2 cells used in this research had not been transfected with NTCP and so the observation of similar NTCP expression between the HepG2 cells and HepaRG cells was surprising. HepaRG cells have been shown to express NTCP that localises to the basolateral membrane and can correctly influx BAs and a variety of substrates into the hepatocytes (Bachour-El Azzi et al., 2015; Donkers et al., 2017; Kotani et al., 2012; Le Vee et al., 2006; Mayati et al., 2018). Proteomic and mRNA analysis between HepaRG cells and 3 different cryopreserved human hepatocytes has revealed that the expression of NTCP was comparable however, no such comparisons of NTCP expression between HepG2 cells and human hepatocytes could be found in the literature (Kotani et al., 2012). Due to the cancer origin of cell lines, it is possible that cells can acquire SNPs leading to genetic drift. In order to minimise this possibility, cell lines should only be cultured up to a specified passage number. The observation of NTCP expression and localisation in HepaRG cells (figure 2.5) replicates numerous observations in the literature and so the utility of the HepaRG cells in this research is not questioned. However, it would be beneficial for future work to characterise the HepG2 cells and determine NTCP expression with more advanced proteomic analysis such as mass spectrometry as was undertaken by Sison-Young et al., as most NTCP characterisation in HepG2 cells has been done at the mRNA

level (Sison-Young et al., 2015). Nonetheless, whilst the HepG2 cells used in this chapter expressed influx and efflux transporters at the proteomic level, immunomicroscopy revealed that they failed to localise at the correct membranes, instead remaining within the cell cytoplasm. In order to emulate the correct physiological characteristics of hepatocytes in humans, it is essential that the hepatic models used for cholestasis studies polarise and have functional transporters. Therefore, due to the results presented in this chapter, it was concluded that 2D cultured HepaRG cells are a suitable model for DIC studies (Penman et al., 2019).

PHH cultures are promoted as the gold standard model for DILI studies as they are thought to most closely resemble hepatocytes within the human body (Atienzar et al., 2016). Due to the low availability of PHH, rodent hepatocytes have been routinely used in cholestasis studies (Woolbright and Jaeschke, 2015). However, rodent hepatocytes also represent a poor model choice for DIC studies. Notably, this is due to differences in biliary transporter expression between PHH and rodent hepatocytes. PHH are able to maintain their transporter activity for 24 h and do not start undergoing dedifferentiation until 72 h, whereas rodent hepatocytes rapidly dedifferentiate and lose their transporter activity (Liang et al., 1993; Rippin et al., 2001). Additionally, the majority of BA efflux in humans occurs at the canalicular membrane whereas in rodent hepatocytes, basolateral efflux via MRP3 and MRP4 are the predominant route of BA efflux (Jemnitz et al., 2010). The differences in transporters between PHH and rodent hepatocytes could result in the generation of data with a lack of *in vivo* relevance and translatability to humans. It is imperative that toxicological studies are utilising the most appropriate *in vitro* models in order to prevent non-predictive or misleading data from being generated.

HepaRG cells are used as the “model system for cholestasis prediction” by their manufacturers and several researchers as they share improved resemblance with PHH than HepG2 cells (Guillouzo et al., 2007; Hendriks et al., 2016; HepaRG.com; Susukida et al., 2016; Woolbright et al., 2016). The utility of HepaRG cells for DIC studies was confirmed by their ability to polarise and resultantly, express functioning biliary transporters. Whilst not assessed in this research, HepaRG cells have been shown to express functional influx transporters using fluorescent BAs such as TCA or other radiolabelled NTCP substrates (Bachour-El Azzi et al., 2015; Kotani et al., 2012; Le Vee et al., 2006; Mayati et al., 2018). The efflux of CMFDA into the bile canaliculi confirmed the functionality of Pgp and MRP2. Whilst the activity of BSEP was not assessed in this study, it has been shown that 2D cultured HepG2

cells express non-functioning BSEP whereas 2D cultured HepaRG cells do (Ramaiahgari et al., 2014; Sharanek et al., 2016). During DIC, biliary transporter constraints by drugs can lead to the retainment of BAs within hepatocytes (Woolbright and Jaeschke, 2015). Therefore, it was essential that the biliary transporters could be inhibited in HepaRG cells in order to recapitulate the toxicity seen in DIC. Inhibition of MRP transporters with MK571 and BSEP with bosentan prevented the efflux of CMFDA into the bile canaliculi, indicating that HepaRG cells could be manipulated to recapture transporter inhibition as seen in DIC (Woolbright and Jaeschke, 2015). Under physiological conditions, the efflux of BAs via the basolateral membrane is negligible however, during cholestasis, the expression of MRP3 and MRP4 are upregulated to act as compensatory mechanisms of BA efflux (Trauner and Boyer, 2003). MK571 is an inhibitor of the MRP family of transporters and has been shown to inhibit MRP3, MRP4 and MRP2 (Gekeler et al., 1995; Lien et al., 2014; Tivnan et al., 2015; Weiss et al., 2007). Therefore, the use of MK571 and bosentan would lead to the retainment of BAs within HepaRG cells, as mechanisms of efflux via the basolateral and canalicular membrane would be inhibited.

The hypothesis for this work was based upon research by Aleo *et al*, in which they found compounds with dual potency to inhibit BSEP and mitochondrial function were associated with a severe case of DILI (Aleo et al., 2014). The expression of biliary transporters important in BA influx and efflux were assessed over time following BA mix treatment. To act as a positive control, the effects of a known mitochondrial toxicant, rotenone, were also assessed on biliary transporter expression and activity following 24 h treatment. There was a temporal reduction in the expression of MRP2 and BSEP following 1000 x BA mix treatment, whereas the expression of NTCP remained unchanged. The decline in MRP2 expression commenced from 24 h treatment with the 1000 x BA mix and by 2 weeks there was negligible expression of MRP2, whereas BSEP expression did not significantly decline until 2 weeks 1000 x BA mix treatment. Furthermore, there was a reduction in the efflux of CMFDA into the bile canaliculi after 24 h treatment with the 1000 x BA mix, indicating that the activity of MRP2 and Pgp had been reduced. Due to the requirement of ATP for BSEP and MRP2 activity, it was hypothesised that an impairment in ATP production by rotenone may lead to transporter dysfunction. However, rotenone treatment did not have an effect on transporter expression or activity in HepaRG cells, thus revealing that mitochondrial toxicity alone is insufficient to predict transporter dysregulation.

It is widely acknowledged that drug-induced BSEP inhibition plays a role in the development of cholestasis as a large proportion of compounds with DILI liabilities have been identified as BSEP inhibitors (Aleo et al., 2014; Dawson et al., 2012; Morgan et al., 2010; Pedersen et al., 2013; Stieger, 2010). Resultantly, the European Medicines Agency have recommended that all compounds undergo BSEP screening during drug development (Kenna, 2014). However, it is important to note that BSEP inhibition alone is insufficient to deem a compound with a DILI liability as there are known BSEP inhibitors that do not cause DILI (Aleo et al., 2014). Interestingly, a repression of BSEP expression, in addition to functional inhibition, has been shown to alter hepatic BA homeostasis and contribute to cholestasis (Garzel et al., 2014). Whilst BSEP alterations have been perceived as an important predictive mechanism for DILI, research has shown that compounds with MRP2, MRP3 and/or MRP4 liabilities, in addition to BSEP, were associated with a greater risk of DILI (Köck et al., 2014; Morgan et al., 2013). Therefore, the identification of alterations in both BSEP and MRP2 in this chapter are consistent with current mechanistic understandings of DILI. The toxicity of DIC is multi-mechanistic and it has been revealed that alterations in bile canaliculi dynamics (constriction and dilation) can be early identifiers of toxicity (Burbank et al., 2016). It would be beneficial for future experiments to conduct time-lapse imaging of HepaRG cells following BA mix treatment to identify any alterations in bile canaliculi dynamics to further strengthen the mechanistic understanding of BA-induced toxicity. Research from BSEP binding assays have revealed that drugs typically inhibit BSEP via competitive inhibition however, non-competitive inhibition can occur (Kenna et al., 2018). Future experiments would benefit from expanding this work by conducting transporter inhibition assays following dual treatment with the BA mixtures and a compound with a DILI liability. This would allow observations of whether transporter activity is reduced due to competitive or non-competitive inhibition and determine whether increasing intracellular BAs levels has the potential to displace drugs from inhibiting biliary transporters. Finally, during cholestasis, the expression of basolateral transporters MRP3 and MRP4 are up-regulated to reduce intracellular BA levels and prevent hepatotoxicity (Boyer, 2013; Boyer et al., 2006). Further research should determine the expression of MRP3 and MRP4 before and after BA mix treatment to determine if compensatory mechanisms of cellular protection have been effected.

The potential clinical impacts of a reduction in the expression of BSEP and MRP2 due to pharmacological action are not fully understood (Chan and Benet, 2018). BSEP is the main transporter responsible for the efflux of bile from hepatocytes and its functionality is essential for normal liver activity. Bile is essential for the digestion of lipids and therefore

failures in secretion due to BSEP repression have the potential to cause malnourishment, fatigue and a lack of fat-soluble vitamins (Milkiewicz and Heathcote, 2004; Werner et al., 2004). Whilst mechanistically different to drug-induced inhibition or repression of BSEP, patients harbouring the genetic condition PFIC2 have a reduction in BSEP transcription and translation, which leads to decreased protein stability and activity, and in some cases complete absence (Byrne et al., 2009; Evason et al., 2011; Ho et al., 2010). These individuals are subjected to early-onset cholestasis, progressive liver injury and fatality if not treated by liver transplantation, thus highlighting the importance of BSEP *in vivo* (Strautnieks et al., 1998). In addition to the transport of glucuronidated and sulphated BAs, MRP2 is also responsible for the efflux of many anti-cancer drugs, leukotrienes and conjugated bilirubin (Akita et al., 2001; Gerk and Vore, 2002). Whilst MRP2 is not the major transporter for BA efflux, a loss of its function could be detrimental to hepatocytes due to effects on other substrates and thus have serious clinical implications. Loss of MRP2 results in the upregulation of MRP3 and MRP4 to act as compensatory mechanisms of efflux (Keppler, 2014). Efflux of bilirubin by MRP3 causes a rise in the levels of conjugated bilirubin in the blood (Konig et al., 1999). *In vivo* experiments in rodents have shown that a reduction in MRP2 leads to conjugated hyperbilirubinemia and jaundice, which is a similar phenotype seen in patients with Dubin-Johnson syndrome, who are deficient in MRP2 (Hashimoto et al., 2002; Kikuchi et al., 2002; Paulusma et al., 1996). Hyperbilirubinemia can induce organ dysfunction due to the cytotoxic potential of bilirubin and in serious cases lead to brain encephalopathy (Sticova and Jirsa, 2013). However, it is important to note that these clinical observations were detected due to a genetic condition whereby biliary transporter expression was significantly reduced or absent (Hashimoto et al., 2002; Kikuchi et al., 2002; Paulusma et al., 1996; Strautnieks et al., 1998). These findings are not representative of inhibition of a biliary transporter by a small molecule thus making it difficult to determine the clinical impacts of a temporal reduction in MRP2 and BSEP activity and expression as observed in this chapter (Chan and Benet, 2018).

The results presented in this chapter have used cell lines cultured in 2D. Whilst 2D culture of hepatic carcinoma lines has been routinely used in DILI studies, advancements in cell culture conditions to create more *in vivo* likeness has led to the development of 3D spheroidal cells. 3D models are said to better recapitulate the 3D structure of the liver via increased cell-cell interaction and interactions with the extracellular matrix (Mandon et al., 2019). Adaptations in cell culture conditions typically revolve around the use of artificial scaffolds acting as matrices for cell growth. There are varieties of matrix mediums ranging from natural

substances such as collagen, gelatin and fibrinogen to synthetic polymers (Luckert et al., 2017).

Adaptations of culture conditions have led to the development of 3D spheroidal HepG2 cells with improved *in vivo* likeness (Miyamoto et al., 2015; Ramaiahgari et al., 2014). Research by Ramaiahgari *et al* found that when HepG2 cells were cultured in 3D with Matrigel, they could be kept in culture for 28 days. Additionally, the cells acquired hepatocyte functions such as albumin secretion, the formation of bile canaliculi, transporter activity and had increased CYP and phase 2 enzymes (Ramaiahgari et al., 2014). Further 3D research using collagen, Matrigel and Alvetex confirmed the results seen by Ramaiahgari *et al*, that 3D culture of HepG2 cells increased *in vivo* resemblance compared to 2D HepG2 cells (Luckert et al., 2017). However, comparison of these results to HepaRG cells revealed that 2D grown HepaRG cells had higher expression and activities of CYP enzymes compared to 2D and 3D grown HepG2 cells (Luckert et al., 2017). In efforts to create simpler methods of 3D culture, HepaRG spheroids have been grown in ultra-low attachment (ULA) plates (Gunness et al., 2013; Mandon et al., 2019; Ramaiahgari et al., 2017). Data revealed that HepaRG spheroids cultured in ULA plates had greater levels of CYP enzymes and a higher sensitivity to genotoxic and DILI compounds than their 2D counterpart (Gunness et al., 2013; Hendriks et al., 2016; Mandon et al., 2019; Ramaiahgari et al., 2017). Whilst it has been shown that there are slight improvements in HepaRG morphology and characteristics when cultured in 3D, there are some limitations with the methodologies for 3D culture. Firstly, 3D cell culture is technically challenging, labour intensive and more expensive when compared with 2D methodologies (Drewitz et al., 2011). Additionally, it has been reported that 3D culture methods can produce less reproducible results than their 2D counterpart due to differences in spheroid size and shape (Miyamoto et al., 2015). Whilst the benefits of culturing HepG2 cells in 3D as opposed to 2D are apparent, the higher cost and proficiency required does not appear to reflect a benefit of increased hepatic function when comparing 2D and 3D HepaRG cells for answering the aims of this thesis. The findings described in this chapter have confirmed the physiological and pharmacological relevance of 2D cultured HepaRG cells as an appropriate model for DIC studies. Resultantly, the remainder of the data presented in this thesis utilising HepaRG cells will be conducted with cells cultured in 2D.

## 2.5 CONCLUSION

The data presented within this chapter has confirmed the utility of HepaRG cells for cholestasis studies over HepG2 cells. HepaRG cells correctly polarised and expressed functional biliary transporters, which could be manipulated with known transporter inhibitors, whereas HepG2 cells failed to polarise. Consequently, it was concluded that 2D cultured HepaRG cells were a physiological and pharmacological suitable model for studying DIC. The study of BA mixture toxicity in HepaRG cells has revealed a temporal reduction in the activity and expression of BSEP and MRP2. Whilst BSEP implications are typically perceived as a predictive mechanism of DILI, research has shown that other ATP-dependent biliary transporters can exacerbate this toxicity. Collectively, alterations to both BSEP and MRP2 could exacerbate DILI however; the predictivity of *in vitro* inhibition to lead to clinical DILI has been questioned. The mitochondrial toxicant rotenone did not cause transporter dysfunction revealing that mitochondrial toxicity alone is insufficient to predict transporter alterations. Despite research indicating BA-mediated mitochondrial toxicity, the mitochondrial dysfunction of the BA mixtures needs to be assessed in HepaRG cells. Only if this relationship is seen can conclusions of the interplay between inhibition of ATP-dependent transporters and mitochondrial function be determined for BAs.

## **Chapter 3**

# **Investigation of Bile Acid-induced Mitochondrial Dysfunction in Isolated Mitochondria and HepaRG Cells**

## CONTENTS

3.1	INTRODUCTION	72
3.2	MATERIALS AND METHODS	74
	3.2.1 Materials	74
	3.2.2 HepG2 Cell Culture	74
	3.2.3 HepaRG Cell Culture	74
	3.2.4 Bile Acid Treatment	74
	3.2.5 Semi-automated Pump Controlled Cell (PCC) Rupture System for the Isolation of Mitochondrial from Cultured Cells	75
	3.2.6 Dual Monitoring of Membrane Potential and Structural Alterations in Isolated Mitochondria	77
	3.2.7 Mitochondrial Membrane Potential in HepaRG Cells	79
	3.2.8 Acute Metabolic Modification Assay	80
	3.2.9 Lactate Dehydrogenase (LDH) Assay	83
	3.2.10 Extracellular Flux Analysis	84
	3.2.11 Statistical Analysis	87
3.3	RESULTS	88
	3.3.1 Examining Mitochondrial Purity from the Crude Mitochondrial Extract	88
	3.3.2 Assessment of the Effects of BA Mixtures and Single BAs on Mitochondrial Membrane Potential and Structural Alterations in Isolated Mitochondria	89
	3.3.3 Assessment of BA Mixture Effects on Mitochondrial Membrane Potential in HepaRG cells	93
	3.3.4 Examining the Mitotoxic Potential of BA Mixtures in HepaRG Cells Following an Acute Metabolic Modification with Galactose Media	94
	3.3.5 Assessment of BA-Induced Temporal Cell Death in HepaRG Cells	96
	3.3.6 Extracellular Flux Analysis of BA Mix-Induced Changes in Mitochondrial Function	97

3.3.7 Examining the Mitotoxic Potential of BA Mixtures Following Biliary Transporter Inhibition in HepaRG Cells	100
3.3.8 Assessment of the Mitotoxic Potential of an alternative BA mixture in isolated mitochondria and HepaRG cells	101
3.4 DISCUSSION	103
3.5 CONCLUSION	110

### 3.1 INTRODUCTION

Bile is an essential fluid in the human body as it aids in the digestion of lipids and lipid-soluble vitamins in the small intestine and acts as a signalling molecule (Thomas et al., 2008; Xie et al., 2001). Despite these critical roles, DIC is characterised by the retention and accumulation of BAs within hepatocytes (Attili et al., 1986). BA hydrophobicity is a determinant of toxicity and protection with the more hydrophobic BAs causing greater levels of injury (Perez and Briz, 2009). The secondary BA, LCA, is recognised as one of the most hydrophobic and cytotoxic BAs, whilst UDCA is recognised as a hydrophilic BA and is currently used in the treatment of cholestatic liver injury (Padda et al., 2011; Perez and Briz, 2009). Notably, drugs with a cholestatic potential cause preferential BA accumulation within hepatocytes and a reduction in BA amidation and sulfation, which consequently leads to an elevation in toxic hydrophobic BAs (Sharanek et al., 2019; Sharanek et al., 2017).

Whilst it is acknowledged that the toxicity of DIC is multi-mechanistic, a vast amount of research has revealed that mitochondrial dysfunction is frequently implicated. However, this research has primarily been conducted in isolated mitochondria, rodent hepatocytes and HepG2 cells, which are inappropriate models for attaining results with human *in vivo* relevance (Palmeira and Rolo, 2004; Rolo et al., 2004; Schulz et al., 2013). Although research has shown that BAs can induce mitochondrial toxicity, research assessing these effects in a more physiologically relevant cell line are lacking. The work presented in Chapter 2 confirmed the suitability of HepaRG cells for cholestasis studies due to their functioning biliary transporters and ability to be manipulated with known biliary transporter inhibitors. Therefore, it was hypothesised that toxic concentrations of BAs would impair mitochondrial bioenergetics in HepaRG cells and cause mitochondrial dysfunction as observed in other models.

The mitochondrial toxicity of the BAs and the BA mixtures were assessed on isolated mitochondria via alterations to mitochondria structure and mitochondrial membrane potential (MMP). Whilst the use of isolated mitochondria is valuable in delineating mechanisms of direct mitochondrial toxicity, the lack of cellular context warrants additional testing within cells in order to observe the mitochondria within their cellular environment (Brand M and Nicholls D 2011). Consequently, the mitochondrial toxicity of the BA mixtures were assessed in isolated mitochondria and whole cells to evaluate the translatability of the effects. A secondary hypothesis of this chapter was that BA-induced toxicity would be detected in both isolated mitochondria and HepaRG whole cells. Resultantly, the work

presented in this chapter aimed to define the role of the mitochondria in DIC and confirm the utility of isolated mitochondria and HepaRG cells for the preclinical assessment of mitochondrial dysfunction.

PHH are recognised as the 'gold standard' cells to use in DILI studies however, limitations with their use prevent their utility (Atienzar et al., 2016). Resultantly, immortalised cell lines of human or rodent origin are typically used during *in vitro* testing. Whilst it is typical for most mammalian cells to generate all of their ATP through OXPHOS within the mitochondria, some immortalised cell lines have different bioenergetics phenotypes (Marroquin et al., 2007; Rodriguez-Enriquez et al., 2001). Despite the presence of a functioning mitochondria and high oxygen levels, some cancer cell lines generate majority of their ATP from glycolysis rather than OXPHOS within the mitochondria, in a phenomenon called the Warburg effect (Rodriguez-Enriquez et al., 2001; Warburg, 1956). This effect can be circumvented by changes to the fuel supply in a process coined the 'Crabtree effect' (Rodriguez-Enriquez et al., 2001). The replacement of glucose in the media with galactose and l-glutamine drives immortalised cells to oxidise pyruvate and glutamine via OXPHOS due to an inadequate supply of ATP from the oxidation of galactose to pyruvate in glycolysis (Marroquin et al., 2007; Reitzer et al., 1979). The use of the acute metabolic modification assay with galactose was employed as a means of screening for direct mitochondrial dysfunction from the BA mixtures in HepaRG cells.

Following this, an extracellular flux analysis (XFe96) was used to gain a comprehensive view of mitochondrial function and BA-induced mitochondrial dysfunction. Real-time measurements of OCR provided evidence of the efficiency of the mitochondria to perform OXPHOS, whilst simultaneously measuring parameters of mitochondrial health. Alterations to MMP were measured in HepaRG cells to provide evidence of downstream impact of mitochondrial dysfunction.

The investigations within this chapter have been conducted in isolated mitochondria and HepaRG whole cells over a duration of time courses in order to examine the relationship between the onset of mitochondrial dysfunction and the initiation of cell death. The application of this range of experiments enabled the mitotoxic potential of the BA mixtures to be examined in both isolated mitochondria and HepaRG cells in order to address the hypotheses of this chapter.

## 3.2 MATERIALS AND METHODS

### 3.2.1 Materials

HepG2 cells were purchased from European Collection of Cell Cultures (ECACC, Salisbury, UK). HepaRG cells, basal media, growth and differentiation additives were purchased from Biopredic International (Saint Grégoire, France). DMEM, media supplements and cell culture reagents were purchased from Life technologies (Paisley, UK). Balch homogeniser was purchased from Isobiotech (Heidelberg, Germany). High precision pump – pump 11 was purchased from Harvard apparatus (Massachusetts, USA). 5,5',6,6'-tetrachloro-1,1',3,3'-tetraethyl benzimidazol carbocyanine iodide (JC-1) was purchased from Abcam (Cambridge, UK). All Extracellular flux analyser (XFe96) consumables were purchased from Agilent (Santa Clara, USA). Rhodamine 123 was purchased from Invitrogen (Carlsbad, USA). Insulin, penicillin-streptomycin, hydrocortisone, L-glutamine, sucrose, 3-(N-morpholino)propanesulfonic acid (MOPS), phosphoric acid, bovine serum albumin (BSA) and all bile acids and salts were purchased from Sigma Aldrich (Missouri, USA). Nitrocellulose membrane and enhanced chemiluminescence (ECL) were purchased from GE Healthcare (Buckinghamshire, UK). Bradford reagent was purchased from Bio-Rad (Hertfordshire, UK). All antibodies were purchased from Abcam (Cambridge, UK) or Santa Cruz Biotechnology (Texas, USA). Williams' E Medium powder (with L-Glutamine, without glucose) was manufactured by United States Biological. Cytotoxicity detection kits were purchased from Roche Diagnostics Ltd (West Sussex, UK).

### 3.2.2 HepG2 Cell Culture

HepG2 cells were maintained and cultured as previously described (Section 2.2.2).

### 3.2.3 HepaRG Cell Culture

HepaRG cells were maintained and cultured as previously described (Section 2.2.3).

### 3.2.4 Bile Acid Treatment

HepaRG cells were treated with BA mixtures as previously described (Section 2.2.4). Isolated mitochondria from HepG2 cells were acutely dosed with BA mixtures and individual BAs which were prepared as 200 x stock solutions and diluted to 0.5 % with a vehicle control in each experiment.

An additional BA mixture composed of the BAs and their respective concentrations found within patients with obstructive cholestasis was prepared (table 3.1) (Woolbright et al., 2015). The additional BA mixture was prepared as a 200 x stock solution in DMSO and the final solvent concentration was diluted to 0.5 % with a vehicle control in each experiment.

**Table 3.1: Composition of the alternative BA mixture composed of the BAs found within the bile of patients with obstructive cholestasis (Woolbright et al., 2015).**

Bile acid	Concentration in serum of patient with cholestasis ( $\mu\text{M}$ )
Lithocholic acid	< 10
Ursodeoxycholic acid	71 $\pm$ 20
Chenodeoxycholic acid	< 10
Deoxycholic acid	25 $\pm$ 16
Cholic acid	< 10
Taurocholic acid	2460 $\pm$ 295
Glycochenodeoxycholic acid	2756 $\pm$ 339
Taurochenodeoxycholic acid	1058 $\pm$ 191
Glycocholic acid	1530 $\pm$ 269
Glycodeoxycholic acid	1152 $\pm$ 355
Taurodeoxycholic acid	607 $\pm$ 320

### 3.2.5 Semi-automated Pump Controlled Cell (PCC) Rupture System for the Isolation of Mitochondrial from Cultured Cells

#### 3.2.5.1 Assay Preparation

2 fully confluent T175 flasks of HepG2 cells were washed with  $\text{Ca}^{2+}$  free PBS, trypsinised (0.25 %) and re-suspended in isolation buffer (300 mM sucrose, 5 mM N-[Tris (hydroxymethyl) methyl]-2-aminoethanesulfonic acid (TES) and 200  $\mu\text{M}$  EGTA) at  $7 \times 10^6$  cells/mL and stored on ice for 15 min.

### 3.2.5.2 Semi-automated Pump Controlled Cell Rupture

Due to time constraints with HepaRG cell culture, mitochondria were isolated from HepG2 cells as described elsewhere by the Pump Controlled Cell Rupture System (PCC) (Schmitt et al., 2013). A 6  $\mu\text{m}$  tungsten carbide ball was inserted into the homogeniser and two 1 mL glass syringes were attached to either side of the homogeniser (figure 3.1). The isolation buffer and assembled homogeniser were kept at 4 °C. 1 mL of cell suspension was passed between the two syringes at a flow rate of 1400  $\mu\text{L}/\text{min}$  four times. To retrieve the maximum amount of homogenate, the system was rinsed with 1 mL of isolation buffer.

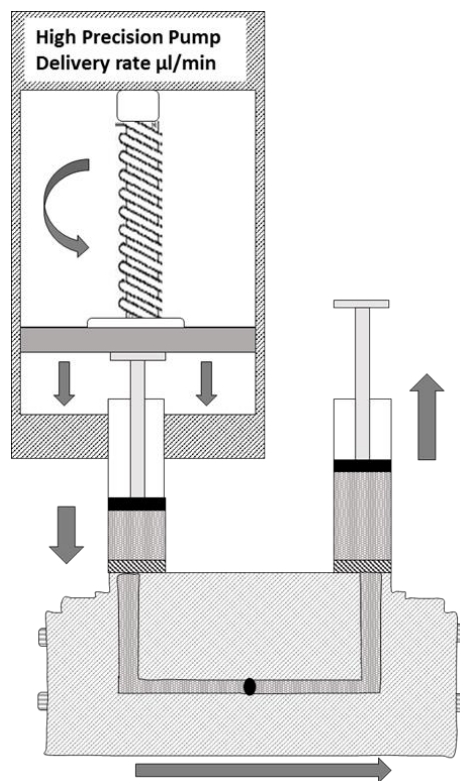


**Figure 3.1: Schematic representation of the Pump controlled cell (PCC) rupture system.** A Balch homogeniser is coupled to an automatic pump. The rate at which the pump turns is constant meaning that the rate at which the syringes are plunged stays constant throughout the mitochondrial isolation. Image adapted from (Schmitt et al., 2013).

This was repeated ten times per isolation. The homogenates were centrifuged at 800 g for 5 min. The supernatant from each tube was retained and centrifuged to pellet the crude mitochondria at 9000 g for 10 mins. The PCC method and centrifugation steps were both conducted at 4 °C.

### 3.2.5.3 Bradford Assay

Total protein content of the mitochondria fraction was determined by a Bradford assay. Briefly, 20  $\mu\text{L}$  of standards in the range of 0 – 0.25 mg/mL BSA and mitochondria (diluted 1:20 in isolation buffer) were added in duplicate to a 96-well plate. Bradford reagent was diluted 1:5 in water and 200  $\mu\text{L}$  was added to each well. Plates were read immediately at 595 nm using a Varioskan™ Flash multimode plate reader with SkanIt™ software.

The assay is centred on the binding of the dye Coomassie Brilliant Blue G250 (CBB) with protein (Bradford, 1976). Binding of the dye with proteins forms a complex which causes a shift in the absorbance maximum from 465 to 595 nm (Bradford, 1976). The formation of the dye-protein complex causes a colour change from red to blue which is proportional with the amount of protein present in the sample (figure 3.2) (Reisner et al., 1975).

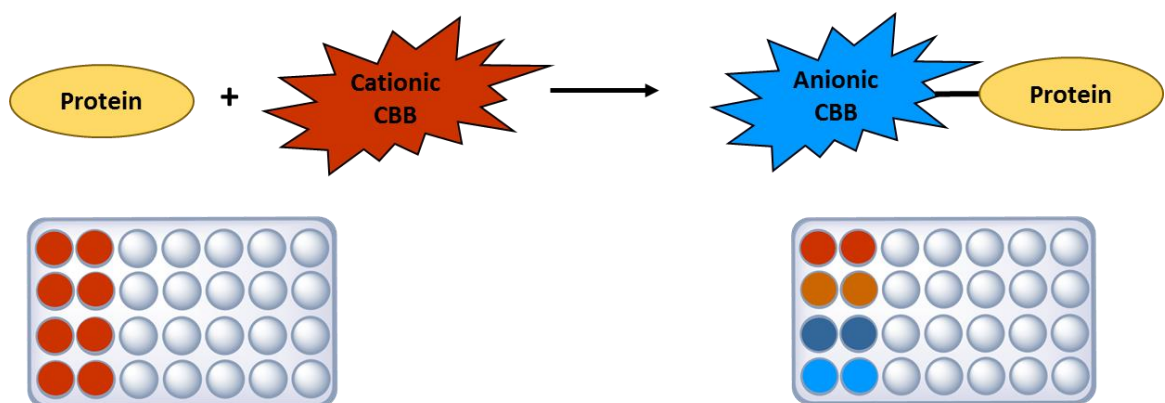


**Figure 3.2: Illustration of the Bradford assay used for protein quantification.** The cationic form of the dye CBB binds with proteins and forms a complex where the CBB is reduced. The protein complex causes a colour change that is proportional with the amount of protein in the sample.

### 3.2.6 Dual Monitoring of Membrane Potential and Structural Alterations in Isolated Mitochondria

MMP was measured with the lipophilic, cationic dye Rhodamine123 (Rh123) under quenching conditions. Rh123 accumulates in the matrix of polarised mitochondria where energisation results in the quenching of Rh123 fluorescence. Loss of MMP results in the release of Rh123 from the matrix and fluorescence recovery (Baracca et al., 2003). Rh123 is preferential for measuring the membrane potential in isolated mitochondria due to its inability to interact with mitochondrial structures or the ETC compared to other dyes (Perry et al., 2011; Scaduto and Grotyohann, 1999).

The induction of the MPT leads to a sudden increase in the permeability of the mitochondrial inner membrane and can be instigated via calcium overload, ROS and inorganic phosphate (Hunter et al., 1976; Kim et al., 2003). The resultant influx of molecules into the mitochondrial matrix leads to swelling of the mitochondria which can be detected via an optical density decrease. Mitochondrial structural alterations were assessed photometrically by light scattering at 540 nm which is within the range of mitochondrial isosbestic point (Fulda et al., 2010).

### 3.2.6.1 Assay Preparation

Isolated mitochondria were diluted in isolation buffer (2 µg/µL). Swelling buffer (0.2 M sucrose, 10 mM MOPS-Tris, 5 mM succinate, 1 mM phosphoric acid, 10 µM EGTA and 2 µM rotenone) was prepared and test compounds were made up in swelling buffer. Calcium (400 µM) and carbonyl cyanide-4- trifluoromethoxyphenylhydrazone (FCCP) (10 µM) were used as positive controls. BAs were diluted 1:4 in swelling buffer. Calcium, FCCP and Rh123 were prepared in swelling buffer and all compounds were kept on ice until used.

Dual monitoring of MMP and structural alterations were performed in the same wells of a black 96-well plate with a transparent base. Experimental setup of each well is shown in table 3.2. Compounds were loaded onto the plate in the following order: swelling buffer, 50 µg mitochondria, calcium/bile acids, FCCP and Rh123. MMP was monitored by the Rh123 quenching method at Excitation 500/20 nm, Emission 528/20 nm and structural changes were monitored photometrically at 540 nm for 45 min using the microplate reader (Thermo Scientific Varioskan Flash). After 45 mins, FCCP (10 µM) was added to each well to dissipate the MMP of any remaining functional mitochondria, thus acting as an internal control.

**Table 3.2: Experimental setup of compounds used to monitor MMP and MPT during BA treatment.**

	Blank (µL)	Positive control (µL)	Positive control for MMP (µL)	Positive control for MPT (µL)	Bile acid incubation (µL)
Swelling buffer	150	125	115	75	75
Mitochondria		25	25	25	25
Bile acid					50
Calcium (400µM)				50	
FCCP (10µM)			10		
Rh123 (500 nM)	50	50	50	50	50

### 3.2.6.2 Assessment of Mitochondrial Purity

Purity of the isolated mitochondria from HepG2 cells was assessed via protein detection of mitochondrial specific and nonspecific proteins using western blot as previously described (Section 2.2.5.3). Mitochondria were lysed in 100  $\mu$ L RIPA buffer.

The membrane was probed with mitochondrial proteins (VDAC, cytochrome C and heat shock protein 60 (Hsp60)), nuclear proteins (histone H3), lysosomal proteins (lysosome-associated membrane protein 2 (Lamp2)) and peroxisomal proteins (peroxisomal membrane protein 70 (PMP70)). Incubation and dilution conditions for the primary and secondary antibodies were dependent on the protein of interest (table 3.3).

**Table 3.3: Western blot incubation conditions for primary and secondary antibodies.** Antibodies were used to assess mitochondrial purity in HepG2 cells.

Protein	Antibody product code	Molecular weight (kDa)	Primary antibody (in 5% milk)	Secondary antibody (in 2% milk)
PMP70	ab3421	70	1:500	Anti-rabbit
Hsp60	ab46798	60	1:20000	Anti-rabbit
Lamp2	ab203224	45	1:500	Anti-rabbit
Actin	ab1801	42	1:5000	Anti-mouse
VDAC	ab15895	31	1:1000	Anti-rabbit
Histone H3	ab201456	15	1:2000	Anti-rabbit
Cytochrome C	SC-13156	14	1:5000	Anti-rabbit

### 3.2.7 Mitochondrial Membrane Potential in HepaRG Cells

#### 3.2.7.1 Assay Preparation and Experimental Design

Undifferentiated HepaRG cells were plated onto collagen coated (50  $\mu$ g/mL rat tail collagen type II in 0.02 M acetic acid) glass coverslides in 12-well plates at 80,000 cells/well and cultured as described (Section 2.2.3). Following differentiation, HepaRG cells were dosed with BA mixtures for 24 h as described (Section 2.2.4) and incubated with JC-1 (1  $\mu$ M) for 1 h in the dark. Following this, cells were washed with PBS and incubated with Hoechst (1:5000) in PBS for 10 min. Cells treated with FCCP (100  $\mu$ M) as a positive control for MMP depolarisation. Cells were mounted using Pro-long gold onto glass microslides. Snap images were taken using a Zeiss Axio Observer.Z1 widefield florescent microscope with Apotome using 40 x oil objective.

The dye allows the identification of energised and de-energised mitochondria (figure 3.3). When mitochondria are fully energised and functioning correctly, the dye forms aggregates that emit red fluorescence with a maximum at 595 nm. Whereas loss of MMP causes the dye to exist as a monomer that emits green fluorescence with a maximum at 488 nm (Perelman et al., 2012).

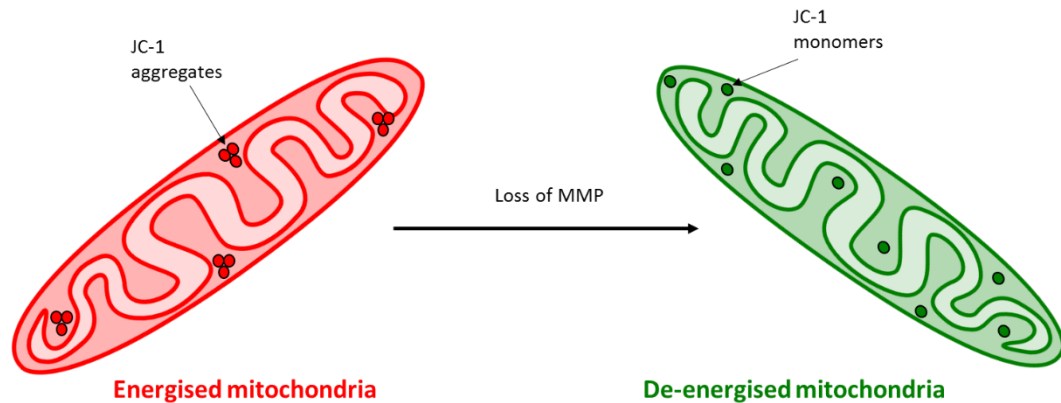


**Figure 3.3: Illustration of the principles of the JC-1 assay.** The JC-1 dye is a membrane permeable dye that is used to monitor MMP. In healthy, energised cells, the dye accumulates in the mitochondria and emits red fluorescence. Loss of MMP causes the dye to exist as a monomer and emits green fluorescence. A decrease in the red/green fluorescence intensity ratio is indicative of membrane depolarisation.

### 3.2.8 Acute Metabolic Modification Assay

Many pharmaceutical companies screen for mitochondrial toxicity during the preclinical stages of drug development via a metabolic modification assay (Blomme and Will, 2016). Despite having functioning mitochondria and adequate supplies of glucose and oxygen, many tumour-derived cell lines generate most of their ATP via glycolysis instead of OXPHOS in a process known as the Warburg effect (Rodriguez-Enriquez et al., 2001; Warburg, 1956). Substitution of the culture media with galactose reduces the yield of ATP produced during glycolysis and increases the cells reliance on OXPHOS, thus exposing compounds with mitochondrial liabilities (Marroquin et al., 2007; Reitzer et al., 1979).

This method was later adapted by Kamalian *et al.*, whereby acute galactose conditioning for 2 h prior to additional compound treatment in galactose media, as opposed to long term galactose conditioning, was sufficient to identify compounds causing direct mitochondrial toxicity (Kamalian et al., 2015).

The assessment of ATP content in galactose media acts as an early marker of mitochondrial function. When assessed alongside cytotoxicity, this assay can provide information whether mitochondrial dysfunction is the cause or the consequence of cytotoxicity (Kamalian et al., 2015). Using this technique, a compound is defined as mitotoxic by calculating  $IC_{50}ATP$  values in glucose and galactose media. An  $IC_{50}ATP_{glu}/IC_{50}ATP_{gal} \geq 2$  is indicative of a compound with a mitochondrial liability (Kamalian et al., 2015; Swiss et al., 2013).

#### *3.2.8.1 Assay Preparation*

Undifferentiated HepaRG cells were plated in collagen coated 96-well cell culture plates at 9000 cells/well and cultured to differentiation as described (Section 2.2.3).

Next, serum-free base media was prepared from glucose-free Williams E powder dissolved in sterile distilled water and supplemented with sodium bicarbonate (3.7 mg/mL), insulin (5 µg/mL) and hydrocortisone (50 µM). To make glucose and galactose media, the base was supplemented with galactose (10 mM) or glucose (11 mM), which is the same concentration of glucose found within the HepaRG differentiation media as told by Biopredic.

#### *3.2.8.2 24 h BA Mix Dosing*

HepaRG cells were washed twice in either serum-free glucose or galactose media before incubation in the respective media (50 µL) for 2 h. BA mixtures were diluted in either serum-free glucose or galactose media to reach a final solvent concentration of 1% (v/v) and added to every well of the plate (50 µL) for 24 h.

#### *3.2.8.3 72 h, 1 week and 2 week BA Mix Dosing*

HepaRG cells were dosed with the BA mixtures in HepaRG culture media for 72 h, 1 week or 2 weeks. Cells were washed twice with either serum-free glucose or galactose media and then incubated in the respective media (100 µL) for 2 h.

#### *3.2.8.4 Inhibition of Biliary Transporters with MK571 and Bosentan*

HepaRG cells were washed twice with either serum-free glucose or galactose media before incubation in the respective media (50 µL) for 2 h. Bosentan (50 µM) and MK571 (30 µM) were diluted in either serum-free glucose or galactose media to reach a final solvent concentration of 1% (v/v) and added to every well of the plate (50 µL) for 30 min. Following this, media containing the inhibitors were aspirated and HepaRG cells were treated in serum-

free glucose or galactose media containing BA mixtures, bosentan and MK571 (100  $\mu$ L) for 24 h.

Following BA mix treatment (24 h) or the 2 h metabolic switch (72 h, 1 week and 2 week), the cell supernatant was removed and 100  $\mu$ L of somatic cell ATP releasing agent was added to each well of the plate to lyse cells. The plate was placed on a shaker for 1 min. Protein was assessed via a standard BCA assay and ATP content was assessed via an ATP bioluminescent assay according to the manufacturer's guidelines.

### 3.2.8.5 ATP Bioluminescent Assay

ATP content was assessed by the addition 10  $\mu$ L of cell lysate and ATP standards to a white-walled 96-well plate. The ATP complete reaction solution was prepared according to the manufacturers guidelines by mixing ATP assay mix with ATP dilution buffer in a 1:25 ratio. 40  $\mu$ L of the complete reaction solution was added to both the cell lysates and the standards and bioluminescence was measured (Varioskan™, Thermo Scientific).

The ATP assay works on the principles of bioluminescence and the resultant light emission being directly proportional to ATP content. The assay kit contains the enzyme luciferase and the substrate luciferin. In the presence of ATP and magnesium, luciferase converts luciferin to the enzyme-bound luciferil adenylate. In the following reaction, the luciferil adenylate undergoes oxidation to form oxyluciferin and light is emitted (figure 3.4) (Chollet and Ribault, 2012).

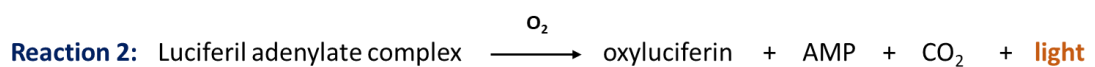


**Figure 3.4: Chemical reactions undergone during the ATP bioluminescent assay.** The assay is based upon the conversion of the substrate luciferin to oxyluciferin by the enzyme luciferase. This reaction requires ATP. The amount of light emitted is directly proportional to the amount of ATP in the cells. Adapted from (Chollet and Ribault, 2012).

### 3.2.8.6 Bicinchoninic Acid (BCA) Assay

Protein was measured as a marker of cell death because once HepaRG cells have reached confluency and are fully differentiated, they do not continue proliferating therefore, any differences in protein can be attributed to cell death (Gripon et al., 2002). Additionally, a BCA assay was used to normalise ATP data to total protein to account for variances in cell seeding density and cell death.

A BCA assay was conducted as described (Section 2.2.5.2) using 10  $\mu\text{L}$  of cell lysate and BCA standards.

### 3.2.9 Lactate Dehydrogenase (LDH) Assay

Undifferentiated HepaRG cells were plated in collagen coated 96-well cell culture plates at 9000 cells/well and cultured as described (Section 2.2.3). Following differentiation, cells were dosed with the BA mixtures for 1 week, as described (Section 2.2.4).

Following this, HepaRG cells were daily dosed with the BA mixtures for an additional week. The supernatant was collected and daily LDH content released into the media was measured using a Cytotoxicity Detection Kit in accordance with the manufacturer's instructions in order to determine the total LDH released into the supernatant. 40  $\mu\text{L}$  supernatant and 40  $\mu\text{L}$  of LDH catalyst-dye solution were added to a clear 96 well plate and incubated at room temperature in the dark for 30 min. The absorbance was read at 490 nm using a Varioskan™ Flash multimode plate reader with SkanIt™ software.

Following 2 weeks of BA mix dosing, the supernatant was removed and the cells were lysed in 100  $\mu\text{L}$  of somatic cell ATP releasing agent. 8  $\mu\text{L}$  of cell lysate was added to a clear 96 well plate and diluted 1:5 with media. 40  $\mu\text{L}$  of LDH catalyst-dye solution was added to the plate. The plate was incubated in the dark at room temperature for 30 min and the absorbance read at 490 nm using a Varioskan™ Flash multimode plate reader with SkanIt™ software.

The LDH retained within the cells was determined by the following formula: Retained LDH =  $\text{LDH in lysate} / (\text{LDH in lysate} + \text{LDH in supernatant})$

The assay works on the principals that necrotic cells have a damaged plasma membrane thus leading to the release of the stable cytoplasmic enzyme LDH into the supernatant (figure 3.5). LDH reduces  $\text{NAD}^+$  to NADH via the oxidation of lactate to pyruvate. A second reaction occurs which sees  $\text{H}^+$  transferred from NADH to the tetrazolium salt present in the cytotoxicity detection kit to form the red formazan. The intensity of the red formazan is

proportional to the amount of LDH released by the cell into the supernatant (Decker and Lohmann-Matthes, 1988).

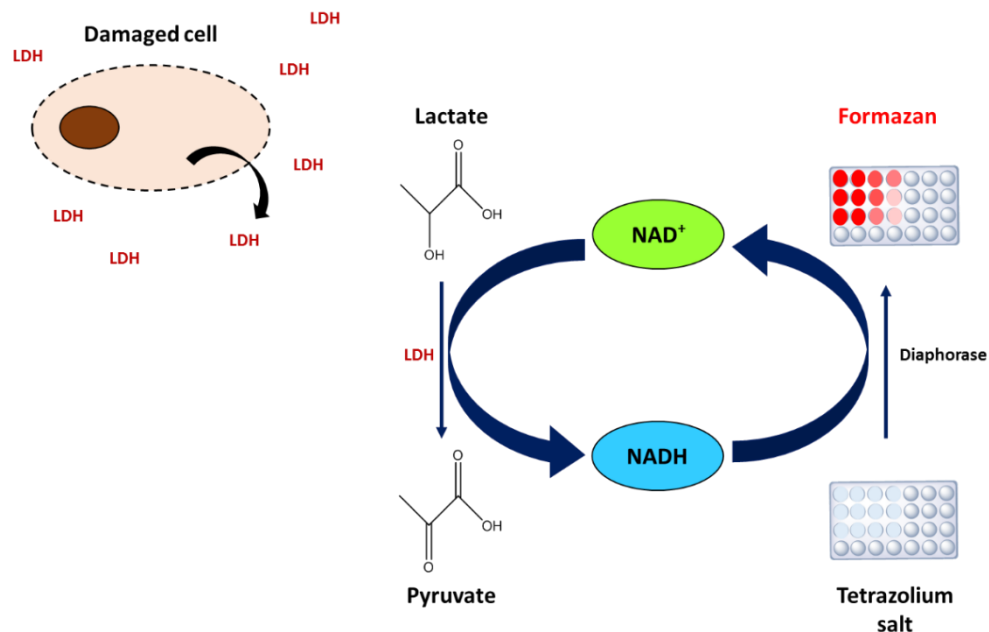


**Figure 3.5: Schematic representation of the principles of the LDH assay used to monitor cell death.** Necrotic cells have a compromised cell membrane which leads to the release of the enzyme LDH into the media. The LDH-catalysed conversion of lactate to pyruvate leads to the reduction of  $\text{NAD}^+$  to NADH. In a second enzymatic reaction,  $\text{H}^+$  are transferred to a tetrazolium salt yielding the red formazan dye that is proportional to the amount of LDH in the sample.

### 3.2.10 Extracellular Flux Analysis

The acute metabolic modification assay is useful in detecting compounds that cause direct mitochondrial dysfunction of the ETC however, it is restricted in its ability to detect compounds that cause mitochondrial dysfunction via alternative mechanisms such as reactive metabolite production or inhibition of fatty acid oxidation (Kamalian et al., 2015). Therefore, if a compound is deemed negative for mitochondrial toxicity, further respiratory analysis should be undertaken for confirmation.

One of the most commonly used instruments for measuring respiratory function is the extracellular flux analyser (Agilent Technologies). The XFe96 analyser uses a 96-well cell culture microplate with a sensor cartridge for each well. Within the sensor cartridge are sensor probes that each contain 2 separate polymer-embedded fluorophores that are sensitive to  $\text{O}_2$  and  $\text{H}^+$  respectively. During each measurement cycle, the sensor cartridge is

lowered 200  $\mu\text{m}$  above the cells creating a transient microchamber. Fiber optic bundles are simultaneously inserted into the sensor probes and emit light that excites the fluorophores. The emitted light from the fluorophores is relative to changes in  $\text{O}_2$  and  $\text{H}^+$  and is measured by a detector within the XFe96 instrument (figure 3.6). Changes related to  $\text{O}_2$  are due to OCR whilst changes in  $\text{H}^+$  are related to ECAR (Ferrick et al., 2008; Perry et al., 2013). After measuring, the sensor cartridge is elevated to allow the media to restore the cells to baseline (Koopman et al., 2016).

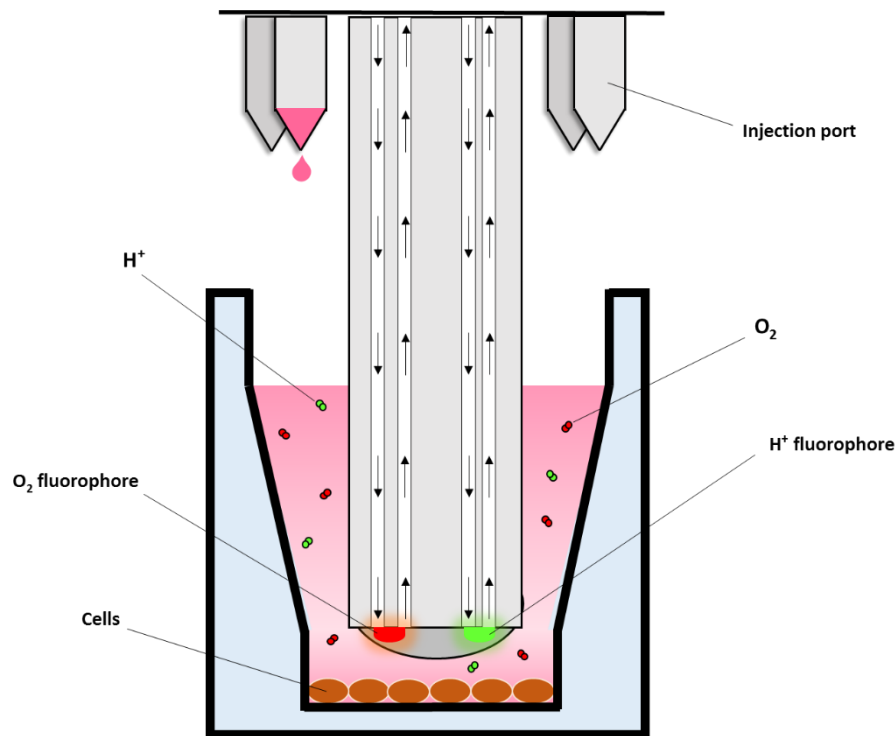


**Figure 3.6: Schematic of the XFe sensor cartridge.** Within each sensor probe are 2 polymer-embedded fluorophores that are sensitive to  $\text{O}_2$  and  $\text{H}^+$ . Fiber optic bundles emit light that excites the fluorophores and a detector measures the emitted light which gives information on changes in OXPHOS and glycolysis.

#### 3.2.10.1 Assay Preparation and Normalisation

Undifferentiated HepaRG cells were plated in collagen coated XFe 96-well cell culture plates at 5000 cells/well as described (Section 2.2.3). Following differentiation, HepaRG cells were dosed with BA mixtures as described (Section 2.2.4). Following completion of the XF stress test assay, media was removed from all wells and cells were lysed in somatic ATP releasing agent (20  $\mu\text{L}$ ). 10  $\mu\text{L}$  of cell lysates were transferred to a clear 96-well plate and a standard BCA assay was conducted as described (Section 2.2.5.2). Protein content per well was used to normalise OCR values.

### 3.2.10.2 Mitochondrial Stress Test

Prior to the start of the assay, culture media was removed and HepaRG cells were incubated at 37°C in 0% CO<sub>2</sub> in unbuffered Seahorse XFe base media (25 mM glucose, 1mM sodium pyruvate and 2mM l-glutamine) with the pH adjusted to 7.4.

Stress test compounds were made in the Seahorse media. The final optimised concentrations of the stress test compounds were oligomycin (1 µM), FCCP (0.25 µM), rotenone (1 µM) and antimycin-A (1µM). 25 µL of the stress test compounds were added to the corresponding port on the sensor cartridge (figure 3.7). No compounds were added to port D on the sensor cartridge in any of the wells.

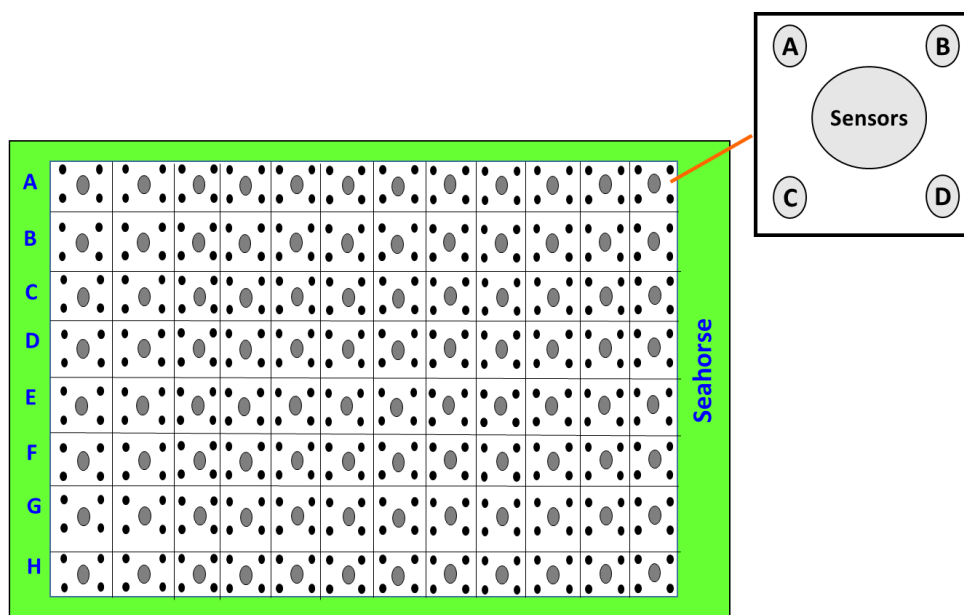


**Figure 3.7:** Illustration of the sensor cartridge provided in the Extracellular Flux Assay Kit. 25 µl of stress test compounds can be loaded in the ports A-D. In these experiments oligomycin was loaded into port A, FCCP into port B and antimycin-A and rotenone into port C. No compounds were loaded into port D.

Before measuring cellular OCR, the XFe96 instrument had been programmed to gently mix the assay media in each well for 10 min to allow the oxygen partial pressure to equilibrate. In order to define a baseline rate, OCR was measured three times before the injection of stress test compounds. Each measurement cycle comprised a 3 min mix followed by 3 min of measurements. Stress test compounds were sequentially injected and 3 measurement cycles were performed before the next compound was injected.

Normalised data was analysed using the Seahorse XF Mito Stress Test Generator from Agilent.

Normalised OCR values were used to calculate non-mitochondrial respiration (NMR = minimum rate measurement after rotenone/antimycin A injection, basal respiration (BR = last measurement before oligomycin injection – NMR), proton leak (PL = minimum measurement after oligomycin injection – NMR), ATP-linked respiration (ALR = BR – PL), maximum respiration (MR = maximum measurement after FCCP injection – NMR) and spare respiratory capacity (SRC = MR – BR) (figure 3.8).

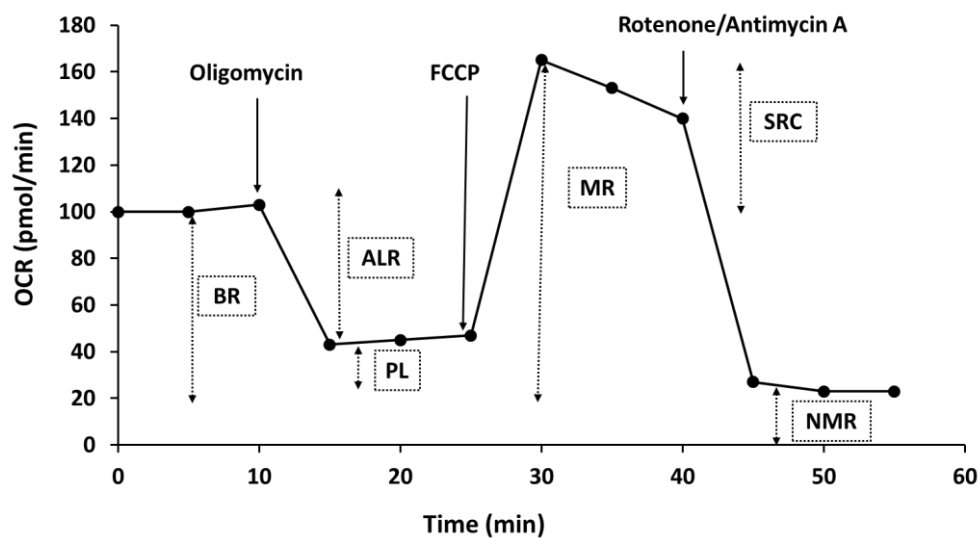


**Figure 3.8: Illustration of a typical mitochondrial stress test trace using injection ports A-C.** OCR data can be manipulated to determine mitochondrial parameters such as basal respiration (BR), ATP-linked respiration (ALR), proton leak (PL), maximum respiration (MR), spare respiratory capacity (SRC) and non-mitochondrial respiration (NMR).

### 3.2.11 Statistical Analysis

Data is expressed from a minimum of three independent experiments. Unless specified otherwise, all results are expressed as mean  $\pm$  standard error of the mean (SEM). Normality was assessed using a Shapiro-Wilk statistical test. Statistical significance compared to the control was determined by a one-way ANOVA with a Dunnett's test for parametric data or a Kruskal-Wallis test for non-parametric data using StatsDirect 3.0.171. Results were considered significant when  $P < 0.05$ .

### 3.3 RESULTS

#### 3.3.1 Examining Mitochondrial Purity from the Crude Mitochondrial Extract

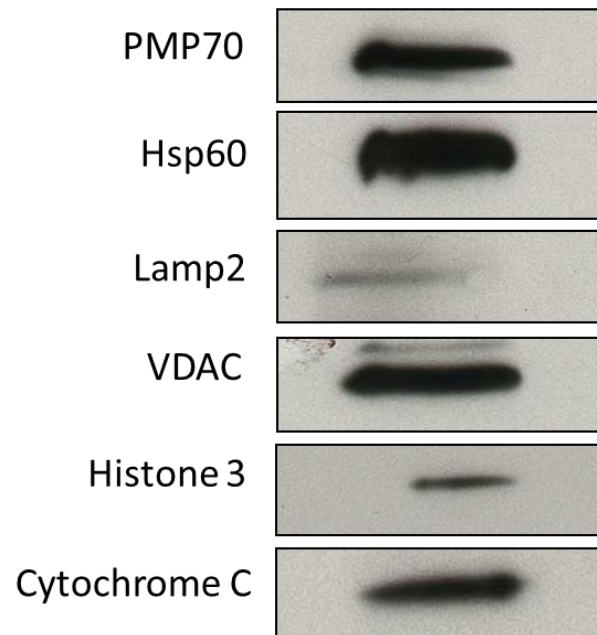


**Figure 3.9: Examining the purity of the crude mitochondrial fraction.** A representative gel of mitochondria from HepG2 cells were isolated via the PCC method and the expression of mitochondrial, peroxisomal, lysosomal and nuclear markers were assessed via western blot.

To assess the purity of the crude mitochondria extract from the mitochondrial isolation, antibodies for mitochondrial, lysosomal, peroxisomal and nuclear markers were measured (figure 3.9). Western blot analysis revealed that there was high expression of the mitochondrial markers Hsp60, VDAC and Cytochrome C confirming successful mitochondria isolation. Mitochondria presented minor contaminations with lysosomes (Lamp2) and nuclear proteins (Histone 3). Crude mitochondria exhibited expression of the peroxisomal protein PMP70 indicating there were contaminations.

### 3.3.2 Assessment of the Effects of BA Mixtures and Single BAs on Mitochondrial Membrane Potential and Structural Alterations in Isolated Mitochondria

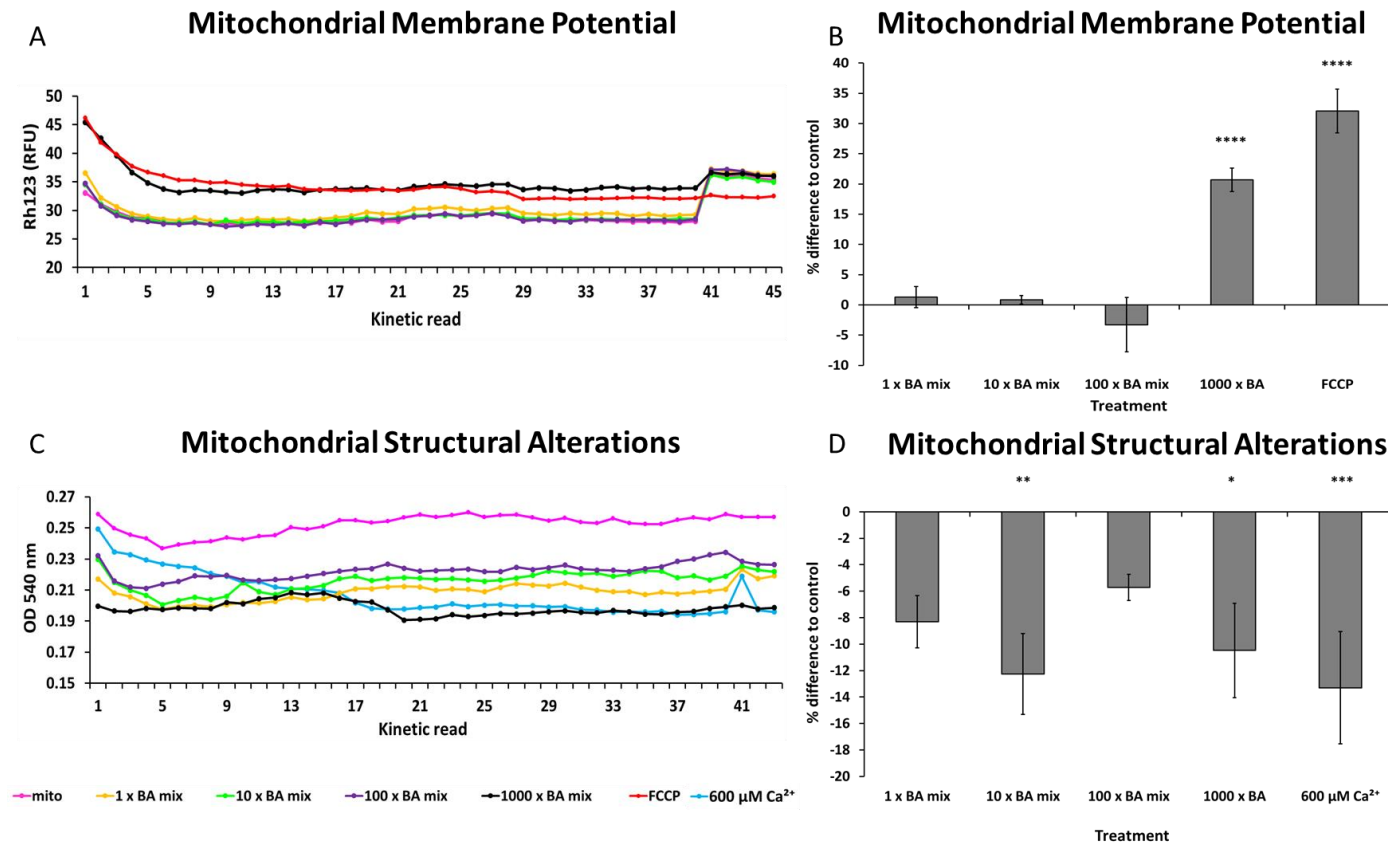


**Figure 3.10: The effects of BA mixtures on MMP and optical density on isolated mitochondria from HepG2 cells.** (A) Representative kinetic traces for the simultaneous measurements of MMP loss (Rh123 fluorescence) and (C) optical density (OD<sub>540nm</sub>). (C) Calculations of percentage difference to mitochondria alone for MMP and (D) optical density at kinetic read 20. FCCP served as an internal control for MMP loss and calcium served as a control for mitochondrial swelling. Statistical significance compared with mitochondria alone; \* P < .05, \*\* P < .01, \*\*\* P < .001, \*\*\*\* P < .0001. Graphical values are displayed as mean  $\pm$  SEM of n = 4 experiments.

The integrity of the inner MMP was assessed via the cationic fluorescent dye Rh123 under quenching conditions in isolated mitochondria from HepG2 cells. The mitochondria generated an inner transmembrane potential that remained stable for 1 h (figure 3.10A). Exposure of isolated mitochondria to the 1000 x BA mix resulted in a loss of MMP as indicated by a  $20.7 \pm 1.9$  % increase in fluorescence when compared to mitochondria alone (figure 3.10B). At kinetic read 40, the uncoupler FCCP was added to all wells to act as an internal control for depolarisation. This resulted in an increase in the fluorescence for mitochondria that had been treated with the 1, 10 and 100 x BA mixtures, revealing that these concentrations had not induced depolarisation of the MMP.

Concomitant optical density measurements at 540 nm were used to assess if the mitochondria had undergone swelling. The induction of the MPT can occur in the presence of high concentrations of calcium and leads to an influx of solutes into the mitochondrial matrix, thus resulting in swelling. Accordingly, calcium was used as a positive control for this experiment. All BA mixtures induced a decrease in optical density, implying mitochondrial swelling or structural alterations (figure 3.10C and D). However, BA mixtures did not result in induction of the MPT as mitochondria still had an intact membrane potential.

## Mitochondrial Membrane Potential

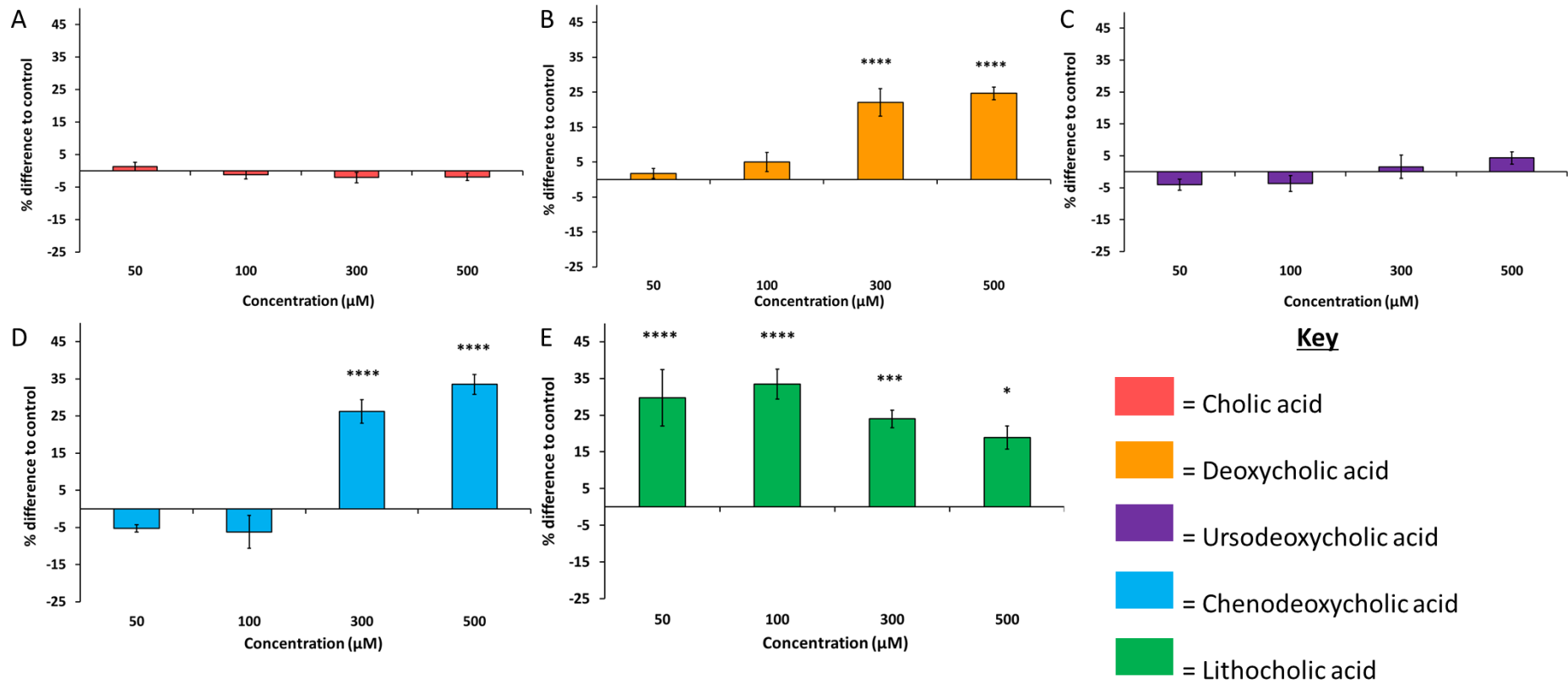


**Figure 3.11: The effects of single BAs on MMP on isolated mitochondria from HepG2 cells.** Calculations of percentage difference to mitochondria alone for MMP at kinetic read 20 for (A) Cholic acid, (B) Deoxycholic acid, (C) Ursodeoxycholic acid, (D) Chenodeoxycholic acid and (E) Lithocholic acid. Statistical significance compared with mitochondria alone; \*  $P < .05$ , \*\*  $P < .01$ , \*\*\*  $P < .001$ , \*\*\*\*  $P < .0001$ . Graphical values are displayed as mean  $\pm$  SEM of a minimum of  $n = 5$ .

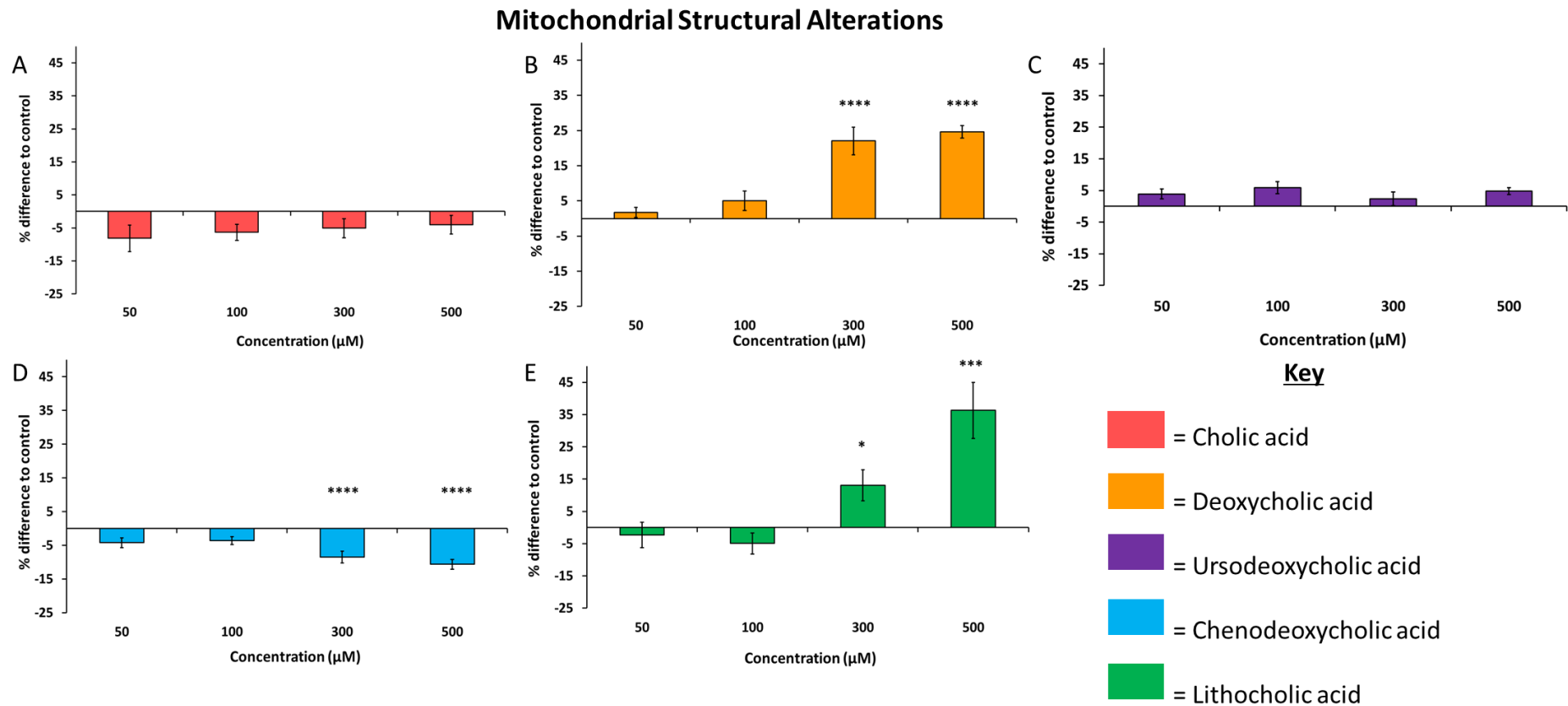


**Figure 3.12: The effects of single BAs on optical density on isolated mitochondria from HepG2 cells.** Calculations of percentage difference to mitochondria alone for optical density at kinetic read 20 for (A) Cholic acid, (B) Deoxycholic acid, (C) Ursodeoxycholic acid, (D) Chenodeoxycholic acid and (E) Lithocholic acid. Statistical significance compared with mitochondria alone; \*  $P < .05$ , \*\*  $P < .01$ , \*\*\*  $P < .001$ , \*\*\*\* $P < .0001$ . Graphical values are displayed as mean  $\pm$  SEM of a minimum of  $n = 5$ .

The mitotoxic potential of the individual BAs found within the BA mixture were also assessed on isolated mitochondria. Exposure of isolated mitochondria to LCA caused a significant increase in fluorescent signal at 50  $\mu\text{M}$  and 100  $\mu\text{M}$  compared to mitochondria alone however, the fluorescent signal started to decrease with 300  $\mu\text{M}$  and 500  $\mu\text{M}$  (figure 3.11E). In addition, both the 300  $\mu\text{M}$  and 500  $\mu\text{M}$  conditions demonstrated a significant increase in optical density (figure 3.12E), which is considered a characteristic of mitochondrial shrinkage or rupture. Alternatively, the hydrophilic BAs CA and UDCA did not induce any significant changes in MMP or optical density. DCA and CDCA induced a significant increase in fluorescent signal at 300  $\mu\text{M}$  and 500  $\mu\text{M}$ , suggestive of membrane depolarisation (figure 3.11B and D) and a significant optical density decrease indicating mitochondrial swelling (figure 3.12B and D).

### 3.3.3 Assessment of the Effects of BA Mixtures on Mitochondrial Membrane Potential in HepaRG cells

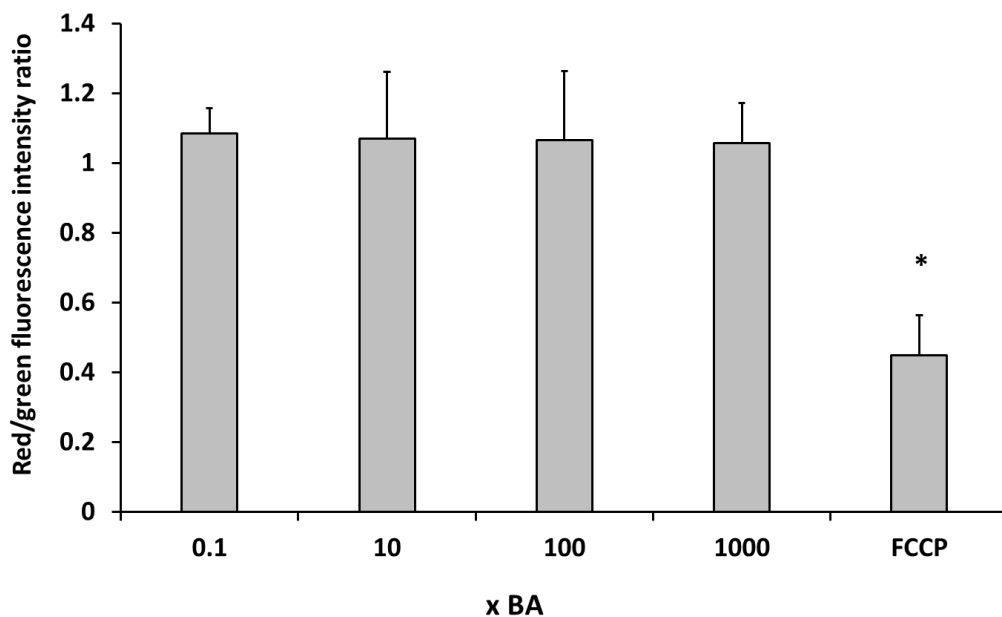


**Figure 3.13: The effects of BA mixtures on MMP in HepaRG cells.** HepaRG cells were treated for 24 h with the BA mixtures and MMP was detected by JC-1 fluorescence. A ratio of the fluorescence intensity of the red aggregate over the green monomer was determined. FCCP was used as a positive control for depolarisation. Statistical significance compared with vehicle control; \*  $P < .05$ , \*\*  $P < .01$ , \*\*\*  $P < .001$ , \*\*\*\* $P < .0001$ .

Assessment of MMP in HepaRG whole cells was monitored using the fluorescent dye JC-1. A reduction in the red/green fluorescent ratio is indicative of loss of MMPP. The BA mixtures

did not induce loss of MMP as there were no differences in the red/green fluorescent ratio (figure 3.13). The positive control FCCP induced a significant MMP loss with a decrease of  $0.4 \pm 0.1$  in the red/green fluorescent ratio.

### **3.3.4 Examining the Mitotoxic Potential of BA Mixtures in HepaRG Cells Following an Acute Metabolic Modification with Galactose Media**

In order to detect BA-induced mitochondrial toxicity in the absence of significant cell death, cellular ATP content and protein were measured in HepaRG cells acutely conditioned to glucose or galactose media (figure 3.14). There were no significant differences in the ATP levels between glucose or galactose media for the time points tested suggesting that the BA mixtures did not cause mitochondrial toxicity via direct ETC dysfunction. According to this technique, a compound is deemed to possess a mitochondrial liability if the ratio between the  $IC_{50}$  ATP values in glucose and galactose media is  $\geq 2$  (Kamalian et al., 2015; Swiss et al., 2013).  $IC_{50}$  values could not be calculated for any of the time points due to an absence of a reduction in cellular ATP content.

Protein was measured as a marker of cell death as on differentiation, HepaRG cells stop proliferating meaning that any loss of protein can be attributed to cell death (Gripon et al., 2002). There was a dose-dependent decrease in protein from 1 week of BA mix dosing and by 2 weeks there was a significant loss of  $39.5 \pm 8.9$  % protein for HepaRG cells dosed with 1000 x BA mix (figure 3.14D). Despite the temporal cell death, ATP levels significantly increased up to  $180 \pm 11.9$  % following 1 week BA mix dosing (figure 3.14C) and then reduced to  $124.6 \pm 13.0$  % by 2 weeks dosing.

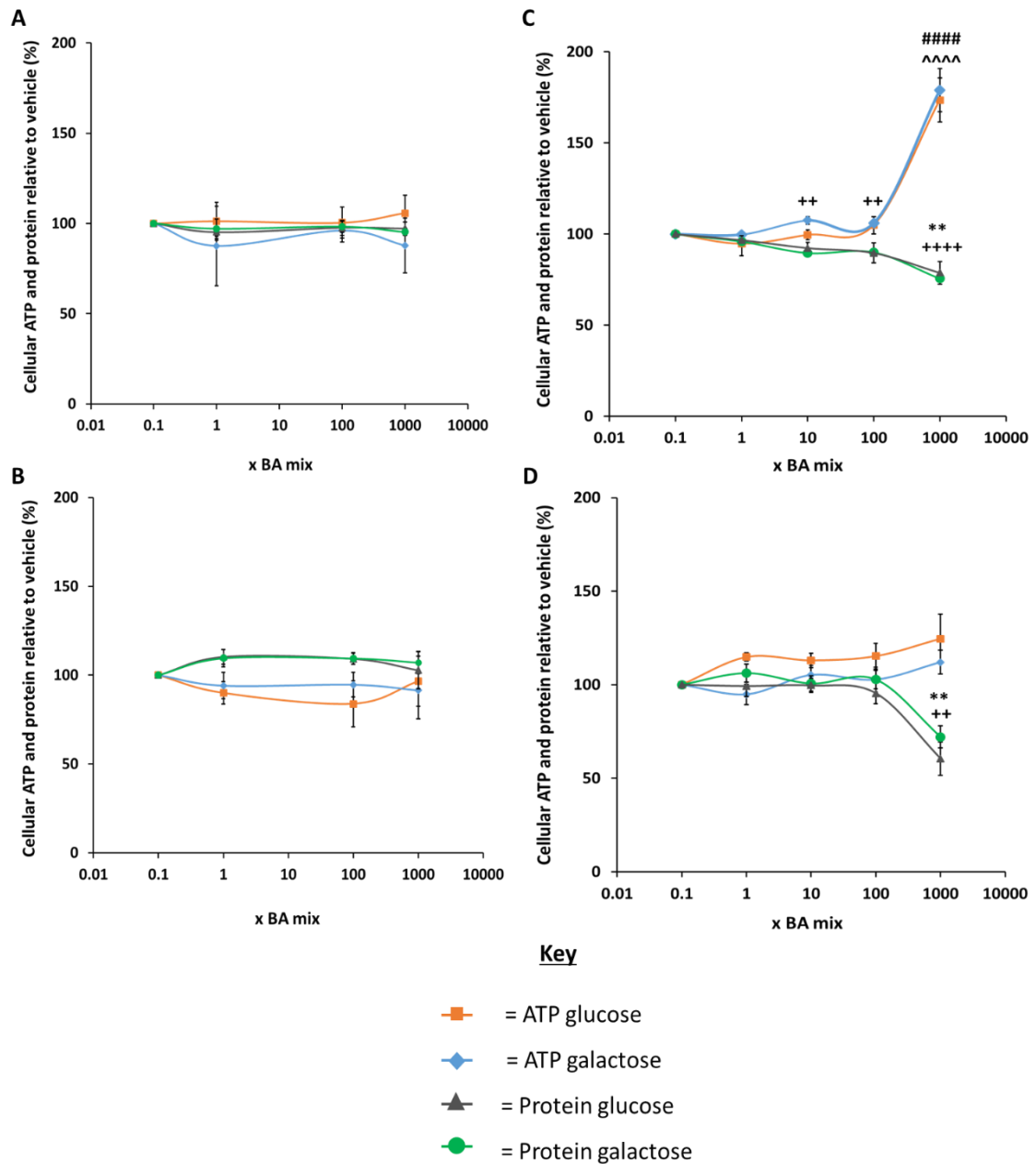


**Figure 3.14: The effects of BA mixtures after (A) 24 h, (B) 72 h, (C) 1 week and (D) 2 weeks on cellular ATP content and protein compared to the vehicle control.** Statistical significance compared with vehicle control; ATP glucose ^  $P < .05$ , ^^  $P < .01$ , ^^^  $P < .001$ , ^^^^  $P < .0001$ , ATP galactose #  $P < .05$ , ##  $P < .01$ , ###  $P < .001$ , ####  $P < .0001$ , protein glucose \*  $P < .05$ , \*\*  $P < .01$ , \*\*\*  $P < .001$ , \*\*\*\*  $P < .0001$  and protein galactose +  $P < .05$ , ++  $P < .01$ , +++  $P < .001$ , ++++  $P < .0001$ . ATP values have been normalised to  $\mu\text{g}$  protein per well. Data are presented as  $\pm$  SEM of  $n = 4$  experiments.

## 3.3.5 Assessment of BA-Induced Temporal Cell Death in HepaRG Cells

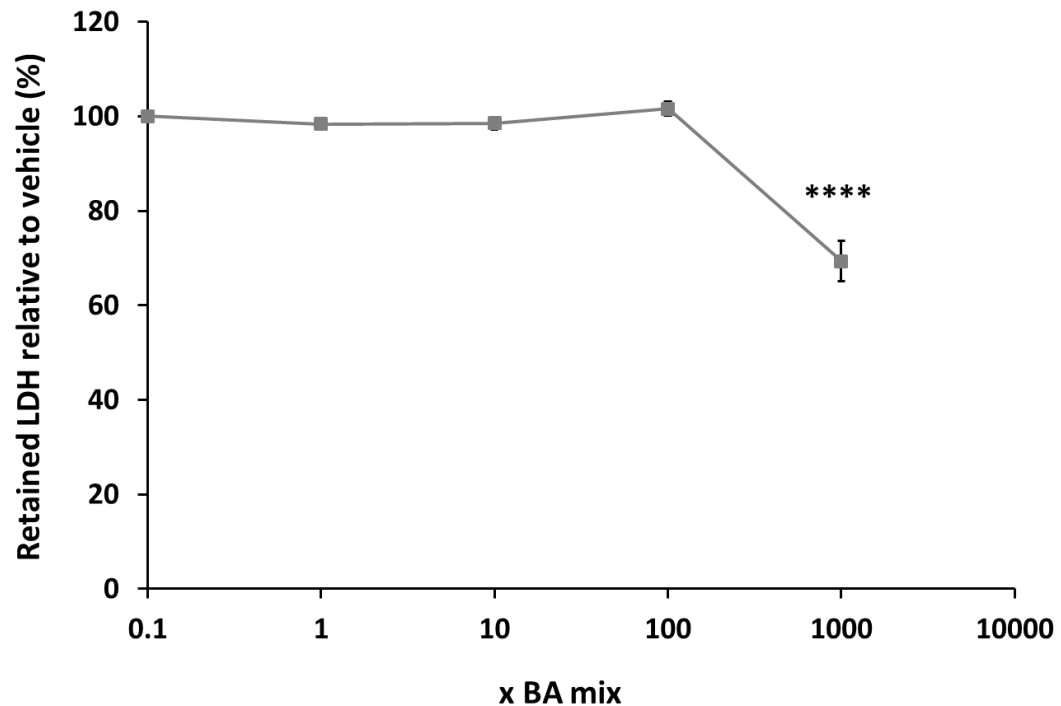


**Figure 3.15: The effects of BA mixtures on cellular retained LDH levels compared to the vehicle control after 2 weeks treatment.** Supernatant was collected daily after 1 week BA mix treatment and HepaRG cells re-dosed for an additional week. LDH content in the lysate was determined and retained LDH was calculated by; LDH in lysate/ (LDH in lysate + supernatant). Statistical significance compared with vehicle control; \* P < .05, \*\* P < .01, \*\*\* P < .001, \*\*\*\*P < .0001.

LDH levels were measured to gain further mechanistic understanding of the time-dependent cell death. The supernatant was collected daily following 1 week of BA mix treatment and the LDH released into the media was measured. There was a significant decrease of  $30.6 \pm 4.3$  % in retained LDH for HepaRG cells dosed with the 1000 x BA mix (figure 3.15).

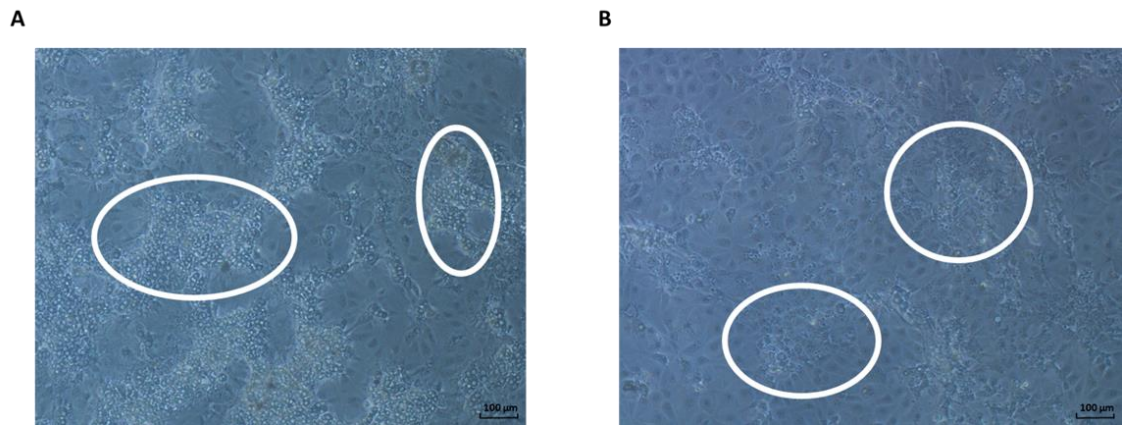


**Figure 3.16: Changes in HepaRG cell morphology following 2 weeks treatment with the 1000 x BA mix.** HepaRG cells are a heterogeneous population containing both hepatocytes and primitive biliary-like cells. Circled areas represent examples of the hepatocyte clusters. (A) Morphology of vehicle treated HepaRG cells. (B) Morphology of HepaRG cells following 2 weeks 1000 x BA mix treatment. There is a loss of the hepatocyte clusters following BA mix treatment. Images were taken using a Nikon Eclipse TS100 optical microscope using a 10 x objective. Scale bar = 100 µm.

Additionally, morphological changes were observed in the HepaRG cells that had been dosed for 2 weeks with the BA mixtures. Vehicle treated HepaRG cells had a mixed population of hepatocytes (figure 3.16A circles) and biliary-like epithelial cells. 2 weeks treatment with the 1000 x BA mix resulted in a loss of the hepatocyte clusters (figure 3.16B circles) whereas biliary-like epithelial cells remained unchanged.

### 3.3.6 Extracellular Flux Analysis of BA Mix-Induced Changes in Mitochondrial Function

XFe96 was used to assess more in-depth parameters of mitochondrial function via a mitochondrial stress test. A representative trace of a stress test in HepaRG cells is displayed in figure 3.8. BA mixtures did not cause a significant change in any of the parameters of mitochondrial function following 24 and 72 h (figure 3.17) or 1 and 2 week treatment (figure 3.18). There was a non-significant decrease in SRC; decreasing to  $68.9 \pm 19.2$  % following 1 week and  $61.9 \pm 18.9$  % following 2 weeks treatment (figure 3.18C) however, all other parameters remained unchanged.

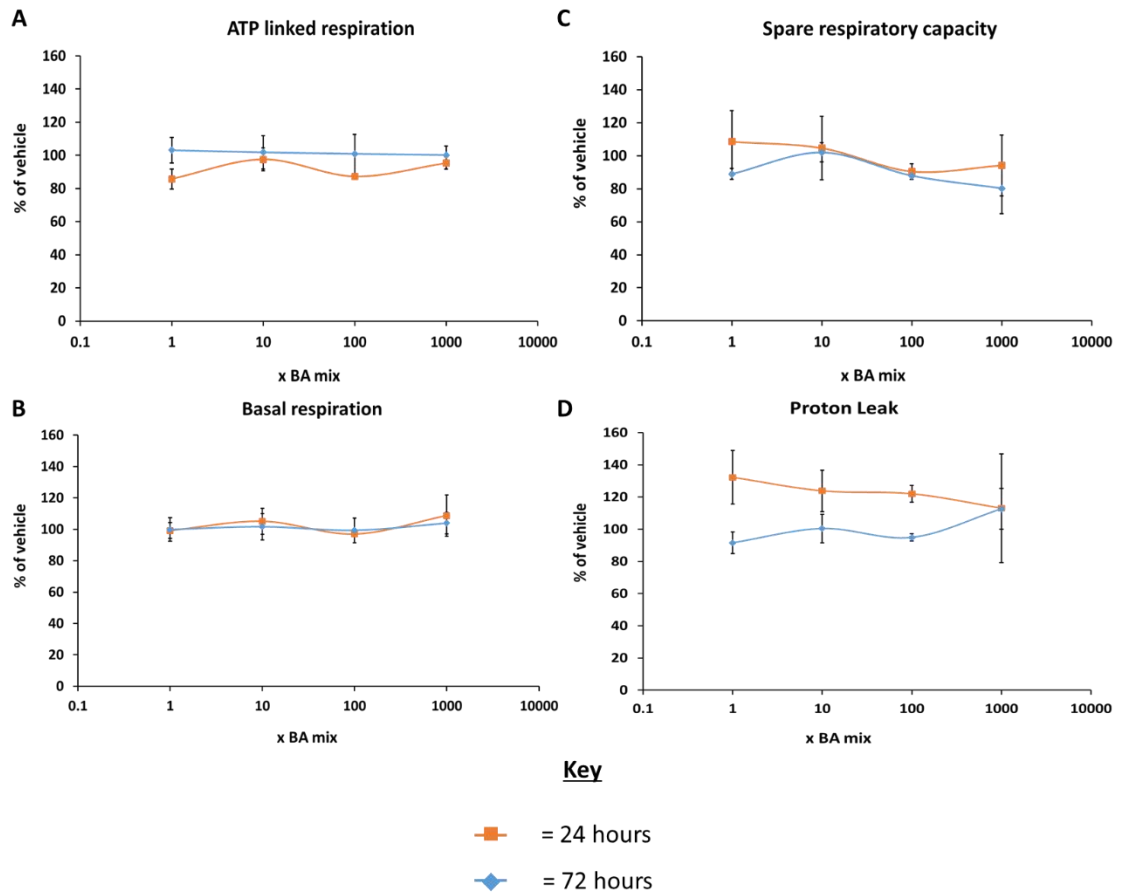


**Figure 3.17: The effects of BA mixtures on mitochondrial OCR after 24 and 72 h treatment.** Mitochondrial parameters; (A) ATP-linked respiration, (B) Basal respiration, (C) Spare respiratory capacity and (D) Proton leak, were calculated from OCR data to allow in-depth analysis of mitochondria after BA treatment. All results were normalised to  $\mu\text{g}$  of protein per well. Data are presented as  $\pm$  SEM of  $n = 4$  experiments.

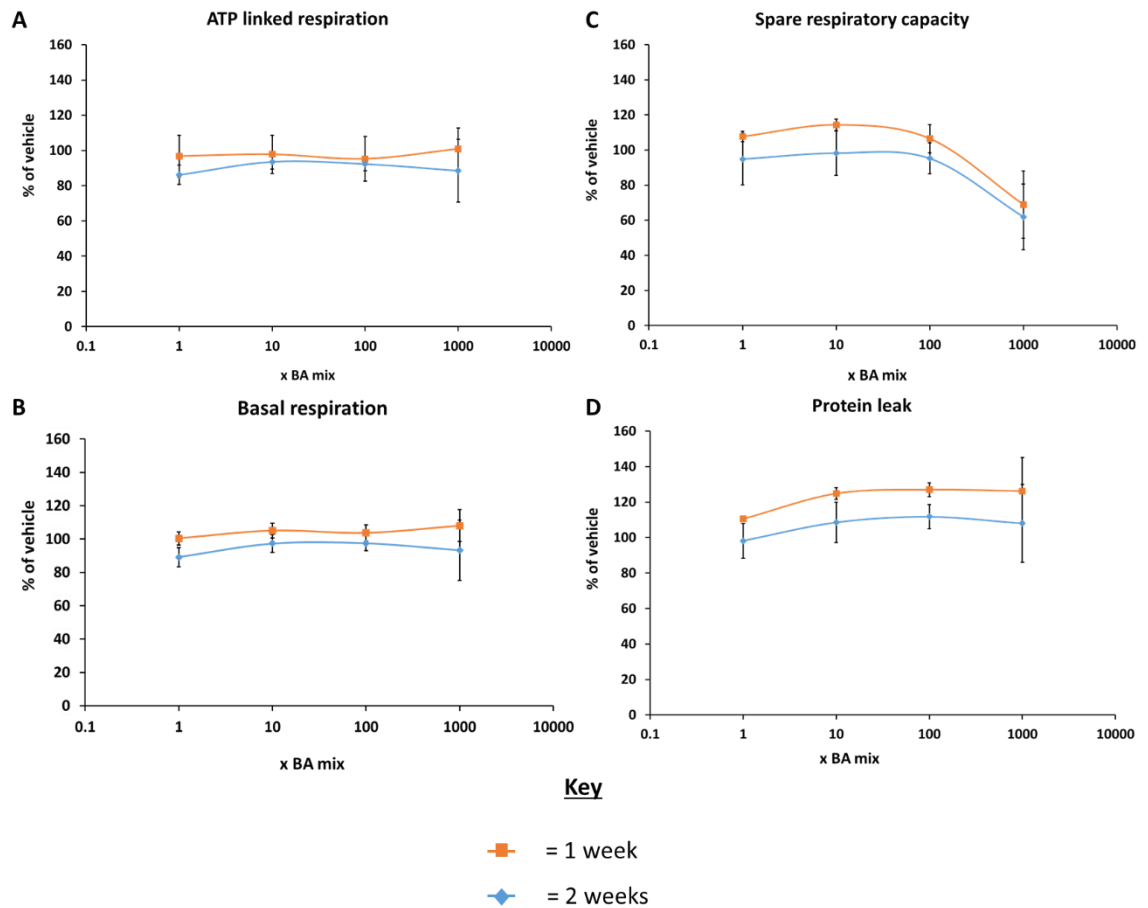


**Figure 3.18: The effects of BA mixtures on mitochondrial OCR after 1 and 2 weeks treatment.** Mitochondrial parameters; (A) ATP-linked respiration, (B) Basal respiration, (C) Spare respiratory capacity and (D) Proton leak, were calculated from OCR data to allow in-depth analysis of mitochondria after BA treatment. All results were normalised to  $\mu\text{g}$  of protein per well. Data are presented as  $\pm$  SEM of  $n = 4$  experiments.

### 3.3.7 Examining the Mitotoxic Potential of BA Mixtures Following Biliary Transporter Inhibition in HepaRG Cells

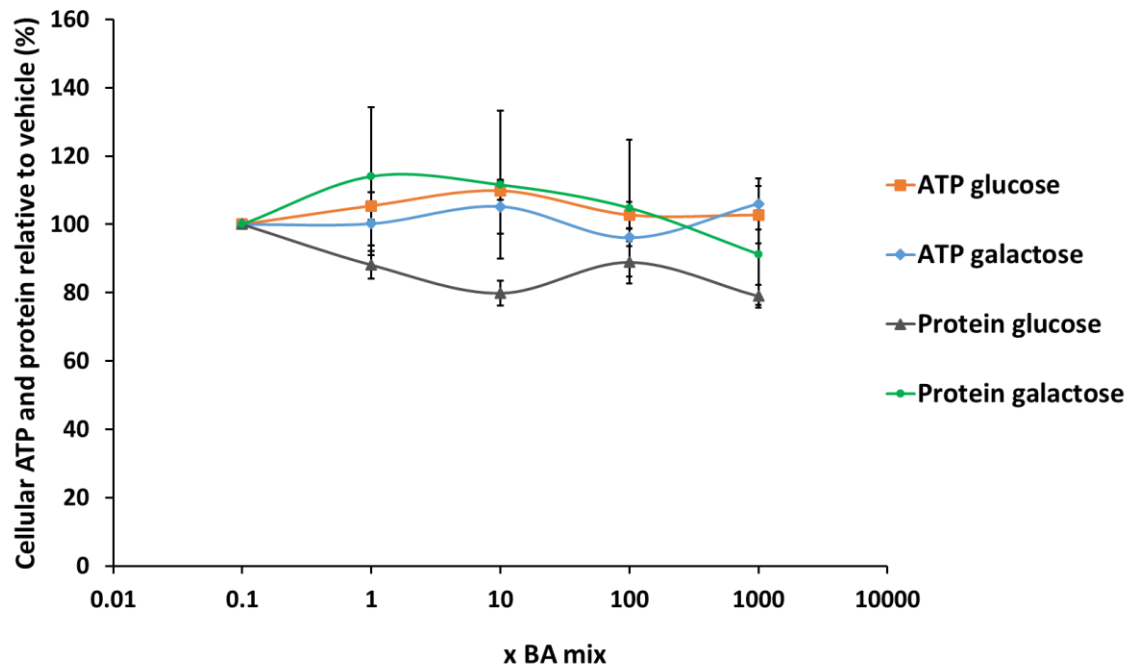


**Figure 3.19:** The effects of BA mixtures on ATP content and protein compared to the vehicle control following 24 h treatment and biliary transporter inhibition with MK571 (MRP inhibitor) and bosentan (BSEP inhibitor). ATP values have been normalised to  $\mu\text{g}$  protein per well. Data are presented as  $\pm$  SEM of  $n = 5$  experiments.

Following confirmation that the biliary transporters could be inhibited in HepaRG cells (chapter 2), HepaRG cells were treated with MK571 and bosentan followed by the BA mixtures in order to create a static pool of BAs within the cells. In the presence of the transporter inhibitors, there were no significant changes in cellular ATP content or protein levels following an acute metabolic modification assay with galactose (figure 3.19). Additionally, respirometry results following a mitochondrial stress test revealed that there were no significant changes in any of the mitochondrial parameters measured (figure 3.20).

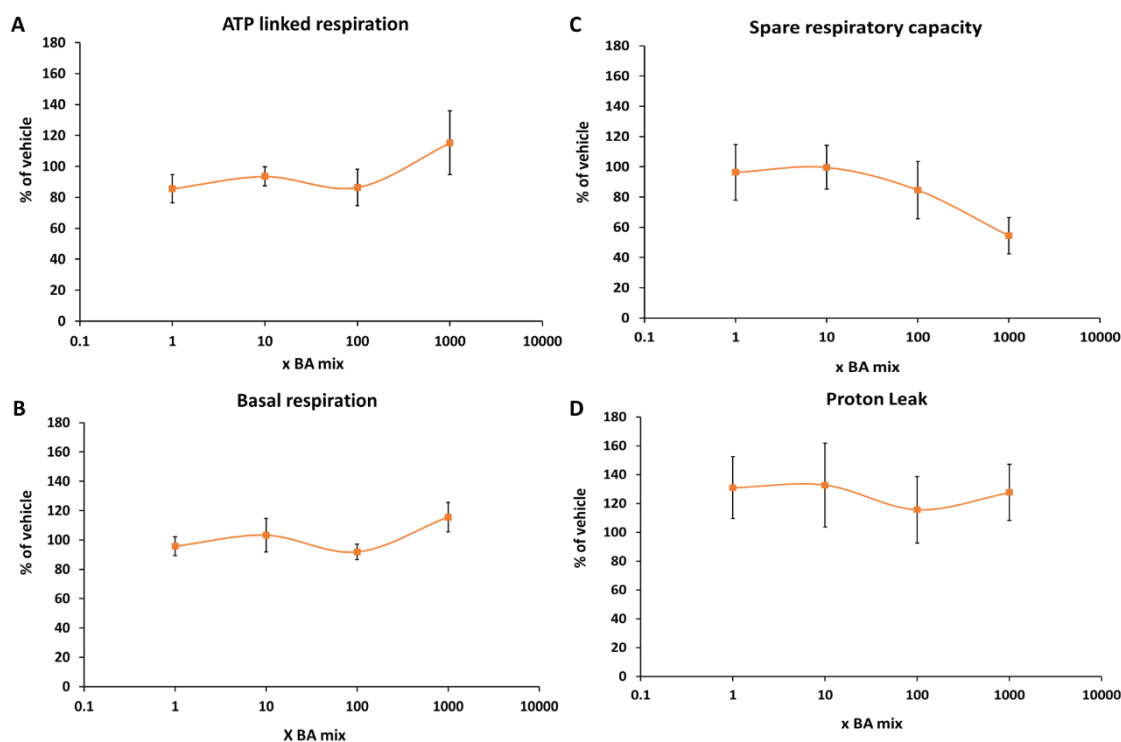


**Figure 3.20: The effects of BA mixtures on mitochondrial OCR following 24 h treatment and biliary transporter inhibition with MK571 (MRP inhibitor) and bosentan (BSEP inhibitor).** Mitochondrial parameters; (A) ATP-linked respiration, (B) Basal respiration, (C) Spare respiratory capacity and (D) Proton leak, were calculated from OCR data to allow in-depth analysis of mitochondria after BA treatment. All results were normalised to  $\mu\text{g}$  of protein per well.

### 3.3.8 Assessment of the Mitotoxic Potential of an Alternative BA Mixture in Isolated Mitochondria and HepaRG Cells

In order to confirm that the composition of the BA mixture was not responsible for the absence of mitochondrial toxicity in HepaRG cells, a second BA mixture composed of the BAs and their respective concentrations found within the bile of patients with obstructive cholestasis was prepared (table 3.1) (Woolbright et al., 2015). The mitotoxic potential of the additional BA mixture was assessed on isolated mitochondria. Exposure of isolated mitochondria to the additional BA mixture caused a significant increase in fluorescence when compared to mitochondria alone of  $20.7 \pm 3.5\%$  (figure 3.21A) whereas there were no significant changes in optical density (figure 3.21B). There was no significant difference in ATP content or retained LDH levels between glucose and galactose media in HepaRG cells exposed to the additional BA mixture for 24 h.

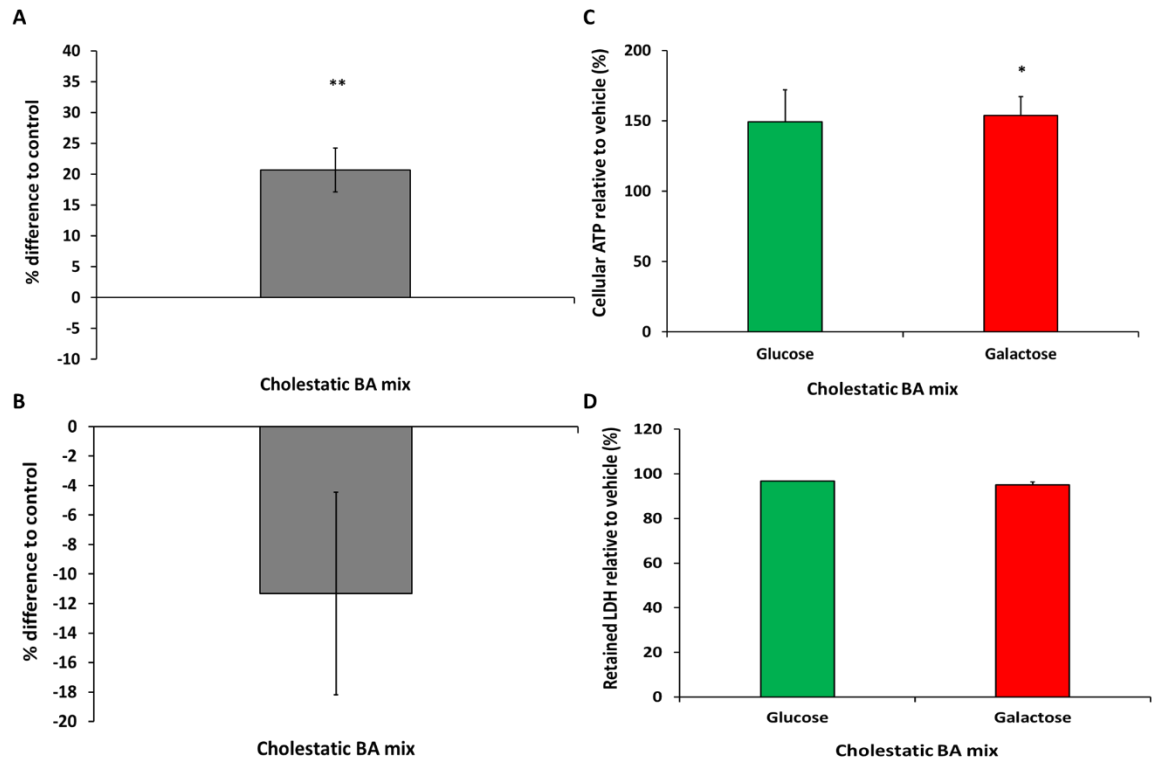


**Figure 3.21: The mitochondrial effects of an additional BA mixture with a composition based upon the concentrations of BAs detected within the bile of patients with cholestasis in isolated mitochondria and HepaRG cells. (A) % difference in MMP and (B) optical density at kinetic read 20 for isolated mitochondria acutely treated with the cholestatic BA mixture compared to control. (C) Changes in cellular ATP in glucose and galactose media and (D) retained LDH in glucose and galactose media in HepaRG cells after 24 h treatment with the cholestatic BA mixture compared to vehicle control. ATP values have been normalised to  $\mu\text{g}$  protein per well. Statistical significance compared with control; \*  $P < 0.05$ , \*\*  $P < 0.01$ , \*\*\*  $P < 0.001$ , \*\*\*\*  $P < 0.0001$ .**

### 3.4 DISCUSSION

Research in isolated mitochondria, HepG2 cells and rodent hepatocytes have demonstrated mitochondrial dysfunction as a mechanism of BA-induced toxicity. However, the findings described in this chapter have shown that BA mixtures do not cause mitochondrial toxicity when examined in a whole cell model with functional biliary transporters and enhanced physiological relevance than prior used models. Nonetheless, their effects upon isolated mitochondria from HepG2 cells confirmed previous reports.

In this thesis, mitochondria were isolated using a novel, semi-automated technique called the PCC (figure 3.1). Traditional methods of mitochondrial isolation were first employed in the 1940's and involved manual homogenisation using a Dounce homogeniser (Hogeboom et al., 1948; Pallotti and Lenaz, 2007). The degree of homogenisation was determined by the speed of the pestle, the number of strokes made and the clearance between the vessel and the pestle (Pallotti and Lenaz, 2007). Due to the physical aspect of this past technique, results lacked reproducibility (Schmitt et al., 2013). The coupling of a Balch homogeniser with a high precision automatic pump led to the creation of the PCC, which has been shown to isolate functionally intact mitochondria (Schmitt et al., 2013). An advantage of the automated method is that the shear force can be controlled via the pump, therefore generating reproducible results (Schmitt et al., 2015). Western blot analysis of the PCC isolated mitochondria from HepG2 cells in this chapter revealed that there was high purity of mitochondria with contaminations of peroxisomes and minor contaminations of lysosomes and nuclear proteins. Despite these contaminations, mitochondria were functional as they responded as expected to positive controls and had a stable membrane potential. Peroxisomes are difficult to eliminate from mitochondria fractions as they share similar densities and thus, sedimentation rates (Satori et al., 2012). However, purification of the crude mitochondria extract can be undertaken via a Nycodenz<sup>®</sup> density gradient centrifugation. Whilst application of the density gradient enriches the mitochondrial fraction and decreases the levels of contaminations, the yield of mitochondria decreases. Additionally, the functional integrity of the isolated mitochondria is time-dependent and so will be reduced due to the extra steps undertaken during the purification process (Schmitt et al., 2015). The functional integrity and quality of the mitochondria were deemed of higher importance than the purity for the experiments conducted in this chapter, and so purification steps were not conducted.

The mitotoxic potential of the BA mixtures were initially assessed in isolated mitochondria from HepG2 cells. The 1000 x BA mixture increased Rh123 fluorescence, indicating depolarisation of the inner mitochondrial membrane and caused mitochondrial structural alterations as signified by the optical density decrease. The changes in mitochondrial structure occurred immediately in comparison to changes in MMP and thus mirror results seen by Schulz et al. in which MMP loss and MPT were late events that occurred quickly at very high doses (Schulz et al., 2013). Notably, it was revealed that mitochondria undergo various stages of structural alterations upon BA exposure from inner membrane rearrangement, outer member detachment, matrix swelling and loss of cristae to finally MOMP and the formation of inner membrane vesicles (IMVs) (Schulz et al., 2013). Despite the mitochondria undergoing structural alterations in this chapter, they were still intact as evidenced by their membrane potential (figure 3.10). These results support previous findings in isolated mitochondria with single BAs, specifically that when administered in combination, BA mixtures caused mitochondrial toxicity (Palmeira and Rolo, 2004; Rolo et al., 2000; Schulz et al., 2013). In order to replicate the results seen by other researchers with single BAs, the mitochondrial toxicity of the individual BAs within the mixture were assessed. BA hydrophobicity is a determinant of toxicity and protection, with the more hydrophobic BAs causing greater levels of hepatocyte injury (Perez and Briz, 2009). The magnitude of hydrophobicity of the single BAs tested in this thesis are UDCA < CA < CDCA < DCA < LCA (Thomas et al., 2008). Exposure of the isolated mitochondria to the hydrophobic BAs LCA, DCA and CDCA resulted in a loss of MMP and significant optical density changes. The decline in fluorescent signal at 300  $\mu$ M and 500  $\mu$ M LCA could be due to auto-quenching of the fluorescent signal due to the rupture of mitochondria. As expected, the hydrophilic BAs CA and UDCA did not induce significant changes in Rh123 fluorescence or optical density. The BA mixtures contain both hydrophobic and hydrophilic BAs. Whilst LCA is the most toxic of the BAs tested, the concentration of LCA in the 1000 x BA mix is low at 8  $\mu$ M (table 2.2). The lowest concentration tested for the individual BAs was 50  $\mu$ M and so it is difficult to make assumptions on the role LCA within the 1000 x mix. However, both DCA and CDCA were present in the 1000 x BA mix at concentrations in which individually they were shown to cause toxicity. CDCA is present at 640  $\mu$ M and DCA at 480  $\mu$ M in the 1000 x BA mix. Given this association, it is plausible that the toxicity of the 1000 x BA mix is attributed to the high concentrations of CDCA and DCA.

Whilst experiments with increasing BA concentrations up to 500  $\mu$ M led to induction of mitochondrial toxicity, it is important to acknowledge that the concentrations of the BAs in

the 1000 x BA mixture are supra-physiological of serum BA levels. However, it has been reported that during cholestasis, intracellular concentrations of BAs can reach up to 800  $\mu\text{M}$  (Greim et al., 1973; Spivey et al., 1993). Additionally, research into BA toxicity in obstructive cholestasis found that there is potential leakage of bile back into the parenchyma that may expose hepatocytes to biliary concentrations of BAs, which are far greater than serum levels (Fickert et al., 2002). Whilst the concentrations of various BAs in serum rises to no  $\geq 20 \mu\text{M}$ , during cholestasis, certain BAs have been reported to reach up to 1 – 5 mM in bile (Woolbright et al., 2015). Together these findings suggest that although the 1000 x BA mixture used in this thesis is supra-physiological of serum levels, it is similar to the concentrations BAs have been postulated to rise to in bile, albeit not identical. In cases of obstructive cholestasis, it is suspected that biliary levels of BAs are responsible for hepatocyte toxicity. However, it remains unclear whether during intrahepatic cholestasis hepatocytes are exposed to such biliary fluids containing high concentrations of BAs. Resultantly, the toxicity of an alternative BA mixture composed of the BAs at levels found within the bile of patients with obstructive cholestasis was assessed on the isolated mitochondria. The use of the alternative BA mixture was to ensure that differences in the composition of the BA mixtures were not responsible for the depolarisation seen in isolated mitochondria. Exposure of isolated mitochondria to the alternative BA mixture resulted in a significant increase in Rh123 fluorescence, signifying depolarisation of the inner mitochondrial membrane. Collectively, the results with both BA mixtures and single BAs support previous findings that mitochondrial dysfunction is a mechanism of BA-induced toxicity when assessed in isolated mitochondria. However, it is important to note that within the human body and in HepaRG cells, BAs can bind to albumin present in serum or FBS (Roda et al., 1982). This therefore questions the translatability of the results detected in this chapter in isolated mitochondria, as it is unlikely that *in vivo* isolated mitochondria would be exposed to such high concentrations of BAs.

Whilst isolated mitochondria are valuable for mechanistic studies as they allow direct interactions between a compound and the mitochondria to be assessed, their lack of cellular context means they lack physiological relevance (Brand M and Nicholls D 2011). However, advancements in techniques have allowed mitochondrial bioenergetics and health to be assessed in whole cells, thus increasing the translatability of the results to an *in vivo* setting. The toxicity of the BA mixtures were examined in HepaRG cells treated with the BA mixtures for 24 h. There were no differences in the red/green fluorescent ratio, indicating that BA mixtures did not induce loss of MMP in whole cells. This contrasts with results seen in HepG2

cells grown in 2D culture in which CDCA resulted in mitochondrial depolarisation (Rolo et al., 2004). Whilst the findings of this research are not disputed, HepG2 cells grown in 2D are an inappropriate cell choice for cholestasis studies as concluded in chapter 2 of this thesis. Therefore, the translatability of the results seen in HepG2 cells may not be an accurate reflection of the pathophysiology in humans (Woolbright and Jaeschke, 2015). The uncoupler FCCP was used as a positive control for depolarisation in both isolated mitochondria and HepaRG cells. Correctly, FCCP induced a significant MMP loss with a decrease of  $0.4 \pm 0.1$  in the red/green fluorescent ratio in HepaRG cells. This apparent disconnection between the activity of BAs and the positive control in isolated organelles versus whole cells may be explained by considering the models physical properties and the chemical structure of the compounds (Palmeira and Rolo, 2004). Whilst BAs do possess an acid dissociable group, they lack other structural moieties that are present in FCCP that aid in its strong uncoupling activity. These include the presence of a bulky lipophilic group and strong electron withdrawing groups (Palmeira and Rolo, 2004). Therefore, the depolarisation observed in isolated mitochondria could be attributed to a direct interaction and immediate access of the BAs on the mitochondria. Alternatively, in whole cells, processes such as conjugation and metabolism could produce less toxic entities that are chemically unable to induce depolarisation (Chiang, 2013).

Research by Kamalian *et al*, confirmed the suitability of HepaRG cells for detecting mitochondrial toxicity via an acute metabolic modification with galactose, using a panel of positive and negative mitotoxic compounds (Kamalian et al., 2018). In support of the experiments measuring MMP, there were also no significant differences in cellular ATP content between glucose or galactose media for all time points tested suggesting BAs do not mediate mitochondrial toxicity via ETC dysfunction in HepaRG whole cells.  $IC_{50ATP}$  values could not be determined for any time-point, as BA mixtures did not result in a loss of ATP. Additionally, there were no differences in ATP content between glucose or galactose media for HepaRG cells exposed to the additional BA mixture. Exposure of HepaRG cells to BA mixtures for 1 week resulted in a significant decrease in protein. Protein continued to decline following 2 weeks dosing for the 1000 x BA mixture suggesting a temporal cytotoxicity. Daily supernatant LDH levels were assessed to gain further confirmation of a time-dependent cell death and verified that the 1000 x BA mixture induced significant cytotoxicity in HepaRG cells following 2 weeks dosing. Despite the significant loss of protein from 1 week of BA mix dosing, ATP levels significantly increased up to  $180 \pm 11.9 \%$  and then reduced to  $124.6 \pm 13.0 \%$  of the vehicle control. HepaRG cells are a heterogeneous population composed of

hepatocytes and primitive biliary-like cells (Marion et al., 2010). Interestingly, observation of changes in cell morphology revealed that there was a loss of hepatocytes in HepaRG cells following 2 weeks BA mix exposure, whereas primitive biliary-like cells remained unchanged. Transported-mediated uptake of BAs into cholangiocytes occurs via the ASBT transporter (Craddock et al., 1998; Hofmann, 2009). It has been revealed that ASBT is mutated in HepaRG cells and therefore, could explain the lack of BA-induced toxicity to the biliary-like-cells in this research due to a primary distribution in hepatocytes (Dianat et al., 2014). The increase in ATP following 1 week of BA mix dosing could be attributed to the biliary-like cells withstanding cytotoxicity by switching off ATP consuming processes to maintain ATP stores for cellular defence mechanisms (Kamalian et al., 2015). Cholangiocytes within the human body are responsible for altering the alkalinity of bile, thereby producing less toxic entities (Hohenester et al., 2012; Tabibian et al., 2013). The absence of toxicity to the biliary-like cells in HepaRG cells could also be attributed to alterations in the alkalinity of the BAs however, these cells are yet to be fully characterised and so their ability to alter bile pH is unknown.

The acute metabolic modification assay is a valuable first-line screening tool for detecting compounds that cause direct toxicity of the ETC however, it is limited in its ability to assess all forms of mitochondrial dysfunction (Kamalian et al., 2015). The use of ATP as a surrogate indicator for mitochondrial function is simplistic and offers no mechanistic insight to the dysfunction occurring. Accordingly, extracellular flux analysis was used to provide more in-depth insight into the mechanisms of BA toxicity as changes in OCR are known to be a more sensitive gauge of mitochondria function (Brand M and Nicholls D 2011).

The treatment of HepaRG cells with BA mixtures did not result in significant changes in any of the OCR parameters measured, supporting the previous findings that the BA mixtures do not induce mitochondrial dysfunction in HepaRG cells. Research has shown that SRC is the most sensitive parameter that is reduced if a compound has a mitochondrial liability (Kamalian et al., 2018). There was a non-significant decrease in SRC following 1 and 2 weeks BA mix exposure however, all other parameters remained unchanged. The time-point at which the decrease in SRC occurred is consistent with the decrease in protein and retained LDH, implying it is a result of cytotoxicity rather than mitotoxicity.

As previously demonstrated, HepaRG cells express functional biliary transporters (chapter 2) (Le Vee et al., 2006). Therefore, it was thought that the lack of mitochondrial toxicity in HepaRG cells could be attributed to the protective role of the biliary transporters and efflux of BAs out of hepatocytes. In order to create a static pool of BAs within the hepatocytes,

HepaRG cells were pre-dosed with MK571 and bosentan and then dosed with the BA mixtures for 24 h. There were no significant differences in cellular ATP content or protein levels in glucose and galactose media. Additionally, there were no significant differences in OCR results from the extracellular flux analysis. Collectively, these results support the findings that even when retained within hepatocytes, BA mixtures do not cause mitochondrial toxicity in HepaRG cells and thus disproves the primary hypothesis of this research.

BA-mediated mitochondrial toxicity has been identified in several studies using isolated mitochondria, rodent hepatocytes and HepG2 cells. These studies have identified mitochondrial dysfunction as a mechanism of BA-induced toxicity due to the activation of apoptosis. Specifically, HepG2 cells and rodent hepatocytes exposed to BAs resulted in an increase in the levels of B-cell lymphoma 2-associated X protein (Bax), caspase 9 and cytochrome c (Rodrigues et al., 1999; Rolo et al., 2004; Schoemaker et al., 2003). In work by Denk et al., the BA  $\beta$ -Muricholic acid, was found to induce loss of MMP and apoptosis in HepG2 cells transfected with NTCP at 25  $\mu$ M following 4 hours treatment (Denk et al., 2012). Whilst these observations are not disputed, their relevance to HepaRG cells and PHH is questioned. Firstly, HepG2 cells do not express functional BSEP, whereas HepaRG cells and PHH do. Therefore, it is plausible that in HepG2-NTCP cells, the BA  $\beta$ -Muricholic acid could have been retained within the cells and caused toxicity, which would not occur in HepaRG cells or PHH. Additionally,  $\beta$ -Muricholic acid is the major BA found within rats and mice and so toxicity could be due to a lack of exposure to a trihydroxylated BA (Denk et al., 2012). Exposure of isolated mitochondria from rodent hepatocytes to BAs resulted in the induction of the MPT, which is a hallmark of apoptosis (Rolo et al., 2003). Furthermore, BAs were shown to tightly bind to isolated mitochondria and instigate the detachment of the mitochondrial inner membrane boundary from the outer mitochondrial membrane, leading to the formation of negatively charged IMVs (Schulz et al., 2013). Whilst these findings are not disputed, they do not reflect the mechanisms of how BAs induce mitochondrial toxicity that then leads to cytotoxicity, but rather how mitochondria dysfunction is implicated in cell death. The activation of apoptosis is a downstream effect of toxicity and so must be activated via another mechanism. In this chapter, upstream processes of mitochondrial function and dysfunction were monitored in HepaRG cells, thus offering greater clarifications into the role of the mitochondria in BA-induced toxicity. Additionally, it is important to note that there are some limitations with the research conducted using rodent hepatocytes and HepG2. There are vast differences in BA concentrations and compositions in rodents and humans.

Rats produce high levels of hydrophilic bile salts such as TCA, whereas humans produce large quantities of toxic glycine-conjugated BAs (Woolbright and Jaeschke, 2015). Resultantly, rodent hepatocytes are overly sensitive to glycine-conjugated BAs, as they are not exposed to such bile salts *in vivo*, leading to conclusions that are not reflective of the pathophysiology in humans (Marrero et al., 1994; Woolbright and Jaeschke, 2015). The work presented in this chapter identified BA-induced mitochondrial toxicity in isolated mitochondria, similar to other researchers however, this mechanism of toxicity was not induced in a more physiologically relevant cell model. This therefore highlights that whilst the use of isolated mitochondria is valuable in determining direct mechanisms of mitochondrial toxicity, their lack of cellular context means conclusions may have limited *in vivo* and clinical relevance, thus disproving the second hypothesis of this research. Notably, that mitochondrial toxicity would be detected in both whole cells and isolated mitochondria. Overall, these studies show that BA-induced mitochondrial toxicity does not precede cytotoxicity in a whole cell model with functional biliary transporters and enhanced suitability for DIC studies.

Finally, the results generated in this chapter can be linked with conclusions drawn from chapter 2. In chapter 2, it was suggested that there could be a mechanistic link between BA-induced mitochondrial dysfunction and biliary transporter alterations. However, the mitotoxic potential of the BA mixtures needed to be determined in HepaRG cells. The evidence presented in this chapter has shown that BA mixtures exert a time-dependent cytotoxicity that is not mediated via the mitochondria in HepaRG cells. Resultantly, it can be concluded that there is not a mechanistic link between mitochondrial dysfunction and ATP-dependent transports in BA-induced toxicity. Interestingly, the identification of temporal cytotoxicity in HepaRG cells was consistent with the periods in which alterations in BSEP and MRP2 were detected in chapter 2 of this thesis. Whilst a reduction in MRP2 can have severe clinical consequences, the reduction is unlikely attributable to the cytotoxicity observed in HepaRG cells due to compensatory mechanisms of BA efflux (Keppler, 2014; Trauner and Boyer, 2003). The toxicity of DIC is multi-mechanistic with reports suggesting destruction of lipid membranes, ROS production, alterations to bile canaliculi dynamics and endoplasmic reticulum stress as mediators of BA-induced toxicity (Adachi et al., 2014; Fahey et al., 1995; Hofmann, 1999b; Perez and Briz, 2009; Sharanek et al., 2016). It is plausible that these mechanisms are activated in tandem however, mitochondrial toxicity is not one of these mechanisms in HepaRG cells.

### 3.5 CONCLUSION

The work presented in this chapter has shown that mitochondrial toxicity does not precede cytotoxicity in HepaRG cells. The detection of BA-induced mitochondrial toxicity in isolated mitochondria did not translate to a whole cell model, thus highlighting limitations of the use of isolated mitochondria when trying to deduce results with *in vivo* relevance. Past research in isolated mitochondria, rodent hepatocytes and HepG2 cells revealed mitochondrial dysfunction as a key mechanism of BA-induced hepatotoxicity. However, there are caveats with this past research including inappropriate species model choice and a lack of a physiologically relevant cell line. Given the enhanced physiological relevance of the research presented in this chapter, in comparison to past studies, it is likely that mitochondrial toxicity is not a mechanism of BA-induced toxicity in humans. As a result of the negative mitotoxic potential of the BA mixtures, it can also be concluded that there is no mechanistic link between inhibition of mitochondrial function and ATP-dependent transporter activity with BAs.

# **Chapter 4**

## **Assessment of the Mitotoxic and Cholestatic Potential of Flucloxacillin in HepaRG cells**

**CONTENTS**

4.1	INTRODUCTION	113
4.2	MATERIALS AND METHODS	115
	4.2.1 Materials	115
	4.2.2 HepaRG Cell Culture	115
	4.2.3 Bile Acid Treatment	115
	4.2.4 Cholestasis Assay	115
	4.2.5 Fluorescence Imaging of Biliary Transporters	116
	4.2.6 Acute Metabolic Modification Assay	116
	4.2.7 Statistical Analysis	117
4.3	RESULTS	118
	4.3.1 Determining the cholestatic potential of flucloxacillin in HepaRG cells	118
	4.3.2 Assessment of the Effects of Flucloxacillin on Cellular ATP and Cell Death Following Acute Metabolic Modification with Galactose Media	118
4.4	DISCUSSION	122
4.5	CONCLUSION	125

## 4.1 INTRODUCTION

Flucloxacillin is an antibiotic of the penicillin class used in the treatment of Gram – positive bacterial infections ranging from skin and soft tissue infections to urinary tract infections (Wing et al., 2017). In the 1980's, several cases of flucloxacillin-induced liver injury were reported with severe cases leading to fatality (Boyd, 2002). Flucloxacillin predominantly causes DILI via cholestatic liver injury with estimated cases to be 8.5 in 100,000 patients (Russmann et al., 2005). Despite this, flucloxacillin still remains the first line treatment of *Staphylococcal* infections in the UK with 2 million prescriptions per year (Andrews and Daly, 2008; Russmann et al., 2005).

The mechanisms underlying flucloxacillin-induced liver injury are currently unknown but thought to be multi-mechanistic. It is known that there is a strong association of human leukocyte antigen (HLA) allele HLA-B\*57:01 with flucloxacillin-induced liver injury, suggestive of activation of the adaptive immune system (Daly et al., 2009). Non-immune mediated mechanisms of flucloxacillin involve molecular events leading to cholestasis. The cholestatic potential of flucloxacillin has been demonstrated in HepaRG cells whereby impairment of the Rho-kinase signalling pathway resulted in bile canaliculi dilation and reduced BA efflux, which was further enhanced by pro-inflammatory cytokines (Burban et al., 2018; Burban et al., 2017; Sharanek et al., 2019). However, the events that bring about activation of the Rho-kinase pathway are yet to be fully defined. Given the bacterial origin of the mitochondria and the potential for many drugs with liver toxicity liabilities to induce mitochondrial toxicity, research has hypothesised that mitochondrial dysfunction may be a method of flucloxacillin-induced liver injury (Kalghatgi et al., 2013; Pessayre et al., 2010). However, this aspect of flucloxacillin toxicity has yet to be fully investigated. Given the suitability of HepaRG cells for studying DIC and DIMT, the aim of this chapter was to assess the mitotoxic and cholestatic potential of flucloxacillin. It was hypothesised that flucloxacillin-induced mitochondrial toxicity is a pre-determinant of cholestatic risk.

The work presented in this chapter is a sub-section of a large, multi-research project to elucidate both non-immune and immune-mediated mechanisms of flucloxacillin-induced hepatotoxicity. In this pilot study, the effects of flucloxacillin upon mitochondrial function were examined via changes in ATP levels and cytotoxicity in HepaRG cells under acute metabolic modification. Results from the overall project revealed that inhibition of MRP2 and Pgp with MK571 and valsopodar led to an increase in intracellular flucloxacillin within HepaRG cells (data not shown). Therefore, the mitotoxic potential of flucloxacillin was

further investigated following biliary transporter inhibition in order to create a static pool of flucloxacillin within hepatocytes (Penman et al., 2019). It has been shown in HepaRG spheroids that dual dosing with a compound with cholestatic potential and BAs presents synergistic toxicity (Hendriks et al., 2016). Notably, this assay has successfully identified chlorpromazine and troglitazone as compounds with cholestatic potential (Hendriks et al., 2016). Therefore, HepaRG cells represent a system with which to investigate concomitant, or sequential activation of cholestatic and mitochondrial dysfunction induced by flucloxacillin.

## 4.2 MATERIALS AND METHODS

### 4.2.1 Materials

HepaRG cells, basal media, growth and differentiation additives were purchased from Biopredic International (Saint Grégoire, France). Cytotoxicity Detection Kit was purchased from Roche Diagnostics Ltd. (West Sussex, UK). Williams' E Medium powder (with L-Glutamine, without glucose) was manufactured by United States Biological. Collagen I rat protein and PBS were purchased from Life Technologies (Paisley, UK). Clear and white 96-well plates were purchased from Fisher Scientific (Loughborough, UK) and Greiner Bio-One (Stonehouse, UK) respectively. All other reagents and chemicals were purchased from Sigma Aldrich (Dorset, UK). Flucloxacillin (Wockharat) was gifted from collaborators.

### 4.2.2 HepaRG Cell Culture

HepaRG cells were maintained and cultured as previously described (Section 2.2.3).

### 4.2.3 Bile Acid Treatment

HepaRG cells were treated with the 1000 x BA mixtures as previously described (Section 2.2.4).

### 4.2.4 Cholestasis Assay

#### 4.2.4.1 Assay Preparation

Undifferentiated HepaRG cells were plated in collagen coated 96-well cell culture plates at 9000 cells/well and cultured to differentiation as described (Section 2.2.3).

Next, serum-free base media was prepared from glucose-free Williams E powder dissolved in sterile distilled water and supplemented with sodium bicarbonate (3.7 mg/mL), insulin (5 µg/mL) and hydrocortisone (50 µM). The base media was supplemented with glucose (11 mM), which is the same concentration of glucose found within the HepaRG differentiation media as told by Biopredic.

#### 4.2.4.2 24 h Flucloxacillin Dosing

Differentiated HepaRG cells were washed twice in serum-free glucose media before incubation in the respective media (50 µL) for 2 h. Flucloxacillin and the 1000 x BA mixture

were diluted in serum-free glucose media to reach a final solvent concentration of 1 % (v/v) and added to all wells of the plate (50  $\mu$ L) for 24 h.

Following drug incubation, HepaRG cells were lysed in somatic cell ATP releasing agent and 10  $\mu$ L was used to assess ATP content and protein content as described (Section 3.2.8.5 and Section 2.2.5.2 respectively).

#### **4.2.5 Fluorescence Imaging of Biliary Transporters**

Undifferentiated HepaRG cells were prepared as described (Section 2.2.6.1). HepaRG cells were incubated with CMFDA (5  $\mu$ M) and Hoechst (1:5000) with or without MK571 (30  $\mu$ M) and valsopodar (12.5  $\mu$ M) in HBSS for 30 mins at 37 °C and images were taken as described (Section 2.2.6.3).

#### **4.2.6 Acute Metabolic Modification Assay**

##### *4.2.6.1 Assay Preparation*

Undifferentiated HepaRG cells were plated in collagen coated 96-well cell culture plates at 9000 cells/well and cultured to differentiation as described (Section 2.2.3).

Serum-free base media was prepared as described above (Section 4.2.4.1). Additionally, galactose media was prepared by supplementing serum-free base with galactose (10 mM).

##### *4.2.6.2 4 or 24 h Flucloxacillin Dosing*

Differentiated HepaRG cells were washed twice in either serum-free glucose or galactose media before incubation in the respective media (50  $\mu$ L) for 2 h. Flucloxacillin and the 1000 x BA mixture were diluted in serum-free glucose or galactose media to reach a final solvent concentration of 1 % (v/v) and added to all wells of the plate (50  $\mu$ L) for 4 or 24 h.

##### *4.2.6.3 Inhibition of Biliary Transporters with MK571 and valsopodar*

HepaRG cells were washed twice with either serum-free glucose or galactose media before incubation in the respective media (50  $\mu$ L) for 2 h. Valsopodar (12.5  $\mu$ M) and MK571 (30  $\mu$ M) were diluted in either serum-free glucose or galactose media to reach a final solvent concentration of 1% (v/v) and added to every well of the plate (50  $\mu$ L) for 30 min. Following this, media containing the inhibitors were aspirated and HepaRG cells were treated in serum-free glucose or galactose media containing flucloxacillin, valsopodar and MK571 (100  $\mu$ L) for 24 h.

Following drug incubation, the supernatant was collected and used to measure lactate dehydrogenase (LDH) released as described (Section 3.2.9). Cells were lysed in somatic cell ATP releasing agent and 10  $\mu$ L was used to assess ATP content and protein content as described (Section 3.2.8.5 and Section 2.2.5.2 respectively). The lysate was dilute (1:5) using media and LDH content within the lysate was measured as described (Section 3.2.9).

#### **4.2.7 Statistical Analysis**

Data is expressed from a minimum of three independent experiments. Unless specified otherwise, all results are expressed as mean  $\pm$  SEM. Normality was assessed using a Shapiro-Wilk statistical test. Statistical significance compared to the control was determined by a one-way ANOVA with a Dunnett's test or a student's t-test for parametric data or the appropriate alternative for non-parametric data using StatsDirect 3.0.171. Results were considered significant when  $P < 0.05$ .

## 4.3 RESULTS

### 4.3.1 Determining the cholestatic potential of flucloxacillin in HepaRG cells

In this assay, the cholestatic risk of a compound is determined by calculating the  $(IC_{50-ATP}$  compound and BA)/ $(IC_{50-ATP}$  compound alone) known as the cholestatic index ( $CI_x$ ) (Hendriks et al., 2016). Compounds are defined as having a cholestatic risk if  $CI_x \leq 0.8$  (Hendriks et al., 2016). The  $IC_{50-ATP}$  value for flucloxacillin alone was  $12.7 \pm 0.6$  mM whereas the  $IC_{50-ATP}$  value for the 1000 x BA mixture and flucloxacillin was  $7.0 \pm 1.1$  mM. A slight increase in toxicity was detected upon exposure to the BA mixture, but based on the  $CI_x$  value, flucloxacillin was classified as a compound that had cholestatic risk ( $CI_x = 0.6 \pm 0.1$ ) (figure 4.1).

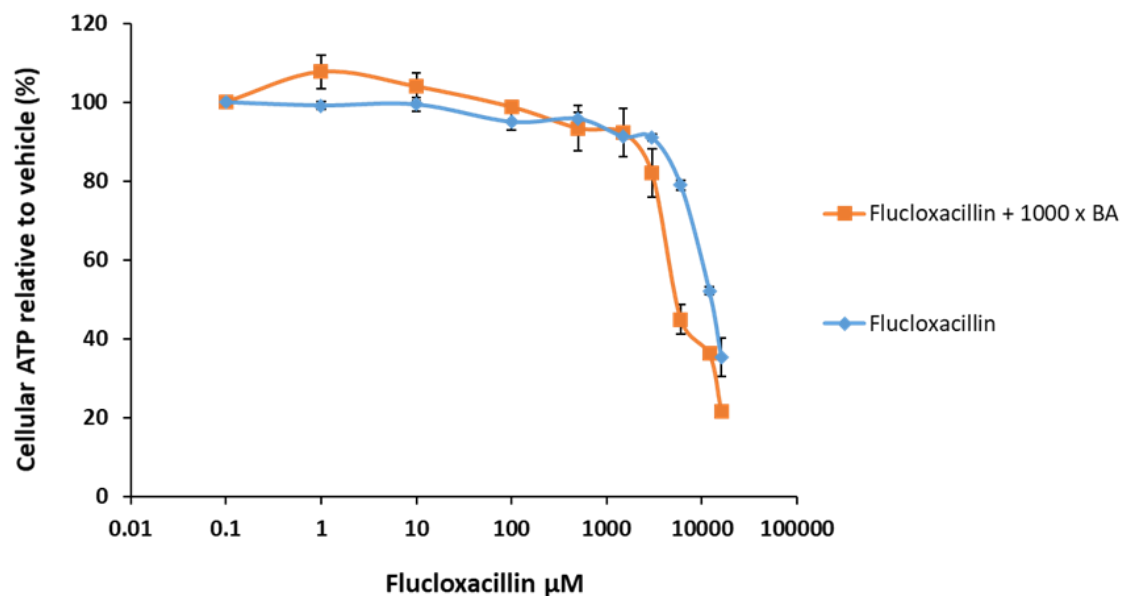
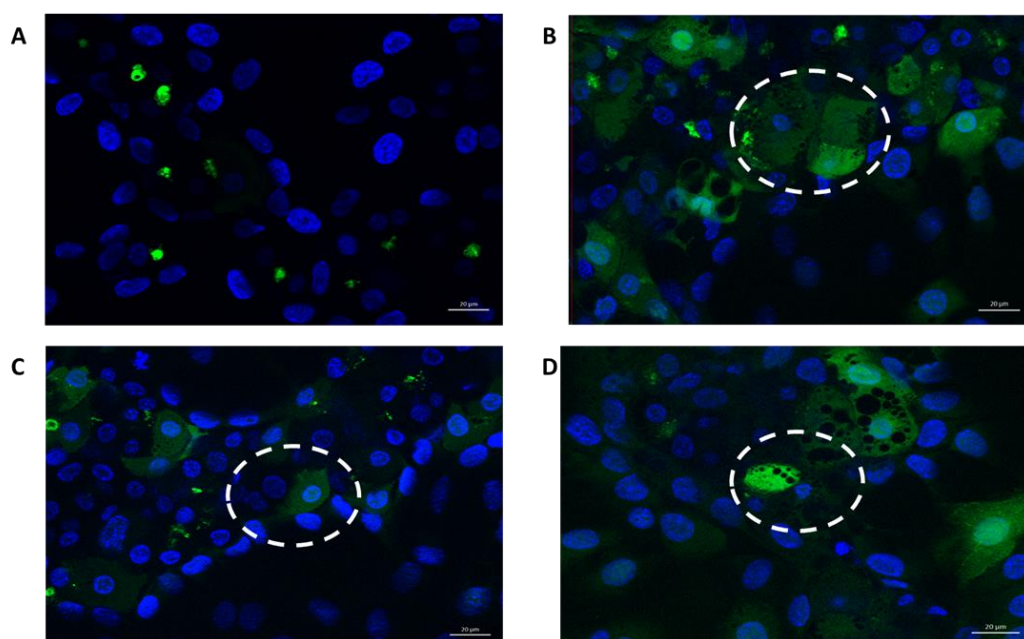


Figure 4.1: The effects on cellular ATP content following 24 hrs exposure of HepaRG cells to flucloxacillin in the presence and absence of a 1000 x bile acid mixture.

### 4.3.2 Assessment of the Effects of Flucloxacillin on Cellular ATP and Cell Death Following Acute Metabolic Modification with Galactose Media

A 30 min treatment with MK571 and valsopodar, was shown to inhibit MRP and Pgp as evidenced by the retainment of CMFDA within the cell cytoplasm (dotted circles in figure 4.2B-D).



**Figure 4.2: Transporter function and inhibition in HepaRG cells with the fluorescent dye CMFDA.** HepaRG cells were treated with (A) CMFDA (5 $\mu$ M) and Hoechst (1:5000) only for 30 minutes; (B) CMFDA, Hoechst and the Pgp inhibitor valsopodar (12.5  $\mu$ M) for 30 minutes; (C) CMFDA, Hoechst and the MRP inhibitor MK571 (30  $\mu$ M) for 30 minutes and (D) CMFDA, Hoechst, valsopodar and MK571 for 30 minutes. Snap images were taken with Apotome on a Zeiss microscope using 40 x objective. Circles indicate CMFDA retained within the cell cytoplasm. Scale bar = 20  $\mu$ m.

According to the metabolic modification assay, a compound is deemed to possess a mitochondrial liability if the ratio between the IC<sub>50</sub> ATP values in glucose and galactose media is  $\geq 2$  (Kamalian et al., 2015; Swiss et al., 2013). IC<sub>50</sub> values were less than 2 for all treatment options (table 4.1).

**Table 4.1: Comparison of IC<sub>50</sub>-ATP levels in glucose and galactose media following flucloxacillin and biliary transporter inhibitors in HepaRG cells.**

Treatment	Concentration (mM)		IC <sub>50</sub> ATPglu/IC <sub>50</sub> ATPgal (P-value)
	IC <sub>50</sub> ATPglu	IC <sub>50</sub> ATPgal	
4 hours flucloxacillin	5.5 $\pm$ 0.7	4.9 $\pm$ 1.0	1.13 (0.61)
4 hours flucloxacillin + MK571	5.4 $\pm$ 1.1	7.7 $\pm$ 2.2	0.71 (0.41)
4 hours flucloxacillin + valsopodar	8.0 $\pm$ 1.2	6.6 $\pm$ 0.9	1.21 (0.37)
4 hours flucloxacillin + MK571 + valsopodar	9.4 $\pm$ 4.7	5.4 $\pm$ 1.6	1.74 (0.25)

24 hours flucloxacillin	12.7 ± 0.6	12.5 ± 0.9	1.01 (0.87)
----------------------------	------------	------------	-------------

Cellular ATP levels decreased in both glucose and galactose media, in the absence of cell death, following 4 hr flucloxacillin treatment (figure 4.3B). This trend was observed in the presence of biliary transporter inhibitors (figure 4.3C-E). However, following 24 hrs flucloxacillin treatment, ATP decrease and cell death occurred concurrently (figure 4A). The absence of a difference in ATP levels between glucose and galactose media for all time points tested suggests that flucloxacillin did not cause mitochondrial dysfunction via direct ETC dysfunction.

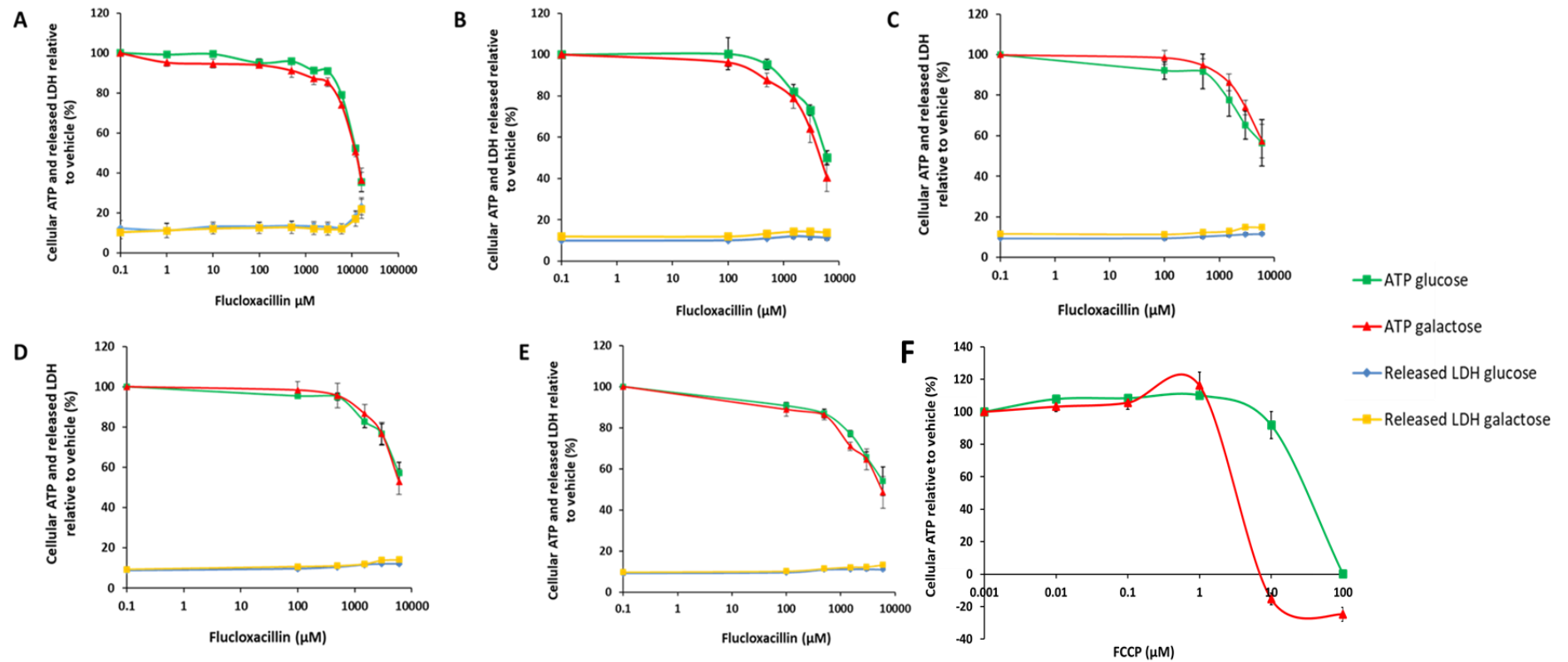


Figure 4.3: The effects of flucloxacillin after (A) 24 hours, (B) 4 hours, (C) 4 hours flucloxacillin and MK571, (D) 4 hours flucloxacillin and valsopodar, (E) 4 hours flucloxacillin, MK571 and valsopodar (F) 24 hours FCCP on cellular ATP content and released LDH compared to the vehicle control. ATP values have been normalised to  $\mu\text{g}$  protein per well.

## 4.4 DISCUSSION

The hepatic cell line, HepaRG, has been used for the successful identification of compounds that are mitochondrial toxicants via direct ETC dysfunction (Kamalian et al., 2018). The dual assessment of ATP content alongside LDH release allows mitochondrial toxicity to be detected prior to the initiation of cytotoxicity (Kamalian et al., 2015). According to this assay, flucloxacillin was not identified to possess a mitochondrial liability (figure 4.3). Due to HepaRG cells expressing functional transporters, it was hypothesised that the absence of flucloxacillin-induced mitochondrial toxicity arises from a failure to retain flucloxacillin within the hepatocytes. Pgp and MRP transporters were inhibited (figure 4.2) and HepaRG cells were dosed with flucloxacillin. Similarly, in the presence of these transporters, there were no significant changes in ATP content in glucose or galactose media. Increasing the duration of the metabolic modification assay and concentrations of compounds used has been shown to reveal mitochondrial toxicity (Kamalian et al., 2015). HepaRG cells were dosed for 24 h with concentrations reaching 16 mM however, the  $IC_{50ATPglu}/IC_{50ATPgal}$  ratio remained less than 2 and there was significant cytotoxicity with 16 mM in both media types. Overall, indicating that ETC dysfunction is not a mechanism of flucloxacillin-induced liver injury in HepaRG cells.

Whilst the differences in  $IC_{50-ATP}$  for flucloxacillin alone and with the 1000 x BA mix were small (12.7 mM vs 7.0 mM), the assay tested was able to successfully classify flucloxacillin as a compound with a cholestatic risk as  $Clx \leq 0.8$  at 0.6 (figure 4.1). Research has shown that the dual treatment of cells with BAs and compounds with a cholestatic liability demonstrate a synergistic toxicity (Chatterjee et al., 2014; Hendriks et al., 2016). The BA mixture used in this chapter is known to not cause mitochondrial toxicity up to 2 weeks of dosing (Penman et al., 2019). Therefore, it is plausible that the small increase in toxicity could be attributed to a synergistic toxicity between flucloxacillin and the BA mixture. However, the absence of mitochondrial dysfunction following 4 and 24 hrs flucloxacillin treatment, but identification of a cholestatic risk following 24 hrs treatment, disproves the hypothesis of this pilot study that mitochondrial toxicity is a pre-determinant of cholestasis. It has been demonstrated that the molecular events leading to flucloxacillin-induced bile canaliculi dilations are attributed to an inhibition of heat shock protein 27 (hsp27) and downstream activation of the phosphoinositide 3-kinase (PI3K)/ protein kinase B (AKT) signalling pathway (Burban et al., 2017). Whilst the PI3K/AKT pathway is typically associated with cellular protection, in HepaRG cells it has also been credited to an

impairment of the Rho-kinase signalling pathway resulting in bile canaliculi dilation and reduced BA efflux (Burban et al., 2017). The results from this pilot study reveal that mitochondrial dysfunction via direct ETC dysfunction is not a molecular event that is involved in flucloxacillin-induced cholestasis.

The most widely accepted theory of the origin and evolution of the mitochondria is the endosymbiotic theory (Martin et al., 2015). This theory postulates that the mitochondria were prokaryotic cells proficient in oxidative mechanisms whilst eukaryotic cells relied on glycolytic pathways for energy production (Whelan and Zuckerbraun, 2013). The two cell types lived symbiotically with the eukaryotic cells acting as a host cell for the prokaryotic cell (Whelan and Zuckerbraun, 2013). During eukaryotic evolution, parts of the mitochondrial genome were transferred to the eukaryotic nuclear DNA and underwent modification to develop nuclear DNA, which encodes genes for glycolysis and OXPHOS (Wallace, 2009). The rest of the mitochondrial genome remained within the mitochondria and is central for transcription of subunits for OXPHOS (Whelan and Zuckerbraun, 2013). Due to the bacterial origin of mitochondria, it was hypothesised that flucloxacillin may target the mitochondria in DILI. Whilst the results from this pilot study show that flucloxacillin does not have any ETC liabilities, other antibiotics have been shown to target mitochondria via other mechanisms (Dewelhenke et al., 2007; Kroon and Van den Bogert, 1983; Lawrence et al., 1993; Moullan et al., 2015). The bactericidal chloramphenicol was shown to cause an increase in lactate production due to an inhibition of mitochondrial protein synthesis (Kroon and Van den Bogert, 1983). The macrolide antibiotics are known to interact with phospholipids and affect lipid fluidity leading to the conclusion that they could alter mitochondrial membrane potential (Dewelhenke et al., 2007; Montenez et al., 1999). Ciprofloxacin, ampicillin and kanamycin were shown to increase levels of mitochondrial superoxides, decrease mitochondrial complex activity and cause a reduction in the MMP (Kalghatgi et al., 2013). Additionally, tetracyclines have been shown to initiate mitochondrial dysfunction by promoting a mitochondria-nuclear protein imbalance, manipulating mitochondrial gene expression and disrupting translation (Jones et al., 2009; Moullan et al., 2015).

Whilst this pilot study failed to link acute mitochondrial dysfunction and cholestasis, it would be a disservice to discredit the potential role of the mitochondria in flucloxacillin-induced toxicity given the multiple roles of the mitochondria in cellular physiology. In this chapter, mitochondrial toxicity was only examined via the acute metabolic modification assay. Given the vast amount of literature in which antibiotics have caused mitochondrial

dysfunction via other mechanisms, further research should be conducted before flucloxacillin is deemed negative for mitochondrial toxicity. Notably, changes in mitochondrial protein synthesis may be a more suitable endpoint.

## 4.5 CONCLUSION

The work presented in this pilot study has demonstrated the utility of 2D cultured HepaRG cells for assessing the cholestatic potential of a compound. The dual treatment of HepaRG cells with a BA mixture and flucloxacillin revealed synergistic toxicity and correctly classified flucloxacillin as a compound with a cholestatic potential. However, initial experiments to determine if flucloxacillin is a mitochondrial toxicant revealed negative mitochondrial dysfunction. It is important to note that this chapter has only focussed upon one assay to identify mitochondrial toxicity. Thus, more mechanistically-focussed experiments should be undertaken before mitochondrial toxicity is not deemed one of the mechanisms of flucloxacillin-induced DILI.

## **Chapter 5**

# **Assessment of the Impact of Mitochondrial Genetic Variation and Susceptibility to Toxicity Using HepG2 Transmitochondrial Cybrids**

**CONTENTS**

5.1	INTRODUCTION	129
5.2	MATERIALS AND METHODS	133
	5.2.1 Materials	133
	5.2.2 HepG2 Cell Culture	133
	5.2.3 Transmitochondrial HepG2 Cell Culture	133
	5.2.4 Assessment of Membrane Potential in Isolated Mitochondria	133
	5.2.5 Acute Metabolic Modification Assay	134
	5.2.6 High-throughput Assessment of Mitochondrial Membrane Potential in HepG2 cells and Cybrids	134
	5.2.7 Assessment of Cellular Superoxide Levels	134
	5.2.8 Assessment of Individual Respiratory Complex Driven Respiration (I-IV)	135
	5.2.9 Mitochondrial Dynamics Assessment via Fluorescence Imaging	137
	5.2.10 Mitochondrial DNA Copy Number via RT-PCR	137
	5.2.11 Proteomic Analysis for Markers of Mitochondrial Biogenesis	139
	5.2.12 Statistical Analysis	139
5.3	RESULTS	140
	5.3.1 Assessment of the Effect of Tolcapone and Entacapone on Mitochondrial Membrane Potential in Isolated Mitochondria	140
	5.3.2 Assessment of the Effects of Tolcapone on Mitochondrial Membrane Potential in HepG2 Cells and Haplogroup H and J Cybrids	142
	5.3.3 Assessment of the Effects of Compounds on Cellular ATP Following Acute Metabolic Modification with Galactose Media	144
	5.3.4 Examining the Effects of Tolcapone on Cellular Superoxide Levels	147
	5.3.5 Assessment of the Effects of Tolcapone-induced Respiratory Complex Dysfunction	149

5.3.6	Assessment of Tolcapone-induced Changes in Mitochondrial Dynamics	151
5.3.7	Examination of the Effects of Tolcapone on mtDNA copy number per cell	153
5.3.8	Assessment of the Effects of Tolcapone on Mitochondrial Biogenesis	156
5.4	DISCUSSION	160
5.5	CONCLUSION	171

## 5.1 INTRODUCTION

Cases of toxicity that are idiosyncratic present the most uncertainty to drug development as they typically only occur when the novel agent is tested on a large population post market (Mosedale and Watkins, 2017). Given the unpredictability of idiosyncratic DILI, its acquisition has been suggested to be characterised, at least in part, by interindividual variation (Chalasani and Björnsson, 2010; Russmann et al., 2009; Uetrecht, 2008). Whilst there have been advancements in the field to identify host nuclear genetics conferring increased susceptibility to idiosyncratic DILI, the pathogenesis is still poorly understood and it has been proposed that DILI may be a complex genetic disorder (Chalasani and Björnsson, 2010; Fontana, 2014).

The mitochondria are a source of interindividual variation as they contain their own genome. The mitochondrial genome encodes core subunits of the ETC and it has been shown that variation within the mitochondrial genome can produce differences in mitochondrial function, disease susceptibility and drug efficacy (Chinnery and Hudson, 2013; Gomez-Duran et al., 2010; Gomez-Duran et al., 2012; Kenney et al., 2014). Given this association, it has been hypothesised that variation in mtDNA could underpin some of the idiosyncrasies associated with DILI by offering another source of interindividual variation (Boelsterli and Lim, 2007). However, there is limited representation of interindividual variation in preclinical models and notably, the role of the mitochondrial genome has been neglected (Mosedale and Watkins, 2017). The ability to study the effects of mtDNA variation and susceptibility to ADRs could prove invaluable in increasing the predictivity of preclinical screening.

The effects of mtDNA variation can be encompassed into preclinical models via the creation of trans-mitochondrial cybrids (section 1.5.1.5). The fusion of  $\rho 0$  cells (devoid of mtDNA) with anucleated cells of known genotype allows the impact of mitochondrial genotype to be assessed against a constant nuclear genetic background (figure 1.13) (Wilkins et al., 2014). At the time of study, there had been no studies examining the influence of mtDNA variation upon susceptibility to drug toxicity in relation to DILI. HepG2 trans-mitochondrial cybrids were generated and kindly donated by Dr Amy Ball, Department of Pharmacology and Therapeutics, The University of Liverpool for the purpose of the research conducted within this chapter. Briefly, HepG2 cells were devoid of their mtDNA via culture in 1  $\mu\text{M}$  ethidium bromide for 8 weeks to create HepG2  $\rho 0$  cells. Freshly-isolated platelets from volunteers of known mitochondrial genotype were fused with HepG2  $\rho 0$  cells using PEG and cultured in a selective growth media devoid of pyruvate and uridine to eliminate unfused  $\rho 0$  cells. The use

of HepG2 trans-mitochondrial cybrids presents an opportunity to identify possible associations between mtDNA haplogroups and susceptibility to idiosyncratic DILI via mitochondrial dysfunction in a cell line routinely used for DILI studies (Ball, 2018).

The cybrids used in this chapter were created from individuals of haplogroup H and J. Haplogroup H is the most common haplogroup in the UK. Haplogroup J is the second most common haplogroup and contains non-synonymous mutations in subunits 3 and 5 within complex I (figure 1.12) (Eupedia, 2018; van Oven, 2015). As the ability to research the mitochondrial genome has advanced, the mitochondrial phylogenetic tree (figure 5.1) has expanded. Notably, as more SNPs have been identified, macro-haplogroups have grown to contain more divisions termed sub-haplogroups. Specifically, the cybrids used in this research belonged to the sub-haplogroup H2a1e1a1 and J1c1e. Out of a selection of ten cybrid cell lines, two of these were selected based upon their high-quality score, which is an indicator of genomic sequencing accuracy. As previously mentioned, HepG2 cells were established from a Caucasian male from Argentina (Aden et al., 1979). It was discovered that HepG2 cells belong to haplogroup B and more specifically, the sub-haplogroup B2c2, which is common amongst Native Americans (Starikovskaya et al., 2005). By comparing haplogroups common in Europe with one common in indigenous Americans, the work presented in this chapter has greater consideration of ethnic diversity and its contributions to susceptibility to drug toxicity.

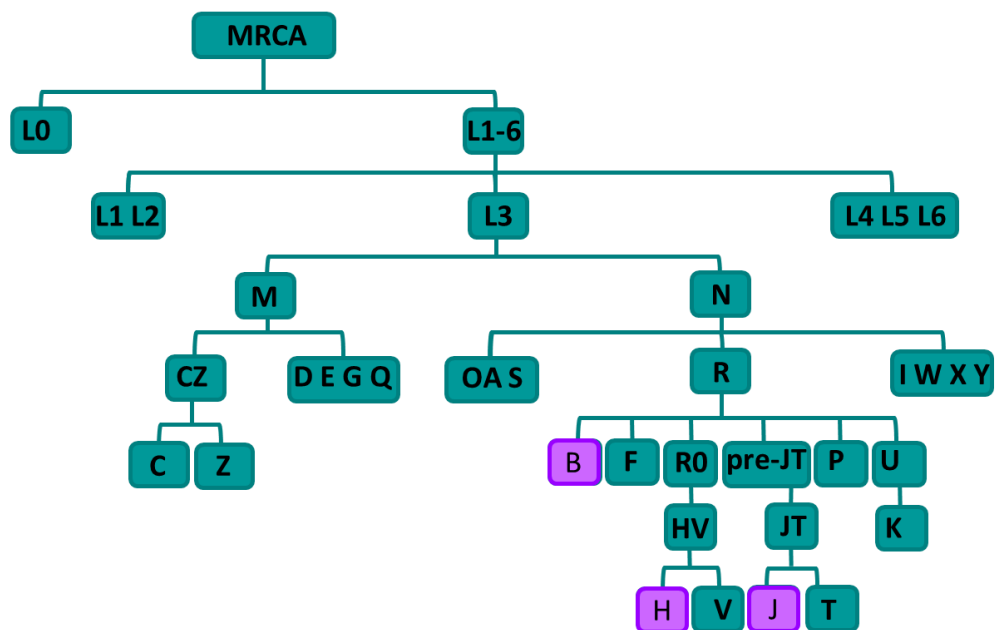


**Figure 5.1: Simplified representation of the mitochondrial phylogenetic tree.** The evolution of mitochondrial macro-haplogroups from the MRCA. The haplogroups investigated in this research are highlighted in purple. Adapted from (van Oven, 2015).

To test differences in susceptibility between haplogroups, a model drug with known mitochondrial toxicity was investigated. Tolcapone is a compound that was developed for the treatment of Parkinson's disease. Tolcapone is a selective inhibitor of the enzyme catechol-O-methyl transferase (COMT). When administered in conjunction with levodopa, a precursor of dopamine, tolcapone prevents the methylation of levodopa and increases its elimination half-life (Dingemans et al., 1995). When tested in clinical trials, tolcapone was revealed to be efficacious and safe. "Off-periods", where patients experience symptoms of tremors and dyskinesia, were greatly reduced and it was concluded that tolcapone in co-administration with levodopa had great clinical benefit (Baas et al., 1997; Dupont et al., 1997; Kurth et al., 1997; Rajput et al., 1997). However, four cases of serious hepatic dysfunction, with three of these resulting in deaths, were reported post-market (Assal et al., 1998). Consequently, tolcapone was issued a black-box warning and is used as a last-resort treatment for those who do not respond to other COMT inhibitors (Borges, 2005). Entacapone was developed as an alternative to tolcapone and is not associated with cases of DILI (Korlipara et al., 2004). However, entacapone is a less potent COMT inhibitor and has a shorter half-life, which results in patients experiencing the symptoms of Parkinson's disease more frequently than if administered tolcapone (Lees, 2008). Tolcapone is a known mitochondrial toxicant and *in vitro* work has revealed it is a mitochondrial uncoupler whereas, entacapone has been shown to have a weak mitochondrial liability (Kamalian et al., 2015). Given the positive clinical effects of tolcapone treatment for individuals with Parkinson's disease, the ability to identify "at risk" individuals based upon their mitochondrial genome could have great impact on the safe usage of tolcapone treatment.

The overall aim of this research was to advance findings obtained from a pilot study of the utility of the HepG2 transmitochondrial cybrids. Notably, in the pilot study, differential susceptibility to DIMT were observed following 2 h tolcapone treatment between haplogroup H and J HepG2 transmitochondrial cybrids (Ball, 2018). The research presented within this chapter aimed to expand on these findings by conducting more in-depth mechanistic assays at different time points to identify the role of mtDNA variation upon susceptibility to tolcapone-induced toxicity. Initial research with the HepG2 cybrids revealed that haplogroup J cybrids were more susceptible to tolcapone-induced ATP depletion and fission than haplogroup H cybrids following 2 h tolcapone treatment (Ball, 2018). Supporting this finding, research using Leber's hereditary optic neuropathy (LHON) fibroblast cybrid models belonging to haplogroups H, J and U revealed that haplogroup J cybrids were more susceptible to uncoupling by toluene and the neurotoxic uncoupler 2,5-hexanedione (Ghelli

et al., 2009). Consequently, the hypothesis of this work was that haplogroup J cybrids would be more susceptible to acute tolcapone-induced mitochondrial toxicity than haplogroup B and H. To screen for acute DIMT, HepG2 cells and haplogroup H and J cybrids were dosed for 2 hours and then subjected to testing using methods previously optimised for isolated mitochondria and whole cells in order to observe immediate mitochondrial response. Namely, alterations to MMP in both isolated mitochondria and whole cells, and ATP quantification in acutely galactose-conditioned cells. Following these evaluations, XFe96 analysis was utilised to assess the activity of specific respiratory complexes within the ETC to gain a more in-depth judgement on respiratory function. In order to evaluate downstream impacts of mitochondrial dysfunction, ROS production was determined. The mitochondria have developed a multitude of coordinated responses to stress in order to minimise cell toxicity (Valera-Alberni and Canto, 2018). In order to investigate differences in mitochondrial protection, final experiments examined changes in mitochondria morphology, dynamics and mtDNA copy number via western blotting, fluorescence imaging and real-time PCR (RT-PCR). The application of these assays following 2 h tolcapone treatment would allow elucidation of differences in acute mitochondrial toxicity and response dependent upon mitochondrial haplogroup.

In order to expand on the initial HepG2 cybrid pilot study, this research extended the dosing regimen to 24 h treatment in order to observe if there were differences in mitochondrial protection or adaptation dependent on mtDNA haplogroup. A meta-analysis of Parkinson's patients and control subjects revealed that haplogroups K, J and T were associated with increased mitochondrial protection and adaptation (Hudson et al., 2013). Whilst genetic associations and cybrid studies are not directly comparable due to differences in the nuclear genome and environmental factors of those in the meta-analysis, investigations of temporal differences in DIMT in cybrids are warranted given the potential for differences in mitochondrial protection and adaptation (Strobbe et al., 2018). As a result, a secondary hypothesis was formulated; haplogroup J cybrids would be able to adapt to mitochondrial dysfunction and therefore be less susceptible to DIMT following 24 h tolcapone treatment. To assess this secondary hypothesis, cells were subjected to testing via the aforementioned *in vitro* assays but following 24 h tolcapone treatment. Collectively, these techniques were used to determine temporal differences in susceptibility to tolcapone toxicity based upon activation of mitochondrial compensatory mechanisms of protection.

## 5.2 MATERIALS AND METHODS

### 5.2.1 Materials

HepG2 cells were purchased from European Collection of Cell Cultures (ECACC, Salisbury, UK). HepG2 transmitochondrial cybrids were gifted from The University of Liverpool (Liverpool, UK). DMEM, media supplements, cell culture reagents and RT-PCR reagents were purchased from Life technologies (Paisley, UK). Balch homogeniser was purchased from Isobiotech (Heidelberg, Germany). High precision pump – pump 11 was purchased from Harvard apparatus (Massachusetts, USA). JC-1 and all antibodies were purchased from Abcam (Cambridge, UK) or Proteintech (Illinois, USA). All Extracellular flux analyser (XFe96) consumables were purchased from Agilent (Santa Clara, USA). Bradford reagent was purchased from Bio-Rad (Hertfordshire, UK). MitoSOX™ dye was purchased from Invitrogen (Carlsbad, USA). DNA mini kit and nuclease-free water were purchased from Qiagen (Manchester, UK). All other reagents and chemicals were purchased from Sigma Aldrich (Dorset, UK) unless otherwise stated.

### 5.2.2 HepG2 Cell Culture

HepG2 cells were maintained and cultured as previously described (Section 2.2.2).

### 5.2.3 Transmitochondrial HepG2 Cell Culture

HepG2 transmitochondrial cybrids were maintained and cultured at 37 °C in 5 % CO<sub>2</sub> in DMEM high-glucose medium (glucose; 25 mM) supplemented with 10 % v/v FBS, sodium pyruvate (1 mM), L-glutamine (4 mM) and HEPES (1 mM) as the same for HepG2 cells (Section 2.2.2).

### 5.2.4 Assessment of Membrane Potential in Isolated Mitochondria

Mitochondria were isolated from HepG2 cells and haplogroup H and J cybrids as previously described (Section 3.2.5). Following successful isolation of mitochondria, loss of MMP was assessed following acute treatment with tolcapone and entacapone (0.975 – 500 μM) as previously described (Section 3.2.6).

### 5.2.5 Acute Metabolic Modification Assay

HepG2 cells and haplogroup H and J cybrids were collected by trypsinisation with 0.25 % trypsin and seeded into collagen coated 96-well plates at  $1 \times 10^5$  cells/well. Cells were maintained as described (Section 2.2.2) for 24 h.

Cells were washed twice in serum-free glucose or galactose media (DMEM supplemented with 25 mM glucose and 4 mM L-glutamine or 10 mM galactose and 6 mM L-glutamine respectively, plus 1 mM HEPES and 1 mM sodium pyruvate) before incubation in the respective media (50  $\mu$ L) for 2 h. Serial dilutions of tolcapone, entacapone, FCCP and rotenone (200 x) were prepared in DMSO and further diluted 1:100 into the appropriate media and added to every well of the plate (50  $\mu$ L) for 2 or 24 h. The final solvent concentration for all experiments was 0.5 % (v/v) DMSO.

Cells were lysed in somatic cell ATP releasing agent and 10  $\mu$ L was used to assess ATP content and protein content as described (Section 3.2.8.5 and Section 2.2.5.2 respectively).

### 5.2.6 High-throughput Assessment of Mitochondrial Membrane Potential in HepG2 cells and Cybrids

Changes in MMP were assayed using the fluorescent dye JC-1 in a plate reader assay. HepG2 cells and haplogroup H and J cybrids were collected by trypsinisation with 0.25 % trypsin and seeded into un-collagen coated, black 96-well plates with a clear base at  $1.5 \times 10^4$  cells/well and incubated overnight in glucose media as described previously (Section 2.2.2). Cells underwent a 2 h galactose metabolic switch and tolcapone dosing in galactose media for 2 or 24 h as previously described (Section 5.2.5).

A lyophilised vial of JC-1 dye was prepared as according to the manufacturer's instructions in order to create a 1 mM stock. Following tolcapone dosing, cells were incubated with JC-1 (1  $\mu$ M) for 30 mins in the dark. Following this, cells were washed with HBSS and 50  $\mu$ L HBSS was added to every well. The fluorometric signal (475/20 nm excitation; 530/15 nm emission; 590/17.5 nm emission) was read on a Varioskan™ Flash multimode plate reader with SkanIt™ software.

### 5.2.7 Assessment of Cellular Superoxide Levels

The development of superoxide occurs at complexes I and III during OXPHOS. Excessive superoxides can lead to mitochondrial dysfunction. The MitoSOX™ Red reagent allows direct

measurements of superoxide levels in live cells where it selectively targets the mitochondrial matrix. Many reagents for measuring superoxide levels are also oxidised by other ROS and reactive nitrogen species however, MitoSOX™ is oxidised merely by superoxide. The oxidation of MitoSOX™ Red leads to an emission of red fluorescence, which can be measured using a plate reader assay (Robinson et al., 2006).

HepG2 cells and haplogroup H and J cybrids were collected by trypsinisation with 0.25 % trypsin and seeded into un-collagen coated, white-walled 96-well plates at  $1 \times 10^5$  cells/well for 2 h dosing and  $5 \times 10^4$  cells/well for 24 h dosing and incubated overnight in glucose media as described previously (Section 2.2.2). Cells underwent a 2 h galactose metabolic switch and tolcapone dosing in galactose media for 2 or 24 h as previously described (Section 4.2.5). MitoSOX™ Red was prepared in DMSO as according to the manufacturer's guidelines in order to create a 5 mM stock. Cells were incubated with MitoSOX™ Red (5  $\mu$ M) diluted in HBSS in the dark for 30 mins (37 °C, 5 % CO<sub>2</sub>). Following this, cells were washed with HBSS and the fluorescent signal (excitation/emission 396/579 nm) was read immediately on a Varioskan™ Flash multimode plate reader with SkanIt™ software.

## 5.2.8 Assessment of Individual Respiratory Complex Driven Respiration (I-IV)

### 5.2.8.1 Assay preparation

The XFe96 analyser was used to assess individual respiratory complex driven respiration (I – IV). HepG2 cells and haplogroup H and J cybrids were collected by trypsinisation with 0.25 % trypsin and seeded into collagen coated XFe96 cell culture microplates (25 x 10<sup>3</sup> cells/100  $\mu$ L medium/well) and incubated overnight. Cells were cultured as described previously (Section 2.2.2).

### 5.2.8.2 Respiratory Complex Assays (I – IV)

The cell culture medium was removed and replaced with mitochondrial assay solutions (MAS) buffer (5 mM MgCl<sub>2</sub>, 220 mM mannitol, 70 mM sucrose, 10 mM KH<sub>2</sub>PO<sub>4</sub>, 2 mM HEPES, 1 mM EGTA and 0.4 % (w/v) fatty acid free BSA, pH 7.2), supplemented with constituents to stimulate oxygen consumption via complex I (4.6 mM ADP, 30 mM malic acid, 22 mM glutamic acid, 0.2 % (w/v) BSA and 1 nM recombinant perfringolysin O (rPFO)), complex II (4.6 mM ADP, 20 mM succinic acid, 1  $\mu$ M rotenone, 0.2 % (w/v) BSA and 1 nM rPFO), complex III (4.6 mM ADP, 500  $\mu$ M duroquinol, 1  $\mu$ M rotenone, 40  $\mu$ M malonic acid, 0.2 % (w/v) BSA and 1 nM rPFO) or complex IV (4.6 mM ADP, 20 mM ascorbic acid, 0.5 mM TMPD (N,N,N',N'-

tetramethyl-p-phenylenediamine), 2  $\mu\text{M}$  antimycin A, 0.2 % (w/v) BSA and 1 nM rPFO). The XFe96 instrument was programmed to measure 3 cycles of mix (30 secs), measure (2 mins) and wait (30 secs) to establish a basal OCR. Tolcapone (15 – 250  $\mu\text{M}$ ) was acutely injected and 3 measurement cycles were performed. Following this, a mitochondrial stress test was conducted as described (Section 3.2.10.2). The site of action of complex-specific substrates and inhibitors is illustrated (figure 5.2).

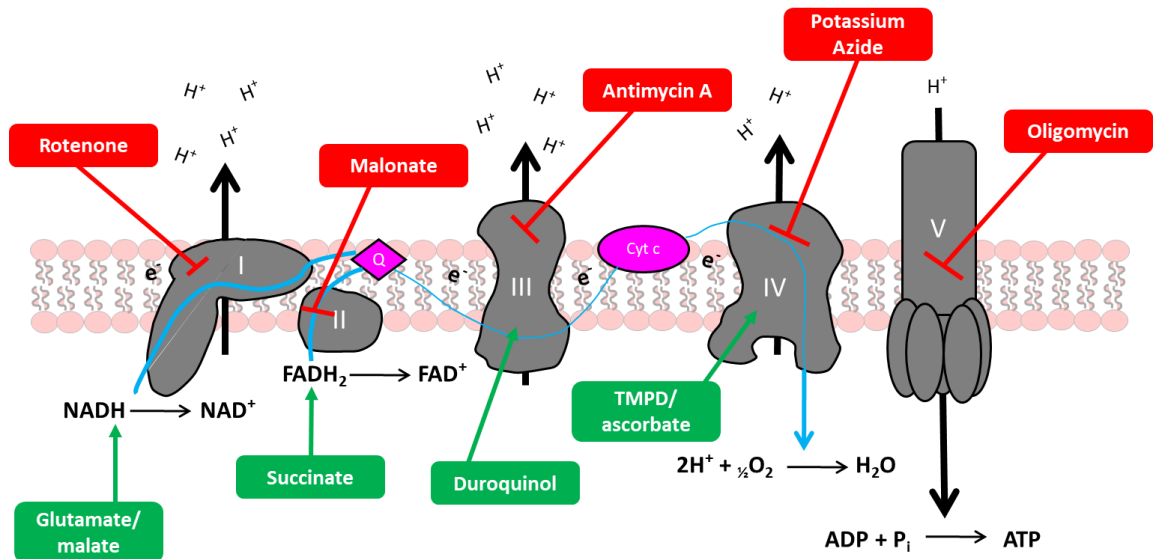


**Figure 5.2: Sites of action of complex-specific substrates (green) and inhibitors (red) used in the mitochondrial respiratory complex assay.** To stimulate oxygen consumption via specific complexes, substrates and inhibitors had to be supplemented into the assay solution.

To measure complex IV activity, the final injection of rotenone/antimycin A was replaced with the complex IV inhibitor, potassium azide (50  $\mu\text{M}$ ). This substitution was essential for the calculation of non-mitochondrial OCR because TMPD/ascorbate undergo reduction-oxidation (REDOX) cycling, which can “consume” oxygen within the assay medium. This can cause significant background signal which could be falsely analysed as complex IV activity (Morgan and Wikstrom, 1991). Complex I – IV activity was defined as maximal respiratory capacity (as a % of basal respiration), normalised to the respective vehicle control.

Following completion of the assay, media was removed from all wells and cells were lysed in somatic ATP releasing agent (20  $\mu\text{L}$ ). 10  $\mu\text{L}$  of cell lysates (diluted 1:1 in somatic ATP releasing agent) were transferred to a clear 96-well plate and a standard Bradford assay was

conducted as described (Section 3.2.5.3). Protein count per well was used to normalise OCR values.

## 5.2.9 Mitochondrial Dynamics Assessment via Fluorescence Imaging

### 5.2.9.1 Assay Preparation

HepG2 cells and haplogroup H and J cybrids were collected by trypsinisation with 0.25 % trypsin and seeded onto collagen coated (50 µg/mL in 0.02 M acetic acid) glass coverslips in 12-well plates at  $5 \times 10^5$  cells/well and incubated overnight in glucose media as described previously (Section 2.2.2). The following day, cells underwent a 2 h galactose metabolic switch and tolcapone dosing in galactose media for 2 or 24 h as previously described (Section 5.2.5).

### 5.2.9.2 Immunofluorescence Analysis of Mitochondrial Dynamics

In order to assess changes in mitochondrial dynamics following 2 and 24 h tolcapone dosing, mitochondria were stained with the marker heat shock protein 70 (Hsp70). Cells were washed, fixed, permeabilised and stained as described in Section 2.2.6.2. Incubation and dilution conditions were dependent on the protein of interest (table 5.1).

Samples were mounted onto glass microslides with Pro-Long Gold anti-fade reagent and left to dry overnight at 4 °C. Snap images were taken using a Zeiss Axio Observer.Z1 widefield fluorescent microscope with Apotome using 60 x oil objective.

**Table 5.1: Immunofluorescence incubation conditions for primary and secondary antibodies.**

Protein	Antibody product code	Primary antibody (in 5% BSA)	Secondary antibody (in 5% BSA)
Hsp70	ab2787	1:1000	Anti-mouse

## 5.2.10 Mitochondrial DNA Copy Number via RT-PCR

### 5.2.10.1 Assay Preparation

HepG2 cells and haplogroup H and J cybrids were collected by trypsinisation with 0.25 % trypsin and seeded into collagen coated 6-well plates at  $1 \times 10^6$  cells/well and incubated overnight in glucose media as described previously (Section 2.2.2). The following day, cells

underwent a 2 h galactose metabolic switch and tolcapone dosing in galactose media for 2 or 24 h as previously described (Section 5.2.5).

### 5.2.10.2 DNA Extraction and Quantification

DNA was extracted using a QIAamp DNA mini kit in accordance with the manufacturer's guidelines. Quantification and quality control of the resultant DNA samples were performed using nanodrop spectrophotometry (Thermo Fisher Scientific, Loughborough, UK). Samples with an  $A_{260/280} > 1.8$  were deemed acceptable for RT-PCR.

### 5.2.10.3 RT-PCR

Relative levels of mtDNA copy number were determined by RT-PCR using primers designed to target a region of mtDNA; ND-1 (complex I subunit) and a region of nuclear DNA; ribonuclease P RNA component H1 (RNase P) (table 5.2). Both primers had different dye-labelled probes (VIC dye-labelled and FAM-labelled), which enabled the simultaneous use of these primers in a single well.

**Table 5.2: Details of the mtDNA and nuclear DNA primers used for RT-PCR.**

Gene	Probe	Location
RNase P (nuclear)	VIC <sup>®</sup> dye-labelled TAMRA <sup>™</sup> probe	Location: chromosome 14, cytoband 14q11.2
ND-1 (mtDNA)	FAM <sup>®</sup> dye-labelled MGB probe	Location: mtDNA 3307-4262

2 x Taqman<sup>®</sup> genotyping master mix (5  $\mu$ L), nuclear DNA primer (0.5  $\mu$ L), mtDNA primer (0.5  $\mu$ L), nuclease-free water (2  $\mu$ L) and 10 ng DNA (2  $\mu$ L) were combined to give a final sample concentration of 1 ng/ $\mu$ L in each well. RT-PCR was performed using a viiA7 RT-PCR system (Life Technologies, UK) according to standard parameters (table 5.3). PCR reactions were performed in duplicate for each DNA sample.

**Table 5.3: Details of the mtDNA and nuclear DNA primers used for RT-PCR.**

Stage	Temperature (°C)	Time
Hold	95	10 mins
Cycle (40 cycles)	95	15 seconds
	60	60 seconds

### 5.2.11 Proteomic Analysis for Markers of Mitochondrial Biogenesis

#### 5.2.11.1 Assay Preparation

HepG2 cells and haplogroup H and J cybrids were collected by trypsinisation with 0.25 % trypsin and seeded into collagen coated 6-well plates at  $1 \times 10^6$  cells/well and incubated overnight in glucose media as described previously (Section 2.2.2). The following day, cells underwent a 2 h galactose metabolic switch and tolcapone dosing in galactose media for 2 or 24 h as previously described (Section 5.2.5). Cells were lysed in 100  $\mu$ L RIPA buffer and protein was quantified using a standard BCA assay as described (Section 2.2.5.2).

#### 5.2.11.2 Western Blot Analysis

20  $\mu$ g of cell lysate was heat-denatured at 95 °C for 5 mins before loading into NuPAGE® 4-12 % Bis-Tris pre-cast gels together with 5  $\mu$ L of Precision Plus Protein™ molecular weight marker. Proteins were subjected to electrophoretic separation, transferred onto nitrocellulose membranes and bands visualised as described (Section 2.2.5.3). Incubation and dilution conditions for the primary and secondary antibodies were dependent on the protein of interest (table 5.4). Densitometry analysis was performed with Image J 1.48 software.

**Table 5.4: Western blot incubation conditions for primary and secondary antibodies.** Summary of primary antibodies, dilution conditions and appropriate secondary HRP-conjugated secondary antibody.

Protein	Antibody product code	Molecular weight (kDa)	Primary antibody (in 5 % milk)	HRP-conjugated Secondary antibody (in 5 % milk)
PGC1- $\alpha$	66369-1-Ig	100	1:1000	Anti-mouse
GAPDH	ab8245	37	1:5000	Anti-mouse
VDAC	ab15895	31	1:1000	Anti-rabbit
TFAM	ab131607	28	1:500	Anti-rabbit

### 5.2.12 Statistical Analysis

Data is expressed from a minimum of three independent experiments. Unless specified otherwise, all results are expressed as mean  $\pm$  SEM. Normality was assessed using a Shapiro-Wilk statistical test. Statistical analyses were performed using StatsDirect 3.0.171. Results were considered significant when  $P < 0.05$ .

## 5.3 RESULTS

### 5.3.1 Assessment of the Effect of Tolcapone and Entacapone on Mitochondrial Membrane Potential in Isolated Mitochondria

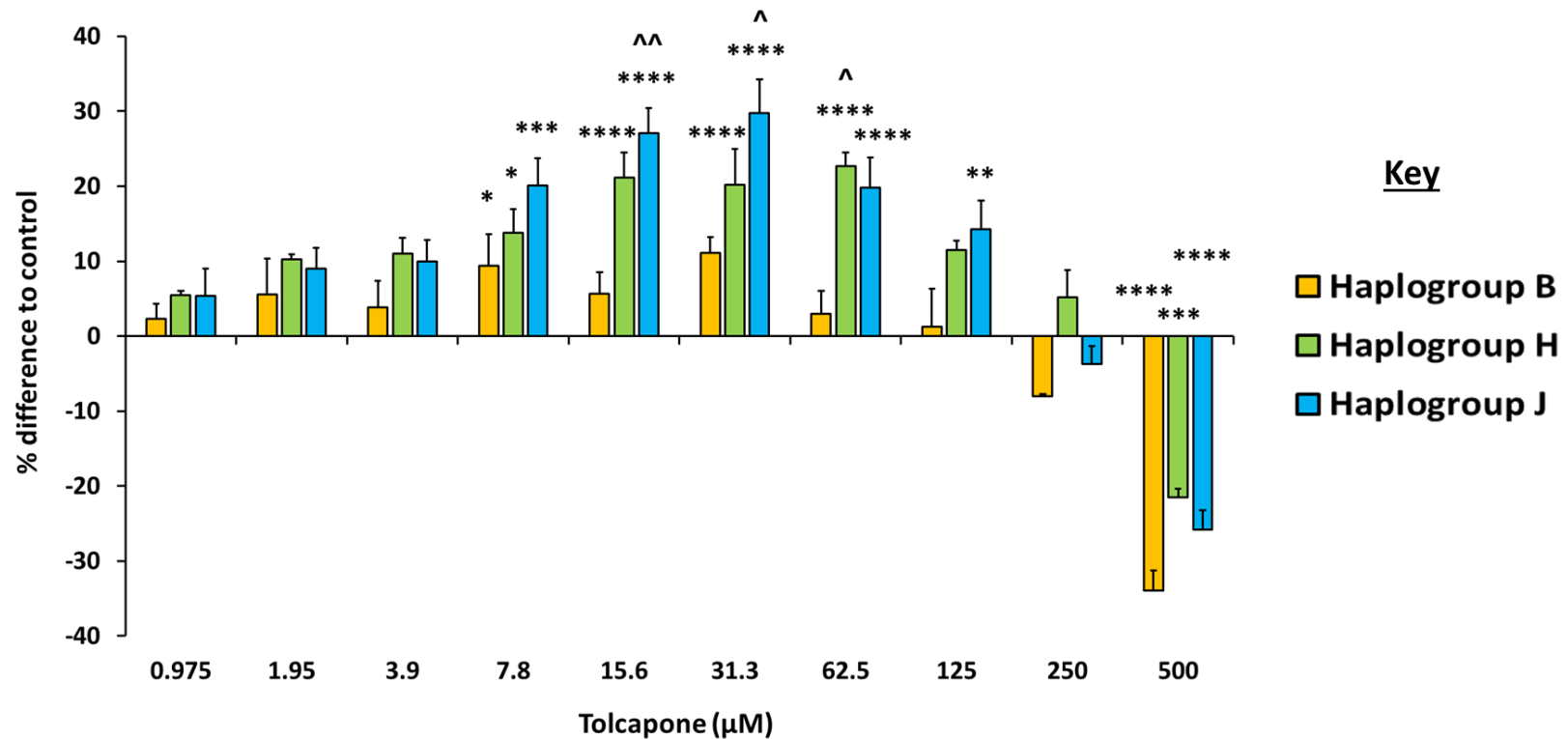


**Figure 5.3:** The effects of tolcapone on MMP on isolated mitochondria from HepG2 cells and haplogroup H and J transmittochondrial HepG2 cybrids. Calculations of percentage difference to mitochondria alone at kinetic read 20 for (A) haplogroup B, (B) haplogroup H (C) haplogroup J. Statistical significance compared with mitochondria alone; \*  $P < .05$ , \*\*  $P < .01$ , \*\*\*  $P < .001$ , \*\*\*\*  $P < .0001$ , between haplogroups; ^  $P < .05$ , ^^  $P < .01$ , ^^  $P < .001$ , ^^  $P < .0001$ .

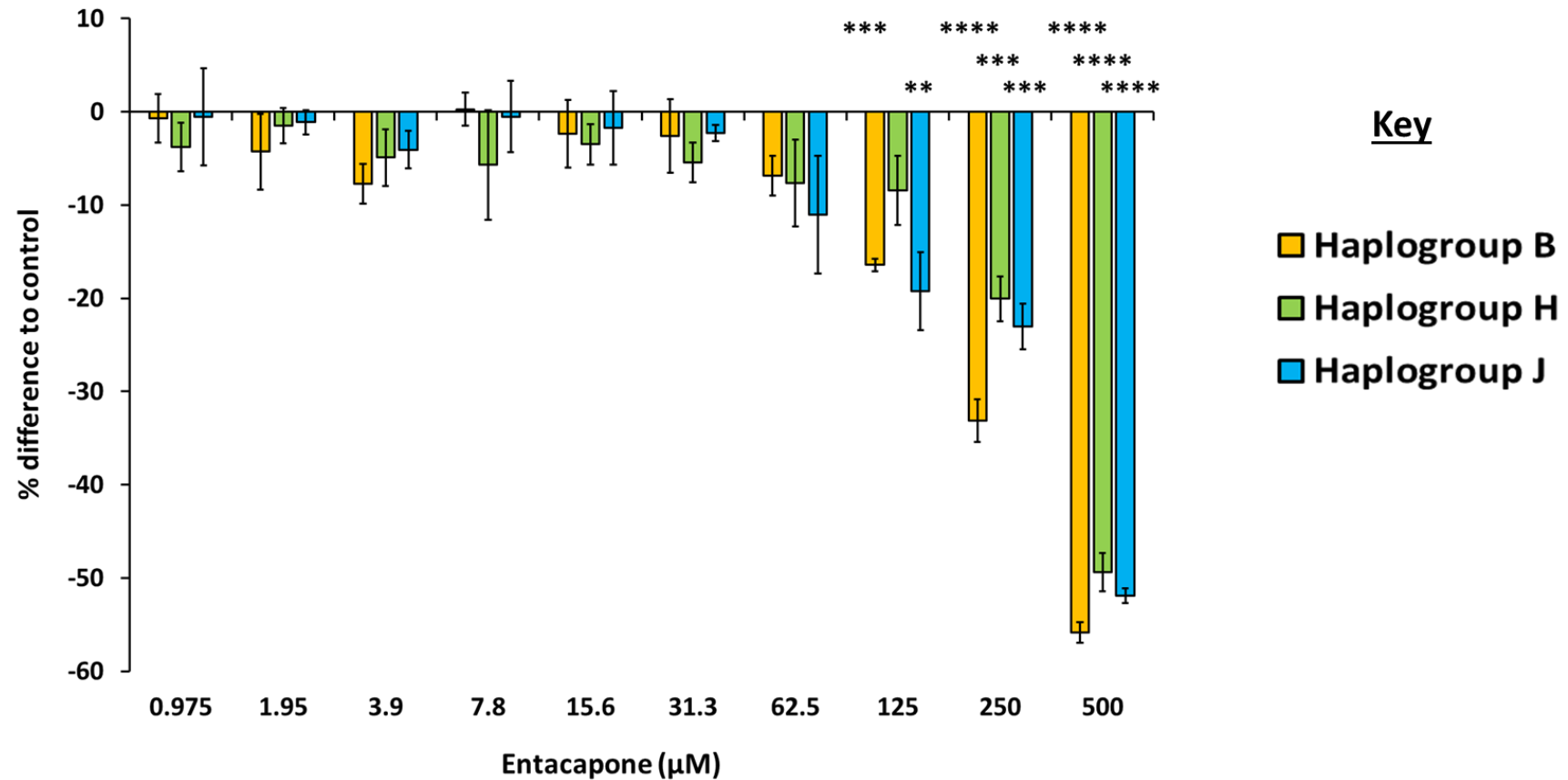


**Figure 5.4: The effects of entacapone on MMP on isolated mitochondria from HepG2 cells and haplogroup H and J transmitochondrial HepG2 cybrids.** Calculations of percentage difference to mitochondria alone at kinetic read 20 for (A) haplogroup B, (B) haplogroup H (C) haplogroup J. Statistical significance compared with mitochondria alone; \*  $P < .05$ , \*\*  $P < .01$ , \*\*\*  $P < .001$ , \*\*\*\* $P < .0001$ , between haplogroups; ^  $P < .05$ , ^^  $P < .01$ , ^^ $P < .001$ , ^^ $P < .0001$ .

The ability of tolcapone and entacapone to alter MMP was assessed on isolated mitochondria. Differential susceptibility to tolcapone-induced depolarisation was detected (figure 5.3). Exposure of haplogroup B mitochondria to 7.8  $\mu\text{M}$  tolcapone resulted in a significant increase of  $9.4 \pm 4.2\%$  in Rh123 fluorescence compared to control mitochondria however, no other concentrations resulted in significant depolarisation and resultantly, a dose-dependent trend was unable to be determined. Haplogroup H and J mitochondria were significantly depolarised in comparison to haplogroup B mitochondria following certain concentrations of tolcapone treatment. Haplogroup J mitochondria were the most susceptible to tolcapone-induced depolarisation as they had the greatest increase in Rh123 fluorescence. This occurred at 31.3  $\mu\text{M}$  tolcapone where there was a  $29.4 \pm 4.4\%$  increase in fluorescence compared to control mitochondria. Loss of MMP following tolcapone treatment was dose-dependent for haplogroup H and J mitochondria however, the highest concentration that the mitochondria were able to tolerate prior to a reduction in Rh123 fluorescence, differed. Whilst still significantly greater than control mitochondria, Rh123 fluorescence started to decline in haplogroup J mitochondria following 62.5  $\mu\text{M}$  tolcapone treatment, whereas fluorescence declined at 125  $\mu\text{M}$  tolcapone for haplogroup H mitochondria (figure 5.3). Increased concentrations of tolcapone resulted in a further decline in Rh123 fluorescence, which is indicative of dye auto-quenching and toxicity (Perry et al., 2011). Exposure of isolated mitochondria to entacapone did not induce significant depolarisation as there were no increases in Rh123 fluorescence (figure 5.4). There were no significant differences in entacapone-induced toxicity between haplogroups.

### **5.3.2 Assessment of the Effects of Tolcapone on Mitochondrial Membrane Potential in Whole Cells**

Assessment of MMP in whole cells was monitored using the fluorescent dye JC-1. A reduction in the red/green fluorescent ratio is indicative of loss of MMP. MMP decreased dose-dependently in all haplogroups following 2 and 24 h tolcapone treatment when compared to the control (figure 5.5). However, there were no overall significant differences in depolarisation between haplogroups at both time points.

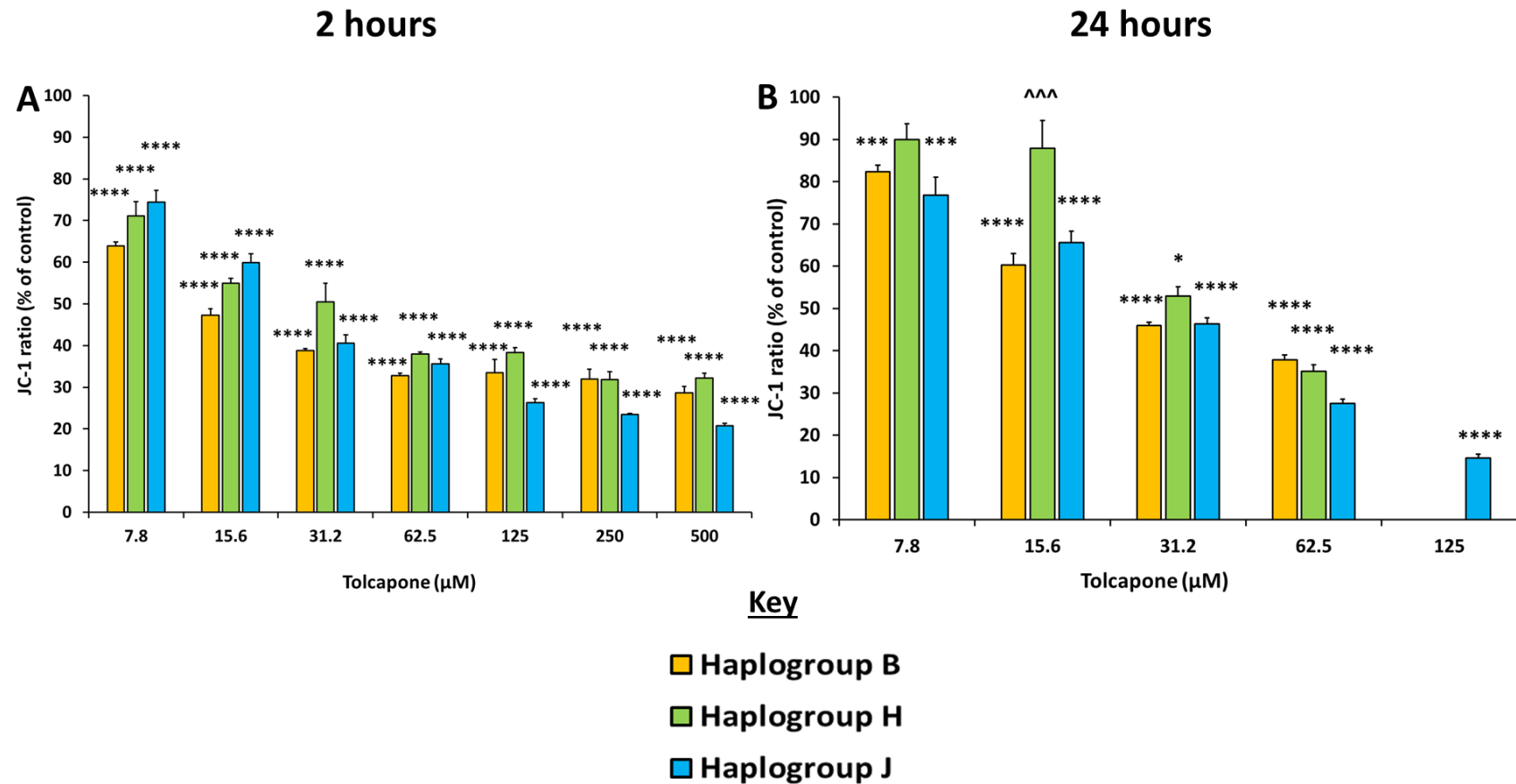


**Figure 5.5: The effects of tolcapone on MMP in HepG2 cells and haplogroup H and J cybrids.** Cells were treated with serial concentrations of tolcapone up to 500  $\mu\text{M}$  in galactose media for (A) 2 h and (B) 24 h and changes to MMP were measured by JC-1 fluorescence. A ratio of the fluorescence intensity of the red aggregate over the green monomer was determined. Statistical significance compared with control; \*  $P < .05$ , \*\*  $P < .01$ , \*\*\*  $P < .001$ , \*\*\*\*  $P < .0001$ , between haplogroups;  $\wedge$   $P < .05$ ,  $\wedge\wedge$   $P < .01$ ,  $\wedge\wedge\wedge$   $P < .001$ ,  $\wedge\wedge\wedge\wedge$   $P < .0001$ .

### 5.3.3 Assessment of the Effects of Compounds on Cellular ATP Following Acute Metabolic Modification with Galactose Media

There were no significant differences in cellular ATP depletion between haplogroups in response to 2 h tolcapone treatment (figure 5.6A). ATP levels following 24 h tolcapone were significantly different between the three haplogroups; haplogroup B exhibited greater ATP content at middle concentrations of tolcapone (31.3 and 62.5  $\mu\text{M}$ ) in comparison to haplogroup H and J (figure 5.6B). Whilst no significant differences between haplogroups were observed in dose-response curves following 2 h tolcapone dosing, comparison of  $\text{IC}_{50}\text{ATP}$  values revealed significant differences (table 5.5). Haplogroup H was less susceptible to tolcapone-induced ATP depletion following 2 h treatment as evidenced by a significantly greater  $\text{IC}_{50}\text{ATP}$  value in comparison to haplogroup B and J (119.6  $\mu\text{M}$  vs 80.7  $\mu\text{M}$  vs 77.8  $\mu\text{M}$ ). However, haplogroup B was less susceptible to tolcapone-induced ATP depletion following 24 h treatment as evidence by a significantly greater  $\text{IC}_{50}\text{ATP}$  value in comparison to haplogroup H and J (86.2  $\mu\text{M}$  vs 39.1  $\mu\text{M}$  vs 58.8  $\mu\text{M}$ ). Comparison of 2 h vs 24 h tolcapone  $\text{IC}_{50}\text{ATP}$  values between the haplogroups revealed that there was a significant difference in haplogroup H however, no significant difference in temporal  $\text{IC}_{50}\text{ATP}$  values were detected for haplogroup B and J (table 5.5).

There were no significant differences in cellular ATP depletion between haplogroups in response to 24 h FCCP treatment (figure 5.6D). Following 2 h FCCP treatment, ATP levels in haplogroup J were significantly greater than haplogroup B and H (figure 5.6C). Consistent with the differences evident in dose-response curves, haplogroup J cybrids were less susceptible to FCCP-induced ATP depletion as evidenced by a significantly greater  $\text{IC}_{50}\text{ATP}$  value following 2 h FCCP treatment in comparison with the other haplogroups (table 5.5). There were no differences in susceptibility to FCCP-induced ATP depletion following 24 h treatment as evidenced by the lack of significant differences in  $\text{IC}_{50}\text{ATP}$  values between haplogroups (table 5.5). Comparison of 2 h and 24 h FCCP  $\text{IC}_{50}\text{ATP}$  values between the three haplogroups revealed that there were no significant differences in FCCP  $\text{IC}_{50}\text{ATP}$  values.

There were no significant differences in cellular ATP depletion between haplogroups in response to 24 h rotenone treatment (figure 5.6F). Following 2 h rotenone treatment, ATP levels in haplogroup J were significantly greater than haplogroup B and H (figure 5.6E). Consistent with the differences evident in dose-response curves, haplogroup J cybrids were less susceptible to rotenone-induced ATP depletion as evidenced by a significantly greater  $\text{IC}_{50}\text{ATP}$  value following 2 h rotenone treatment in comparison with the other haplogroups

(table 5.5). However, there were no differences in susceptibility to rotenone-induced ATP depletion following 24 h treatment as evidenced by the lack of significant differences in  $IC_{50}ATP$  values between haplogroups (table 5.5). Comparison of 2 h and 24 h rotenone  $IC_{50}ATP$  values between the three haplogroups revealed that there was a significant difference in rotenone  $IC_{50}ATP$  for haplogroup J (table 5.5).

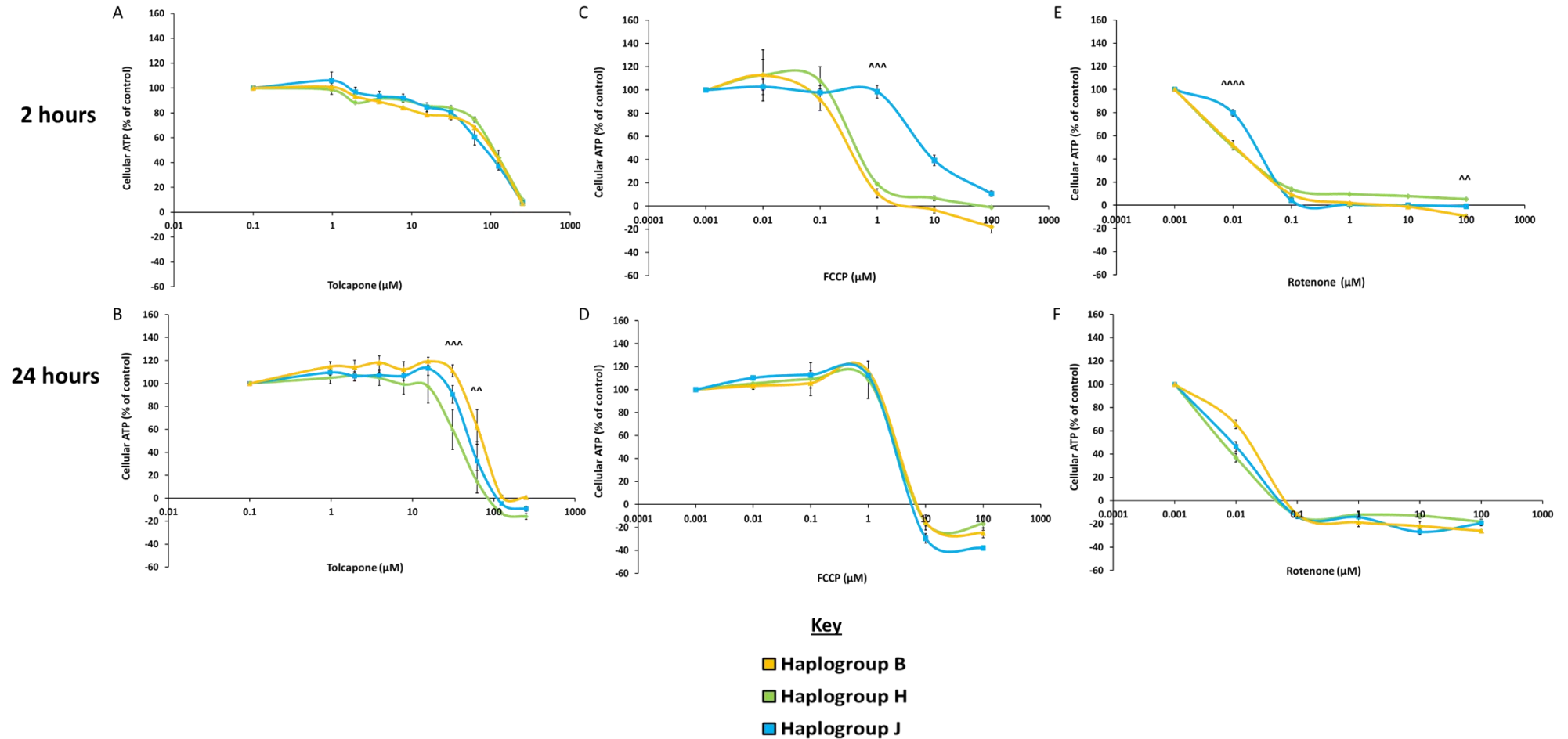


**Figure 5.6: The effects of (A) 2 h tolcapone, (B) 24 h tolcapone, (C) 2 h FCCP, (D) 24 h FCCP, (E) 2 h rotenone and (F) 24 h rotenone treatment on cellular ATP content following an acute metabolic modification with galactose media in HepG2 cells (haplogroup B) and haplogroup H and J cybrids. Statistical significance between haplogroups;  $^{\wedge}$   $P < .05$ ,  $^{\wedge\wedge}$   $P < .01$ ,  $^{\wedge\wedge\wedge}$   $P < .001$ ,  $^{\wedge\wedge\wedge\wedge}$   $P < .0001$ . ATP values have been normalised to  $\mu\text{g}$  protein per well.**

**Table 5.5: Comparison of IC<sub>50</sub> values of tolcapone, FCCP and rotenone in HepG2 cells (haplogroup B) and haplogroup H and J cybrids following 2 and 24 h treatment.** Statistical significance between haplogroups; ^ P < .05, ^^ P < .01, ^^^ P < .001, ^^^^ P < .0001

Parameter	Concentration (μM)			Significance		
	B	H	J	B	H	J
Tolcapone ATP content IC <sub>50</sub> 2 h	80.7 ± 6.4	119.6 ± 10.9	77.8 ± 12.0		^	
Tolcapone ATP content IC <sub>50</sub> 24 h	86.2 ± 8.5	39.1 ± 7.9	58.8 ± 10.9	^^		
Tolcapone ATP content IC <sub>50</sub> 2 h vs 24 h					^^^	
FCCP ATP content IC <sub>50</sub> 2 h	0.4 ± 0.1	0.6 ± 0.1	8.2 ± 1.6			^^
FCCP ATP content IC <sub>50</sub> 24 h	4.3 ± 1.3	2.4 ± 0.4	5.4 ± 0.8			
FCCP ATP content IC <sub>50</sub> 2 h vs 24 h						
Rotenone ATP content IC <sub>50</sub> 2 h	0.01 ± 0.002	0.009 ± 0.002	0.02 ± 0.002			^
Rotenone ATP content IC <sub>50</sub> 24 h	0.01 ± 0.0003	0.009 ± 0.0003	0.01 ± 0.0003			
Rotenone ATP content IC <sub>50</sub> 2 h vs 24 h						^^

### 5.3.4 Examining the Effects of Tolcapone on Cellular Superoxide Levels

There were no significant changes in cellular superoxide levels compared to the control for all haplogroups following 2 h tolcapone treatment (figure 5.7A). Following 24 h tolcapone treatment, superoxide levels significantly increased in haplogroup B and were  $366.8 \pm 121.5$  % of the control. Following increased concentrations of tolcapone, MitoSOX readings could not be obtained in haplogroup B due to cell death. There was a significant increase of  $155.3 \pm 14.6$  % in superoxide levels when compared to the control following 62.5 μM tolcapone treatment in haplogroup H cybrids. MitoSOX readings could not be obtained for 125 μM tolcapone in haplogroup H cybrids due to cell death. However, there was a very significant increase in superoxide levels following 125 μM tolcapone treatment in haplogroup J cybrids of  $1235.6 \pm 71.2$  % of the control. 1 μM antimycin A was used as a positive control for ROS production. In all haplogroups, there was a significant increase in mitoSOX reading when compared to the control following antimycin A treatment.

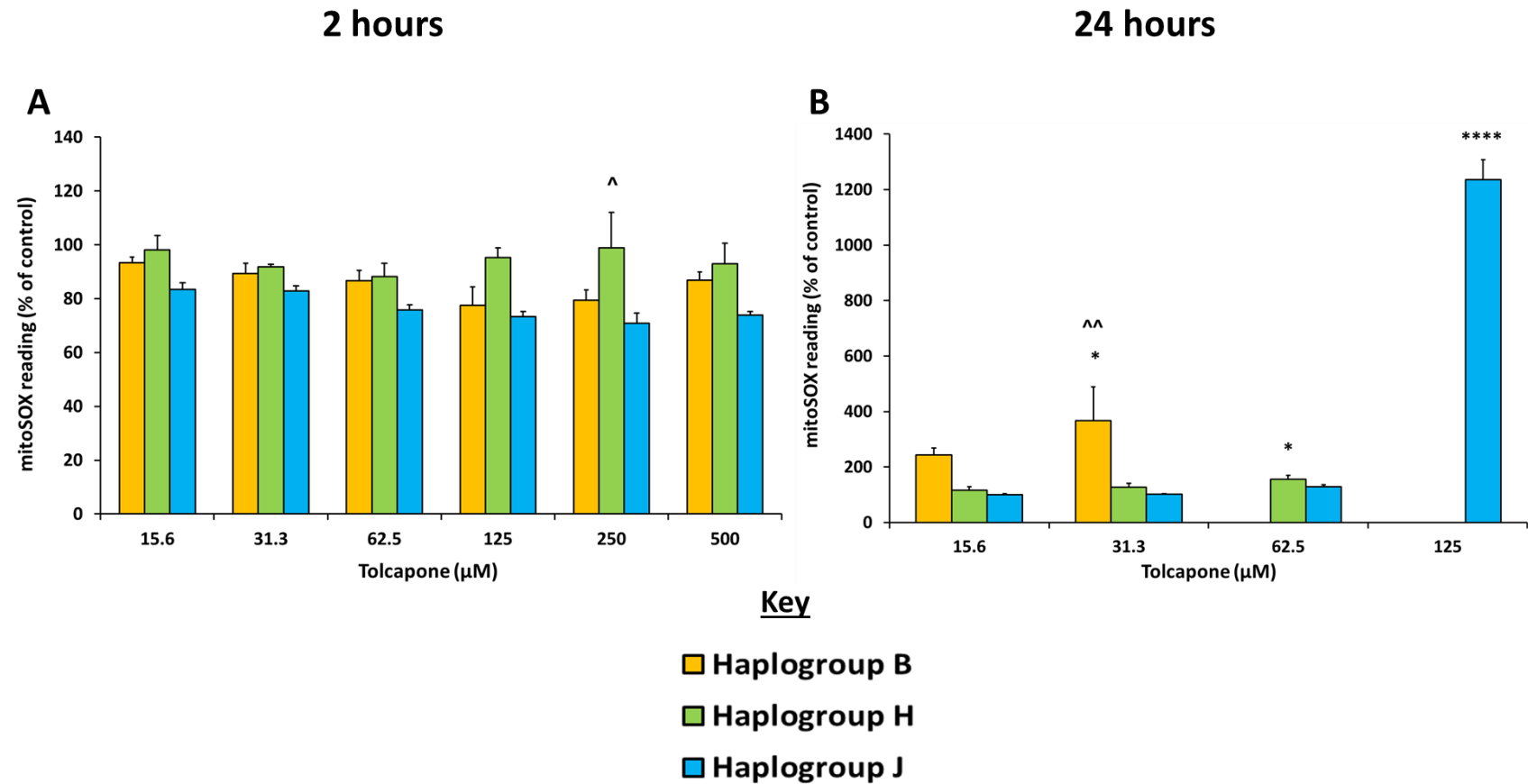


**Figure 5.7: The effects of tolcapone on cellular superoxide levels.** Cells were treated with serial concentrations of tolcapone up to 500  $\mu\text{M}$  in galactose media for (A) 2 h and (B) 24 h, and changes to superoxide levels were measured using the MitoSOX™ Red reagent. All results were normalised to  $\mu\text{g}$  protein per well. Statistical significance compared with control; \*  $P < .05$ , \*\*  $P < .01$ , \*\*\*  $P < .001$ , \*\*\*\* $P < .0001$ , between haplogroups; ^  $P < .05$ , ^^  $P < .01$ , ^^<sup>^</sup>  $P < .001$ , ^^<sup>^</sup><sup>^</sup>  $P < .0001$ .

### 5.3.5 Assessment of the Effects of Tolcapone-induced respiratory complex dysfunction

In order to assess individual complex driven respiration, HepG2 cells and transmitochondrial cybrids were permeabilised using rPFO and assayed using solutions containing specific substrates and inhibitors for the complex of interest. Cells were acutely treated with tolcapone followed by a mitochondrial stress test. There were no significant changes in complex I – IV activity for haplogroup B when compared to the control. A significant reduction in complex I – III driven respiration was observed haplogroup H and J cybrids. In haplogroup H, maximum reductions in complex I activity were  $79.0 \pm 1.6$  % of the control and in haplogroup J were  $81.9 \pm 1.2$  % of the control (figure 5.8A). Maximum decreases in complex II activity were  $79.5 \pm 3.5$  % of the control in haplogroup H cybrids and  $88.7 \pm 0.9$  % of the control in haplogroup J cybrids (figure 5.8B). A maximal reduction in complex III activity was observed in haplogroup H cybrids at  $73.6 \pm 0.3$  % of the control and  $89.1 \pm 3.0$  % of the control in haplogroup J cybrids (figure 5.8C). A significant reduction in complex IV activity compared to the control was observed in haplogroup J cybrids. Maximal reductions were  $86.9 \pm 3.6$  % of the control following 250  $\mu$ M tolcapone treatment in haplogroup J cybrids (figure 5.8D). Whilst significant reductions in complex driven respiration were detected when compared to the control, they were minor and so  $IC_{50}$  values could not be calculated. Comparison of changes to individual complex activity between haplogroups revealed that overall there were no differences.

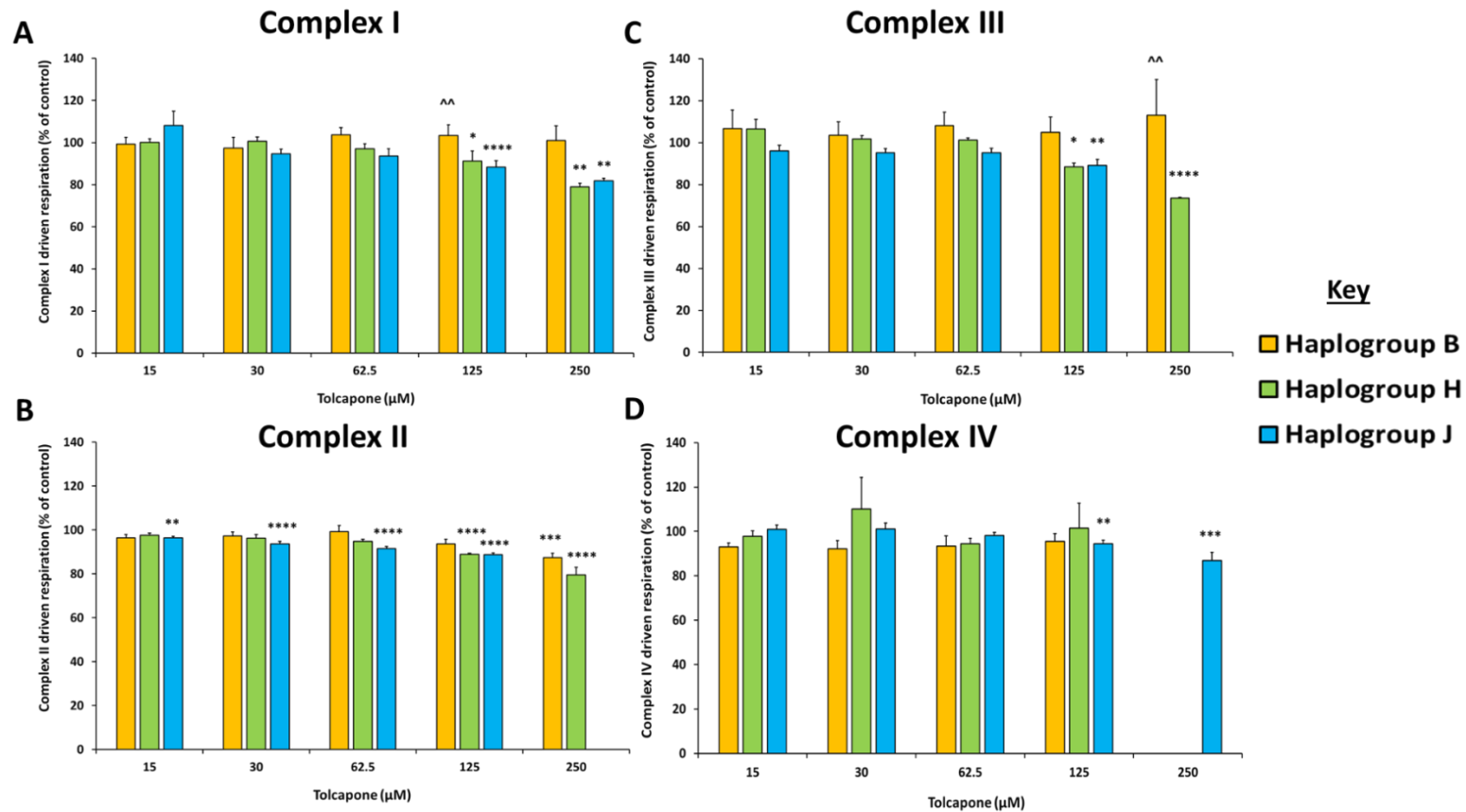


**Figure 5.8: The effect of acute tolcapone exposure upon the activity of the mitochondrial respiratory complexes (I – IV).** Cells were permeabilised and acutely dosed with tolcapone (0 – 500 µM) before conducting a mitochondrial stress test using an extracellular flux analyser XFe96 instrument. Complex driven respiration (activity) was defined as maximal respiration (as a % of basal respiration) as a % of vehicle control. All results were normalised to µg protein per well. Statistical significance compared with control; \* P < .05, \*\* P < .01, \*\*\* P < .001, \*\*\*\* P < .0001, between haplogroups; ^ P < .05, ^^ P < .01, ^^ ^ P < .001, ^^ ^ ^ P < .0001. Data are presented as mean + SEM of n = 5 experiments.

### 5.3.6 Assessment of Tolcapone-induced Changes in Mitochondrial Dynamics

In order to assess changes in mitochondrial dynamics and morphology, cells were immunostained with Hsp70. Using this antibody in H1299 cells, changes in mitochondria morphology have been documented (Milani et al., 2019). In vehicle treated H1299 cells, mitochondria appear in a filamentous network, whereas treatment with 100 nM A-1210477 induces extensive mitochondrial fragmentation (figure 5.9) (Milani et al., 2019).

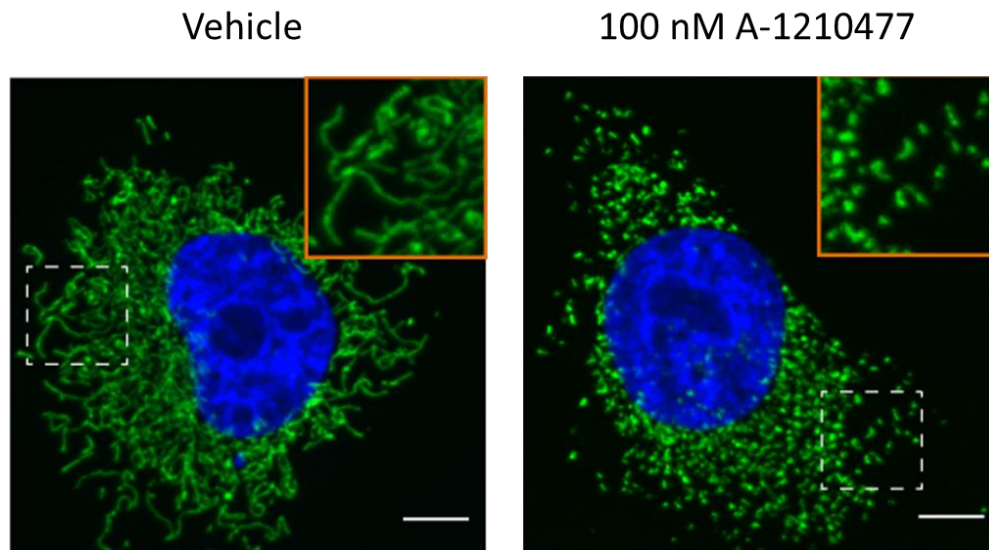


**Figure 5.9: Assessment of changes in H1299 cells exposed to Z-VAD.fmk (30  $\mu$ M) for 30 mins followed by 100 nM A-1210477 for 4 h. Mitochondrial morphology was assessed by immunostaining with Hsp70 antibody. Scale bar = 10  $\mu$ m (Milani et al., 2019).**

There were no differences in mitochondrial dynamics upon treatment with tolcapone (figure 5.10 and 5.11) when compared to vehicle treated cells or between the three haplogroups. Control treated cells for all three haplogroups exhibited fragmented mitochondria at 2 and 24 h. Mitochondria remained fragmented upon tolcapone treatment at both time points for all haplogroups.

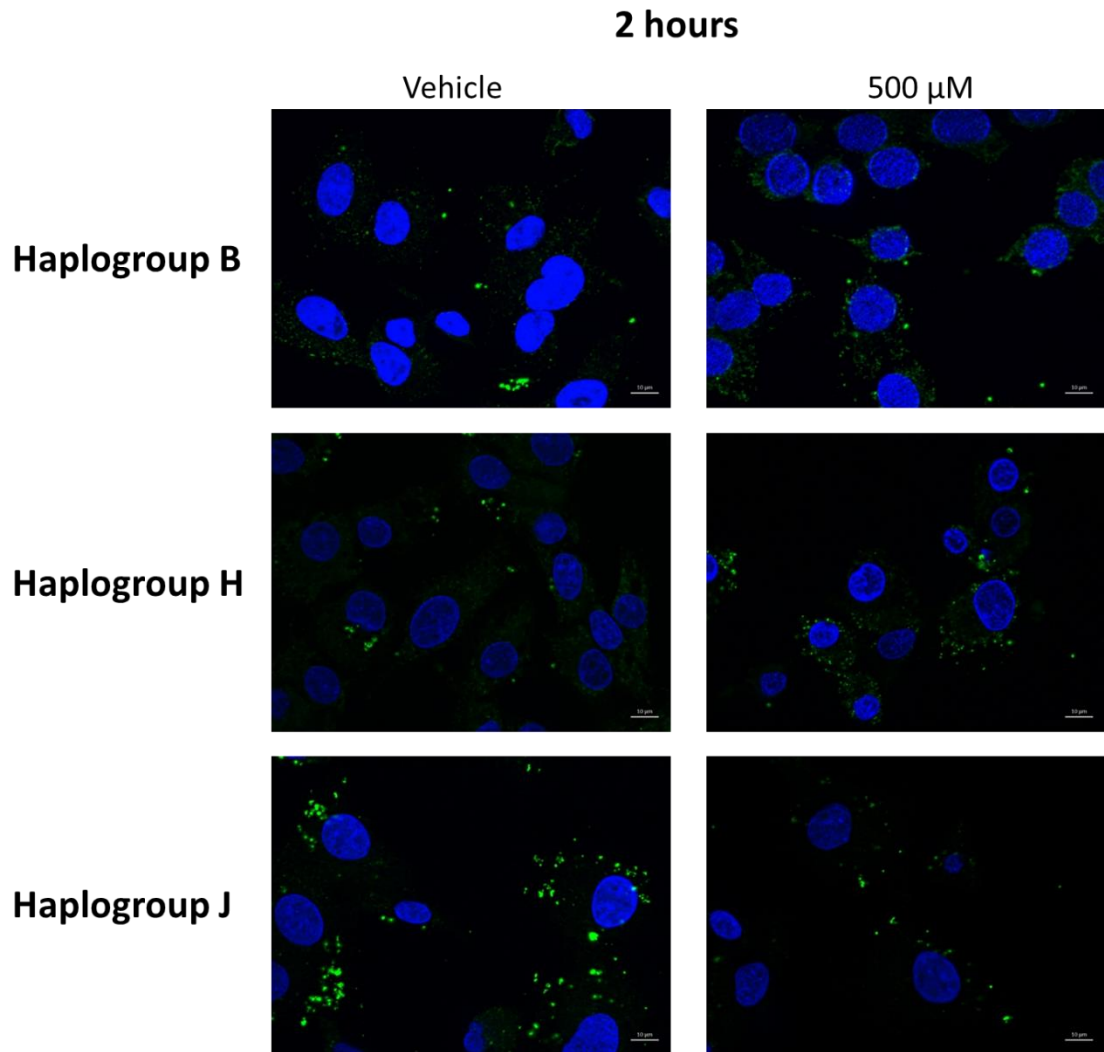


**Figure 5.10: Assessment of mitochondrial dynamics following 2 h dosing with 500  $\mu$ M tolcapone in galactose media in HepG2 cells (haplogroup B) and haplogroup H and J cybrids.** Cells were fixed with 4 % PFA and stained with Hsp70 antibody (green) to assess mitochondrial integrity following 2 h tolcapone treatment. Cells were incubated with Hoechst (blue). Snap images with Apotome were taken using a Zeiss microscope using 60 x oil objective. Scale bar = 10  $\mu$ m.

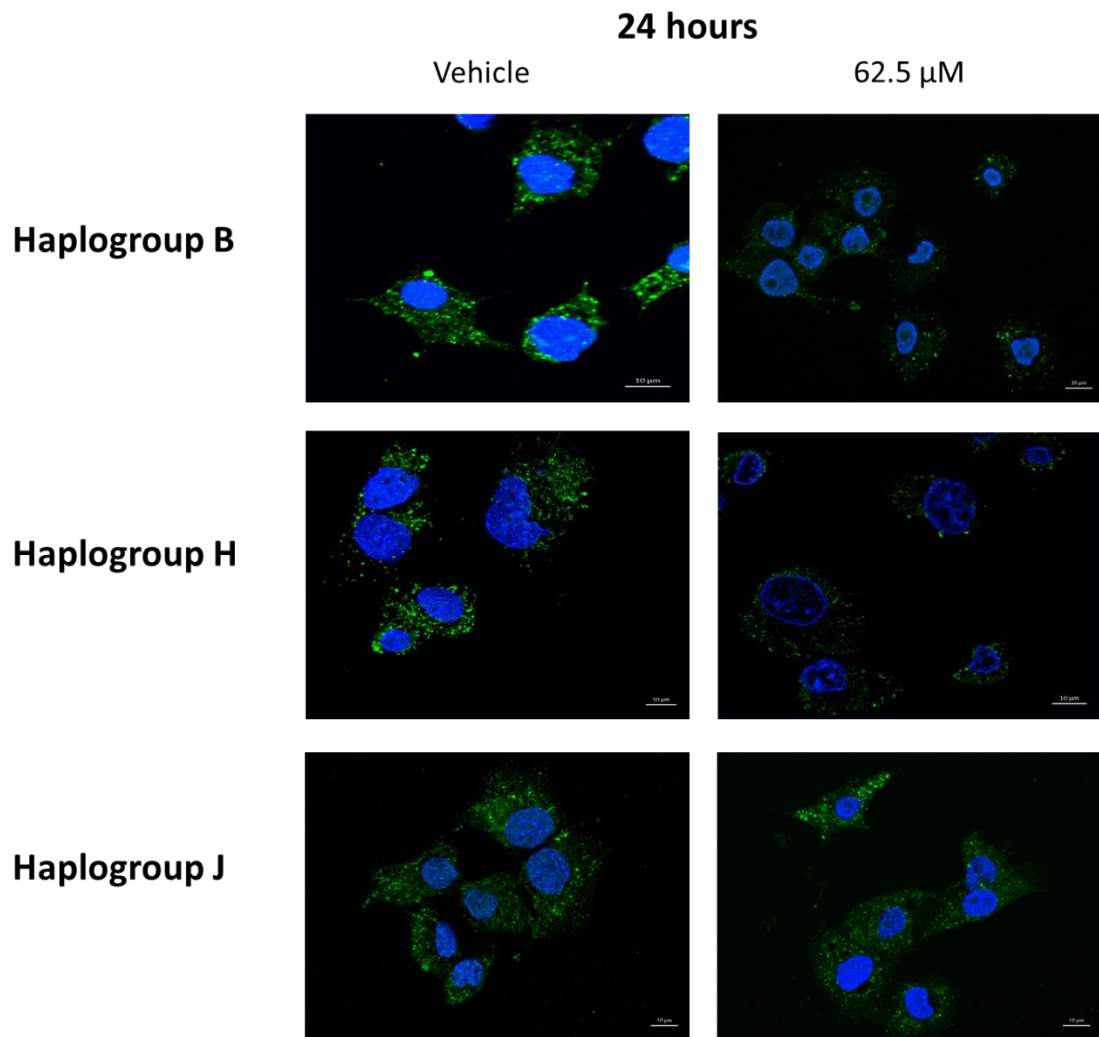


**Figure 5.11: Assessment of mitochondrial dynamics following 24 h dosing with 500  $\mu$ M tolcapone in galactose media in HepG2 cells (haplogroup B) and haplogroup H and J cybrids.** Cells were fixed with 4 % PFA and stained with Hsp70 antibody (green) to assess mitochondrial integrity following 2 h tolcapone treatment. Cells were incubated with Hoechst (blue). Snap images with Apotome were taken using a Zeiss microscope using 60 x oil objective. Scale bar = 10  $\mu$ m.

### 5.3.7 Examination of the Effects of Tolcapone on mtDNA copy number per cell

Changes to the number of mtDNA copies per cell following 2 and 24 h tolcapone dosing were determined using RT-PCR with primers designed to amplify one region of nuclear DNA (RNaseP) and one region of mtDNA (ND-1). There were no significant differences in mtDNA copy number when compared to the control for haplogroup B and J following 2 h tolcapone treatment (figure 5.12A). MtDNA copy number significantly decreased in haplogroup H cybrids to  $80.0 \pm 2.2$  % when compared to the control following 2 h tolcapone treatment. There were no significant differences in mtDNA copy number per cell between haplogroups

following 2 h tolcapone treatment. Following 24 h tolcapone treatment, mtDNA copy number per cell was significantly reduced when compared to the control in haplogroup H cybrids (figure 5.12B). Maximal reductions of  $29.1 \pm 3.6$  % of the control were achieved following treatment with 62.5  $\mu$ M tolcapone. However, there were no significant differences in mtDNA copy number when compared to the control for haplogroup B and J. Following 24 h tolcapone treatment, a significant difference in mtDNA copy number per cell was detected between haplogroups. MtDNA copy number was significantly lower in haplogroup H cybrids when compared with haplogroup B and J (figure 5.12B).

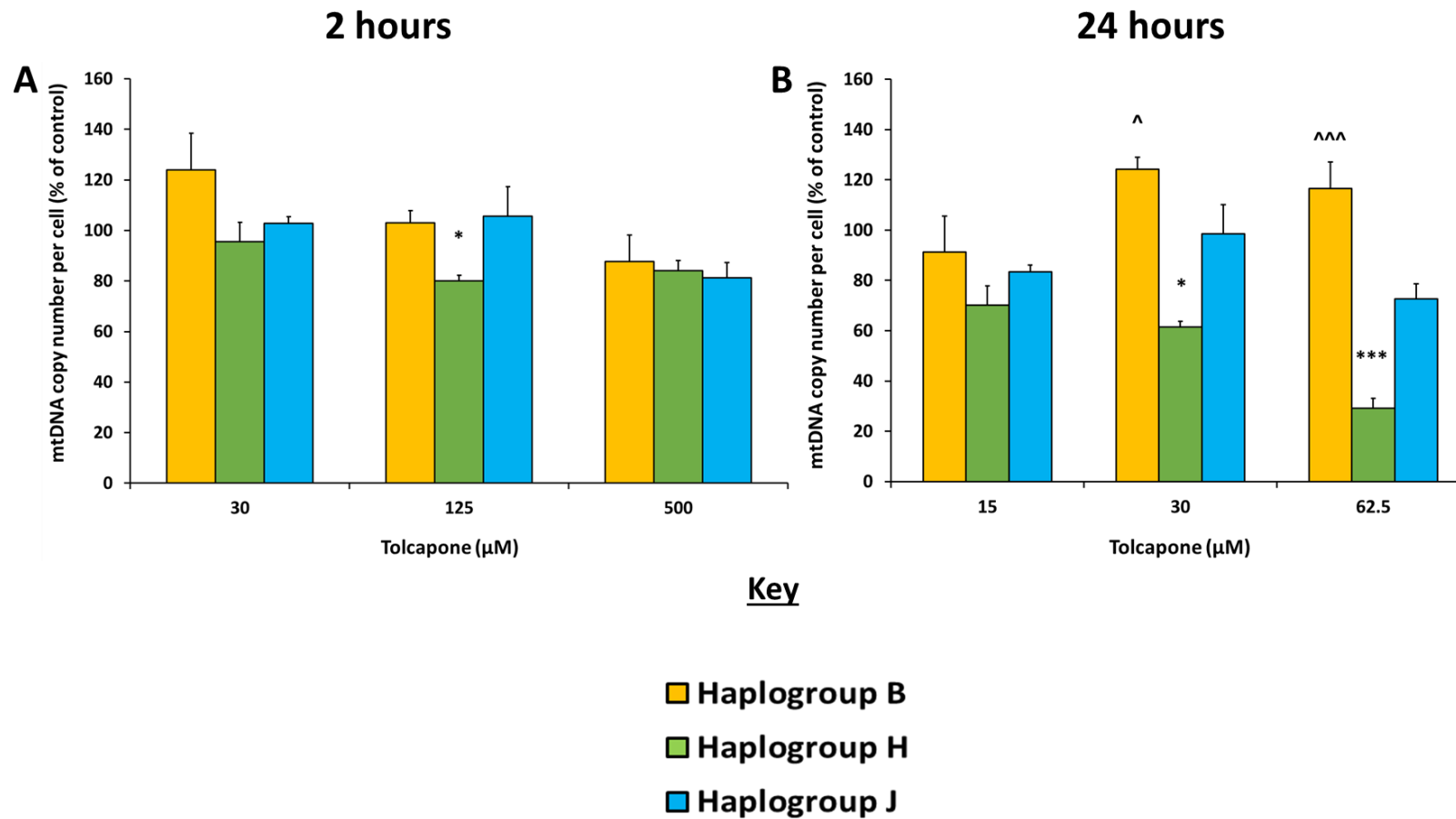


**Figure 5.12: Assessment of changes to cellular mtDNA content per cell in HepG2 cells (haplogroup B) and haplogroup H and J cybrids treated with tolcapone for 2 and 24 h.** Cells were treated with tolcapone in galactose media for (A) 2 and (B) 24 h. A region of nuclear DNA and mtDNA were amplified using RT-PCR in order to calculate the number of mtDNA copies per cells. Statistical significance compared with control; \*  $P < .05$ , \*\*  $P < .01$ , \*\*\*  $P < .001$ , \*\*\*\*  $P < .0001$ , between haplogroups; <sup>^</sup>  $P < .05$ , <sup>^^</sup>  $P < .01$ , <sup>^^^</sup>  $P < .001$ , <sup>^^^^</sup>  $P < .0001$ .

### 5.3.8 Assessment of the Effects of Tolcapone on Mitochondrial Biogenesis

In order to explore changes in mitochondrial mass and the activation of mitochondrial biogenesis, proteins involved in the mitochondrial biogenesis cascade (TFAM and PGC1- $\alpha$ ) and a mitochondrial marker (VDAC) were assessed following 2 and 24 h tolcapone treatment.

There were no significant differences in the expression of VDAC when compared to the control for haplogroup B and H following 2 h tolcapone treatment (figure 5.13A). However, VDAC expression significantly increased when compared to the control in haplogroup J cybrids following 2 h tolcapone treatment. Significant increases were observed at 500  $\mu$ M tolcapone and were  $132.7 \pm 7.6$  % of the control. Consistent with the differences evident when compared to the control, haplogroup J cybrids had a greater expression of VDAC compared to haplogroup B and H following high doses of tolcapone for 2 h (125 and 500  $\mu$ M). Following 24 h tolcapone treatment, there was a non-significant increase in the expression of VDAC in haplogroup H and J cybrids however, there was a significant dose-dependent increase in the expression of VDAC in haplogroup B cells (figure 5.13B). The maximal significant increase in VDAC expression occurred following 62.5  $\mu$ M tolcapone treatment and was  $151.3 \pm 9.9$  % of the control in haplogroup B. There were no significant differences in VDAC expression between haplogroups following 24 hours tolcapone treatment.

Whilst there were no significant changes in the expression of TFAM when compared to the control for all 3 haplogroups following 2 h tolcapone treatment, the expression of TFAM in haplogroup B cells was significantly greater than haplogroup H and J cybrids at 500  $\mu$ M tolcapone (figure 5.14A). Following 2 h treatment with 500  $\mu$ M tolcapone, the expression of TFAM compared to the control was  $128.6 \pm 17.6$  % in haplogroup B,  $72.3 \pm 12.2$  % in haplogroup H and  $93.3 \pm 11.2$  % in haplogroup J. There were no significant changes in the expression of TFAM when compared to the control or between haplogroups following 24 h tolcapone treatment (figure 5.14B).

There were no significant changes in the expression of PGC1- $\alpha$  when compared to the vehicle for all 3 haplogroups, nor was there a significant difference in the expression of PGC1- $\alpha$  between haplogroups following 2 and 24 h tolcapone treatment (figure 5.15A and B).

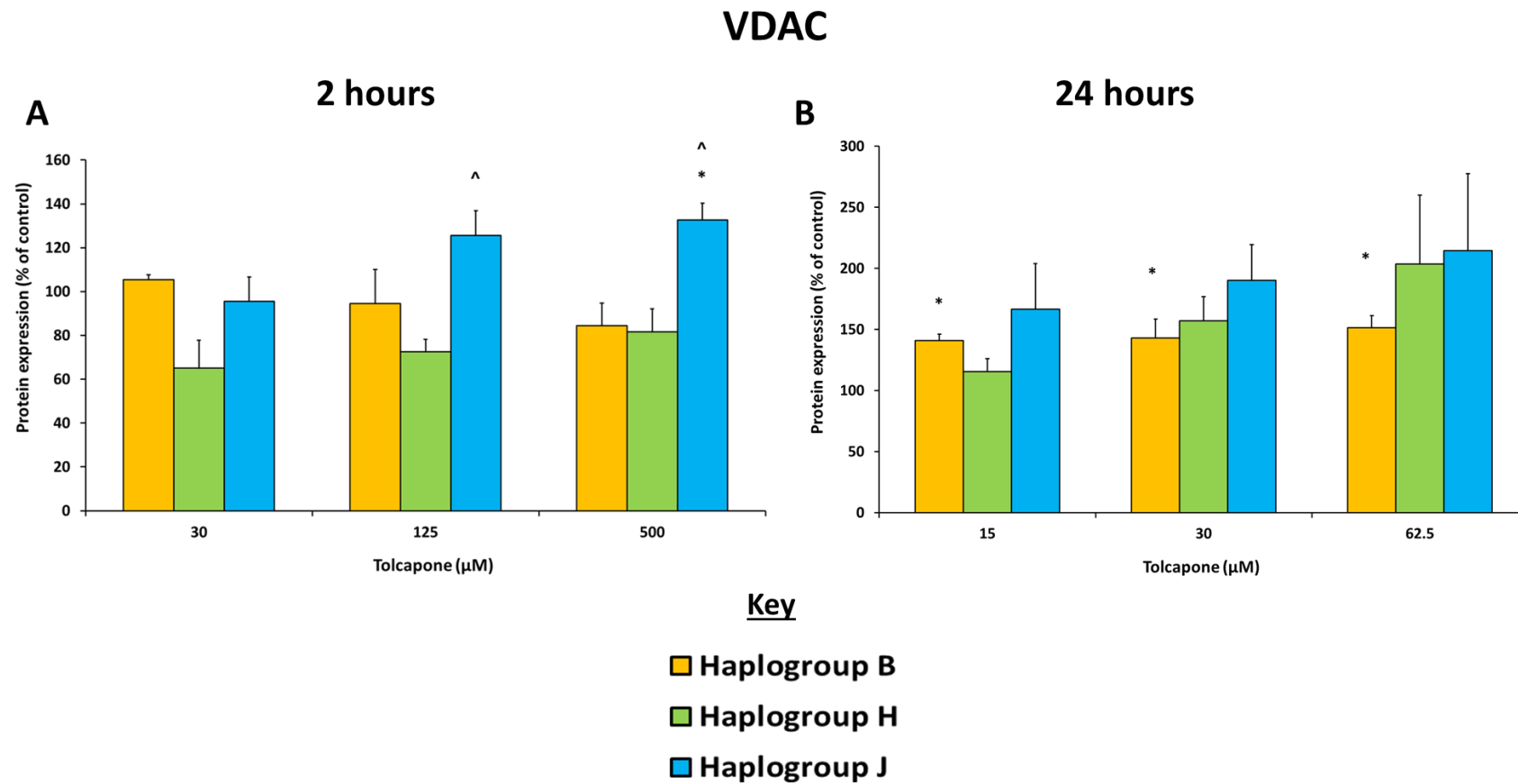


**Figure 5.13: Assessment of changes to VDAC expression in HepG2 cells (haplogroup B) and haplogroup H and J cybrids treated with tolcapone for 2 and 24 h.** Cells were treated with tolcapone in galactose media for (A) 2 and (B) 24 h and 20 µg of lysate protein was separated by gel electrophoresis and probed for VDAC. GAPDH was used as a loading control. The bands were quantified using Image J. Statistical significance compared with control; \*  $P < .05$ , \*\*  $P < .01$ , \*\*\*  $P < .001$ , \*\*\*\* $P < .0001$ , between haplogroups; ^  $P < .05$ , ^^  $P < .01$ , ^^^  $P < .001$ , ^^^^ $P < .0001$ .

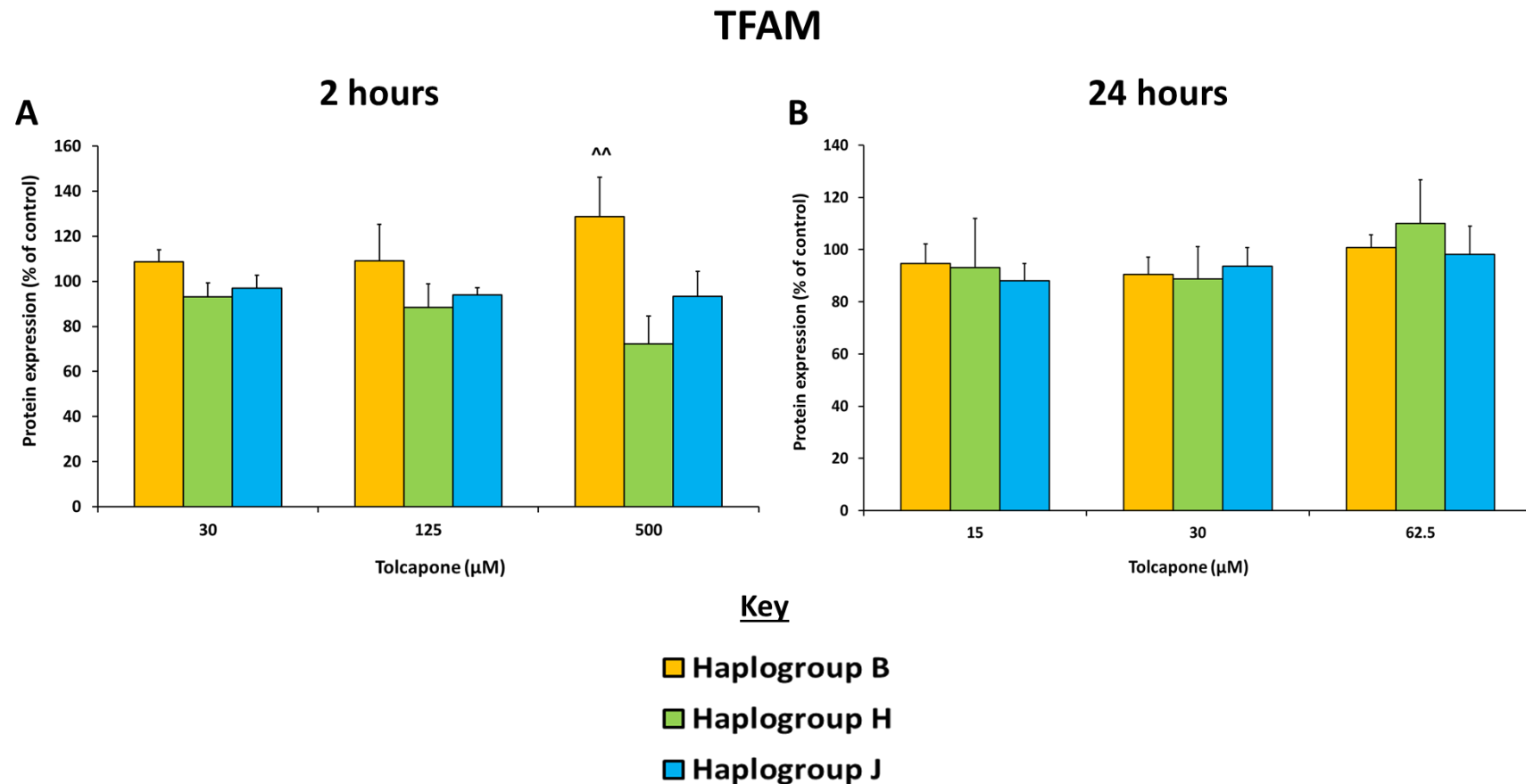


**Figure 5.14: Assessment of changes to TFAM expression in HepG2 cells (haplogroup B) and haplogroup H and J cybrids treated with tolcapone for 2 and 24 h.** Cells were treated with tolcapone in galactose media for (A) 2 and (B) 24 h and 20 µg of lysate protein was separated by gel electrophoresis and probed for TFAM. GAPDH was used as a loading control. The bands were quantified using Image J. Statistical significance compared with control; \* P < .05, \*\* P < .01, \*\*\* P < .001, \*\*\*\*P < .0001, between haplogroups; ^ P < .05, ^^ P < .01, ^^ P < .001, ^^^P < .0001.

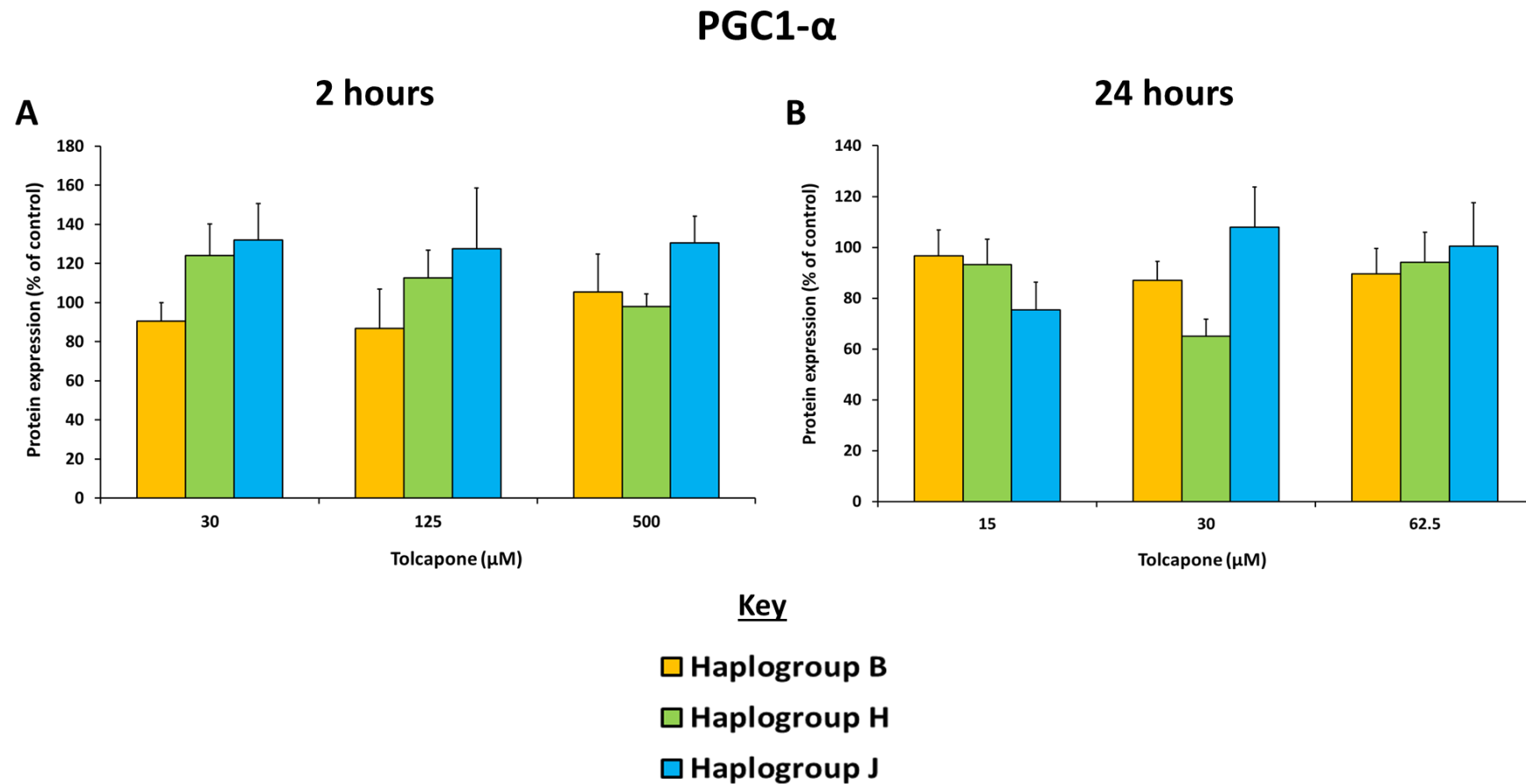


**Figure 5.15: Assessment of changes to PGC1- $\alpha$  expression in HepG2 cells (haplogroup B) and haplogroup H and J cybrids treated with tolcapone for 2 and 24 h.** Cells were treated with tolcapone in galactose media for (A) 2 and (B) 24 h and 20  $\mu\text{g}$  of lysate protein was separated by gel electrophoresis and probed for PGC1- $\alpha$ . GAPDH was used as a loading control. The bands were quantified using Image J. Statistical significance compared with control; \*  $P < .05$ , \*\*  $P < .01$ , \*\*\*  $P < .001$ , \*\*\*\* $P < .0001$ , between haplogroups; ^  $P < .05$ , ^^  $P < .01$ , ^^^  $P < .001$ , ^^^^ $P < .0001$ .

## 5.4 DISCUSSION

Due to the idiosyncrasies associated with DILI, it is acknowledged that individual factors are important in defining susceptibility to toxicity (Chalasanani and Björnsson, 2010; Russmann et al., 2009; Uetrecht, 2008). However, there is limited representation of interindividual variation within the models used during preclinical screening and importantly, the role of the mitochondrial genome has been neglected (Mosedale and Watkins, 2017). Whilst different *in vitro* assays were conducted to study acute and adaptive mitochondrial dysfunction, the primary focus of the research presented within this chapter was on the utility of the HepG2 cybrids as novel, personalised *in vitro* model for studying differential susceptibility to DIMT. Notably, whether differential susceptibility could be identified for a compound with a hepatotoxic risk and mitochondrial liability when assessed in the cybrids. Therefore, the overall aim of the research presented within this chapter was to investigate the effects of mtDNA variation upon susceptibility to tolcapone-induced toxicity using HepG2 transmitochondrial cybrids.

**Table 5.6: Single nucleotide polymorphisms (SNPs) identified in HepG2 cells and the haplogroup H and J cybrid used in this study**

Macro-haplogroup	Sub-haplogroup	SNPs characteristic of this haplogroup
B	B2c2	73G 146C 263G 827G 1438G 2706G 3547G 4755C 4769G 4820A 4977C 6473T 7028T 7241G 8860G 9950C 10373A 11177T 11719A 13590A 14757C 14766T 15326G 15535T 16217C 16295T 16519C
H	H2a1e1a1	263G 575T 750G 751G 951A 8860G 15326G 16124C 16148T 16166G 16354T
J	J1c1e	185A 228A 263G 295T 462T 482C 489C 750G 1438G 3010A 3394C 4216C 4769G 7028T 8860G 10398G 10454C 11251G 11719A 12612G 13708A 14766T 14798C 15326G 15452A 16069T 16126C 16368C

To assess differences in acute mitochondrial dysfunction, initial experiments were conducted in isolated mitochondria acutely treated with tolcapone and entacapone in order to observe immediate interactions between the compounds and the mitochondria. Tolcapone is a chemical uncoupler that works by binding and transporting protons across the inner mitochondrial membrane into the matrix via simple diffusion in the same manner as FCCP (Benz and McLaughlin, 1983). Haplogroup-specific differences in depolarisation in isolated

mitochondria were detected following acute treatment with tolcapone and entacapone (figure 5.3 and 4). Notably, haplogroup B mitochondria were the least susceptible to tolcapone-induced depolarisation as evidenced by the lack of a significant increase in Rh123, whereas haplogroup J mitochondria were the most susceptible, thus supporting the initial hypothesis of this research that haplogroup J would be more susceptible to acute mitochondrial dysfunction. Research utilising cybrids with East Asian haplogroups (haplogroup M and N) found that cybrids containing the mtDNA SNP m.10398A>G exhibited higher uncoupled respiration (Zhou et al., 2017). This SNP is characteristic of sub-haplogroup J1c1e (table 5.6), which is the sub-haplogroup of the cybrid used in this research, and therefore, could explain the increased uncoupling observed following tolcapone and entacapone treatment in the haplogroup J isolated mitochondria in comparison to haplogroup H and B isolated mitochondria (figure 5.3 and 4). Whilst these experiments suggest that this particular mtDNA variant is a determinant for drug-induced MMP depolarisation, further investigations are required. In addition to haplogroups J and M, the m.10398A>G SNP is also present in haplogroups B5, I and K and can have advantageous or detrimental effects (Li et al., 2014; Zhou et al., 2017). Consideration of single SNPs should therefore not be mistaken for a focus upon interactions with other alleles and nuclear-modifier genes that can alter the phenotype of the mtDNA variant (Chinnery and Hudson, 2013; Wallace, 2013). Nonetheless, future experiments of this type would benefit from the generation of cybrids belonging to haplogroups M, I, K and B5 to examine whether a similar susceptibility to tolcapone-induced depolarisation is evident as in haplogroup J mitochondria. It would also be beneficial to treat isolated mitochondria from different haplogroups to a panel of uncouplers to see if the effects are compound specific or the same for all uncouplers.

The removal of mitochondria from their cellular environment is beneficial as it allows direct interactions between a compound and the mitochondria to be investigated however lacks physiological relevance (Brand M and Nicholls D, 2011). Therefore, in order to increase the translatability of the results detected in isolated mitochondria, additional assays were conducted in whole cells (Brand M and Nicholls D, 2011). To assess acute toxicity, assays were conducted following 2 h of tolcapone treatment, whereas cells were dosed for 24 h in order to observe mitochondrial adaptations. Whilst differential loss of MMP was detected in isolated mitochondria, this observation was not seen at either time-point in whole cells (figure 5.5). Tolcapone correctly induced depolarisation in whole cells however, there were no clear differences between haplogroups as was observed in isolated mitochondria. Given

that the cybrids contain the same nuclear background as the parental HepG2 cell, any processes that could alter the metabolism or distribution of tolcapone should remain constant, which could explain the lack of haplogroup-specific results in whole cells. Removal of the mitochondria from their cellular environment ensues direct interaction with compounds and forgoes cellular processes such as metabolism and distribution (Brand M and Nicholls D, 2011).

Comparison of tolcapone  $IC_{50ATP}$  values revealed that there were time-dependent variances to haplogroup-specific differences in toxicity. Supporting the primary hypothesis, haplogroup J; and also haplogroup B, were identified as the most susceptible haplogroups to tolcapone-induced ATP depletion following 2 h tolcapone treatment in comparison to haplogroup H (table 5.5). The observation of enhanced susceptibility to drug toxicity in haplogroup J cybrids in comparison to haplogroup H cybrids is consistent with results found in other studies and supports the results observed in this study by which haplogroup J isolated mitochondria were the most susceptible to tolcapone-induced depolarisation (Gomez-Duran et al., 2012; Strobbe et al., 2018). However, following 24 h treatment, haplogroup J and H were the most susceptible to tolcapone induced ATP depletion. Notably, there were no significant differences between 2 h and 24 h  $IC_{50ATP}$  values for haplogroup B and J but haplogroup H significantly declined (table 5.5). This observation revealed that in haplogroup H cybrids, toxicity temporally accumulated, whereas in parental HepG2 cells and haplogroup J cybrids, toxicity was sustained at the 2 h level without further toxicity. This observation somewhat supports the secondary hypothesis of this research as it was hypothesised that haplogroup J cybrids would be able to adapt to mitochondrial dysfunction following 24 h tolcapone treatment. The absence of change in 2 h and 24 h  $IC_{50ATP}$  values for haplogroup J cybrids could be suggestive of activation of compensatory mechanisms of mitochondrial protection. To see if this temporal difference was common amongst chemical uncouplers and other mitochondrial toxicants, cells were treated with the mitochondrial poison FCCP and the complex I inhibitor rotenone for 2 and 24 h. Haplogroup J cybrids were revealed to be the least susceptible to FCCP and rotenone-induced ATP depletion after 2 h dosing. This finding contrasts with the trend for  $IC_{50ATP}$  values observed following 2 h tolcapone treatment in which haplogroup J cybrids were identified as the most susceptible to ATP-depletion. This finding also contrasts with results from other researchers using rotenone in which haplogroup J was found to be more susceptible to rotenone-induced mitochondrial dysfunction than haplogroup H (Strobbe et al., 2018). However, it is important to note that in most studies, susceptibility is considered in comparison with the other

haplogroups in the sample population, rather than as a risk in isolation (Penman et al., 2020a). Consequently, the results generated will be dependent on the haplogroups tested. The results presented in this chapter compared haplogroups J1 with H2 and B2, whereas in the research conducted by Strobbe *et al*, cybrids belonging to haplogroup H1 were utilised (Strobbe et al., 2018). Therefore, differences in sub-haplogroup level could account for the different haplogroup trends reported following rotenone treatment.

To identify any additional mitochondrial liabilities that could elucidate non-uncoupling mediated mechanisms of tolcapone, the activity of individual respiratory complexes were measured in permeabilised cells following acute tolcapone treatment. No significant differences in individual complex activity were detected in HepG2 cells (haplogroup B) when compared to vehicle control cells (figure 5.8). However, there was a dose-dependent decrease in complex driven respiration for complex I, II and III in haplogroup H and J cybrids and in complex IV in for haplogroup J cybrids. Overall, there were no significant differences in loss of complex activity between haplogroups, which does not support the finding of increased susceptibility to acute tolcapone-induced depolarisation in haplogroup J mitochondria or tolcapone-induced ATP depletion in haplogroup J cybrids (figure 5.3 and table 5.5). The observation of significant reduced complex IV activity in haplogroup J cybrids is not surprising given that the J1 sub-haplogroup is characterised by the SNP m.3010A>G (table 5.6) (Pacheu-Grau et al., 2013). This SNP is also common in the H1 sub-haplogroup and therefore is not present in the haplogroup H cybrid tested in this thesis, which belongs to sub-haplogroup H2 (Pacheu-Grau et al., 2013). The presence of the m.3010A>G allele has been shown to cause a reduction in the expression of cytochrome c oxidase (complex IV) and could account for the reduced complex IV activity in haplogroup J cybrids in this chapter but not haplogroups B and H (Pacheu-Grau et al., 2013).

The findings of an inhibition of complex I, II and IV activity support findings by Grünig *et al* in permeabilised HepaRG cells and suggest a multi-mechanistic toxicity of tolcapone (Grünig et al., 2017). Albeit, in Grünig *et al* work, 24 h tolcapone treatment resulted in an approximate 20 % reduction in complex activity, which is consistent with the greatest reduction in complex activity following acute tolcapone treatment seen in this work, thus implying that complex inhibition does not increase temporally (Grünig et al., 2017). Whilst the results of Grünig *et al* are not disputed, their capacity to cause toxicity are questioned given the marginal declines in complex activity detected. Several researchers have shown that it is possible to inhibit substantial complex activity before a critical phenotype is observed in a

phenomenon called the 'biochemical threshold effect' (Rossignol et al., 2003). Whilst differing rates have been observed, approximately 75 – 85 % inhibition of an individual complex was required to cause toxicity (James et al., 1996; Letellier et al., 1994; Rossignol et al., 1999). Additionally, the reductions in complex activity seen in this study were marginal when compared to other compounds shown to be complex inhibitors using the same methodology described in this chapter, implying that complex inhibition is not a mechanism of tolcapone-induced mitochondrial dysfunction (Ball et al., 2016; Felser et al., 2013).

Inhibition of complexes within the ETC has the potential to cause superoxide formation (Turrens, 2003). However, there were no significant differences in superoxide levels for all haplogroups when compared to the control following 2 h tolcapone treatment or between haplogroups (figure 5.7A). The lack of changes in superoxide formation therefore supports the findings of minimal differences in complex activity following acute tolcapone treatment (figure 4.8). Excessive production of ROS at the ETC has the potential to cause mitochondrial dysfunction due to damage to lipids, proteins and mtDNA. Research has demonstrated that there is a positive correlation between loss of MMP and ROS production (Korshunov et al., 1997; Turrens, 2003). Tolcapone induced a significant increase in cellular superoxide levels following 24 h dosing for all haplogroups (figure 5.7B) however, differential levels of cell death meant that superoxide formation could not be determined for all concentrations amongst the haplogroups. Following 24 h treatment with 125  $\mu$ M tolcapone, haplogroup J cybrids had the greatest superoxide formation (figure 5.7B) and greatest loss of MMP (figure 5.5B) than haplogroup H and B cybrids, thus supporting the mechanistic link between loss of MMP and ROS formation. Enhanced uncoupling can affect electron flow and so it is plausible that in all haplogroups, reverse electron flow could lead to superoxide formation (Zorova et al., 2018).

The mitochondria have a wealth of structural and functional features that make them vulnerable to stress. In order to prevent this insult from causing cellular injury, the mitochondria have evolved to be able to detect, regulate and adapt to protect mitochondrial function. There are multiple compensatory mechanisms of mitochondrial protection including mitochondrial dynamics, mitophagy, biogenesis and the mitochondrial unfolded protein response (Barbour and Turner, 2014; Valera-Alberni and Canto, 2018). The secondary hypothesis of this research was that haplogroup J cybrids would be able to temporally adapt to mitochondrial dysfunction and therefore be less susceptible to DIMT following 24 h tolcapone treatment. The lack of change in 2 h and 24 h  $IC_{50ATP}$  values for haplogroup J and

B cells was suggestive of activation of mitochondrial protective mechanisms (table 5.5). However, the significant reduction in  $IC_{50}ATP$  in haplogroup H cybrids following 24 h tolcapone treatment suggested that compensatory mechanisms of mitochondrial protection were not activated in haplogroup H. In order to assess differential adaptive response, *in vitro* assays were conducted to measure changes in mitochondrial dynamics (section 1.3.4.1) and mitochondrial biogenesis (section 1.3.4.2) following 2 and 24 h tolcapone treatment.

Mitochondria are dynamic organelles, repeatedly cycling between fission and fusion (Rosdahl et al., 2016). There is a complex interplay between fission and fusion as both can act as quality control mechanisms (Valera-Alberni and Canto, 2018). Mitochondrial dynamics did not change following 2 or 24 h tolcapone treatment in all haplogroups indicating that changes in mitochondrial dynamics were not a mechanism of mitochondrial protection. In all haplogroups, mitochondria appeared fragmented in control cells and remained fragmented upon tolcapone treatment. This contrasts with findings from the initial pilot study conducted with the HepG2 cybrids where it was concluded that fission increased dose-dependently in haplogroup J cybrids following 2 h tolcapone treatment (Ball, 2018). Due to the qualitative nature of the immunofluorescence used in this chapter, it was not possible to tell if any changes in the number of fragmented mitochondria were due to an increase in fission or the production of new mitochondria. Given the complex interchange in mitochondrial dynamics, it would be beneficial for future studies to use more quantitative methodologies. During the initial pilot study of the HepG2 cybrids, mitochondrial dynamics were assessed using a high-throughput, automated microscope (Operetta CLS (PerkinElmer)) coupled with a machine-learning platform called PhenoLOGIC™ (Ball, 2018). Other researchers have also used time-lapsed videos and machine-learning derived algorithms to successfully generate unbiased, quantitative information on mitochondrial morphology and movement (Leonard et al., 2015; Zahedi et al., 2018). The use of these methodologies would allow visualisation of the progression of cellular stress and changes in mitochondrial morphology in real-time as well as distinguish morphological classes, which was not possible in the scope of this work (Leonard et al., 2015; Zahedi et al., 2018).

Mitochondrial biogenesis is the process by which cells increase their mitochondrial mass, typically in response to an increase in ATP demand or compromised ATP synthesis (Valera-Alberni and Canto, 2018). Therefore, it was plausible that there could be haplogroup-specific differential activation of mitochondrial biogenesis. Due to the complexity of mitochondrial biogenesis, it is advised that multiple endpoints are measured to establish the extent of

mitochondrial biogenesis (Medeiros, 2008). Proposed initial investigations are to assess the relative area occupied by mitochondria using immunofluorescence however, the aforementioned limitations of this approach meant conclusions on biogenesis or mitochondrial fission could not be determined. Other recommended end-points include mtDNA copy number determination and western blotting of proteins regulated during the biogenesis cascade. MtDNA encodes core subunits of the ETC alongside tRNA and rRNA (Calvo and Mootha, 2010). MtDNA copy number is tightly regulated to meet the energy needs of the cells as mtDNA replication and transcription will increase mitochondrial mass (Moyes et al., 1998). There were no significant differences in mtDNA copy number compared to the control for any haplogroup following 2 h tolcapone treatment (figure 5.12A). However, mtDNA copy number significantly decreased dose-dependently following 24 h tolcapone treatment in haplogroup H cybrids (figure 5.12B). Notably, following 24 h tolcapone treatment, haplogroup B mtDNA copy number was significantly greater than that of haplogroup H (figure 5.12B). This trend mirrors the temporal changes in  $IC_{50}ATP$  values following 24 h tolcapone treatment in haplogroup H compared to haplogroup B and J (table 5.5) and could thereby explain the loss of metabolic capacity of haplogroup H cybrid due to an inability to increase mtDNA copy number for replication and creation of new mitochondria. There were no significant changes in the expression of proteins regulated during the biogenesis cascade; TFAM and PGC1- $\alpha$ , when compared to the control or between haplogroups at both time-points (figure 5.14 and 5.15). Collectively, these findings do not suggest an activation of mitochondrial biogenesis following 24 h tolcapone treatment and imply that another mechanism of mitochondrial adaptation and protection is activated in haplogroup B and J, thus disproving the secondary hypothesis of this work.

VDAC levels were assessed to determine potential increases in mitochondrial mass. There was a significant dose-dependent increase in the expression of VDAC in haplogroup J cybrids following 2 h tolcapone treatment and a significant increase in VDAC expression in haplogroup B after 24 h (figure 5.13). In addition to its role in molecule movement, VDAC is hypothesised to be a part of the MPT pore (figure 1.11), whose opening leads to apoptosis (section 1.3.3.2) (Vianello et al., 2012). Work by Zheng *et al* demonstrated that treatment of a myeloma cell line with arsenic trioxide led to an increase in the expression of VDAC and enhanced apoptosis (Zheng et al., 2004). Therefore, it is plausible that the increases in VDAC expression observed in this chapter could be attributed to the cells attempting to prevent further cell injury by activating apoptosis.

The activation of mitochondrial quality controls is a complex process involving multiple mechanisms, all of which were not discussed in this chapter. It is therefore possible that many processes can occur simultaneously within a mitochondrion or a mitochondria population (Valera-Alberni and Canto, 2018). Whilst it is recommended to monitor many end-points of biogenesis, the complexity of the signalling cascade means that it could be possible to miss a step in the biogenesis gene programme (Medeiros, 2008). Whilst no differences in TFAM and PGC1- $\alpha$  expression were detected amongst the haplogroups, haplogroup-specific differences in mtDNA copy number were observed. There were no significant increases in mtDNA copy number, thereby suggesting that mitochondrial biogenesis was not activated as a compensatory mechanism of mitochondrial protection in haplogroups B and J. However, the loss of mtDNA copy number in haplogroup H cybrids following 24 h tolcapone treatment suggests an inability to replicate, which could explain the temporal change in toxicity.

The work presented within this chapter has identified haplogroup-specific differences in susceptibility to tolcapone-induced toxicity following 2 and 24 h dosing for certain *in vitro* assays. There are many methods to measure mitochondrial function and dysfunction and determining which will have better predictive value of *in vivo* toxicity can be compound and model specific. The endpoints assessed in this chapter represent a fraction of functions that could be perturbed during DIMT and may be affected by mitochondrial haplogroup. The identification of a significant reduction in complex I driven respiration in haplogroup H and J cybrids warrants further investigations into secondary outcomes of perturbations at complex I. This could be investigated via measuring changes in NAD<sup>+</sup>/NADH. When functioning correctly, NADH binds to complex I and is oxidised to NAD<sup>+</sup> thus leading to an increase in the NAD<sup>+</sup>/NADH ratio (Vinogradov and Grivennikova, 2016). Therefore, investigations into the NAD<sup>+</sup>/NADH ratio would provide further clarification for tolcapone-induced complex I inhibition in haplogroup H and J cybrids. As previously mentioned, tolcapone treatment resulted in 3 deaths, which led to it receiving a Black Box warning (Assal et al., 1998). A liver biopsy from one of the patients revealed steatosis in adjacent hepatocytes (Assal et al., 1998; Spahr et al., 2000). Grünig *et al* conducted experiments in HepaRG cells where it was revealed that 24 h exposure to tolcapone resulted in an inhibition of palmitate metabolism and caused lipid accumulation, thus supporting findings of steatosis (Grünig et al., 2018). Consequently, future experiments could be conducted to determine if there is differential inhibition of  $\beta$ -oxidation amongst the haplogroups using the XFe96 analyser.

Whilst the results presented in this chapter highlight HepG2 transmitochondrial cybrids as a novel model that can be utilised in DILI screening, their use is in its infancy and thus their limitations should be considered. Firstly, the generation of the cybrids is a labour-intensive process involving an 8-week treatment of HepG2 cells with low dose ethidium bromide to generate HepG2  $\rho 0$  cells. The use of low dose ethidium bromide is routinely used to deplete mtDNA without affecting nuclear DNA (Desjardins et al., 1985; Hayakawa et al., 1998; Zylber et al., 1969). However, the consequent high passage number of the HepG2  $\rho 0$  cells used in cybrid generation has the potential to alter cell growth rate, morphology and response to stimuli in comparison to lower passages (<20 cells) (Briske-Anderson et al., 1997; Esquenet et al., 1997). MtDNA is constantly changing in a process known as heteroplasmy (Stewart and Chinnery, 2015). The selective pressures endured during cybrid generation may have induced a change in heteroplasmy, meaning that the genotypes of the individuals mtDNA may have altered (Shtolz and Mishmar, 2019). Additionally, the parental HepG2 cells had not undergone the same selective pressures as the cybrids. These limitations could be tackled by genotyping the cybrids to see the current genotype and the effects of time and selection pressures on shifts in heteroplasmy. It would also be valuable if HepG2 transmitochondrial cybrids were generated from an individual belonging to haplogroup B in order to see if the same results as the parental HepG2 cells were gained. It is also important to note that mitochondrial haplogroups are not the only way in which mtDNA-mediated changes in mitochondrial function can occur. Specific mtDNA polymorphisms have been found to be contributing factors for some ADRs however, can be found in multiple sub-haplogroups. Additionally, haplogroup-specific nuclear DNA interactions and nuclear-modifier genes that have the potential to alter the phenotypic response of mtDNA variants have been identified (Chinnery and Gomez-Duran, 2018; Chinnery and Hudson, 2013; Craven et al., 2017). Finally, future experiments may benefit from the generation of cybrids using the platelets of individuals whom have experienced clinical cases of DILI. In research by Zhao et al., osteosarcoma transmitochondrial cybrids were created from a Chinese family who had suffered from antibiotic-induced toxicity. In their experiments, *in vivo* toxicity translated to *in vitro* toxicity when the cybrids were dosed with paromomycin (Zhao et al., 2004; Zhao et al., 2005). Therefore, it would be interesting to see if susceptibility to clinical DILI translates to the HepG2 cybrid model.

Nonetheless, the results presented in this chapter have confirmed the utility of HepG2 transmitochondrial cybrids for the study of differential susceptibility to DIMT. Using this model, differential susceptibility in toxicity were identified following measurements of MMP

in isolated mitochondria and ATP content and mtDNA copy number in whole cells (figure 5.16). By combining results from MMP in isolated mitochondria and  $IC_{50}ATP$  values, haplogroup J cybrids were the most susceptible to tolcapone-induced mitochondrial toxicity at short time points (acute dosing and 2 h). Whereas when this dosing regimen was extended to 24 h, haplogroup H cybrids were more susceptible to toxicity as evidenced by their lower  $IC_{50}ATP$  (table 5.5) value and reduction in mtDNA copy number (figure 5.12B). This research provides preliminary evidence that mitochondrial haplogroups do influence susceptibility to drug toxicity and supports the tenet that variation in mtDNA could underpin some of the idiosyncrasies associated with DILI (Boelsterli and Lim, 2007). It is important to note that due to the multi-mechanistic toxicity of DILI, there are a plethora of *in vitro* assays to identify toxicity (Atienzar et al., 2016). As such, differential toxicity was identified in 3 out of the 8 assays conducted within this chapter. This does not mean that these assays have an overall better predictive value for a clinical manifestation of DILI however, highlight the need to also consider drug-specific mechanisms when choosing *in vitro* assays (Atienzar et al., 2016; Kenna and Uetrecht, 2018). Overall, the observation of differential susceptibility to toxicity using this novel model, confirms the utility of HepG2 transmitochondrial cybrids for personalised medicine and drug safety screening.

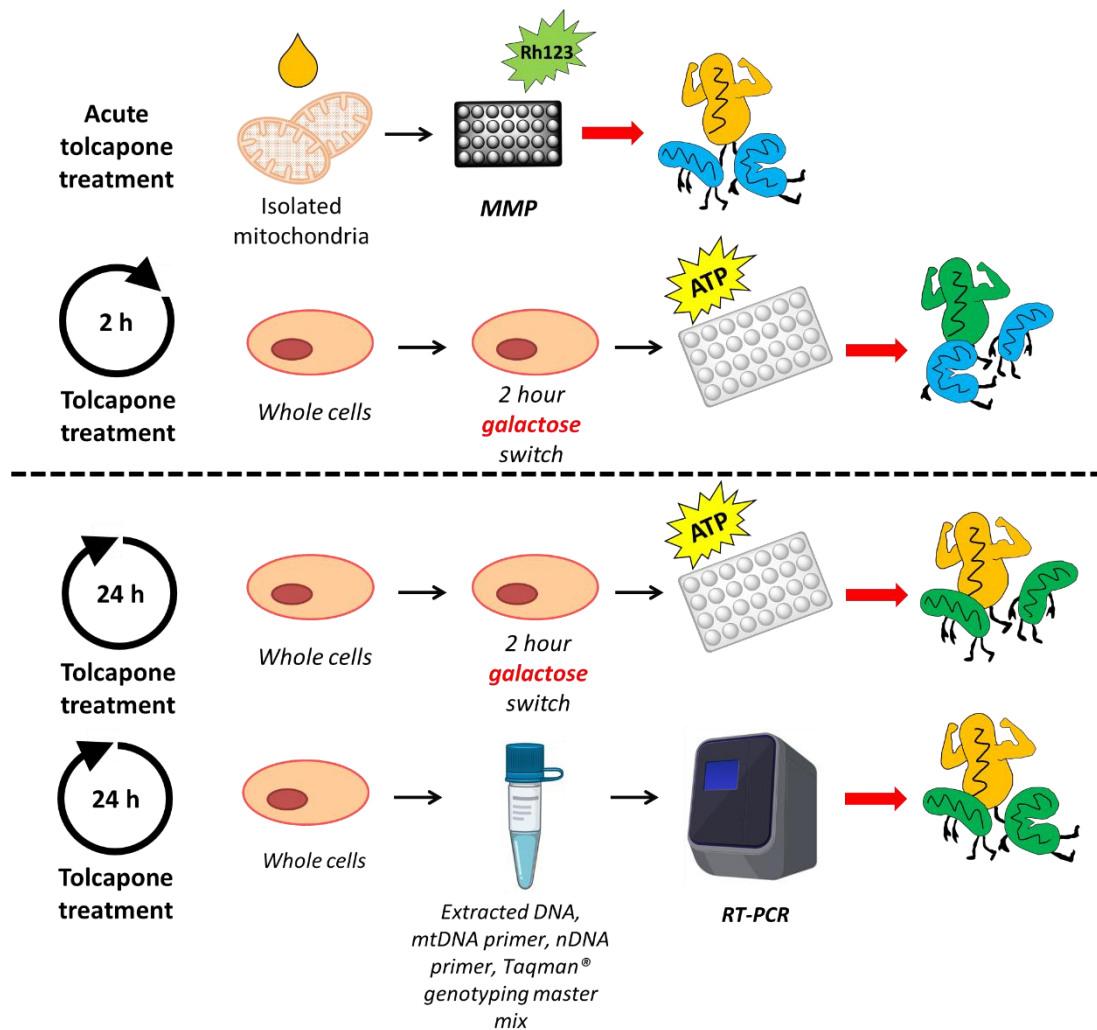


**Figure 5.16: Schematic representation of differential susceptibility to tolcapone-induced mitochondrial toxicity following 2 and 24 h treatment.** Following acute tolcapone treatment, isolated mitochondria from haplogroup J were the most susceptible to tolcapone-induced MMP depletion. Following 2 h tolcapone treatment, haplogroup H cybrids were the least susceptible to tolcapone-induced ATP depletion whereas following 24 h tolcapone treatment, haplogroup H cybrids were the most susceptible. Haplogroup H cybrids were also the most susceptible to mtDNA copy number depletion following 24 h tolcapone treatment.

## 5.5 CONCLUSION

The lack of inter-individual variation in pre-clinical screening and lack of genetic diversity in *in vivo* models emphasises the need for novel, preclinical models that account for differences in the nuclear and mitochondrial genome (Mosedale and Watkins, 2017; Pereira et al., 2012). Using HepG2 transmitochondrial cybrids, differential susceptibility to tolcapone-induced mitochondrial dysfunction was identified dependent on mitochondrial haplogroup and length of exposure to tolcapone. Notably, haplogroup J was the most susceptible haplogroup to acute-mitochondrial dysfunction whereas haplogroup H was more susceptible following 24 h treatment. The inability to reliably identify 'at risk' individuals has prohibited many drugs from gaining regulatory approval and caused many to be withdrawn from the market (Watkins, 2011). The goal of personalised medicine is to deliver bespoke treatment, predict clinical outcomes and offer alternative therapies based upon an individual's genetics (Schwab and Schaeffeler, 2012). The identification of haplogroup-specific differences in tolcapone toxicity could prove invaluable in the stratification of tolcapone treatment given the positive results associated with its use in Parkinson's disease (Lees, 2008). Whilst this research focussed on one compound and three macro-haplogroups, the results could present a paradigm for other compounds. This research therefore confirms the utility of HepG2 transmitochondrial cybrids for the study of DILI and presents a promising utility of the model in personalised medicine.

# **Chapter 6**

## **General Discussion**

The aim of drug development is the creation of a drug candidate with efficacy against its intended therapeutic target (Mohs and Greig, 2017). However, the success of a new candidate drug can be dampened if toxicity arises post-market. The detection of ADRs following drug approval poses a significant concern given the potential for fatalities and the time and high cost associated with drug development. Hepatotoxicity is one of the most reported ADRs and thus the screening for the potential of a drug to cause DILI is routinely undertaken during preclinical development (Kullak-Ublick et al., 2017). Whilst it is acknowledged that DILI can arise due to a plethora of mechanisms, it is also governed by complex genetic and non-genetic factors meaning that there are significant limitations in its preclinical detection (Chalasan and Björnsson, 2010; Roth and Lee, 2017; Ulrich, 2007). Nonetheless, advances in the field have identified multiple *in vitro* assays for the screening of DILI (Kenna and Uetrecht, 2018). However, the predictive value of these assays are often questioned given that *in vitro* toxicity does not always translate to a clinical manifestation of hepatotoxicity (Atienzar et al., 2016; Roth and Lee, 2017). This in part could be explained by the suitability of the models used during preclinical screening. Failure to employ models with suitable phenotypic characteristics, or those that are not representative of inter-individual variation, can lead to toxicity being undetected, missed or exaggerated (figure 6.1). Therefore, it is essential that *in vitro* assays are conducted in the most appropriate models in order to deliver results with *in vivo* relevance and predictive value. Consequently, the overall aim of this thesis was to assess the pharmacological and toxicological utility of advanced hepatic models, including HepaRG cells and transmitochondrial cybrids, for the study of defined mechanisms of toxicity associated with DILI. Specifically, mitochondrial dysfunction and transporter implications, which are frequently reported to be implicated in DILI.

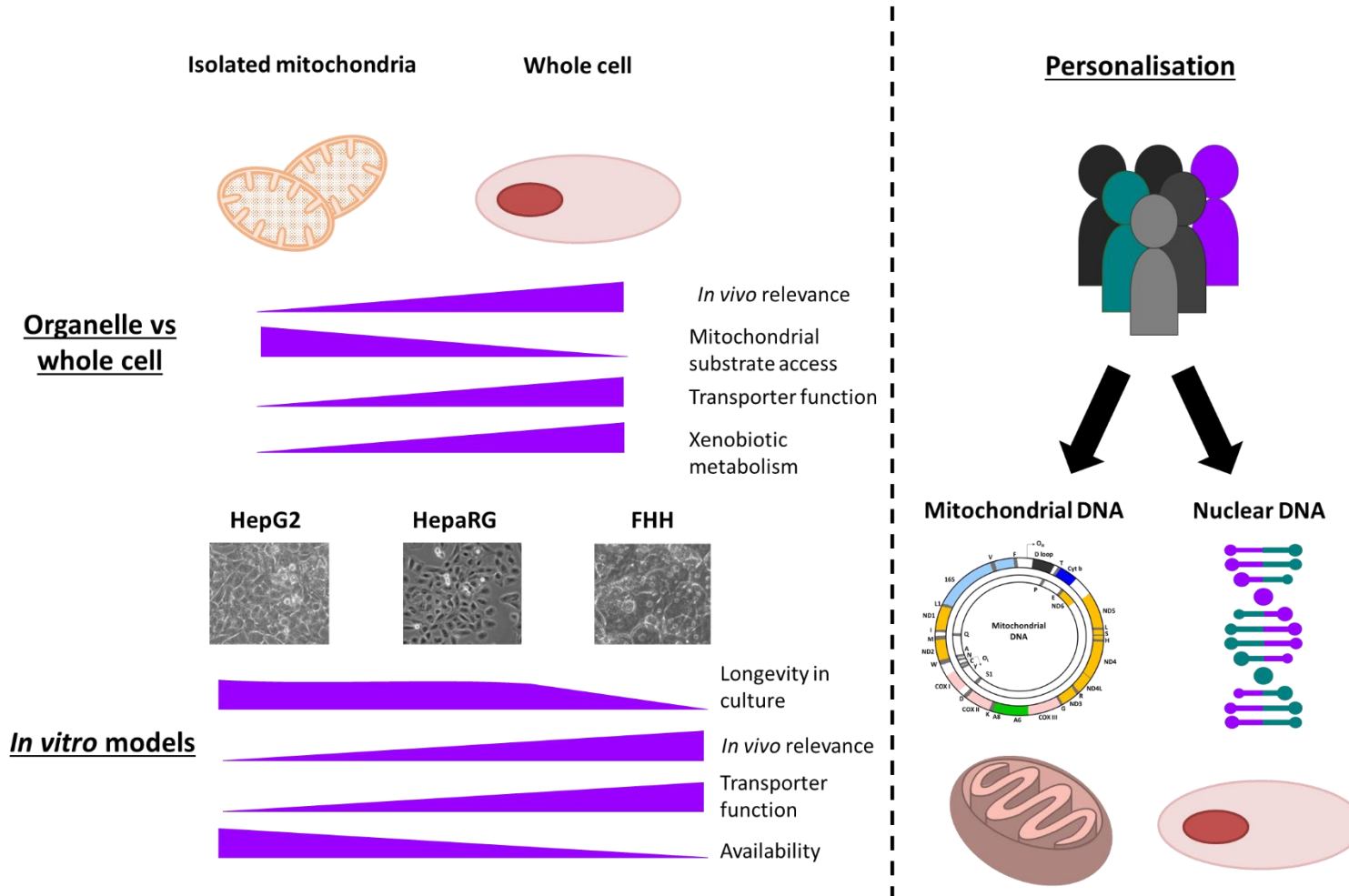


**Figure 6.1: Schematic representation of factors that must be considered when choosing the most appropriate model to answer experimental questions.** This thesis identified physiological relevance and personalisation of models as important factors which must be considered.

Investigations conducted within this thesis confirmed the utility of 2D grown HepaRG cells for the study of DIC over 2D cultured HepG2 cells. This was concluded following an observation of polarisation and transporter function in HepaRG cells but inability in HepG2 cells (chapter 2). Additionally, 2D cultured HepaRG cells have been shown to express functional bile canaliculi networks and metabolic activity more comparable with PHH than other cell lines (Burbank et al., 2016; Guillouzo et al., 2007). Following the use of HepaRG cells, this research identified biliary transporter dysfunction as a mechanism of BA-induced toxicity but not mitochondrial dysfunction, contrary to the accepted understanding based upon data from simpler models. This observation was an important finding as it has long been hypothesised that BA-induced toxicity was mediated via mitochondrial dysfunction (Palmeira and Rolo, 2004; Rolo et al., 2004; Schulz et al., 2013). The detection of BA-induced mitochondrial toxicity in isolated mitochondria did not translate to a whole cell model, thus highlighting limitations of using isolated organelles when trying to deduce results with *in vivo* relevance (chapter 3). This observation does not discredit the use of isolated mitochondria as their application is good for initial mechanistic studies and in cases where substrates and inhibitors are not directly accessible to the mitochondria when in their cellular environment (Brand M and Nicholls D, 2011). Nonetheless, mitochondria within their cellular environment do not behave as single entities but are complex signalling organelles that communicate with other mitochondria and the cell (Valera-Alberni and Canto, 2018). Therefore, in order to expand on findings in isolated mitochondria, additional experiments in whole cells should be conducted in order to increase physiological relevance.

The 3D cultivation of cells has been revealed to increase *in vivo* likeness (Miyamoto et al., 2015; Ramaiahgari et al., 2017). Therefore, in order to further advance the research conducted within this thesis, future experiments with 3D cultured HepaRG cells and cybrids should be employed. Whilst 2D cultured HepaRG cells share an improved resemblance with PHH, 3D spheroidal cultivation has been shown to enhance their phenotype further by improving functionality and sensitivity to drugs (Gunness et al., 2013; Hendriks et al., 2016; Mandon et al., 2019; Ramaiahgari et al., 2017). *In situ*, within the body, cells are surrounded by an extracellular matrix (ECM) and interact with other cells in a 3D environment. In order to recapitulate this 3D environment, cell culture techniques have been advanced to include the use of natural and synthetic hydrogels, scaffolds, scaffold free techniques and flow culture systems (Bachmann et al., 2015). PHH, HepG2 and HepaRG cells have successfully been cultured in 3D with enhanced *in vivo* likeness than

their 2D counterparts including increased sensitivity to drugs, enhanced bile canaliculi formation, increased albumin synthesis and elevated CYP and transporter levels (Hamilton et al., 2001; Saavedra et al., 2003; Schyschka et al., 2013).

Therefore, the findings of this thesis could be advanced via 3D culture of HepaRG cells. A popular method of 3D culture, which has been highly commercialised, are scaffold free techniques, with the hanging-drop method being a common technique used to generate spheroids (Bachmann et al., 2015). Cell number and spheroid size is an important factor to consider during development as oxygen and nutrient diffusion can be impeded leading to a necrotic core (Bachmann et al., 2015). Nonetheless, PHH, HepG2 and HepaRG spheroids have successfully been generated with enhanced *in vivo* likeness than their 2D counterparts. In order to recapitulate the complex physiology of the liver, 3D cell culture conditions have been further advanced to contain co-cultures of hepatocytes and non-parenchymal cells (Roth and Lee, 2017). The primary cells within the liver lobule are hepatocytes but sinusoidal cells make up the remainder and include Kupffer cells, stellate cells and endothelial cells (Jacobs et al., 2010; Kietzmann, 2017). HepG2 and human hepatocyte spheroids have successfully been co-cultured with non-parenchymal cells generating spheroids with enhanced albumin and urea secretion, increased culture times and improved sensitivity to repeated drug exposure when compared with the single-cultured spheroid (Lee et al., 2014; Messner et al., 2013). It would therefore be beneficial if future studies were to repeat the assays conducted within chapter 3 of this thesis using HepaRG spheroids cultured via the hanging drop method with and without the addition of non-parenchymal cells in order to see if the same results are achieved. The enhanced physiological relevance of 3D cultured HepaRG spheroids may allow questions regarding whether mitochondrial dysfunction is a mechanism of toxicity in humans to be better informed than using 2D results (Gunness et al., 2013).

Advances in genetic screening and technologies has led to an improved understanding that variation within the genome can affect response to therapy (Agyeman and Ofori-Asenso, 2015). The concept of personalised medicine has become popular, with the goals to deliver bespoke treatment, predict clinical outcomes and offer alternative therapies based upon an individual's genetics (Schwab and Schaeffeler, 2012). The role of the mitochondrial genome has typically been neglected during personalised medicine however, over the last 20 years, our knowledge and understanding of the mitochondrial genome has greatly advanced due to next generation sequencing (NGS) (Chinnery and Hudson, 2013). Notably, it is now

understood that specific mitochondrial haplogroups or genetic variants are associated with disease susceptibility, drug efficacy and ADRs (Boelsterli and Lim, 2007; Chinnery and Gomez-Duran, 2018; Chinnery and Hudson, 2013; Grady et al., 2011; Guzman-Fulgencio et al., 2013; Hart et al., 2013; Hulgan et al., 2012; Medrano et al., 2018; Wallace, 2013).

Supporting this tenet, an additional finding of the results presented within this thesis were that personalisation of models at the mitochondrial genome level is an important factor that should be considered during preclinical screening. Notably, the research presented within chapter 5 confirmed the utility of HepG2 transmitochondrial cybrids for studying the effects of mtDNA variation and susceptibility to DILI. Using the HepG2 cybrids, temporal differences in tolcapone-induced mitochondrial toxicity were identified between haplogroups B, H and J. Although the findings presented in chapter 5 were only for one drug, this may present a paradigm for other compounds and warrants the use of HepG2 cybrids by the pharmaceutical industry for screening other compounds with DILI liabilities. Whilst only preliminary results, the identification of haplogroup-specific differences in tolcapone toxicity in chapter 5 has promising implications for patients with Parkinson's disease given that tolcapone has been shown to have greater efficacy than entacapone (Lees, 2008). Following additional research, there could be the potential to stratify tolcapone treatment for Parkinson's patients based upon identification of 'at risk' individuals, ultimately leading to improvements in patient quality of life.

Given the lack of genetic diversity within clinical trials and the high costs associated with multi-centre clinical trials, there is a need to develop new strategies to bridge preclinical and clinical outcomes (Clark et al., 2019; Fermini et al., 2018). The identification of haplogroup-specific differences in susceptibility to toxicity has the potential to improve preclinical investigations of DILI with the overall aim of identifying 'at risk' individuals and improving drug safety. Therefore, the pharmaceutical industry may benefit from utilising a panel of HepG2 cybrids representative of different haplogroups and sub-haplogroups in order to gain a better understanding of mitochondrial associations and ADRs. However, cybrid generation is a labour intensive process meaning the development of cybrids from multiple haplogroups and sub-haplogroups may not be amenable for the pharmaceutical industry and the need for high-throughput screening and short execution times (Szymański et al., 2012). Genome association studies have revolutionised the field of personalised medicine by allowing individual's entire genome to be screened for specific variants and SNPs that are associated with a phenotype or outcome (Visscher et al., 2017). In terms of the mitochondrial genome, sequencing has revealed that individuals belonging to

haplogroup L are associated with protection from non-alcoholic steatohepatitis (NASH) (Mehta et al., 2016). Additionally, NGS of tuberculosis patient's blood revealed that individuals harbouring multiple nonsynonymous variants in subunits ND1 and ND5 of complex I were more susceptible to isoniazid-induced liver injury (Lee et al., 2019). It would therefore be beneficial for more genome association studies to be conducted in order to identify specific haplogroups and mtDNA variants that are associated with liver disease or DILI, as opposed to creating and screening cybrids belonging to every haplogroup, which would be a labour-intensive process. Once we have a greater understanding of mtDNA associations and ADRs, cybrid generation for specific haplogroups based upon geography or disease phenotype could then be employed within the pharmaceutical industry.

Whilst it is acknowledged that genetic factors can influence susceptibility to ADRs, non-genetic factors such as age, sex, diet, poly-pharmacy, physical activity and pre-existing diseases can also be implicated (Ulrich, 2007). It is recognised that being over the age of 50 years and being female sex increases the likelihood of developing DILI (Pauli-Magnus and Meier, 2006). Pre-existing liver disease is known to worsen symptoms of DILI and in some cases, increase susceptibility. For example, patients with cholestatic alcoholic hepatitis were found to have a reduction in the mRNA and protein expression levels of BSEP and NTCP (Zollner et al., 2001). Therefore, it could be plausible that adaptive changes in hepatocyte biliary transporters due to pre-existing liver disease could be an added risk of developing DILI (Pauli-Magnus and Meier, 2006). *In silico* modelling in response to tolcapone and entacapone was conducted using a simulated human population (SimPops™) with added variability factors to account for interindividual susceptibility to DILI (Longo et al., 2016). It was found that those with compromised mitochondrial function were at an increased risk of developing DILI. Individuals with NASH are associated with defects in the ETC (Pérez-Carreras et al., 2003). The inclusion of a subset of individuals with mitochondrial abnormalities due to NASH were included in the SimPops™ model and allowed for an investigation of the influence of prior ETC dysfunction and tolcapone-mediated toxicity (Longo et al., 2016). This observation supports the hypothesis that personalised mitochondrial function is important in DILI and should be considered in preclinical screening. *In vitro* assays could attempt to simulate individuals with compromised mitochondrial function by pre-dosing cells with low doses of rotenone, as such to not fully inhibit complex I activity, and thereby allowing ATP generation via electron entry at complex II of the ETC.

There are a plethora of models that can be used for the preclinical screening of DILI. As such, a certain model may be better suited for detecting some DILI mechanisms than others (Atienzar et al., 2016). However, due to the multi-mechanistic toxicity of DILI, none of the models can address all of the mechanisms and no single *in vitro* assay appears to have greater predictive value to a clinical manifestation of toxicity than the other (Atienzar et al., 2016; Kenna and Uetrecht, 2018). This highlights the need for biomarkers with mechanistic value for DILI (Kenna and Uetrecht, 2018). Mitochondria can act as crucial regulators of the innate immune system through the release of mitochondrial specific damage associated molecular patterns (mtDAMPs), which engage with various pattern-recognition receptors (Grazioli and Pugin, 2018). It has been suggested that the release of mtDNA during mitochondrial dysfunction could act as an mtDAMP and thus biomarker for mitochondrial toxicity (Grazioli and Pugin, 2018). MtDNA encompasses remnants of bacterial nucleic acid sequences and is methylated in a different way from nuclear DNA meaning that the innate immune system could mistake mtDNA as a foreign pathogen (Rodríguez-Nuevo and Zorzano, 2019). Therefore, future efforts should be made to further investigate the role of mtDNA as a potential biomarker for mitochondrial dysfunction and whether this biomarker could be of predictive value for DILI.

In conclusion, this work has achieved its overall aim of assessing the pharmacological and toxicological utility of HepaRG cells and HepG2 transmitochondrial cybrids for screening mechanisms of toxicity associated with DILI. In order to advance our mechanistic understanding of DILI, it is essential that the most appropriate models are utilised during preclinical screening. Failure to employ the correct models can lead to the generation of data that lacks *in vivo* applicability. Overall, this thesis has highlighted the importance of ensuring that the models utilised during preclinical screening are physiologically relevant for the defined pathophysiological condition being tested in order to ensure data with *in vivo* relevance is generated. Additionally, this thesis has shown that personalisation of models at the mitochondrial genome level is of importance during preclinical screening. It is only by utilising models with enhanced physiological relevance that the field can improve predictive values of *in vitro* assays and our ability to accurately predict clinical outcomes of DILI.

# **Bibliography**

- Abdel-Misih, S.R., Bloomston, M., 2010. Liver anatomy. *Surg Clin North Am* 90, 643-653.
- Adachi, T., Kaminaga, T., Yasuda, H., Kamiya, T., Hara, H., 2014. The involvement of endoplasmic reticulum stress in bile acid-induced hepatocellular injury. *J Clin Biochem Nutr* 54, 129-135.
- Aden, D.P., Fogel, A., Plotkin, S., Damjanov, I., Knowles, B.B., 1979. Controlled synthesis of HBsAg in a differentiated human liver carcinoma-derived cell line. *Nature* 282, 615-616.
- Agyeman, A.A., Ofori-Asenso, R., 2015. Perspective: Does personalized medicine hold the future for medicine? *J Pharm Bioallied Sci* 7, 239-244.
- Akita, H., Suzuki, H., Ito, K., Kinoshita, S., Sato, N., Takikawa, H., Sugiyama, Y., 2001. Characterization of bile acid transport mediated by multidrug resistance associated protein 2 and bile salt export pump. *Biochim Biophys Acta* 1511, 7-16.
- Aleo, M.D., Luo, Y., Swiss, R., Bonin, P.D., Potter, D.M., Will, Y., 2014. Human drug-induced liver injury severity is highly associated with dual inhibition of liver mitochondrial function and bile salt export pump. *Hepatology* 60, 1015-1022.
- Anderson, S., Bankier, A.T., Barrell, B.G., de Bruijn, M.H., Coulson, A.R., Drouin, J., Eperon, I.C., Nierlich, D.P., Roe, B.A., Sanger, F., Schreier, P.H., Smith, A.J., Staden, R., Young, I.G., 1981. Sequence and organization of the human mitochondrial genome. *Nature* 290, 457-465.
- Andrews, E., Daly, A.K., 2008. Flucloxacillin-induced liver injury. *Toxicology* 254, 158-163.
- Aninat, C., Piton, A., Glaise, D., Le Charpentier, T., Langouet, S., Morel, F., Guguen-Guillouzo, C., Guillouzo, A., 2006. Expression of cytochromes P450, conjugating enzymes and nuclear receptors in human hepatoma HepaRG cells. *Drug Metab Dispos* 34, 75-83.
- Assal, F., Spahr, L., Hadengue, A., Rubbia-Brandt, L., Burkhard, P.R., 1998. Tolcapone and fulminant hepatitis. *Lancet* 352, 958.
- Atienzar, F.A., Blomme, E.A., Chen, M., Hewitt, P., Kenna, J.G., Labbe, G., Moulin, F., Pognan, F., Roth, A.B., Suter-Dick, L., Ukairo, O., Weaver, R.J., Will, Y., Dambach, D.M., 2016. Key Challenges and Opportunities Associated with the Use of In Vitro Models to Detect Human DILI: Integrated Risk Assessment and Mitigation Plans. 2016, 9737920.
- Attili, A.F., Angelico, M., Cantafora, A., Alvaro, D., Capocaccia, L., 1986. Bile acid-induced liver toxicity: relation to the hydrophobic-hydrophilic balance of bile acids. *Med Hypotheses* 19, 57-69.
- Axelson, M., Mörk, B., Aly, A., Wisén, O., Sjövall, J., 1989. Concentrations of cholestenic acids in plasma from patients with liver disease. *J Lipid Res* 30, 1877-1882.
- Baas, H., Beiske, A.G., Ghika, J., Jackson, M., Oertel, W.H., Poewe, W., Ransmayr, G., 1997. Catechol-O-methyltransferase inhibition with tolcapone reduces the "wearing off" phenomenon and levodopa requirements in fluctuating parkinsonian patients. *J Neurol Neurosurg Psychiatry* 63, 421-428.
- Bachmann, A., Moll, M., Gottwald, E., Nies, C., Zantl, R., Wagner, H., Burkhardt, B., Sánchez, J.J., Ladurner, R., Thasler, W., Damm, G., Nussler, A.K., 2015. 3D Cultivation Techniques for Primary Human Hepatocytes. *Microarrays (Basel)* 4, 64-83.
- Bachour-El Azzi, P., Sharanek, A., Burban, A., Li, R., Guével, R.L., Abdel-Razzak, Z., Stieger, B., Guguen-Guillouzo, C., Guillouzo, A., 2015. Comparative Localization and Functional Activity of the Main Hepatobiliary Transporters in HepaRG Cells and Primary Human Hepatocytes. *Toxicol Sci* 145, 157-168.
- Ball, A.L., 2018. Generation and Validation of Transmitochondrial Cybrid and Platelet Models to Investigate the Effect of Mitochondrial Genotype upon DrugInduced Liver Injury, Department of Molecular and Clinical Pharmacology. The University of Liverpool.
- Ball, A.L., Kamalian, L., Alfirevic, A., Lyon, J.J., Chadwick, A.E., 2016. Identification of the Additional Mitochondrial Liabilities of 2-Hydroxyflutamide When Compared With its Parent Compound, Flutamide in HepG2 Cells. *Toxicological Sciences* 153, 341-351.

- Ballatori, N., Li, N., Fang, F., Boyer, J.L., Christian, W.V., Hammond, C.L., Ost alpha-Ost beta: A key membrane transporter of bile acids and conjugated steroids. *Front Biosci* 14, 2829-2844.
- Baracca, A., Sgarbi, G., Solaini, G., Lenaz, G., 2003. Rhodamine 123 as a probe of mitochondrial membrane potential: evaluation of proton flux through FO during ATP synthesis. *Biochimica et Biophysica Acta (BBA) - Bioenergetics* 1606, 137-146.
- Barbour, J.A., Turner, N., 2014. Mitochondrial stress signaling promotes cellular adaptations. *Int J Cell Biol* 2014, 156020.
- Barker, S., 1944. The direct colorimetric determination of urea in blood and urine. *J. Biol. Chem* 152, 453-463.
- Benedetti, A., Di Sario, A., Marucci, L., Svegliati-Baroni, G., Schteingart, C.D., Ton-Nu, H.T., Hofmann, A.F., 1997. Carrier-mediated transport of conjugated bile acids across the basolateral membrane of biliary epithelial cells. *Am J Physiol* 272, G1416-1424.
- Benz, R., McLaughlin, S., 1983. The molecular mechanism of action of the proton ionophore FCCP (carbonylcyanide p-trifluoromethoxyphenylhydrazone). *Biophys J* 41, 381-398.
- Bernardi, P., 1999. Mitochondrial transport of cations: channels, exchangers, and permeability transition. *Physiol Rev* 79, 1127-1155.
- Billington, D., Evans, C.E., Godfrey, P.P., Coleman, R., 1980. Effects of bile salts on the plasma membranes of isolated rat hepatocytes. *Biochem J* 188, 321-327.
- Blomme, E.A., Will, Y., 2016. Toxicology Strategies for Drug Discovery: Present and Future. *Chem Res Toxicol* 29, 473-504.
- Boelsterli, U.A., Lim, P.L.K., 2007. Mitochondrial abnormalities—A link to idiosyncratic drug hepatotoxicity? *Toxicology and Applied Pharmacology* 220, 92-107.
- Borges, N., 2005. Tolcapone in Parkinson's disease: liver toxicity and clinical efficacy. *Expert Opinion on Drug Safety* 4, 69-73.
- Borst, P., Evers, R., Kool, M., Wijnholds, J., 2000. A family of drug transporters: the multidrug resistance-associated proteins. *J Natl Cancer Inst* 92, 1295-1302.
- Boyd, I.W., 2002. The role of the Australian Adverse Drug Reactions Advisory Committee (ADRAC) in monitoring drug safety. *Toxicology* 181-182, 99-102.
- Boyer, J.L., 2013. Bile Formation and Secretion. *Compr Physiol* 3, 1035-1078.
- Boyer, J.L., Trauner, M., Mennone, A., Soroka, C.J., Cai, S.Y., Moustafa, T., Zollner, G., Lee, J.Y., Ballatori, N., 2006. Upregulation of a basolateral FXR-dependent bile acid efflux transporter OSTalpha-OSTbeta in cholestasis in humans and rodents. *Am J Physiol Gastrointest Liver Physiol* 290, G1124-1130.
- Boyer, P.D., 1993. The binding change mechanism for ATP synthase--some probabilities and possibilities. *Biochim Biophys Acta* 1140, 215-250.
- Bradford, M.M., 1976. A rapid and sensitive method for the quantitation of microgram quantities of protein utilizing the principle of protein-dye binding. *Anal Biochem* 72, 248-254.
- Brand M, D., Nicholls D, G., 2011. Assessing mitochondrial dysfunction in cells. *Biochem J* 435, 297-312.
- Brand M, D., Nicholls D, G., 2011. Assessing mitochondrial dysfunction in cells. *Biochem J* 435, 297-312.
- Brand, M.D., Pakay, J.L., Ocloo, A., Kokoszka, J., Wallace, D.C., Brookes, P.S., Cornwall, E.J., 2005. The basal proton conductance of mitochondria depends on adenine nucleotide translocase content. *Biochem J* 392, 353-362.
- Brandt, U., Trumppower, B., 1994. The Protonmotive Q Cycle in Mitochondria and Bacteria. *Critical Reviews in Biochemistry and Molecular Biology* 29, 165-197.
- Brinkman, K., Kakuda, T.N., 2000. Mitochondrial toxicity of nucleoside analogue reverse transcriptase inhibitors: a looming obstacle for long-term antiretroviral therapy? *Curr Opin Infect Dis* 13, 5-11.

- Briske-Anderson, M.J., Finley, J.W., Newman, S.M., 1997. The influence of culture time and passage number on the morphological and physiological development of Caco-2 cells. *Proc Soc Exp Biol Med* 214, 248-257.
- Brobst, D., L. Staudinger, J., 2017. Nuclear Receptor Signaling in HepaRG Cells.
- Bunn, C.L., Wallace, D.C., Eisenstadt, J.M., 1974. Cytoplasmic inheritance of chloramphenicol resistance in mouse tissue culture cells. *Proc Natl Acad Sci U S A* 71, 1681-1685.
- Burban, A., Sharanek, A., Guguen-Guillouzo, C., Guillouzo, A., 2018. Endoplasmic reticulum stress precedes oxidative stress in antibiotic-induced cholestasis and cytotoxicity in human hepatocytes. *Free Radic Biol Med* 115, 166-178.
- Burban, A., Sharanek, A., Hue, R., Gay, M., Routier, S., Guillouzo, A., Guguen-Guillouzo, C., 2017. Penicillinase-resistant antibiotics induce non-immune-mediated cholestasis through HSP27 activation associated with PKC/P38 and PI3K/AKT signaling pathways. *Scientific Reports* 7, 1815.
- Burbank, M.G., Burban, A., Sharanek, A., Weaver, R.J., Guguen-Guillouzo, C., Guillouzo, A., 2016. Early Alterations of Bile Canaliculi Dynamics and the Rho Kinase/Myosin Light Chain Kinase Pathway Are Characteristics of Drug-Induced Intrahepatic Cholestasis. *Drug Metab Dispos* 44, 1780-1793.
- Burr, S.P., Pezet, M., Chinnery, P.F., 2018. Mitochondrial DNA Heteroplasmy and Purifying Selection in the Mammalian Female Germ Line. 60, 21-32.
- Byrne, J.A., Strautnieks, S.S., Ihrke, G., Pagani, F., Knisely, A.S., Linton, K.J., Mieli-Vergani, G., Thompson, R.J., 2009. Missense mutations and single nucleotide polymorphisms in ABCB11 impair bile salt export pump processing and function or disrupt pre-messenger RNA splicing. *Hepatology* 49, 553-567.
- Byrne, J.A., Strautnieks, S.S., Mieli-Vergani, G., Higgins, C.F., Linton, K.J., Thompson, R.J., 2002. The human bile salt export pump: characterization of substrate specificity and identification of inhibitors. *Gastroenterology* 123, 1649-1658.
- Byrne, J.A., Strautnieks, S.S., Mieli-Vergani, G., Higgins, C.F., Linton, K.J., Thompson, R.J., The human bile salt export pump: Characterization of substrate specificity and identification of inhibitors. *Gastroenterology* 123, 1649-1658.
- Calvo, S.E., Mootha, V.K., 2010. The mitochondrial proteome and human disease. *Annu Rev Genomics Hum Genet* 11, 25-44.
- Capaldi, R.A., Aggeler, R., 2002. Mechanism of the F(1)F(0)-type ATP synthase, a biological rotary motor. *Trends Biochem Sci* 27, 154-160.
- Cerec, V., Glaise, D., Garnier, D., Morosan, S., Turlin, B., Drenou, B., Gripon, P., Kremsdorf, D., Guguen-Guillouzo, C., Corlu, A., 2007. Transdifferentiation of hepatocyte-like cells from the human hepatoma HepaRG cell line through bipotent progenitor. *Hepatology* 45, 957-967.
- Chalasan, N., Bjornsson, E., 2010. Risk factors for idiosyncratic drug-induced liver injury. *Gastroenterology* 138, 2246-2259.
- Chan, R., Benet, L.Z., 2018. Measures of BSEP Inhibition In Vitro Are Not Useful Predictors of DILI. *Toxicol Sci* 162, 499-508.
- Chatterjee, S., Richert, L., Augustijns, P., Annaert, P., 2014. Hepatocyte-based in vitro model for assessment of drug-induced cholestasis. *Toxicol Appl Pharmacol* 274, 124-136.
- Chazotte, B., 2011a. Labeling lysosomes in live cells with LysoTracker. *Cold Spring Harb Protoc* 2011, pdb.prot5571.
- Chazotte, B., 2011b. Labeling mitochondria with MitoTracker dyes. *Cold Spring Harb Protoc* 2011, 990-992.
- Chiang, J.Y., 2002. Bile acid regulation of gene expression: roles of nuclear hormone receptors. *Endocr Rev* 23, 443-463.
- Chiang, J.Y., 2009. Bile acids: regulation of synthesis. *J Lipid Res* 50, 1955-1966.

- Chiang, J.Y.L., 2013. Bile Acid Metabolism and Signaling. *Compr Physiol* 3, 1191-1212.
- Chinnery, P.F., Gomez-Duran, A., 2018. Oldies but Goldies mtDNA Population Variants and Neurodegenerative Diseases. *Front Neurosci* 12.
- Chinnery, P.F., Hudson, G., 2013. Mitochondrial genetics. *Br Med Bull* 106, 135-159.
- Choi, J.M., Oh, S.J., Lee, J.Y., Jeon, J.S., Ryu, C.S., Kim, Y.M., Lee, K., Kim, S.K., 2015. Prediction of Drug-Induced Liver Injury in HepG2 Cells Cultured with Human Liver Microsomes. *Chem Res Toxicol* 28, 872-885.
- Chollet, R., Ribault, S.b., 2012. Use of ATP Bioluminescence for Rapid Detection and Enumeration of Contaminants: The Milliflex Rapid Microbiology Detection and Enumeration System.
- Clark, L.T., Watkins, L., Piña, I.L., Elmer, M., Akinboboye, O., Gorham, M., Jamerson, B., McCullough, C., Pierre, C., Polis, A.B., Puckrein, G., Regnante, J.M., 2019. Increasing Diversity in Clinical Trials: Overcoming Critical Barriers. *Current Problems in Cardiology* 44, 148-172.
- Coe, K.J., Jia, Y., Ho, H.K., Rademacher, P., Bammler, T.K., Beyer, R.P., Farin, F.M., Woodke, L., Plymate, S.R., Fausto, N., Nelson, S.D., 2007. Comparison of the cytotoxicity of the nitroaromatic drug flutamide to its cyano analogue in the hepatocyte cell line TAMH: evidence for complex I inhibition and mitochondrial dysfunction using toxicogenomic screening. *Chem Res Toxicol* 20, 1277-1290.
- Colombo, B., Felicetti, L., Baglioni, C., 1965. Inhibition of protein synthesis by cycloheximide in rabbit reticulocytes. *Biochem Biophys Res Commun* 18, 389-395.
- Contreras, L., Drago, I., Zampese, E., Pozzan, T., 2010. Mitochondria: The calcium connection. *Biochimica et Biophysica Acta (BBA) - Bioenergetics* 1797, 607-618.
- Craddock, A.L., Love, M.W., Daniel, R.W., Kirby, L.C., Walters, H.C., Wong, M.H., Dawson, P.A., 1998. Expression and transport properties of the human ileal and renal sodium-dependent bile acid transporter. *Am J Physiol* 274, G157-169.
- Craven, L., Alston, C.L., Taylor, R.W., Turnbull, D.M., 2017. Recent Advances in Mitochondrial Disease. *Annu Rev Genomics Hum Genet* 18, 257-275.
- Crouch, S.P., Kozlowski, R., Slater, K.J., Fletcher, J., 1993. The use of ATP bioluminescence as a measure of cell proliferation and cytotoxicity. *J Immunol Methods* 160, 81-88.
- Cui, L., Yoon, S., Schinazi, R.F., Sommadossi, J.P., 1995. Cellular and molecular events leading to mitochondrial toxicity of 1-(2-deoxy-2-fluoro-1-beta-D-arabinofuranosyl)-5-iodouracil in human liver cells. *J Clin Invest* 95, 555-563.
- Daly, A.K., Donaldson, P.T., Bhatnagar, P., Shen, Y., Pe'er, I., Floratos, A., Daly, M.J., Goldstein, D.B., John, S., Nelson, M.R., Graham, J., Park, B.K., Dillon, J.F., Bernal, W., Cordell, H.J., Pirmohamed, M., Aithal, G.P., Day, C.P., 2009. HLA-B\*5701 genotype is a major determinant of drug-induced liver injury due to flucloxacillin. *Nat Genet* 41, 816-819.
- Dawson, S., Stahl, S., Paul, N., Barber, J., Kenna, J.G., 2012. In vitro inhibition of the bile salt export pump correlates with risk of cholestatic drug-induced liver injury in humans. *Drug Metab Dispos* 40, 130-138.
- de Kroon, A.I., Dolis, D., Mayer, A., Lill, R., de Kruijff, B., 1997. Phospholipid composition of highly purified mitochondrial outer membranes of rat liver and *Neurospora crassa*. Is cardiolipin present in the mitochondrial outer membrane? *Biochim Biophys Acta* 1325, 108-116.
- de Vree, J.M.L., Jacquemin, E., Sturm, E., Cresteil, D., Bosma, P.J., Aten, J., Deleuze, J.F., Desrochers, M., Burdelski, M., Bernard, O., Elferink, R., Hadchouel, M., 1998. Mutations in the MDR3 gene cause progressive familial intrahepatic cholestasis. *Proc Natl Acad Sci U S A* 95, 282-287.
- Decker, T., Lohmann-Matthes, M.-L., 1988. A quick and simple method for the quantitation of lactate dehydrogenase release in measurements of cellular cytotoxicity and tumor necrosis factor (TNF) activity. *J Immunol Methods* 115, 61-69.

- Degli Esposti, D., Hamelin, J., Bosselut, N., Saffroy, R., Sebagh, M., Pommier, A., Martel, C., Lemoine, A., 2012. Mitochondrial Roles and Cytoprotection in Chronic Liver Injury. *Biochem Res Int* 2012.
- Denk, G.U., Kleiss, C.P., Wimmer, R., Vennegeerts, T., Reiter, F.P., Schulz, S., Zischka, H., Rust, C., 2012. Tauro- $\beta$ -muricholic acid restricts bile acid-induced hepatocellular apoptosis by preserving the mitochondrial membrane potential. *Biochem Biophys Res Commun* 424, 758-764.
- Denver, D.R., Morris, K., Lynch, M., Vassilieva, L.L., Thomas, W.K., 2000. High direct estimate of the mutation rate in the mitochondrial genome of *Caenorhabditis elegans*. *Science* 289, 2342-2344.
- Desjardins, P., Frost, E., Morais, R., 1985. Ethidium bromide-induced loss of mitochondrial DNA from primary chicken embryo fibroblasts. *Mol Cell Biol* 5, 1163-1169.
- Dianat, N., Dubois-Pot-Schneider, H., Steichen, C., Desterke, C., Leclerc, P., Raveux, A., Combettes, L., Weber, A., Corlu, A., Dubart-Kupperschmitt, A., 2014. Generation of functional cholangiocyte-like cells from human pluripotent stem cells and HepaRG cells. *Hepatology* 60, 700-714.
- DiMasi, J.A., Grabowski, H.G., Hansen, R.W., 2015. The cost of drug development. *N Engl J Med* 372, 1972.
- DiMauro, S., Schon, E.A., 2003. Mitochondrial respiratory-chain diseases. *N Engl J Med* 348, 2656-2668.
- Dingemans, J., Jorga, K., Zürcher, G., Schmitt, M., Sedek, G., Da Prada, M., Van Brummelen, P., 1995. Pharmacokinetic-pharmacodynamic interaction between the COMT inhibitor tolcapone and single-dose levodopa. *Br J Clin Pharmacol* 40, 253-262.
- Donato, M.T., Tolosa, L., Gomez-Lechon, M.J., 2015. Culture and Functional Characterization of Human Hepatoma HepG2 Cells. *Methods Mol Biol* 1250, 77-93.
- Donkers, J.M., Zehnder, B., van Westen, G.J.P., Kwakkenbos, M.J., AP, I.J., Oude Elferink, R.P.J., Beuers, U., Urban, S., van de Graaf, S.F.J., 2017. Reduced hepatitis B and D viral entry using clinically applied drugs as novel inhibitors of the bile acid transporter NTCP. *Sci Rep* 7, 15307.
- Drewitz, M., Helbling, M., Fried, N., Bieri, M., Moritz, W., Lichtenberg, J., Kelm, J.M., 2011. Towards automated production and drug sensitivity testing using scaffold-free spherical tumor microtissues. *Biotechnol J* 6, 1488-1496.
- Duchen, M.R., Szabadkai, G., 2010. Roles of mitochondria in human disease. *Essays Biochem* 47, 115-137.
- Dudkina, N.V., Sunderhaus, S., Boekema, E.J., Braun, H.P., 2008. The higher level of organization of the oxidative phosphorylation system: mitochondrial supercomplexes. *J Bioenerg Biomembr* 40, 419-424.
- Duewelhenke, N., Krut, O., Eysel, P., 2007. Influence on Mitochondria and Cytotoxicity of Different Antibiotics Administered in High Concentrations on Primary Human Osteoblasts and Cell Lines. *Antimicrobial Agents and Chemotherapy* 51, 54-63.
- Dupont, E., Burgunder, J.M., Findley, L.J., Olsson, J.E., Dorflinger, E., 1997. Tolcapone added to levodopa in stable parkinsonian patients: a double-blind placebo-controlled study. Tolcapone in Parkinson's Disease Study Group II (TIPS II). *Mov Disord* 12, 928-934.
- Dykens, J.A., Jamieson, J.D., Marroquin, L.D., Nadanaciva, S., Xu, J.J., Dunn, M.C., Smith, A.R., Will, Y., 2008. In Vitro Assessment of Mitochondrial Dysfunction and Cytotoxicity of Nefazodone, Trazodone, and Buspirone. *Toxicological Sciences* 103, 335-345.
- Esquenet, M., Swinnen, J.V., Heyns, W., Verhoeven, G., 1997. LNCaP prostatic adenocarcinoma cells derived from low and high passage numbers display divergent responses not only to androgens but also to retinoids. *J Steroid Biochem Mol Biol* 62, 391-399.

- Eupedia, 2018. Distribution of European mitochondrial DNA (mtDNA) haplogroups by region in percentage.
- Evans, M.J., Scarpulla, R.C., 1990. NRF-1: a trans-activator of nuclear-encoded respiratory genes in animal cells. *Genes Dev* 4, 1023-1034.
- Evason, K., Bove, K.E., Finegold, M.J., Knisely, A.S., Rhee, S., Rosenthal, P., Miethke, A.G., Karpen, S.J., Ferrell, L.D., Kim, G.E., 2011. Morphologic findings in progressive familial intrahepatic cholestasis 2 (PFIC2): correlation with genetic and immunohistochemical studies. *Am J Surg Pathol* 35, 687-696.
- Faber, K.N., Muller, M., Jansen, P.L., 2003. Drug transport proteins in the liver. *Adv Drug Deliv Rev* 55, 107-124.
- Fahey, D.A., Carey, M.C., Donovan, J.M., 1995. Bile acid/phosphatidylcholine interactions in mixed monomolecular layers: differences in condensation effects but not interfacial orientation between hydrophobic and hydrophilic bile acid species. *Biochemistry* 34, 10886-10897.
- Felser, A., Blum, K., Lindinger, P.W., Bouitbir, J., Krähenbühl, S., 2013. Mechanisms of hepatocellular toxicity associated with dronedarone--a comparison to amiodarone. *Toxicol Sci* 131, 480-490.
- Ferdinandusse, S., Houten, S.M., 2006. Peroxisomes and bile acid biosynthesis. *Biochimica et Biophysica Acta (BBA) - Molecular Cell Research* 1763, 1427-1440.
- Fermini, B., Coyne, K.P., Coyne, S.T., 2018. Challenges in designing and executing clinical trials in a dish studies. *J Pharmacol Toxicol Methods* 94, 73-82.
- Ferrick, D.A., Neilson, A., Beeson, C., 2008. Advances in measuring cellular bioenergetics using extracellular flux. *Drug Discov Today* 13, 268-274.
- Fickert, P., Zollner, G., Fuchsbichler, A., Stumptner, C., Weiglein, A.H., Lammert, F., Marschall, H.U., Tsybrovskyy, O., Zatloukal, K., Denk, H., Trauner, M., 2002. Ursodeoxycholic acid aggravates bile infarcts in bile duct-ligated and Mdr2 knockout mice via disruption of cholangioles. *Gastroenterology* 123, 1238-1251.
- Fini, A., Roda, A., 1987. Chemical properties of bile acids. IV. Acidity constants of glycine-conjugated bile acids. *J Lipid Res* 28, 755-759.
- Fontana, R.J., 2014. Pathogenesis of idiosyncratic drug-induced liver injury and clinical perspectives. *Gastroenterology* 146, 914-928.
- Forster, F., Volz, A., Fricker, G., 2008. Compound profiling for ABCC2 (MRP2) using a fluorescent microplate assay system. *Eur J Pharm Biopharm* 69, 396-403.
- Friedrich, T., Bottcher, B., 2004. The gross structure of the respiratory complex I: a Lego System. *Biochim Biophys Acta* 1608, 1-9.
- Fromenty, B., Fisch, C., Berson, A., Letteron, P., Larrey, D., Pessayre, D., 1990a. Dual effect of amiodarone on mitochondrial respiration. Initial protonophoric uncoupling effect followed by inhibition of the respiratory chain at the levels of complex I and complex II. *J Pharmacol Exp Ther* 255, 1377-1384.
- Fromenty, B., Fisch, C., Labbe, G., Degott, C., Deschamps, D., Berson, A., Letteron, P., Pessayre, D., 1990b. Amiodarone inhibits the mitochondrial beta-oxidation of fatty acids and produces microvesicular steatosis of the liver in mice. *J Pharmacol Exp Ther* 255, 1371-1376.
- Fromenty, B., Pessayre, D., 1995. Inhibition of mitochondrial beta-oxidation as a mechanism of hepatotoxicity. *Pharmacol Ther* 67, 101-154.
- Fulda, S., Galluzzi, L., Kroemer, G., 2010. Targeting mitochondria for cancer therapy. *Nat Rev Drug Discov* 9, 447-464.
- Garzel, B., Yang, H., Zhang, L., Huang, S.M., Polli, J.E., Wang, H., 2014. The role of bile salt export pump gene repression in drug-induced cholestatic liver toxicity. *Drug Metab Dispos* 42, 318-322.

- Gekeler, V., Ise, W., Sanders, K.H., Ulrich, W.R., Beck, J., 1995. The leukotriene LTD4 receptor antagonist MK571 specifically modulates MRP associated multidrug resistance. *Biochem Biophys Res Commun* 208, 345-352.
- Gerets, H.H., Tilmant, K., Gerin, B., Chanteux, H., Depelchin, B.O., Dhalluin, S., Atienzar, F.A., 2012a. Characterization of primary human hepatocytes, HepG2 cells, and HepaRG cells at the mRNA level and CYP activity in response to inducers and their predictivity for the detection of human hepatotoxins. *Cell Biol Toxicol* 28, 69-87.
- Gerets, H.H.J., Tilmant, K., Gerin, B., Chanteux, H., Depelchin, B.O., Dhalluin, S., Atienzar, F.A., 2012b. Characterization of primary human hepatocytes, HepG2 cells, and HepaRG cells at the mRNA level and CYP activity in response to inducers and their predictivity for the detection of human hepatotoxins. *Cell Biology and Toxicology* 28, 69-87.
- Gerk, P.M., Vore, M., 2002. Regulation of expression of the multidrug resistance-associated protein 2 (MRP2) and its role in drug disposition. *J Pharmacol Exp Ther* 302, 407-415.
- Gerloff, T., Stieger, B., Hagenbuch, B., Madon, J., Landmann, L., Roth, J., Hofmann, A.F., Meier, P.J., 1998. The sister of P-glycoprotein represents the canalicular bile salt export pump of mammalian liver. *J Biol Chem* 273, 10046-10050.
- Ghelli, A., Porcelli, A.M., Zanna, C., Vidoni, S., Mattioli, S., Barbieri, A., Iommarini, L., Pala, M., Achilli, A., Torroni, A., Rugolo, M., Carelli, V., 2009. The background of mitochondrial DNA haplogroup J increases the sensitivity of Leber's hereditary optic neuropathy cells to 2,5-hexanedione toxicity. *PLoS One* 4, e7922.
- Gissen, P., Arias, I.M., 2015. Structural and functional hepatocyte polarity and liver disease. *J Hepatol* 63, 1023-1037.
- Godoy, P., Hewitt, N.J., Albrecht, U., Andersen, M.E., Ansari, N., Bhattacharya, S., Bode, J.G., Bolleyn, J., Borner, C., Bottger, J., Braeuning, A., Budinsky, R.A., Burkhardt, B., Cameron, N.R., Camussi, G., Cho, C.S., Choi, Y.J., Craig Rowlands, J., Dahmen, U., Damm, G., Dirsch, O., Donato, M.T., Dong, J., Dooley, S., Drasdo, D., Eakins, R., Ferreira, K.S., Fonsato, V., Fraczek, J., Gebhardt, R., Gibson, A., Glanemann, M., Goldring, C.E., Gomez-Lechon, M.J., Groothuis, G.M., Gustavsson, L., Guyot, C., Hallifax, D., Hammad, S., Hayward, A., Haussinger, D., Hellerbrand, C., Hewitt, P., Hoehme, S., Holzhutter, H.G., Houston, J.B., Hrach, J., Ito, K., Jaeschke, H., Keitel, V., Kelm, J.M., Kevin Park, B., Kordes, C., Kullak-Ublick, G.A., LeCluyse, E.L., Lu, P., Luebke-Wheeler, J., Lutz, A., Maltman, D.J., Matz-Soja, M., McMullen, P., Merfort, I., Messner, S., Meyer, C., Mwinyi, J., Naisbitt, D.J., Nussler, A.K., Olinga, P., Pampaloni, F., Pi, J., Pluta, L., Przyborski, S.A., Ramachandran, A., Rogiers, V., Rowe, C., Schelcher, C., Schmich, K., Schwarz, M., Singh, B., Stelzer, E.H., Stieger, B., Stober, R., Sugiyama, Y., Tetta, C., Thasler, W.E., Vanhaecke, T., Vinken, M., Weiss, T.S., Widera, A., Woods, C.G., Xu, J.J., Yarborough, K.M., Hengstler, J.G., 2013. Recent advances in 2D and 3D in vitro systems using primary hepatocytes, alternative hepatocyte sources and non-parenchymal liver cells and their use in investigating mechanisms of hepatotoxicity, cell signaling and ADME. *Arch Toxicol* 87, 1315-1530.
- Gomez-Duran, A., Pacheu-Grau, D., Lopez-Gallardo, E., Diez-Sanchez, C., Montoya, J., Lopez-Perez, M.J., Ruiz-Pesini, E., 2010. Unmasking the causes of multifactorial disorders: OXPHOS differences between mitochondrial haplogroups. *Hum Mol Genet* 19, 3343-3353.
- Gomez-Duran, A., Pacheu-Grau, D., Martinez-Romero, I., Lopez-Gallardo, E., Lopez-Perez, M.J., Montoya, J., Ruiz-Pesini, E., 2012. Oxidative phosphorylation differences between mitochondrial DNA haplogroups modify the risk of Leber's hereditary optic neuropathy. *Biochim Biophys Acta* 1822, 1216-1222.
- Grady, B.J., Samuels, D.C., Robbins, G.K., Selph, D., Canter, J.A., Pollard, R.B., Haas, D.W., Shafer, R., Kalams, S.A., Murdock, D.G., Ritchie, M.D., Hulgand, T., 2011. Mitochondrial genomics and CD4 T-cell count recovery after antiretroviral therapy initiation in AIDS clinical trials group study 384. *J Acquir Immune Defic Syndr* 58, 363-370.

- Grazioli, S., Pugin, J., 2018. Mitochondrial Damage-Associated Molecular Patterns: From Inflammatory Signaling to Human Diseases. *Front Immunol* 9, 832.
- Greim, H., Czygan, P., Schaffner, F., Popper, H., 1973. Determination of bile acids in needle biopsies of human liver. *Biochemical Medicine* 8, 280-286.
- Gripon, P., Rumin, S., Urban, S., Le Seyec, J., Glaise, D., Cannie, I., Guyomard, C., Lucas, J., Trepo, C., Guguen-Guillouzo, C., 2002. Infection of a human hepatoma cell line by hepatitis B virus. *Proc Natl Acad Sci U S A* 99, 15655-15660.
- Grünig, D., Felser, A., Bouitbir, J., Krähenbühl, S., 2017. The catechol-O-methyltransferase inhibitors tolcapone and entacapone uncouple and inhibit the mitochondrial respiratory chain in HepaRG cells. *Toxicol In Vitro* 42, 337-347.
- Grünig, D., Felser, A., Duthaler, U., Bouitbir, J., Krähenbühl, S., 2018. Effect of the Catechol-O-Methyltransferase Inhibitors Tolcapone and Entacapone on Fatty Acid Metabolism in HepaRG Cells. *Toxicol Sci* 164, 477-488.
- Guillouzo, A., Corlu, A., Aninat, C., Glaise, D., Morel, F., Guguen-Guillouzo, C., 2007. The human hepatoma HepaRG cells: a highly differentiated model for studies of liver metabolism and toxicity of xenobiotics. *Chem Biol Interact* 168, 66-73.
- Gunness, P., Mueller, D., Shevchenko, V., Heinzle, E., Ingelman-Sundberg, M., Noor, F., 2013. 3D organotypic cultures of human HepaRG cells: a tool for in vitro toxicity studies. *Toxicol Sci* 133, 67-78.
- Gureev, A.P., Shaforostova, E.A., Popov, V.N., 2019. Regulation of Mitochondrial Biogenesis as a Way for Active Longevity: Interaction Between the Nrf2 and PGC-1 $\alpha$  Signaling Pathways. *Frontiers in Genetics* 10.
- Gurtu, V., Kain, S.R., Zhang, G., 1997. Fluorometric and colorimetric detection of caspase activity associated with apoptosis. *Anal Biochem* 251, 98-102.
- Guzman-Fulgencio, M., Berenguer, J., Micheloud, D., Fernandez-Rodriguez, A., Garcia-Alvarez, M., Jimenez-Sousa, M.A., Bellon, J.M., Campos, Y., Cosin, J., Aldamiz-Echevarria, T., Catalan, P., Lopez, J.C., Resino, S., 2013. European mitochondrial haplogroups are associated with CD4+ T cell recovery in HIV-infected patients on combination antiretroviral therapy. *J Antimicrob Chemother* 68, 2349-2357.
- Hagenbuch, B., Dawson, P., 2004. The sodium bile salt cotransport family SLC10. *Pflugers Arch* 447, 566-570.
- Hamilton, G.A., Jolley, S.L., Gilbert, D., Coon, D.J., Barros, S., LeCluyse, E.L., 2001. Regulation of cell morphology and cytochrome P450 expression in human hepatocytes by extracellular matrix and cell-cell interactions. *Cell Tissue Res* 306, 85-99.
- Hart, A.B., Samuels, D.C., Hulgan, T., 2013. The other genome: a systematic review of studies of mitochondrial DNA haplogroups and outcomes of HIV infection and antiretroviral therapy. *AIDS Rev* 15, 213-220.
- Hashimoto, K., Uchiumi, T., Konno, T., Ebihara, T., Nakamura, T., Wada, M., Sakisaka, S., Maniwa, F., Amachi, T., Ueda, K., Kuwano, M., 2002. Trafficking and functional defects by mutations of the ATP-binding domains in MRP2 in patients with Dubin-Johnson syndrome. *Hepatology* 36, 1236-1245.
- Haugland, R.P., 1996. Assays for cell viability, proliferation and function. *The Handbook of Fluorescent Probes and Research Chemicals*, 365-398.
- Hayakawa, T., Noda, M., Yasuda, K., Yorifuji, H., Taniguchi, S., Miwa, I., Sakura, H., Terauchi, Y., Hayashi, J., Sharp, G.W., Kanazawa, Y., Akanuma, Y., Yazaki, Y., Kadowaki, T., 1998. Ethidium bromide-induced inhibition of mitochondrial gene transcription suppresses glucose-stimulated insulin release in the mouse pancreatic beta-cell line betaHC9. *J Biol Chem* 273, 20300-20307.
- Hendriks, D.F.G., Fredriksson Puigvert, L., Messner, S., Mortiz, W., Ingelman-Sundberg, M., 2016. Hepatic 3D spheroid models for the detection and study of compounds with cholestatic liability. *6*, 35434.

- HepaRG.com, HepaRG. The most innovative and useful hepatic cell line.
- Herrmann, J.M., Riemer, J., 2010. Oxidation and reduction of cysteines in the intermembrane space of mitochondria: multiple facets of redox control. *Antioxid Redox Signal* 13, 1323-1326.
- Heslop, J.A., Rowe, C., Walsh, J., Sison-Young, R., Jenkins, R., Kamalian, L., Kia, R., Hay, D., Jones, R.P., Malik, H.Z., Fenwick, S., Chadwick, A.E., Mills, J., Kitteringham, N.R., Goldring, C.E.P., Kevin Park, B., 2017. Mechanistic evaluation of primary human hepatocyte culture using global proteomic analysis reveals a selective dedifferentiation profile. *Arch Toxicol* 91, 439-452.
- Hirst, J., 2009. Towards the molecular mechanism of respiratory complex I. *Biochem J* 425, 327-339.
- Ho, R.H., Leake, B.F., Kilkenny, D.M., Meyer Zu Schwabedissen, H.E., Glaeser, H., Kroetz, D.L., Kim, R.B., 2010. Polymorphic variants in the human bile salt export pump (BSEP; ABCB11): functional characterization and interindividual variability. *Pharmacogenet Genomics* 20, 45-57.
- Hofmann, A.F., 1963. The function of bile salts in fat absorption. The solvent properties of dilute micellar solutions of conjugated bile salts. *Biochem J* 89, 57-68.
- Hofmann, A.F., 1999a. Bile Acids: The Good, the Bad, and the Ugly. *News Physiol Sci* 14, 24-29.
- Hofmann, A.F., 1999b. The continuing importance of bile acids in liver and intestinal disease. *Archives of Internal Medicine* 159, 2647-2658.
- Hofmann, A.F., 2009. The enterohepatic circulation of bile acids in mammals: form and functions. *Front Biosci (Landmark Ed)* 14, 2584-2598.
- Hofmann, M., Zgouras, D., Samaras, P., Schumann, C., Henzel, K., Zimmer, G., Leuschner, U., 1999. Small and Large Unilamellar Vesicle Membranes as Model System for Bile Acid Diffusion in Hepatocytes. *Archives of Biochemistry and Biophysics* 368, 198-206.
- Hogeboom, G.H., Schneider, W.C., Pallade, G.E., 1948. Cytochemical studies of mammalian tissues; isolation of intact mitochondria from rat liver; some biochemical properties of mitochondria and submicroscopic particulate material. *J Biol Chem* 172, 619-635.
- Hohenester, S., Wenniger, L.M., Paulusma, C.C., van Vliet, S.J., Jefferson, D.M., Elferink, R.P., Beuers, U., 2012. A biliary HCO<sub>3</sub><sup>-</sup> umbrella constitutes a protective mechanism against bile acid-induced injury in human cholangiocytes. *Hepatology* 55, 173-183.
- Hollensworth, S.B., Shen, C., Sim, J.E., Spitz, D.R., Wilson, G.L., LeDoux, S.P., 2000. Glial cell type-specific responses to menadione-induced oxidative stress. *Free Radic Biol Med* 28, 1161-1174.
- Homolya, L., Varadi, A., Sarkadi, B., 2003. Multidrug resistance-associated proteins: Export pumps for conjugates with glutathione, glucuronate or sulfate. *Biofactors* 17, 103-114.
- Hudson, G., Nalls, M., Evans, J.R., Breen, D.P., Winder-Rhodes, S., Morrison, K.E., Morris, H.R., Williams-Gray, C.H., Barker, R.A., Singleton, A.B., Hardy, J., Wood, N.E., Burn, D.J., Chinnery, P.F., 2013. Two-stage association study and meta-analysis of mitochondrial DNA variants in Parkinson disease. *Neurology* 80, 2042-2048.
- Hulgan, T., Robbins, G.K., Kalams, S.A., Samuels, D.C., Grady, B., Shafer, R., Murdock, D.G., Selph, D., Haas, D.W., Pollard, R.B., 2012. T cell activation markers and African mitochondrial DNA haplogroups among non-Hispanic black participants in AIDS clinical trials group study 384. *PLoS One* 7, e43803.
- Hunter, D.R., Haworth, R.A., Southard, J.H., 1976. Relationship between configuration, function, and permeability in calcium-treated mitochondria. *J Biol Chem* 251, 5069-5077.
- Hüttemann, M., Lee, I., Samavati, L., Yu, H., Doan, J.W., 2007. Regulation of mitochondrial oxidative phosphorylation through cell signaling. *Biochimica et Biophysica Acta (BBA) - Molecular Cell Research* 1773, 1701-1720.

- Hynes, J., Marroquin, L.D., Ogurtsov, V.I., Christiansen, K.N., Stevens, G.J., Papkovsky, D.B., Will, Y., 2006. Investigation of drug-induced mitochondrial toxicity using fluorescence-based oxygen-sensitive probes. *Toxicol Sci* 92, 186-200.
- Hynes, J., Nadanaciva, S., Swiss, R., Carey, C., Kirwan, S., Will, Y., 2013. A high-throughput dual parameter assay for assessing drug-induced mitochondrial dysfunction provides additional predictivity over two established mitochondrial toxicity assays. *Toxicol In Vitro* 27, 560-569.
- Ienco, E.C., Simoncini, C., Orsucci, D., Petrucci, L., Filosto, M., Mancuso, M., Siciliano, G., 2011. May "Mitochondrial Eve" and Mitochondrial Haplogroups Play a Role in Neurodegeneration and Alzheimer's Disease? *International Journal of Alzheimer's Disease* 2011, 11.
- Jacobs, F., Wisse, E., De Geest, B., 2010. The Role of Liver Sinusoidal Cells in Hepatocyte-Directed Gene Transfer. *Am J Pathol* 176, 14-21.
- Jacquemin, E., 2012. Progressive familial intrahepatic cholestasis. *Clin Res Hepatol Gastroenterol* 36 Suppl 1, S26-35.
- James, A.M., Wei, Y.H., Pang, C.Y., Murphy, M.P., 1996. Altered mitochondrial function in fibroblasts containing MELAS or MERRF mitochondrial DNA mutations. *Biochem J* 318 ( Pt 2), 401-407.
- Jancova, P., Anzenbacher, P., Anzenbacherova, E., 2010. Phase II drug metabolizing enzymes. *Biomed Pap Med Fac Univ Palacky Olomouc Czech Repub* 154, 103-116.
- Jemnitz, K., Veres, Z., Vereczkey, L., 2010. Contribution of high basolateral bile salt efflux to the lack of hepatotoxicity in rat in response to drugs inducing cholestasis in human. *Toxicol Sci* 115, 80-88.
- Jonckheere, A.I., Smeitink, J.A.M., Rodenburg, R.J.T., 2012. Mitochondrial ATP synthase: architecture, function and pathology. *J Inher Metab Dis* 35, 211-225.
- Jones, C.N., Miller, C., Tenenbaum, A., Spremulli, L.L., Saada, A., 2009. Antibiotic effects on mitochondrial translation and in patients with mitochondrial translational defects. *Mitochondrion* 9, 429-437.
- Kalghatgi, S., Spina, C.S., Costello, J.C., Liesa, M., Morones-Ramirez, J.R., Slomovic, S., Molina, A., Shirihai, O.S., Collins, J.J., 2013. Bactericidal antibiotics induce mitochondrial dysfunction and oxidative damage in Mammalian cells. *Sci Transl Med* 5, 192ra185.
- Kamalian, L., Chadwick, A.E., Bayliss, M., French, N.S., Monshouwer, M., Snoeys, J., Park, B.K., 2015. The utility of HepG2 cells to identify direct mitochondrial dysfunction in the absence of cell death. *Toxicol In Vitro* 29, 732-740.
- Kamalian, L., Douglas, O., Jolly, C., Snoeys, J., Simic, D., Monshouwer, M., Williams, D.P., Kevin Park, B., Chadwick, A.E., 2018. The utility of HepaRG cells for bioenergetic investigation and detection of drug-induced mitochondrial toxicity. *Toxicology in Vitro*.
- Kenna, J.G., 2014. Current Concepts in Drug-Induced Bile Salt Export Pump (BSEP) Interference. *Curr Protoc Toxicol* 61, 23.27.21-15.
- Kenna, J.G., Taskar, K.S., Battista, C., Bourdet, D.L., Brouwer, K.L.R., Brouwer, K.R., Dai, D., Funk, C., Hafey, M.J., Lai, Y., Maher, J., Pak, Y.A., Pedersen, J.M., Polli, J.W., Rodrigues, A.D., Watkins, P.B., Yang, K., Yucha, R.W., 2018. Can Bile Salt Export Pump Inhibition Testing in Drug Discovery and Development Reduce Liver Injury Risk? An International Transporter Consortium Perspective. *Clin Pharmacol Ther* 104, 916-932.
- Kenna, J.G., Uetrecht, J., 2018. Do In Vitro Assays Predict Drug Candidate Idiosyncratic Drug-Induced Liver Injury Risk? *Drug Metab Dispos*, dmd.118.082719.
- Kennedy, J.A., Unger, S.A., Horowitz, J.D., 1996. Inhibition of carnitine palmitoyltransferase-1 in rat heart and liver by perhexiline and amiodarone. *Biochem Pharmacol* 52, 273-280.
- Kenney, M.C., Chwa, M., Atilano, S.R., Falatoonzadeh, P., Ramirez, C., Malik, D., Tarek, M., Del Carpio, J.C., Nesburn, A.B., Boyer, D.S., Kuppermann, B.D., Vawter, M.P., Jazwinski, S.M., Miceli, M.V., Wallace, D.C., Udar, N., 2014. Molecular and bioenergetic differences

- between cells with African versus European inherited mitochondrial DNA haplogroups: implications for population susceptibility to diseases. *Biochim Biophys Acta* 1842, 208-219.
- Keppler, D., 2014. The Roles of MRP2, MRP3, OATP1B1, and OATP1B3 in Conjugated Hyperbilirubinemia. *Drug Metab Dispos* 42, 561-565.
- Khan, P., Idrees, D., Moxley, M.A., Corbett, J.A., Ahmad, F., von Figura, G., Sly, W.S., Waheed, A., Hassan, M.I., 2014. Luminol-Based Chemiluminescent Signals: Clinical and Non-clinical Application and Future Uses. *Appl Biochem Biotechnol* 173, 333-355.
- Khetani, S.R., Kanchagar, C., Ukairo, O., Krzyzewski, S., Moore, A., Shi, J., Aoyama, S., Aleo, M., Will, Y., 2013. Use of micropatterned cocultures to detect compounds that cause drug-induced liver injury in humans. *Toxicol Sci* 132, 107-117.
- Kietzmann, T., 2017. Metabolic zonation of the liver: The oxygen gradient revisited. *Redox Biol* 11, 622-630.
- Kikuchi, S., Hata, M., Fukumoto, K., Yamane, Y., Matsui, T., Tamura, A., Yonemura, S., Yamagishi, H., Keppler, D., Tsukita, S., Tsukita, S., 2002. Radixin deficiency causes conjugated hyperbilirubinemia with loss of Mrp2 from bile canalicular membranes. *Nat Genet* 31, 320-325.
- Kim, J.S., He, L., Lemasters, J.J., 2003. Mitochondrial permeability transition: a common pathway to necrosis and apoptosis. *Biochem Biophys Res Commun* 304, 463-470.
- Kirkinezos, I.G., Bacman, S.R., Hernandez, D., Oca-Cossio, J., Arias, L.J., Perez-Pinzon, M.A., Bradley, W.G., Moraes, C.T., 2005. Cytochrome c association with the inner mitochondrial membrane is impaired in the CNS of G93A-SOD1 mice. *J Neurosci* 25, 164-172.
- Knobeloch, D., Ehnert, S., Schyschka, L., Buchler, P., Schoenberg, M., Kleeff, J., Thasler, W.E., Nussler, N.C., Godoy, P., Hengstler, J., Nussler, A.K., 2012. Human hepatocytes: isolation, culture, and quality procedures. *Methods Mol Biol* 806, 99-120.
- Knowles, B.B., Howe, C.C., Aden, D.P., 1980. Human hepatocellular carcinoma cell lines secrete the major plasma proteins and hepatitis B surface antigen. *Science* 209, 497-499.
- Köck, K., Ferslew, B.C., Netterberg, I., Yang, K., Urban, T.J., Swaan, P.W., Stewart, P.W., Brouwer, K.L.R., 2014. Risk Factors for Development of Cholestatic Drug-Induced Liver Injury: Inhibition of Hepatic Basolateral Bile Acid Transporters Multidrug Resistance-Associated Proteins 3 and 4. *Drug Metab Dispos* 42, 665-674.
- Kon, K., Kim, J.S., Jaeschke, H., Lemasters, J.J., 2004. Mitochondrial permeability transition in acetaminophen-induced necrosis and apoptosis of cultured mouse hepatocytes. *Hepatology* 40, 1170-1179.
- Konig, J., Rost, D., Cui, Y., Keppler, D., 1999. Characterization of the human multidrug resistance protein isoform MRP3 localized to the basolateral hepatocyte membrane. *Hepatology* 29, 1156-1163.
- Koopman, M., Michels, H., Dancy, B.M., Kamble, R., Mouchiroud, L., Auwerx, J., Nollen, E.A.A., Houtkooper, R.H., 2016. A screening-based platform for the assessment of cellular respiration in *Caenorhabditis elegans*. *Nat Protoc* 11, 1798-1816.
- Korlipara, L.V., Cooper, J.M., Schapira, A.H., 2004. Differences in toxicity of the catechol-O-methyl transferase inhibitors, tolcapone and entacapone to cultured human neuroblastoma cells. *Neuropharmacology* 46, 562-569.
- Korshunov, S.S., Skulachev, V.P., Starkov, A.A., 1997. High protonic potential actuates a mechanism of production of reactive oxygen species in mitochondria. *FEBS Lett* 416, 15-18.
- Kotani, N., Maeda, K., Debori, Y., Camus, S., Li, R., Chesne, C., Sugiyama, Y., 2012. Expression and transport function of drug uptake transporters in differentiated HepaRG cells. *Mol Pharm* 9, 3434-3441.
- Krebs, H.A., 1937. The citric acid cycle. *Science, Technology and Management*, 5.
- Kroon, A.M., Van den Bogert, C., 1983. Antibacterial drugs and their interference with the biogenesis of mitochondria in animal and human cells. *Pharm Weekbl Sci* 5, 81-87.

- Kruiswijk, F., Labuschagne, C.F., Vousden, K.H., 2015. p53 in survival, death and metabolic health: a lifeguard with a licence to kill. *Nature Reviews Molecular Cell Biology* 16, 393.
- Kühlbrandt, W., 2015. Structure and function of mitochondrial membrane protein complexes. *BMC Biol* 13.
- Kukat, C., Wurm, C.A., Spahr, H., Falkenberg, M., Larsson, N.G., Jakobs, S., 2011. Super-resolution microscopy reveals that mammalian mitochondrial nucleoids have a uniform size and frequently contain a single copy of mtDNA. *Proc Natl Acad Sci U S A* 108, 13534-13539.
- Kullak-Ublick, G.A., Andrade, R.J., Merz, M., End, P., Benesic, A., Gerbes, A.L., Aithal, G.P., 2017. Drug-induced liver injury: recent advances in diagnosis and risk assessment. *Gut*.
- Kullak-Ublick, G.A., Beuers, U., Paumgartner, G., 1996. Molecular and functional characterization of bile acid transport in human hepatoblastoma HepG2 cells. *Hepatology* 23, 1053-1060.
- Kullak-Ublick, G.A., Stieger, B., Hagenbuch, B., Meier, P.J., 2000. Hepatic transport of bile salts. *Semin Liver Dis* 20, 273-292.
- Kurth, M.C., Adler, C.H., Hilaire, M.S., Singer, C., Waters, C., LeWitt, P., Chernik, D.A., Dorflinger, E.E., Yoo, K., 1997. Tolcapone improves motor function and reduces levodopa requirement in patients with Parkinson's disease experiencing motor fluctuations: a multicenter, double-blind, randomized, placebo-controlled trial. Tolcapone Fluctuator Study Group I. *Neurology* 48, 81-87.
- Kuznetsov, A.V., Veksler, V., Gellerich, F.N., Saks, V., Margreiter, R., Kunz, W.S., 2008. Analysis of mitochondrial function in situ in permeabilized muscle fibers, tissues and cells. *Nat Protoc* 3, 965-976.
- Lagouge, M., Larsson, N.G., 2013. The role of mitochondrial DNA mutations and free radicals in disease and ageing. *J Intern Med* 273, 529-543.
- Lam, P., Wang, R., Ling, V., 2005. Bile acid transport in sister of P-glycoprotein (ABCB11) knockout mice. *Biochemistry* 44, 12598-12605.
- Larrey, D., 2002. Epidemiology and Individual Susceptibility to Adverse Drug Reactions Affecting the Liver. *Semin Liver Dis* 22, 145-156.
- Lasser, K.E., Allen, P.D., Woolhandler, S.J., Himmelstein, D.U., Wolfe, S.M., Bor, D.H., 2002. Timing of new black box warnings and withdrawals for prescription medications. *Jama* 287, 2215-2220.
- Lawrence, J.W., Darkin-Rattray, S., Xie, F., Neims, A.H., Rowe, T.C., 1993. 4-Quinolones cause a selective loss of mitochondrial DNA from mouse L1210 leukemia cells. *J Cell Biochem* 51, 165-174.
- Le Dinh, T., Freneaux, E., Labbe, G., Letteron, P., Degott, C., Geneve, J., Berson, A., Larrey, D., Pessayre, D., 1988. Amineptine, a tricyclic antidepressant, inhibits the mitochondrial oxidation of fatty acids and produces microvesicular steatosis of the liver in mice. *J Pharmacol Exp Ther* 247, 745-750.
- Le Vee, M., Jigorel, E., Glaise, D., Gripon, P., Guguen-Guillouzo, C., Fardel, O., 2006. Functional expression of sinusoidal and canalicular hepatic drug transporters in the differentiated human hepatoma HepaRG cell line. *Eur J Pharm Sci* 28, 109-117.
- Lee, H.W., Kook, Y.-M., Lee, H.J., Park, H., Koh, W.-G., 2014. A three-dimensional co-culture of HepG2 spheroids and fibroblasts using double-layered fibrous scaffolds incorporated with hydrogel micropatterns. *RSC Advances* 4, 61005-61011.
- Lee, L.N., Huang, C.T., Hsu, C.L., Chang, H.C., Jan, I.S., Liu, J.L., Sheu, J.C., Wang, J.T., Liu, W.L., Wu, H.S., Chang, C.N., Wang, J.Y., 2019. Mitochondrial DNA Variants in Patients with Liver Injury Due to Anti-Tuberculosis Drugs. *J Clin Med* 8.
- Lee, W.M., 2003. Drug-induced hepatotoxicity. *N Engl J Med* 349, 474-485.
- Lees, A.J., 2008. Evidence-based efficacy comparison of tolcapone and entacapone as adjunctive therapy in Parkinson's disease. *CNS Neurosci Ther* 14, 83-93.

- Lefebvre, P., Cariou, B., Lien, F., Kuipers, F., Staels, B., 2009. Role of bile acids and bile acid receptors in metabolic regulation. *Physiol Rev* 89, 147-191.
- Lemasters, J.J., Holmuhamedov, E., 2006. Voltage-dependent anion channel (VDAC) as mitochondrial governor--thinking outside the box. *Biochim Biophys Acta* 1762, 181-190.
- Leonard, A.P., Cameron, R.B., Speiser, J.L., Wolf, B.J., Peterson, Y.K., Schnellmann, R.G., Beeson, C.C., Rohrer, B., 2015. Quantitative analysis of mitochondrial morphology and membrane potential in living cells using high-content imaging, machine learning, and morphological binning. *Biochimica et Biophysica Acta (BBA) - Molecular Cell Research* 1853, 348-360.
- Letellier, T., Heinrich, R., Malgat, M., Mazat, J.P., 1994. The kinetic basis of threshold effects observed in mitochondrial diseases: a systemic approach. *Biochem J* 302 ( Pt 1), 171-174.
- Lewis, W., Levine, E.S., Griniuviene, B., Tankersley, K.O., Colacino, J.M., Sommadossi, J.P., Watanabe, K.A., Perrino, F.W., 1996. Fialuridine and its metabolites inhibit DNA polymerase gamma at sites of multiple adjacent analog incorporation, decrease mtDNA abundance, and cause mitochondrial structural defects in cultured hepatoblasts. *Proc Natl Acad Sci U S A* 93, 3592-3597.
- Li, T., Apte, U., 2015. Bile acid metabolism and signaling in cholestasis, inflammation and cancer. *Adv Pharmacol* 74, 263-302.
- Li, Y.J., Minear, M.A., Qin, X., Rimmler, J., Hauser, M.A., Allingham, R.R., Igo, R.P., Lass, J.H., Iyengar, S.K., Klintworth, G.K., Afshari, N.A., Gregory, S.G., 2014. Mitochondrial polymorphism A10398G and Haplogroup I are associated with Fuchs' endothelial corneal dystrophy. *Invest Ophthalmol Vis Sci* 55, 4577-4584.
- Liang, D., Hagenbuch, B., Stieger, B., Meier, P.J., 1993. Parallel decrease of Na(+)-taurocholate cotransport and its encoding mRNA in primary cultures of rat hepatocytes. *Hepatology* 18, 1162-1166.
- Libra, A., Ferneti, C., Lorusso, V., Visigalli, M., Anelli, P.L., Staud, F., Tiribelli, C., Pascolo, L., 2006. Molecular determinants in the transport of a bile acid-derived diagnostic agent in tumoral and nontumoral cell lines of human liver. *J Pharmacol Exp Ther* 319, 809-817.
- Lien, L.M., Chen, Z.C., Chung, C.L., Yen, T.L., Chiu, H.C., Chou, D.S., Huang, S.Y., Sheu, J.R., Lu, W.J., Lin, K.H., 2014. Multidrug resistance protein 4 (MRP4/ABCC4) regulates thrombus formation in vitro and in vivo. *Eur J Pharmacol* 737, 159-167.
- Lin, K.K., Goodell, M.A., 2011. Chapter 2 - Detection of Hematopoietic Stem Cells by Flow Cytometry, In: Darzynkiewicz, Z., Holden, E., Orfao, A., Telford, W., Wlodkowic, D. (Eds.), *Methods Cell Biol.* Academic Press, pp. 21-30.
- Lindahl, P.E., Oberg, K.E., 1961. The effect of rotenone on respiration and its point of attack. *Exp Cell Res* 23, 228-237.
- Liu, Y., Chen, X.J., 2013. Adenine Nucleotide Translocase, Mitochondrial Stress, and Degenerative Cell Death. *Oxid Med Cell Longev* 2013.
- Longo, D., Yang, Y., Watkins, P., Howell, B., Siler, S., 2016. Elucidating Differences in the Hepatotoxic Potential of Tolcapone and Entacapone With DILIsym<sup>®</sup>, a Mechanistic Model of Drug-Induced Liver Injury. *CPT: Pharmacometrics & Systems Pharmacology* 5, 31-39.
- Lorico, A., Masturzo, P., Villa, S., Salmona, M., Semeraro, N., De Gaetano, G., 1986. Gentisic acid: an aspirin metabolite with multiple effects on human blood polymorphonuclear leukocytes. *Biochemical Pharmacology* 35, 2443-2445.
- Louisa, M., Suyatna, F.D., Wanandi, S.I., Asih, P.B.S., Syafruddin, D., 2016. Differential expression of several drug transporter genes in HepG2 and Huh-7 cell lines. *Adv Biomed Res* 5.
- Luckert, C., Schulz, C., Lehmann, N., Thomas, M., Hofmann, U., Hammad, S., Hengstler, J.G., Braeuning, A., Lampen, A., Hessel, S., 2017. Comparative analysis of 3D culture methods on human HepG2 cells. *Arch Toxicol* 91, 393-406.

- Maillette de Buy Wenniger, L., Beuers, U., 2010a. Bile salts and cholestasis. *Digestive and Liver Disease* 42, 409-418.
- Maillette de Buy Wenniger, L., Beuers, U., 2010b. Bile salts and cholestasis. *Dig Liver Dis* 42, 409-418.
- Mandon, M., Huet, S., Dubreil, E., Fessard, V., Le Hégarat, L., 2019. Three-dimensional HepaRG spheroids as a liver model to study human genotoxicity in vitro with the single cell gel electrophoresis assay. *Scientific Reports* 9, 10548.
- Mannella, C.A., 1998. Conformational Changes in the Mitochondrial Channel Protein, VDAC, and Their Functional Implications. *Journal of Structural Biology* 121, 207-218.
- Marin, J.J., Mangas, D., Martinez-Diez, M.C., El-Mir, M.Y., Briz, O., Serrano, M.A., 2003. Sensitivity of bile acid transport by organic anion-transporting polypeptides to intracellular pH. *Biochim Biophys Acta* 1611, 249-257.
- Marion, M.-J., Hantz, O., Durantel, D., 2010. The HepaRG Cell Line: Biological Properties and Relevance as a Tool for Cell Biology, Drug Metabolism, and Virology Studies, In: Maurel, P. (Ed.), *Hepatocytes: Methods and Protocols*. Humana Press, Totowa, NJ, pp. 261-272.
- Marrero, I., Sanchez-Bueno, A., Cobbold, P.H., Dixon, C.J., 1994. Tauroolithocholate and tauroolithocholate 3-sulphate exert different effects on cytosolic free Ca<sup>2+</sup> concentration in rat hepatocytes. *Biochem J* 300 ( Pt 2), 383-386.
- Marroquin, L.D., Hynes, J., Dykens, J.A., Jamieson, J.D., Will, Y., 2007. Circumventing the Crabtree effect: replacing media glucose with galactose increases susceptibility of HepG2 cells to mitochondrial toxicants. *Toxicol Sci* 97, 539-547.
- Martin, W.F., Garg, S., Zimorski, V., 2015. Endosymbiotic theories for eukaryote origin. *Philosophical Transactions of the Royal Society B: Biological Sciences* 370.
- Masubuchi, Y., Kano, S., Horie, T., 2006. Mitochondrial permeability transition as a potential determinant of hepatotoxicity of antidiabetic thiazolidinediones. *Toxicology* 222, 233-239.
- Mayati, A., Moreau, A., Le Vée, M., Bruyère, A., Jouan, E., Denizot, C., Parmentier, Y., Fardel, O., 2018. Functional polarization of human hepatoma HepaRG cells in response to forskolin. *Sci Rep* 8, 16115.
- Mazunin, I.O., Levitskii, S.A., Patrushev, M.V., Kamenski, P.A., 2015. Mitochondrial matrix processes. *Biochemistry (Moscow)* 80, 1418-1428.
- McCord, J.M., Fridovich, I., 1969. Superoxide dismutase. An enzymic function for erythrocyte (hemocytin). *J Biol Chem* 244, 6049-6055.
- Medeiros, D.M., 2008. Assessing mitochondria biogenesis. *Methods* 46, 288-294.
- Medrano, L.M., Gutiérrez-Rivas, M., Blanco, J., García, M., Jiménez-Sousa, M.A., Pacheco, Y.M., Montero, M., Iribarren, J.A., Bernal, E., Martínez, O.J., Benito, J.M., Rallón, N., Resino, S., CoRis, the, H.I.V.B.i.i.t.S.A.R.N.P.R.I.S.E., 2018. Mitochondrial haplogroup H is related to CD4+ T cell recovery in HIV infected patients starting combination antiretroviral therapy. *Journal of Translational Medicine* 16, 343.
- Mehta, R., Jeiran, K., Koenig, A.B., Otgonsuren, M., Goodman, Z., Baranova, A., Younossi, Z., 2016. The role of mitochondrial genomics in patients with non-alcoholic steatohepatitis (NASH). *BMC Medical Genetics* 17, 63.
- Meier, P.J., Stieger, B., 2002. Bile salt transporters. *Annu Rev Physiol* 64, 635-661.
- Mersch-Sundermann, V., Knasmüller, S., Wu, X.J., Darroudi, F., Kassie, F., 2004. Use of a human-derived liver cell line for the detection of cytoprotective, antigenotoxic and cogenotoxic agents. *Toxicology* 198, 329-340.
- Messner, S., Agarkova, I., Moritz, W., Kelm, J.M., 2013. Multi-cell type human liver microtissues for hepatotoxicity testing. *Arch Toxicol* 87, 209-213.
- Milani, M., Beckett, A.J., Al-Zabeeby, A., Luo, X., Prior, I.A., Cohen, G.M., Varadarajan, S., 2019. DRP-1 functions independently of mitochondrial structural perturbations to facilitate BH3 mimetic-mediated apoptosis. *Cell Death Discovery* 5, 117.

- Milkiewicz, P., Heathcote, E.J., 2004. Fatigue in chronic cholestasis. *Gut* 53, 475-477.
- Mimaki, M., Wang, X., McKenzie, M., Thorburn, D.R., Ryan, M.T., 2012. Understanding mitochondrial complex I assembly in health and disease. *Biochimica et Biophysica Acta (BBA) - Bioenergetics* 1817, 851-862.
- Mitchell, S.L., Goodloe, R., Brown-Gentry, K., Pendergrass, S.A., Murdock, D.G., Crawford, D.C., 2014. Characterization of mitochondrial haplogroups in a large population-based sample from the United States. *Hum Genet* 133, 861-868.
- Miyamoto, Y., Ikeuchi, M., Noguchi, H., Yagi, T., Hayashi, S., 2015. Spheroid Formation and Evaluation of Hepatic Cells in a Three-Dimensional Culture Device. *Cell Med* 8, 47-56.
- Mohs, R.C., Greig, N.H., 2017. Drug discovery and development: Role of basic biological research. *Alzheimers Dement (N Y)* 3, 651-657.
- Montenez, J.P., Van Bambeke, F., Piret, J., Brasseur, R., Tulkens, P.M., Mingeot-Leclercq, M.P., 1999. Interactions of macrolide antibiotics (Erythromycin A, roxithromycin, erythromyclamine [Dirithromycin], and azithromycin) with phospholipids: computer-aided conformational analysis and studies on acellular and cell culture models. *Toxicol Appl Pharmacol* 156, 129-140.
- Moreno-Sanchez, R., Bravo, C., Vasquez, C., Ayala, G., Silveira, L.H., Martinez-Lavin, M., 1999. Inhibition and uncoupling of oxidative phosphorylation by nonsteroidal anti-inflammatory drugs: study in mitochondria, submitochondrial particles, cells, and whole heart. *Biochem Pharmacol* 57, 743-752.
- Morgan, J.E., Wikstrom, M., 1991. Steady-state redox behavior of cytochrome c, cytochrome a, and CuA of cytochrome c oxidase in intact rat liver mitochondria. *Biochemistry* 30, 948-958.
- Morgan, R.E., Trauner, M., van Staden, C.J., Lee, P.H., Ramachandran, B., Eschenberg, M., Afshari, C.A., Qualls, C.W., Jr., Lightfoot-Dunn, R., Hamadeh, H.K., 2010. Interference with bile salt export pump function is a susceptibility factor for human liver injury in drug development. *Toxicol Sci* 118, 485-500.
- Morgan, R.E., van Staden, C.J., Chen, Y., Kalyanaraman, N., Kalanzi, J., Dunn, R.T., 2nd, Afshari, C.A., Hamadeh, H.K., 2013. A multifactorial approach to hepatobiliary transporter assessment enables improved therapeutic compound development. *Toxicol Sci* 136, 216-241.
- Mosedale, M., Watkins, P.B., 2017. Drug-induced liver injury: Advances in mechanistic understanding that will inform risk management. *Clin Pharmacol Ther* 101, 469-480.
- Moullan, N., Mouchiroud, L., Wang, X., Ryu, D., Williams, Evan G., Mottis, A., Jovaisaite, V., Frochoux, Michael V., Quiros, Pedro M., Deplancke, B., Houtkooper, Riekelt H., Auwerx, J., 2015. Tetracyclines Disturb Mitochondrial Function across Eukaryotic Models: A Call for Caution in Biomedical Research. *Cell Reports* 10, 1681-1691.
- Moyes, C.D., Battersby, B.J., Leary, S.C., 1998. Regulation of muscle mitochondrial design. *The Journal of Experimental Biology* 201, 299-307.
- Munoz-Pinedo, C., Guio-Carrion, A., Goldstein, J.C., Fitzgerald, P., Newmeyer, D.D., Green, D.R., 2006. Different mitochondrial intermembrane space proteins are released during apoptosis in a manner that is coordinately initiated but can vary in duration. *Proc Natl Acad Sci U S A* 103, 11573-11578.
- Murphy, M.P., 2009. How mitochondria produce reactive oxygen species. *Biochem J* 417, 1-13.
- Müsch, A., 2014. The unique Polarity Phenotype of Hepatocytes. *Exp Cell Res* 328, 276-283.
- Nachlas, M.M., Margulies, S.I., Goldberg, J.D., Seligman, A.M., 1960. The determination of lactic dehydrogenase with a tetrazolium salt. *Anal Biochem* 1, 317-326.
- Nadanaciva, S., Bernal, A., Aggeler, R., Capaldi, R., Will, Y., 2007a. Target identification of drug induced mitochondrial toxicity using immunocapture based OXPHOS activity assays. *Toxicol In Vitro* 21, 902-911.

- Nadanaciva, S., Dykens, J.A., Bernal, A., Capaldi, R.A., Will, Y., 2007b. Mitochondrial impairment by PPAR agonists and statins identified via immunocaptured OXPHOS complex activities and respiration. *Toxicol Appl Pharmacol* 223, 277-287.
- Nadanaciva, S., Rana, P., Beeson, G.C., Chen, D., Ferrick, D.A., Beeson, C.C., Will, Y., 2012. Assessment of drug-induced mitochondrial dysfunction via altered cellular respiration and acidification measured in a 96-well platform. *Journal of Bioenergetics and Biomembranes* 44, 421-437.
- Nair, R., Raina, S., Keshavarz, T., J.P. Kerrigan, M., 2011. Application of fluorescent indicators to analyse intracellular calcium and morphology in filamentous fungi.
- Nissinen, E., Kaheinen, P., Penttila, K.E., Kaivola, J., Linden, I.B., 1997. Entacapone, a novel catechol-O-methyltransferase inhibitor for Parkinson's disease, does not impair mitochondrial energy production. *Eur J Pharmacol* 340, 287-294.
- O'Brien, P.J., Irwin, W., Diaz, D., Howard-Cofield, E., Krejsa, C.M., Slaughter, M.R., Gao, B., Kaludercic, N., Angeline, A., Bernardi, P., Brain, P., Hougham, C., 2006. High concordance of drug-induced human hepatotoxicity with in vitro cytotoxicity measured in a novel cell-based model using high content screening. *Arch Toxicol* 80, 580-604.
- Ostapowicz, G., Fontana, R.J., Schiødt, F.V., et al., 2002. REsults of a prospective study of acute liver failure at 17 tertiary care centers in the united states. *Annals of Internal Medicine* 137, 947-954.
- Pacheu-Grau, D., Gomez-Duran, A., Iglesias, E., Lopez-Gallardo, E., Montoya, J., Ruiz-Pesini, E., 2013. Mitochondrial antibiograms in personalized medicine. *Hum Mol Genet* 22, 1132-1139.
- Pachkoria, K., Lucena, M.I., Molokhia, M., Cueto, R., Carballo, A.S., Carvajal, A., Andrade, R.J., 2007. Genetic and molecular factors in drug-induced liver injury: a review. *Curr Drug Saf* 2, 97-112.
- Padda, M.S., Sanchez, M., Akhtar, A.J., Boyer, J.L., 2011. DRUG INDUCED CHOLESTASIS. *Hepatology* 53, 1377-1387.
- Pallotti, F., Lenaz, G., 2007. Isolation and subfractionation of mitochondria from animal cells and tissue culture lines. *Methods Cell Biol* 80, 3-44.
- Palmeira, C.M., Rolo, A.P., 2004. Mitochondrially-mediated toxicity of bile acids. *Toxicology* 203, 1-15.
- Pandak, W.M., Ren, S., Marques, D., Hall, E., Redford, K., Mallonee, D., Bohdan, P., Heuman, D., Gil, G., Hylemon, P., 2002. Transport of Cholesterol into Mitochondria Is Rate-limiting for Bile Acid Synthesis via the Alternative Pathway in Primary Rat Hepatocytes. *Journal of Biological Chemistry* 277, 48158-48164.
- Paradies, G., Paradies, V., De Benedictis, V., Ruggiero, F.M., Petrosillo, G., 2014. Functional role of cardiolipin in mitochondrial bioenergetics. *Biochimica et Biophysica Acta (BBA) - Bioenergetics* 1837, 408-417.
- Park, B.K., Kitteringham, N.R., Maggs, J.L., Pirmohamed, M., Williams, D.P., 2005. The role of metabolic activation in drug-induced hepatotoxicity. *Annu Rev Pharmacol Toxicol* 45, 177-202.
- Patel, M.S., Korotchkina, L.G., 2006. Regulation of the pyruvate dehydrogenase complex. *Biochem Soc Trans* 34, 217-222.
- Paul, M.K., Kequiv, R., Mukhopadhyay, A.K., 2008. Characterization of rat liver mitochondrial permeability transition pore by using mitochondrial swelling assay. *African Journal of Pharmacy and Pharmacology* 2, 014-021.
- Pauli-Magnus, C., Meier, P.J., 2006. Hepatobiliary transporters and drug-induced cholestasis. *Hepatology* 44, 778-787.
- Paulusma, C.C., Bosma, P.J., Zaman, G.J., Bakker, C.T., Otter, M., Scheffer, G.L., Scheper, R.J., Borst, P., Oude Elferink, R.P., 1996. Congenital jaundice in rats with a mutation in a multidrug resistance-associated protein gene. *Science* 271, 1126-1128.

- Pedersen, J.M., Matsson, P., Bergstrom, C.A., Hoogstraate, J., Noren, A., LeCluyse, E.L., Artursson, P., 2013. Early identification of clinically relevant drug interactions with the human bile salt export pump (BSEP/ABCB11). *Toxicol Sci* 136, 328-343.
- Penman, S.L., Carter, A.S., Chadwick, A.E., 2020a. Investigating the importance of individual mitochondrial genotype in susceptibility to drug-induced toxicity. *Biochemical Society Transactions*.
- Penman, S.L., Carter, A.S., Chadwick, A.E., 2020b. Investigating the importance of individual mitochondrial genotype in susceptibility to drug-induced toxicity. *Biochem Soc Trans* 48, 787-797.
- Penman, S.L., Sharma, P., Aerts, H., Park, B.K., Weaver, R.J., Chadwick, A.E., 2019. Differential toxic effects of bile acid mixtures in isolated mitochondria and physiologically relevant HepaRG cells. *Toxicology in Vitro*, 104595.
- Pereira, C.V., Oliveira, P.J., Will, Y., Nadanaciva, S., 2012. Mitochondrial bioenergetics and drug-induced toxicity in a panel of mouse embryonic fibroblasts with mitochondrial DNA single nucleotide polymorphisms. *Toxicology and Applied Pharmacology* 264, 167-181.
- Perelman, A., Wachtel, C., Cohen, M., Haupt, S., Shapiro, H., Tzur, A., 2012. JC-1: alternative excitation wavelengths facilitate mitochondrial membrane potential cytometry. *Cell Death Dis* 3, e430.
- Pérez-Carreras, M., Del Hoyo, P., Martín, M.A., Rubio, J.C., Martín, A., Castellano, G., Colina, F., Arenas, J., Solis-Herruzo, J.A., 2003. Defective hepatic mitochondrial respiratory chain in patients with nonalcoholic steatohepatitis. *Hepatology* 38, 999-1007.
- Perez, M.J., Briz, O., 2009. Bile-acid-induced cell injury and protection. *World J Gastroenterol* 15, 1677-1689.
- Perkins, E.J., Bao, W., Guan, X., Ang, C.Y., Wolfinger, R.D., Chu, T.M., Meyer, S.A., Inouye, L.S., 2006. Comparison of transcriptional responses in liver tissue and primary hepatocyte cell cultures after exposure to hexahydro-1, 3, 5-trinitro-1, 3, 5-triazine. *BMC Bioinformatics* 7 Suppl 4, S22.
- Perry, A.J., Rimmer, K.A., Mertens, H.D.T., Waller, R.F., Mulhern, T.D., Lithgow, T., Gooley, P.R., 2008. Structure, topology and function of the translocase of the outer membrane of mitochondria. *Plant Physiology and Biochemistry* 46, 265-274.
- Perry, C.G., Kane, D.A., Lanza, I.R., Neuffer, P.D., 2013. Methods for assessing mitochondrial function in diabetes. *Diabetes* 62, 1041-1053.
- Perry, S.W., Norman, J.P., Barbieri, J., Brown, E.B., Gelbard, H.A., 2011. Mitochondrial membrane potential probes and the proton gradient: a practical usage guide. *Biotechniques* 50, 98-115.
- Persson, M., Loye, A.F., Mow, T., Hornberg, J.J., 2013. A high content screening assay to predict human drug-induced liver injury during drug discovery. *J Pharmacol Toxicol Methods* 68, 302-313.
- Pessayre, D., Mansouri, A., Berson, A., Fromenty, B., 2010. Mitochondrial involvement in drug-induced liver injury. *Handb Exp Pharmacol*, 311-365.
- Pirmohamed, M., James, S., Meakin, S., Green, C., Scott, A.K., Walley, T.J., Farrar, K., Park, B.K., Breckenridge, A.M., 2004. Adverse drug reactions as cause of admission to hospital: prospective analysis of 18 820 patients. *Bmj* 329, 15-19.
- Porter, T.D., Coon, M.J., 1991. Cytochrome P-450. Multiplicity of isoforms, substrates, and catalytic and regulatory mechanisms. *J Biol Chem* 266, 13469-13472.
- Rajput, A.H., Martin, W., Saint-Hilaire, M.H., Dorflinger, E., Pedder, S., 1997. Tolcapone improves motor function in parkinsonian patients with the "wearing-off" phenomenon: a double-blind, placebo-controlled, multicenter trial. *Neurology* 49, 1066-1071.
- Ramaiahgari, S.C., den Braver, M.W., Hershers, B., Terpstra, V., Commandeur, J.N., van de Water, B., Price, L.S., 2014. A 3D in vitro model of differentiated HepG2 cell spheroids with

- improved liver-like properties for repeated dose high-throughput toxicity studies. *Arch Toxicol* 88, 1083-1095.
- Ramaiahgari, S.C., Waidyanatha, S., Dixon, D., DeVito, M.J., Paules, R.S., Ferguson, S.S., 2017. From the Cover: Three-Dimensional (3D) HepaRG Spheroid Model With Physiologically Relevant Xenobiotic Metabolism Competence and Hepatocyte Functionality for Liver Toxicity Screening. *Toxicol Sci* 159, 124-136.
- Reisner, A.H., Nemes, P., Bucholtz, C., 1975. The use of Coomassie Brilliant Blue G250 perchloric acid solution for staining in electrophoresis and isoelectric focusing on polyacrylamide gels. *Anal Biochem* 64, 509-516.
- Reitzer, L.J., Wice, B.M., Kennell, D., 1979. Evidence that glutamine, not sugar, is the major energy source for cultured HeLa cells. *J Biol Chem* 254, 2669-2676.
- Rice, G.C., Bump, E.A., Shrieve, D.C., Lee, W., Kovacs, M., 1986. Quantitative analysis of cellular glutathione by flow cytometry utilizing monochlorobimane: some applications to radiation and drug resistance in vitro and in vivo. *Cancer Res* 46, 6105-6110.
- Rippin, S.J., Hagenbuch, B., Meier, P.J., Stieger, B., 2001. Cholestatic expression pattern of sinusoidal and canalicular organic anion transport systems in primary cultured rat hepatocytes. *Hepatology* 33, 776-782.
- Roberts, M.S., Magnusson, B.M., Burczynski, F.J., Weiss, M., 2002. Enterohepatic circulation: physiological, pharmacokinetic and clinical implications. *Clin Pharmacokinet* 41, 751-790.
- Robinson, K.M., Janes, M.S., Pehar, M., Monette, J.S., Ross, M.F., Hagen, T.M., Murphy, M.P., Beckman, J.S., 2006. Selective fluorescent imaging of superoxide in vivo using ethidium-based probes. *Proc Natl Acad Sci U S A* 103, 15038-15043.
- Roda, A., Cappelleri, G., Aldini, R., Roda, E., Barbara, L., 1982. Quantitative aspects of the interaction of bile acids with human serum albumin. *J Lipid Res* 23, 490-495.
- Rodrigues, C.M., Ma, X., Linehan-Stieers, C., Fan, G., Kren, B.T., Steer, C.J., 1999. Ursodeoxycholic acid prevents cytochrome c release in apoptosis by inhibiting mitochondrial membrane depolarization and channel formation. *Cell Death Differ* 6, 842-854.
- Rodríguez-Enriquez, S., Juárez, O., Rodríguez-Zavala, J.S., Moreno-Sánchez, R., 2001. Multisite control of the Crabtree effect in ascites hepatoma cells. *Eur J Biochem* 268, 2512-2519.
- Rodríguez-Nuevo, A., Zorzano, A., 2019. The sensing of mitochondrial DAMPs by non-immune cells. *Cell Stress* 3, 195-207.
- Rolo, A.P., Oliveira, P.J., Moreno, A.J., Palmeira, C.M., 2000. Bile acids affect liver mitochondrial bioenergetics: possible relevance for cholestasis therapy. *Toxicol Sci* 57, 177-185.
- Rolo, A.P., Oliveira, P.J., Moreno, A.J., Palmeira, C.M., 2003. Chenodeoxycholate induction of mitochondrial permeability transition pore is associated with increased membrane fluidity and cytochrome c release: protective role of carvedilol. *Mitochondrion* 2, 305-311.
- Rolo, A.P., Palmeira, C.M., Holy, J.M., Wallace, K.B., 2004. Role of Mitochondrial Dysfunction in Combined Bile Acid-Induced Cytotoxicity: The Switch Between Apoptosis and Necrosis. *Toxicological Sciences* 79, 196-204.
- Rosdah, A.A., J, K.H., Delbridge, L.M., Disting, G.J., Lim, S.Y., 2016. Mitochondrial fission - a drug target for cytoprotection or cytodestruction? *Pharmacol Res Perspect* 4, e00235.
- Rossignol, R., Faustin, B., Rocher, C., Malgat, M., MAZAT, J.-P., Letellier, T., 2003. Mitochondrial threshold effects. *Biochem J* 370, 751-762.
- Rossignol, R., Malgat, M., Mazat, J.P., Letellier, T., 1999. Threshold effect and tissue specificity. Implication for mitochondrial cytopathies. *J Biol Chem* 274, 33426-33432.
- Roth, A.D., Lee, M.-Y., 2017. Idiosyncratic Drug-Induced Liver Injury (IDILI): Potential Mechanisms and Predictive Assays. *BioMed Research International* 2017, 9176937.

- Ruiz-Pesini, E., Mishmar, D., Brandon, M., Procaccio, V., Wallace, D.C., 2004. Effects of purifying and adaptive selection on regional variation in human mtDNA. *Science* 303, 223-226.
- Russell, D.W., 2003. The enzymes, regulation, and genetics of bile acid synthesis. *Annu Rev Biochem* 72, 137-174.
- Russmann, S., Kaye, J.A., Jick, S.S., Jick, H., 2005. Risk of cholestatic liver disease associated with flucloxacillin and flucloxacillin prescribing habits in the UK: cohort study using data from the UK General Practice Research Database. *Br J Clin Pharmacol* 60, 76-82.
- Russmann, S., Kullak-Ublick, G.A., Grattagliano, I., 2009. Current concepts of mechanisms in drug-induced hepatotoxicity. *Curr Med Chem* 16, 3041-3053.
- Saavedra, Y.G., Mateescu, M.A., Averill-Bates, D.A., DenizEAU, F., 2003. Polyvinylalcohol three-dimensional matrices for improved long-term dynamic culture of hepatocytes. *J Biomed Mater Res A* 66, 562-570.
- Salabei, J.K., Gibb, A.A., Hill, B.G., 2014. Comprehensive measurement of respiratory activity in permeabilized cells using extracellular flux analysis. *Nat Protoc* 9, 421-438.
- Satori, C.P., Kostal, V., Arriaga, E.A., 2012. Review on recent advances in the analysis of isolated organelles. *Anal Chim Acta* 753, 8-18.
- Scaduto, R.C., Grotyohann, L.W., 1999. Measurement of mitochondrial membrane potential using fluorescent rhodamine derivatives. *Biophys J* 76, 469-477.
- Scarpulla, R.C., 2008. Transcriptional paradigms in mammalian mitochondrial biogenesis and function. *Physiol Rev* 88, 611-638.
- Schlame, M., Ren, M., 2009. The role of cardiolipin in the structural organization of mitochondrial membranes. *Biochim Biophys Acta* 1788, 2080-2083.
- Schmitt, S., Eberhagen, C., Weber, S., Aichler, M., Zischka, H., 2015. Isolation of mitochondria from cultured cells and liver tissue biopsies for molecular and biochemical analyses. *Methods Mol Biol* 1295, 87-97.
- Schmitt, S., Saathoff, F., Meissner, L., Schropp, E.-M., Lichtmannegger, J., Schulz, S., Eberhagen, C., Borchard, S., Aichler, M., Adamski, J., Plesnila, N., Rothenfusser, S., Kroemer, G., Zischka, H., 2013. A semi-automated method for isolating functionally intact mitochondria from cultured cells and tissue biopsies. *Anal Biochem* 443, 66-74.
- Schoemaker, M.H., Gommans, W.M., Conde de la Rosa, L., Homan, M., Klok, P., Trautwein, C., van Goor, H., Poelstra, K., Haisma, H.J., Jansen, P.L., Moshage, H., 2003. Resistance of rat hepatocytes against bile acid-induced apoptosis in cholestatic liver injury is due to nuclear factor-kappa B activation. *J Hepatol* 39, 153-161.
- Schon, E.A., DiMauro, S., Hirano, M., 2012. Human mitochondrial DNA: roles of inherited and somatic mutations. *Nat Rev Genet* 13, 878-890.
- Schrenk, D., Gant, T.W., Preisegger, K.H., Silverman, J.A., Marino, P.A., Thorgeirsson, S.S., 1993. Induction of multidrug resistance gene expression during cholestasis in rats and nonhuman primates. *Hepatology* 17, 854-860.
- Schultz, B.E., Chan, S.I., 2001. Structures and proton-pumping strategies of mitochondrial respiratory enzymes. *Annu Rev Biophys Biomol Struct* 30, 23-65.
- Schulz, S., Schmitt, S., Wimmer, R., Aichler, M., Eisenhofer, S., Lichtmannegger, J., Eberhagen, C., Artmann, R., Tookos, F., Walch, A., Krappmann, D., Brenner, C., Rust, C., Zischka, H., 2013. Progressive stages of mitochondrial destruction caused by cell toxic bile salts. *Biochim Biophys Acta* 1828, 2121-2133.
- Schwab, M., Schaeffeler, E., 2012. Pharmacogenomics: a key component of personalized therapy. *Genome medicine*, p. 93.
- Schyschka, L., Sánchez, J.J., Wang, Z., Burkhardt, B., Müller-Vieira, U., Zeilinger, K., Bachmann, A., Nadalin, S., Damm, G., Nussler, A.K., 2013. Hepatic 3D cultures but not 2D cultures preserve specific transporter activity for acetaminophen-induced hepatotoxicity. *Arch Toxicol* 87, 1581-1593.

- Sgro, C., Clinard, F., Ouazir, K., Chanay, H., Allard, C., Guilleminet, C., Lenoir, C., Lemoine, A., Hillon, P., 2002. Incidence of drug-induced hepatic injuries: a French population-based study. *Hepatology* 36, 451-455.
- Sharanek, A., Burban, A., Burbank, M., Le Guevel, R., Li, R., Guillouzo, A., Guguen-Guillouzo, C., 2016. Rho-kinase/myosin light chain kinase pathway plays a key role in the impairment of bile canaliculi dynamics induced by cholestatic drugs. *Scientific Reports* 6, 24709.
- Sharanek, A., Burban, A., Ciriaci, N., Guillouzo, A., 2019. Pro-inflammatory cytokines enhance dilatation of bile canaliculi caused by cholestatic antibiotics. *Toxicol In Vitro* 58, 51-59.
- Sharanek, A., Burban, A., Humbert, L., Guguen-Guillouzo, C., Rainteau, D., Guillouzo, A., 2017. Progressive and Preferential Cellular Accumulation of Hydrophobic Bile Acids Induced by Cholestatic Drugs Is Associated with Inhibition of Their Amidation and Sulfation. *Drug Metab Dispos* 45, 1292-1303.
- Shtolz, N., Mishmar, D., 2019. The Mitochondrial Genome—on Selective Constraints and Signatures at the Organism, Cell, and Single Mitochondrion Levels. *Frontiers in Ecology and Evolution* 7.
- Sison-Young, R.L., Mitsa, D., Jenkins, R.E., Mottram, D., Alexandre, E., Richert, L., Aerts, H., Weaver, R.J., Jones, R.P., Johann, E., Hewitt, P.G., Ingelman-Sundberg, M., Goldring, C.E., Kitteringham, N.R., Park, B.K., 2015. Comparative Proteomic Characterization of 4 Human Liver-Derived Single Cell Culture Models Reveals Significant Variation in the Capacity for Drug Disposition, Bioactivation, and Detoxication. *Toxicol Sci* 147, 412-424.
- Smith, P.K., Krohn, R.I., Hermanson, G.T., Mallia, A.K., Gartner, F.H., Provenzano, M.D., Fujimoto, E.K., Goeke, N.M., Olson, B.J., Klenk, D.C., 1985. Measurement of protein using bicinchoninic acid. *Anal Biochem* 150, 76-85.
- Solmaz, S.R., Hunte, C., 2008. Structure of complex III with bound cytochrome c in reduced state and definition of a minimal core interface for electron transfer. *J Biol Chem* 283, 17542-17549.
- Spahr, L., Rubbia-Brandt, L., Burkhard, P.R., Assal, F., Hadengue, A., 2000. Tolcapone-related fulminant hepatitis: electron microscopy shows mitochondrial alterations. *Dig Dis Sci* 45, 1881-1884.
- Spivey, J.R., Bronk, S.F., Gores, G.J., 1993. Glycochenodeoxycholate-induced lethal hepatocellular injury in rat hepatocytes. Role of ATP depletion and cytosolic free calcium. *J Clin Invest* 92, 17-24.
- Stapelbroek, J.M., van Erpecum, K.J., Klomp, L.W.J., Houwen, R.H.J., 2010. Liver disease associated with canalicular transport defects: Current and future therapies. *J Hepatol* 52, 258-271.
- Starikovskaya, E.B., Sukernik, R.I., Derbeneva, O.A., Volodko, N.V., Ruiz-Pesini, E., Torroni, A., Brown, M.D., Lott, M.T., Hosseini, S.H., Huoponen, K., Wallace, D.C., 2005. Mitochondrial DNA diversity in indigenous populations of the southern extent of Siberia, and the origins of Native American haplogroups. *Ann Hum Genet* 69, 67-89.
- Stevens, J.L., Baker, T.K., 2009. The future of drug safety testing: expanding the view and narrowing the focus. *Drug Discov Today* 14, 162-167.
- Stewart, J.B., Chinnery, P.F., 2015. The dynamics of mitochondrial DNA heteroplasmy: implications for human health and disease. *Nat Rev Genet* 16, 530-542.
- Sticova, E., Jirsa, M., 2013. New insights in bilirubin metabolism and their clinical implications. *World J Gastroenterol* 19, 6398-6407.
- Stieger, B., 2010. Role of the bile salt export pump, BSEP, in acquired forms of cholestasis. *Drug Metab Rev* 42, 437-445.
- Stieger, B., Fattinger, K., Madon, J., Kullak-Ublick, G.A., Meier, P.J., 2000. Drug- and estrogen-induced cholestasis through inhibition of the hepatocellular bile salt export pump (Bsep) of rat liver. *Gastroenterology* 118, 422-430.

- Strautnieks, S.S., Bull, L.N., Knisely, A.S., Kocoshis, S.A., Dahl, N., Arnell, H., Sokal, E., Dahan, K., Childs, S., Ling, V., Tanner, M.S., Kagalwalla, A.F., Nemeth, A., Pawlowska, J., Baker, A., Mieli-Vergani, G., Freimer, N.B., Gardiner, R.M., Thompson, R.J., 1998. A gene encoding a liver-specific ABC transporter is mutated in progressive familial intrahepatic cholestasis. *Nat Genet* 20, 233-238.
- Strobbe, D., Caporali, L., Iommarini, L., Maresca, A., Montopoli, M., Martinuzzi, A., Achilli, A., Olivieri, A., Torroni, A., Carelli, V., Ghelli, A., 2018. Haplogroup J mitogenomes are the most sensitive to the pesticide rotenone: Relevance for human diseases. *Neurobiol Dis* 114, 129-139.
- Su, Y., Zhang, X., Sinko, P.J., 2004. Human Organic Anion-Transporting Polypeptide OATP-A (SLC21A3) Acts in Concert with P-Glycoprotein and Multidrug Resistance Protein 2 in the Vectorial Transport of Saquinavir in Hep G2 Cells. *Molecular Pharmaceutics* 1, 49-56.
- Sun, Y., Qi, Y., Peng, B., Li, W., 2017. NTCP-Reconstituted In Vitro HBV Infection System. *Methods Mol Biol* 1540, 1-14.
- Susukida, T., Sekine, S., Nozaki, M., Tokizono, M., Oizumi, K., Horie, T., Ito, K., 2016. Establishment of a Drug-Induced, Bile Acid-Dependent Hepatotoxicity Model Using HepaRG Cells. *J Pharm Sci* 105, 1550-1560.
- Swiss, R., Niles, A., Cali, J.J., Nadanaciva, S., Will, Y., 2013. Validation of a HTS-amenable assay to detect drug-induced mitochondrial toxicity in the absence and presence of cell death. *Toxicol In Vitro* 27, 1789-1797.
- Szymański, P., Markowicz, M., Mikiciuk-Olasik, E., 2012. Adaptation of high-throughput screening in drug discovery-toxicological screening tests. *Int J Mol Sci* 13, 427-452.
- Tabibian, J.H., Masyuk, A.I., Masyuk, T.V., O'Hara, S.P., LaRusso, N.F., 2013. Physiology of Cholangiocytes. *Compr Physiol* 3.
- Thomas, C., Pellicciari, R., Pruzanski, M., Auwerx, J., Schoonjans, K., 2008. Targeting bile-acid signalling for metabolic diseases. *Nat Rev Drug Discov* 7, 678-693.
- Tivnan, A., Zakaria, Z., O'Leary, C., Kogel, D., Pokorný, J.L., Sarkaria, J.N., Prehn, J.H., 2015. Inhibition of multidrug resistance protein 1 (MRP1) improves chemotherapy drug response in primary and recurrent glioblastoma multiforme. *Front Neurosci* 9, 218.
- Trauner, M., Boyer, J.L., 2003. Bile salt transporters: molecular characterization, function, and regulation. *Physiol Rev* 83, 633-671.
- Treyer, A., Müsch, A., 2013. Hepatocyte Polarity. *Compr Physiol* 3, 243-287.
- Tujios, S., Fontana, R.J., 2011. Mechanisms of drug-induced liver injury: from bedside to bench. *Nat Rev Gastroenterol Hepatol* 8, 202-211.
- Turrens, J.F., 2003. Mitochondrial formation of reactive oxygen species. *J Physiol* 552, 335-344.
- Uetrecht, J., 2008. Idiosyncratic drug reactions: past, present, and future. *Chem Res Toxicol* 21, 84-92.
- Uetrecht, J., Naisbitt, D.J., 2013. Idiosyncratic Adverse Drug Reactions: Current Concepts. *Pharmacol Rev* 65, 779-808.
- Ulrich, R.G., 2007. Idiosyncratic toxicity: a convergence of risk factors. *Annu Rev Med* 58, 17-34.
- Valera-Alberni, M., Canto, C., 2018. Mitochondrial stress management: a dynamic journey. *Cell Stress* 2, 253-274.
- van der Giezen, M., Tovar, J., 2005. Degenerate mitochondria. *EMBO Rep* 6, 525-530.
- van Helvoort, A., Smith, A.J., Sprong, H., Fritzsche, I., Schinkel, A.H., Borst, P., van Meer, G., 1996. MDR1 P-glycoprotein is a lipid translocase of broad specificity, while MDR3 P-glycoprotein specifically translocates phosphatidylcholine. *Cell* 87, 507-517.
- van Oven, M., 2015. PhyloTree Build 17: Growing the human mitochondrial DNA tree. *Forensic Science International: Genetics Supplement Series* 5, e392-e394.

- van Oven, M., Kayser, M., 2009. Updated comprehensive phylogenetic tree of global human mitochondrial DNA variation. *Hum Mutat* 30, E386-394.
- Vianello, A., Casolo, V., Petrusa, E., Peresson, C., Patui, S., Bertolini, A., Passamonti, S., Braidot, E., Zancani, M., 2012. The mitochondrial permeability transition pore (PTP) — An example of multiple molecular exaptation? *Biochimica et Biophysica Acta (BBA) - Bioenergetics* 1817, 2072-2086.
- Vinogradov, A.D., Grivennikova, V.G., 2016. Oxidation of NADH and ROS production by respiratory complex I. *Biochimica et Biophysica Acta (BBA) - Bioenergetics* 1857, 863-871.
- Virbasius, J.V., Scarpulla, R.C., 1994. Activation of the human mitochondrial transcription factor A gene by nuclear respiratory factors: a potential regulatory link between nuclear and mitochondrial gene expression in organelle biogenesis. *Proc Natl Acad Sci U S A* 91, 1309-1313.
- Visscher, P.M., Wray, N.R., Zhang, Q., Sklar, P., McCarthy, M.I., Brown, M.A., Yang, J., 2017. 10 Years of GWAS Discovery: Biology, Function, and Translation. *Am J Hum Genet* 101, 5-22.
- Wallace, D., 2009. Mitochondria, Bioenergetics, and the Epigenome in Eukaryotic and Human Evolution. *Cold Spring Harb Symp Quant Biol* 74, 383-393.
- Wallace, D.C., 2013. A mitochondrial bioenergetic etiology of disease. *J Clin Invest* 123, 1405-1412.
- Walters, H.C., Craddock, A.L., Fusegawa, H., Willingham, M.C., Dawson, P.A., 2000. Expression, transport properties, and chromosomal location of organic anion transporter subtype 3. *Am J Physiol Gastrointest Liver Physiol* 279, G1188-1200.
- Walther, D.M., Rapaport, D., 2009. Biogenesis of mitochondrial outer membrane proteins. *Biochimica et Biophysica Acta (BBA) - Molecular Cell Research* 1793, 42-51.
- Wang, J., Tian, R., Shan, Y., Li, J., Gao, H., Xie, C., Ma, Y., Wu, Y., Ji, B., Gu, S., Xu, M., 2020. Metabolomics study of the metabolic changes in hepatoblastoma cells in response to NTCP/SLC10A1 overexpression. *Int J Biochem Cell Biol* 125, 105773.
- Warburg, O., 1956. On the origin of cancer cells. *Science* 123, 309-314.
- Watkins, P.B., 2011. Drug safety sciences and the bottleneck in drug development. *Clin Pharmacol Ther* 89, 788-790.
- Weisiger, R.A., Fridovich, I., 1973. Superoxide dismutase. Organelle specificity. *J Biol Chem* 248, 3582-3592.
- Weiss, J., Theile, D., Ketabi-Kiyanvash, N., Lindenmaier, H., Haefeli, W.E., 2007. Inhibition of MRP1/ABCC1, MRP2/ABCC2, and MRP3/ABCC3 by nucleoside, nucleotide, and non-nucleoside reverse transcriptase inhibitors. *Drug Metab Dispos* 35, 340-344.
- Werner, A., Kuipers, F., Verkade, H.J., 2004. Fat absorption and lipid metabolism in cholestasis. *Molecular Pathogenesis of Cholestasis*, 314-328.
- Wester, K., Jonsson, A.K., Spigset, O., Druid, H., Hagg, S., 2008. Incidence of fatal adverse drug reactions: a population based study. *Br J Clin Pharmacol* 65, 573-579.
- Whelan, S.P., Zuckerbraun, B.S., 2013. Mitochondrial Signaling: Forwards, Backwards, and In Between. *Oxid Med Cell Longev* 2013, 10.
- Wilkins, H.M., Carl, S.M., Swerdlow, R.H., 2014. Cytoplasmic hybrid (cybrid) cell lines as a practical model for mitochondrial pathies. *Redox Biol* 2, 619-631.
- Wing, K., Bhaskaran, K., Pealing, L., Root, A., Smeeth, L., van Staa, T.P., Klungel, O.H., Reynolds, R.F., Douglas, I., 2017. Quantification of the risk of liver injury associated with flucloxacillin: a UK population-based cohort study. *Journal of Antimicrobial Chemotherapy* 72, 2636-2646.
- Wiseman, A., Attardi, G., 1978. Reversible tenfold reduction in mitochondria DNA content of human cells treated with ethidium bromide. *Mol Gen Genet* 167, 51-63.
- Wojtczak, L., Zablocki, K., 2008. Basic Mitochondrial Physiology in Cell Viability and Death, In: Dykens, J.A., Will, Y. (Eds.), *Drug-Induced Mitochondrial Dysfunction*.

- Woolbright, B.L., Dorko, K., Antoine, D.J., Clarke, J.I., Gholami, P., Li, F., Kumer, S.C., Schmitt, T.M., Forster, J., Fan, F., Jenkins, R.E., Park, B.K., Hagenbuch, B., Olyae, M., Jaeschke, H., 2015. Bile Acid-Induced Necrosis in Primary Human Hepatocytes and in Patients with Obstructive Cholestasis. *283*, 168-177.
- Woolbright, B.L., Jaeschke, H., 2015. Critical Factors in the Assessment of Cholestatic Liver Injury In Vitro. *Methods Mol Biol* 1250, 363-376.
- Woolbright, B.L., McGill, M.R., Yan, H., Jaeschke, H., 2016. Bile Acid-Induced Toxicity in HepaRG Cells Recapitulates the Response in Primary Human Hepatocytes. *Basic Clin Pharmacol Toxicol* 118, 160-167.
- Xiang, X., Han, Y., Neuvonen, M., Laitila, J., Neuvonen, P.J., Niemi, M., 2010. High performance liquid chromatography-tandem mass spectrometry for the determination of bile acid concentrations in human plasma. *J Chromatogr B Analyt Technol Biomed Life Sci* 878, 51-60.
- Xie, W., Radominska-Pandya, A., Shi, Y., Simon, C.M., Nelson, M.C., Ong, E.S., Waxman, D.J., Evans, R.M., 2001. An essential role for nuclear receptors SXR/PXR in detoxification of cholestatic bile acids. *Proc Natl Acad Sci U S A* 98, 3375-3380.
- Yang, K., Köck, K., Sedykh, A., Tropsha, A., Brouwer, K.L.R., 2013. An updated review on drug-induced cholestasis: Mechanisms and investigation of physicochemical properties and pharmacokinetic parameters. *Journal of Pharmaceutical Sciences* 102, 3037-3057.
- Yoneda, M., Miyatake, T., Attardi, G., 1994. Complementation of mutant and wild-type human mitochondrial DNAs coexisting since the mutation event and lack of complementation of DNAs introduced separately into a cell within distinct organelles. *Mol Cell Biol* 14, 2699-2712.
- Youle, R.J., van der Bliek, A.M., 2012. Mitochondrial Fission, Fusion, and Stress. *Science* 337, 1062-1065.
- Zahedi, A., On, V., Phandthong, R., Chaili, A., Remark, G., Bhanu, B., Talbot, P., 2018. Deep Analysis of Mitochondria and Cell Health Using Machine Learning. *Scientific Reports* 8, 16354.
- Zamek-Gliszczyński, M.J., Hoffmaster, K.A., Nezasa, K., Tallman, M.N., Brouwer, K.L., 2006. Integration of hepatic drug transporters and phase II metabolizing enzymes: mechanisms of hepatic excretion of sulfate, glucuronide, and glutathione metabolites. *Eur J Pharm Sci* 27, 447-486.
- Zamzami, N., Larochette, N., Kroemer, G., 2005. Mitochondrial permeability transition in apoptosis and necrosis. *Cell Death Differ* 12 Suppl 2, 1478-1480.
- Zhao, H., Li, R., Wang, Q., Yan, Q., Deng, J.H., Han, D., Bai, Y., Young, W.Y., Guan, M.X., 2004. Maternally inherited aminoglycoside-induced and nonsyndromic deafness is associated with the novel C1494T mutation in the mitochondrial 12S rRNA gene in a large Chinese family. *Am J Hum Genet* 74, 139-152.
- Zhao, H., Young, W.Y., Yan, Q., Li, R., Cao, J., Wang, Q., Li, X., Peters, J.L., Han, D., Guan, M.X., 2005. Functional characterization of the mitochondrial 12S rRNA C1494T mutation associated with aminoglycoside-induced and non-syndromic hearing loss. *Nucleic Acids Res* 33, 1132-1139.
- Zheng, Y., Shi, Y., Tian, C., Jiang, C., Jin, H., Chen, J., Almasan, A., Tang, H., Chen, Q., 2004. Essential role of the voltage-dependent anion channel (VDAC) in mitochondrial permeability transition pore opening and cytochrome c release induced by arsenic trioxide. *Oncogene* 23, 1239-1247.
- Zhou, H., Nie, K., Qiu, R., Xiong, J., Shao, X., Wang, B., Shen, L., Lyu, J., Fang, H., 2017. Generation and Bioenergetic Profiles of Cybrids with East Asian mtDNA Haplogroups. *Oxid Med Cell Longev* 2017, 1062314.
- Zollner, G., Fickert, P., Zenz, R., Fuchsichler, A., Stumptner, C., Kenner, L., Ferenci, P., Stauber, R.E., Krejs, G.J., Denk, H., Zatloukal, K., Trauner, M., 2001. Hepatobiliary

- transporter expression in percutaneous liver biopsies of patients with cholestatic liver diseases. *Hepatology* 33, 633-646.
- Zorova, L.D., Popkov, V.A., Plotnikov, E.Y., Silachev, D.N., Pevzner, I.B., Jankauskas, S.S., Babenko, V.A., Zorov, S.D., Balakireva, A.V., Juhaszova, M., Sollott, S.J., Zorov, D.B., 2018. Mitochondrial membrane potential. *Anal Biochem* 552, 50-59.
- Zuliani, T., Duval, R., Jayat, C., Schnébert, S., Andre, P., Dumas, J.M., Ratinaud, M.-H., 2003. Sensitive and Reliable JC-1 and TOTO-3 Double Staining to Assess Mitochondrial Transmembrane Potential and Plasma Membrane Integrity: Interest for Cell Death Investigations.
- Zylber, E., Vesco, C., Penman, S., 1969. Selective inhibition of the synthesis of mitochondria-associated RNA by ethidium bromide. *J Mol Biol* 44, 195-204.